Optimisation of the Lister strain of vaccinia virus for use as an anticancer immunotherapeutic agent

Jahangir Ahmed

April 2015

Submitted in partial fulfilment of the requirements of the
Degree of Doctor of Philosophy

Barts Cancer Institute
Barts and the London School of Medicine
Queen Mary University of London
London EC1M 6BQ

Statement of originality

I, Jahangir Ahmed confirm that the research included within this thesis is my own work or that where it has been carried out in collaboration with, or supported by others, that it is duly acknowledged below and my contribution indicated. Previously published material is also acknowledged below.

I attest that I have exercised reasonable care to ensure that the work is original, and does not to the best of my knowledge break any UK law, infringe any third party's copyright or other intellectual Property Right, or contain any confidential material.

I accept that the College has the right to use plagiarism detection software to check the electronic version of the thesis.

I can confirm that this thesis has not been previously submitted for the award of a degree by this or any other university.

6th April 2015

This project was performed in collaboration with the Dr Yaohe Wang's team at the Sino-British Research Centre for Molecular Oncology (Zhengzhou University, China), where some animal experiments were performed, as indicated in the main body of the text.

Much of "Chapter 1 Introduction" was used to write a book chapter entitled "The Lister strain of vaccinia virus as an anticancer therapeutic" in the third edition of "Gene Therapy of Cancer" published in October 2013(1).

Abstract

The premise of this project was to engineer a novel viral platform with the capacity to enhance antitumour immunity. To this effect, the N1L gene was disrupted in a Lister strain vaccinia viral backbone that had previously been engineered to be tumour selective (VVL15ΔN1L) and armed with transgenes encoding murine and human versions of GMCSF and IL12.

In vitro, they retained potency for infecting, replicating in and killing a panel of murine, Syrian hamster and human cancer cells; all viruses were able to express their transgenes to detectable levels upon infection of every tumour cell line.

In comparison to the parental virus (VVL15), VVL15ΔN1L administration into immune competent *in vivo* tumour models (of pancreatic and lung cancer) led to enhanced intra-tumour (IT) infiltration of neutrophils as well as markedly elevated circulating numbers of natural killer (NK) cells. VVL15ΔN1L also enhanced the tumour infiltration of CD8+ cells. Functional immunoassays and flow cytometric analysis of T cells provided evidence of enhanced tumour specific adaptive immunity.

In comparison to VVL15, IT VVL15ΔN1L significantly reduced the growth of subcutaneously implanted syngeneic pancreatic tumours. This effect was predominantly due to cytotoxic lymphocytes, evidenced by the complete abrogation of efficacy upon repeating the experiment in mice that had been depleted of CD8+ cells. A similar treatment schedule reduced the formation of lung metastases from a primary spontaneously metastasising syngeneic lung cancer model; and translated into prolonged short-term post-operative survival when used as neoadjuvant to surgical resection. Efficacy in this context was contrastingly, due to an elevation in systemic NK cells; concurrent depletion of NK cells (but not CD4+ or CD8+ cells) completely abrogated the survival advantage.

The IL12 transgene armed recombinant was the most effective antitumour therapeutic. Its IT administration into pancreatic tumours led to complete tumour eradication in over 80% of tumour bearing mice and was effective in slowing the growth of other aggressive flank tumours. Neoadjuvant administration of VVL15ΔN1L-mIL12 into

metastatic lung cancers dramatically prolonged long-term post-surgical survival, with apparent cure of 88% of mice.

Table of contents

Table of figures

List of tables

Index of abbreviations

ADCC	Antigen dependent cellular cytotoxicity
ANOVA	Analysis of Variance
APC	Antigen presenting cell
APC	Allophycocyanin (fluorophore)
ASC	Apoptosis-associated speck-like protein containing a caspase recruitment domain
ATCC	American Type Culture Collection
ATP	Adenosine triphosphate
BAMACAN	Basement membrane-associated chondroitin sulfate proteoglycan
BSA	Bovine serum albumin
BSU	Biological services unit
BCI	Barts Cancer Institute
Bcl	B cell lymphoma
CCR	CC chemokine receptor
CXCR	CXC chemokine receptor
CEV	Cell-associated virion
CPN	Copenhagen strain of VV
CTC	Circulating tumour cell
CTD	Cytosine deaminase
CD	Cluster of differentiation
CLIP	Class II-associated invariant chain peptide
sCM	Stock culture medium
mCM	Marrow culture medium
tCM	T cell culture medium
CMV	Cytomegalovirus
COX	Cyclooxygenase
CRUK	Cancer Research UK
CSC	Cancer stem cell
CT	Computed Tomography
CTL	Cytotoxic T-Lymphocyte
CTLA	Cytotoxic T-Lymphocyte Antigen
dH2O	Distilled water

DAB	3, 3’ diaminobenzidine tetrahydrochloride
DAMP	Damage associated molecular pattern
DC	Dendritic cells
DCT	Dopachrome tautomerase
DMEM	Dulbecco's modified eagle medium
DMSO	Dimethyl sulfoxide
DNA	Deoxyribonucleic acid
EBV	Epstein-Barr Virus
EDTA	Ethylenediaminetetraacetic acid
EEV	Extracellular enveloped virion
EGF	Epidermal growth factor
EGFR	Epidermal growth factor receptor
ELISA	Enzyme linked immunosorbent assay
ER	Endoplasmic reticulum
EtBr	Ethidium bromide
EtOH	Ethanol
FDA	United States Food and Drug Administration
FGF	Fibroblast growth factor
FACS	Fluorescence activated cell sorting
FB	Flow cytometry buffer
FC	Fluorocytosine
FCS	Foetal calf serum
FITC	Fluorescein isothiocyanate
FLT	FMS-related tyrosine kinase
FMO	Fluorescence minus one
FU	Fluorouracil
GFP	Green fluorescent protein
GMCSF	Granulocyte macrophage colony-stimulating factor
H&E	Haematoxylin and eosin
HCC	Hepatocellular carcinoma
HDACI	Histone deacetylase inhibitor
HER	Human epidermal growth factor receptor
HMGB	High mobility group protein B
HPF	High power field

HPV	Human papilloma virus
HSP	Heat shock protein
HSV	Herpes Simplex virus
ICD	Immunogenic cell death
IκB	Inhibitor of κB
IKK	IκB kinase
IFN	Interferon
IHC	Immunohistochemistry
IL	Interleukin
IMV	Intracellular mature virion
INT	2-(4-Iodophenyl)-3-(4-nitrophenyl)-5-phenyl-2H-tetrazolium
IP10	Interferon gamma-induced protein-10
IRF	Interferon regulatory transcription factor
IT	Intratumoural
IV	Intravenous
JA	Jahangir Ahmed
JAK	Janus kinase
KIR	Killer immunoglobulin like receptors
LB	Luria Bertani
LD50	Lethal dose for 50% of animals
LDH	Lactate dehydrogenase
LDL	Low density lipoprotein
LIVP	The Moscow derivative of the Lister strain VV
LMP	Low melting point
MCP	Monocyte chemotactic protein
MDSC	Myeloid derived suppressor cells
MHC	Major histocompatibility complex
MIC	MHC class 1 related chains
MMC	Mitomycin C
MMP	Matrix metalloproteinases
MRD	Minimal residual disease
MTS	3-(4,5-dimethylthiazol-2-yl)-5-(3-carboxymethoxyphenyl)-2-(4-sulfophenyl)-2H-tetrazolium
MVA	Modified vaccinia Ankara

MOI	Multiplicity of infection
NDV	Newcastle Disease Virus
NCR	Natural cytotoxicity receptor
NEB	New England Biolabs
NF	Nuclear factor
NK	Natural killer
NLRP	NOD like receptor family, pyrin domain containing
NOD	Nucleotide oligomerisation domain
dNTP	Deoxyribonucleotide triphosphate
NYCBOH	New York City Board of Health strain of VV
OD	Optical density
ORF	Open reading frame
OV	Oncolytic virus
OVT	Oncolytic virotherapy
PAMP	Pathogen associated molecular pattern
PBS	Phosphate buffered saline
PCR	Polymerase chain reaction
PD	Programmed cell death
PDGF	Platelet derived growth factor
PE	Phycoerythrin
PerCP	Peridinin-chlorophyll
PFU	Plaque forming unit
PMS	Phenazine methosulfate
PRR	Pattern Recognition Receptor
PVP	Primary viral passage
RAG	Recombination activation gene
RAGE	Receptor for advanced glycation end products
RANTES	Regulated on activation, normal T cell expressed and secreted
RBC	Red blood cell
RIG	Retinoic acid inducible gene
RFP	Red fluorescent protein
RNA	Ribonucleic acid
RPMI	Roswell Park Memorial Institute (medium)
RT	Room temperature

SBRCMO	Sino-British Research Centre for Molecular Oncology, China
SC	Subcutaneous
S-HRP	Streptavidin horse radish peroxidase
STAT	Signal transducers and activators of transcription
STR	Short tandem repeat
TAE	Tris base, acetic acid and EDTA, electrophoresis buffer
TAA	Tumour associated antigen
TAM	Tumour associated macrophage
TAP	Transporter associated with antigen processing
TCID	Tissue culture infective dose
TCR	T cell receptor
TEB	Tissue extraction buffer
Th	T helper
TGF	Transforming growth factor
TIL	Tumour infiltrating lymphocyte
TIM	T cell immunoglobulin and mucin
TLR	Toll like receptor
TME	Tumour microenvironment
TNF	Tumour necrosis factor
TRAIL	TNF-related apoptosis-inducing ligand
T-reg	T regulatory cells
T-Vec	Talimogene laherparepvec
UV	Ultraviolet
VEGF	Vascular endothelial growth factor
VGF	Vaccinia growth factor
VV	Vaccinia virus
VVL	Lister strain of vaccinia virus
VSV	Vesicular stomatitis virus
VTK	Vaccinia thymidine kinase enzyme
WP	Well plate
WR	Western Reserve strain of VV
WRDD	Western Reserve double deleted
YW	Yaohe Wang

Chapter 1 Introduction

Vaccinia virus (VV) played a prominent role in one of the greatest achievements in medical history; the eradication of smallpox (caused by Variola virus). This occurred in the late 1970s, having claimed the lives of half a billion people worldwide in the preceding three centuries (2, 3).

The origin of VV remains obscure. Whilst the related cowpox virus was used for initial immunization; by the early 20th century VV had become the foremost smallpox vaccine (3, 4). Although Variola is no longer present in any population, threats of bioterrorism from laboratory-preserved derivatives maintain the potential need for rapid widespread vaccination. Vaccine development therefore still remains active. In addition, VV has found utility in other roles, including the immunotherapeutic prevention of other infectious diseases (5) as well as in the treatment of cancer (6). With regard to the latter, the earliest studies (which mainly used replication-attenuated VV recombinants for fear of toxicity) were relatively disappointing in clinical trials.

Second generation replication-competent VVs retain their ability to lyse tumour cells and spread through tumour tissue. Recent advances in deoxyribonucleic acid (DNA) recombinant technology (facilitating rational manipulation of the viral backbone), coupled with knowledge gains in the fields of molecular virology and cancer cell biology, have aided the development of safe and efficacious replication-competent oncolytic VVs. These are currently at the forefront of the most promising novel anticancer agents.

Different VV strains were used in different areas of the world for mass vaccination. The anticancer potential of the Lister strain (VVL), which was popular in Europe has been the focus of our research group and is the platform upon which the current project is based.

This introduction aims to review oncolytic virotherapy (OVT) using VV as an archetypal example. As our group has chosen to develop the Lister strain platform, studies using this strain will feature prominently. However illustrative lessons from

studies that have utilised other viral platforms will be also be referred to where appropriate.

1.1 Advantages of vaccinia virus as an onco-therapeutic agent

VV is a member of the poxvirus family, which can be broadly divided into those that infect vertebrates (Chordopox) and those that infect insects (Entomopox). VV belongs to the group Orthopoxvirae, a genus of the Chordopox subdivision. Structurally, its protein core surrounds a double-stranded linear sequence of DNA that approximates 192 kbp (see http://www.ncbi.nlm.nih.gov/genbank and http://www.poxvirus.org) with its free ends linked by hairpin loops. This contains approximately 200, largely non-overlapping genes, some of which are duplicated due to their position in inverted terminal repeat sequences (7).

The capacity of VV strains to stably accommodate up to 25 kbp of exogenous DNA with little hindrance to infectivity makes it an ideal vector for use in vaccination and gene therapy (8). VVs have several other inherent features that make them particularly suitable for development as oncolytic agents for cancer treatment.

VVs have an efficient life cycle, leading to the rapid destruction of infected cells and indeed tissue via local dissemination (9). Viral replication occurs in juxtanuclear "factories," commencing one to two hours following infection. During this time, host cell nucleic acid synthesis completely shuts down as cellular resources are diverted toward viral production (10). The initial viral replication cycle is usually complete by eight hours, at which time the first extracellular virions are shed. Infected cells are usually lysed approximately 48 hours post infection. Up to 10,000 viral genome copies per cell may ultimately be produced, of which half will be packaged into infectious particles (11-13).

VV strains have a broad tumour cell tropism. Unlike other oncolytic viruses (OVs), cellular entry is not dependent on specific surface receptors (that would otherwise limit entry to those select tumour cells expressing these) but appears to involve a number of

nonspecific membrane fusion pathways (14, 15). During its life cycle, VV may appear in four infectious forms, differing in the number of layers and composition of the encapsulating lipoprotein membrane(s) (9) (figure 1.1)

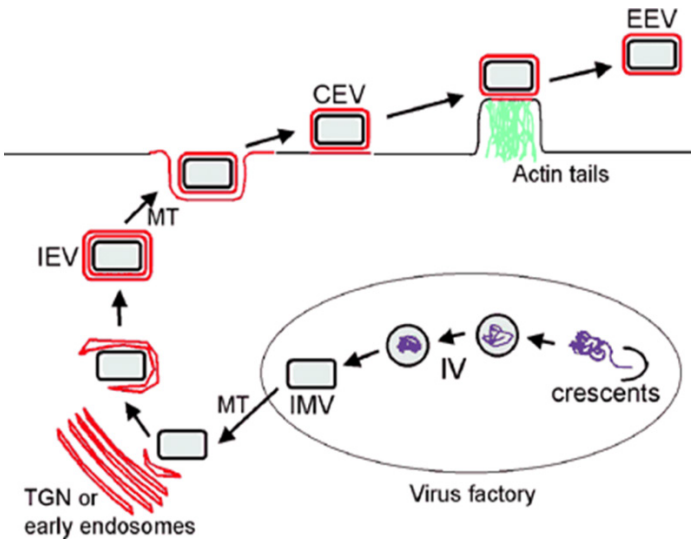

Figure 1.1 The different morphological forms of vaccinia virus during replication (16)

TGN: trans golgi network; MT: microtubules; IV: immature virus; IMV: intracellular mature virus; IEV: intracellular enveloped virus; CEV: cell associated enveloped virus; EEV: extracellular enveloped virus.

Cellular entry of the two major forms, IMV (intracellular mature virion) and EEV (extracellular enveloped virion), is morphologically different (17). The single IMV envelope fuses with the cell membrane, releasing its naked core directly into the cytoplasm, whereas the double-layered EEV particle is first engulfed by endocytosis. Its outer membrane is subsequently disrupted by the low endosomal pH allowing the inner membrane to fuse with the endosomal membrane to release the nucleoprotein core into the cytoplasm.

The relative molecular independence of the life cycle of VV, in comparison to other OVs such as the adenovirus genre makes it more resistant to alterations in host cell biology (18, 19). Uniquely, infectious vaccinia virions are pre-packed with virally encoded proteins; notably a virus-specific ribonucleic acid (RNA) polymerase accompanied by enzymes responsible for further mRNA processing and various early transcription factors (9). Viral transcription can therefore commence almost

immediately after cellular entry, within the cytoplasm. The minimal reliance on host cellular proteins for replication makes it difficult for the host cell to effect defensive manoeuvres based on alteration of its gene transcription profile. VVs may be genetically safer compared with other virus families, because their life cycle is entirely cytoplasmic, with little possibility of host chromosomal integration.

VVs have the potential to be efficacious following systemic administration, a feature that would enable targeting of metastatic disease (20). VVs have acquired various mechanisms to evade host defences (discussed later) and their different morphological forms are antigenically distinct. Following infection, the relatively stable IMVs form the majority of virion particles in a host. They are brick shaped and measure 300 × 200 × 120 nm. IMVs may be released only upon cell lysis. Upon release via cellular burst, abundant immunogenic viral proteins on their single lipoprotein envelope rapidly stimulate both innate and adaptive host defence mechanisms. A cell-associated virion (CEV) (figure 1.1) resembles a particle just about to bud off from the host cell and affords a means of direct cell-to-cell dissemination. If it does bud off into the systemic circulation, in contrast to IMVs, it maintains the additional host cell lipoprotein bilayer, which enables the resulting particle (EEV) to be (relatively) antigenically quiet (16). This, coupled with viral transmembrane proteins that antagonize components of innate (complement) and adaptive (neutralizing antibodies) systemic host defence, permits widespread dissemination of EEVs (21-26). Current mass viral production techniques, which depend on co-culture in a standard cell line, produce mainly IMVs. Strategies to induce the intra-host production of proportionately more EEV forms of VV are an active area of research (27).

Advanced solid tumours often harbour areas of hypoxia secondary to outgrowth from and/or destruction of local vasculature. This contributes to the aggressive, treatment-resistant phenotype of several cancers (28, 29). Hypoxia is detrimental to the efficacy of other types of OVs (30-32). In contrast, our group has demonstrated that hypoxia does not impair the replication or oncolysis mediated by VVL; its oncolytic potency against some tumour cells may even be enhanced in such an environment (33).

As described for other OVs VVL appears not to discriminate between “normal” cancer cells and cancer “stem like” cells (CSCs) (34, 35). In one study, a VVL recombinant demonstrated enhanced infectivity and replication in human breast CSCs compared to their non-stem like counterparts (34). There is accumulating evidence that at least some human solid tumours are initiated and driven by CSCs. CSCs are thought to be chemotherapeutic and radiation resistant and have been causally linked to failure of these modalities to prevent recurrence (36-38).

Finally, a wealth of historic clinical data, accrued mainly from its use as a vaccine, confirms the excellent safety profile of VV. Nevertheless, in the extremely unlikely event of unchecked viral replication, effective antiviral treatment options are currently available (39, 40).

1.2 Vaccinia virus cancer selectivity

1.2.1 Inherent tumour selectivity

Several VV strains have demonstrated tumour specificity and antitumour efficacy in preclinical models of malignancy (6, 20, 41, 42). Molecular drivers of oncogenesis are often conducive to viral replication. Indeed the hallmarks of cancer could almost be renamed as those that enable successful viral infection (43, 44). For example many tumour cells contain mutations that inactivate common cellular defence mechanisms that in normal cells act to counter both invading pathogens and tumourigenesis. These include defects in interferon (IFN) and apoptotic pathways (20, 45, 46). Tysome et al. (19) compared the replication of a VVL recombinant in cultured normal human keratinocytes with that in its malignant counterpart (SCC25). There was minimal viral replication in the former, even when infected with five times the dose of virus used to infect the SCC25 cells.

Oncogenic mutations that result in excess stimulation of the cell cycle may promote viral replication, mainly due to the provision of a large nucleotide pool. For example,

the epidermal growth factor receptor (EGFR) pathway is overactive in many, if not all, solid malignancies (47). Interestingly, VV may actively drive this pathway as part of its infectious cycle: VV DNA encodes a secreted epidermal growth factor (EGF) homologue, vaccinia growth factor (VGF), which binds to EGFRs on neighbouring cells, stimulating their replication; effectively priming them for imminent virus invasion (48, 49).

Tumours usually harbour very rich but disorganized and "leaky" blood supplies (50). Large gaps between endothelial cells readily allow the large VV particles to leave the circulation at these junctures (42). Vascular permeability may be increased by elevations in temperature. Chang et al. demonstrated a 100-fold increase in uptake of systemically delivered VV by tumour following localized heat treatment (51). Some VV strains have tropism for ovaries (49), which has been at least partially attributed to their relatively permeable blood supply.

Another potential mechanism for the inherent tumour selectivity of VV may relate to the overexpression of vascular endothelial growth factor (VEGF) within tumour micro environment(TME)s. VEGF is a major effector of angioneogenesis (50). Our group has recently demonstrated enhanced VVL uptake by various solid tumour cell models in the presence of VEFG. This appears to be effected by stimulation of the AKT signalling pathway, that ultimately leads to enhanced viral endocytosis (52).

1.2.2 Engineered selectivity

In general however, viral tumour selectivity is the exception rather than the rule. Viral infection of and replication in normal cells is enhanced by their phylogenetic acquisition of host genes that stimulate cell division, inactivate growth suppression or apoptosis and facilitate the high-jacking of cellular energetics in normal cells.

Investigators have attempted to enhance tumour selectivity and thus safety of VV by genetic manipulation. Traditionally, strategies have relied on disrupting viral genes that are essential for replication in normal cells but not required for replication in cancer cells. The most popular of these in VV, has been disruption of the gene encoding the

vaccinia thymidine kinase (VTK) enzyme. VTK is essential for the synthesis of deoxyribonucleotides particularly in cells with low nucleotide pools, as is the case in most normal, well-differentiated mammalian cells. Tumour cells, however, usually have an abundance of nucleotides. VTK gene-deleted recombinant VVs have demonstrated enhanced tumour selectivity in a number of *in vivo* tumour models (6). For example, disruption of the VTK gene in the neurovirulent laboratory-derived Western Reserve (WR) VV strain reduced viral colonization and replication in the mouse central nervous system following intravenous (IV) administration, without affecting tumour tropism (20, 49).

The VVL derivative from Moscow (LIVP) used by our group and others (53, 54) has a premature stop codon in the locus that encodes VTK (the J2R gene) (55). Interestingly, near complete deletion of the J2R locus, in our case by replacing a significant section of the coding sequence with marker transgenes encoding luciferase and lacZ enzymes (forming the VVL recombinant, VVL15), further enhanced the tumour selectivity of LIVP (Hughes et al., in press, Gene Therapy).

Other candidate genes that could be disrupted include those involved in combatting host cell defence mechanisms. Numerous tumour types have defective apoptotic pathways and could thereby facilitate the selective replication of viruses harbouring mutations in anti-apoptotic genes. Specific candidates include the anti-apoptotic serpin proteins SP1 and SP2 (56); F1L, which inhibits the release of cytochrome c; and N1L, a structural B cell lymphoma(Bcl)-2 homologue with additional functions (57) (discussed later). Although deliberate disruption of these and other genes should theoretically enhance tumour selectivity, viral replication and oncolytic potency often deteriorate in proportion to the extent of genetic manipulation (58). Thus, a VV in which both SP1 and SP2 coding sequences were disrupted was severely attenuated compared to viruses harbouring deletions in either sequence alone (55, 59). In our experience, a disruption in the J2R locus of LIVP is all that is required to strike a good balance between tumour selectivity and antitumour efficacy. For other strains however, particularly the more virulent ones such as WR, additional genetic disruption may be required prior to potential clinical use. Indeed the WR strain of VV required deletions of both VTK and VGF genes (49) (WR double deleted mutant (WRDD)) to obtain a tumour specific

variant that was significantly less virulent than either single deleted or wild-type viral counterparts.

Finally, other innovative strategies have been utilised more recently to enhance tumour specificity. One such includes the genomic incorporation of tissue or hypoxia specific promoters, to conditionally drive key viral gene products upon infection of target tissue (60) or hypoxic environments (61, 62) respectively. Along similar principles, tissue specific post translational targeting strategies have also been recently used. Hikichi et al. (63) illustrated this with an attenuated VVL virus in which the B5R gene (essential for intracellular viral trafficking) was reconstituted with an additional 3' sequence complementary to the microRNA, Let-7a. Let-7a is commonly down-regulated in tumour cells, whereas normal cells contain it in abundance. Translation of the recombinant B5R mRNA (and consequent virus production) could therefore only take place in tumour cells.

1.3 Unique characteristics of the Lister strain of VV

Different strains of VV were used in different areas of the world in mass vaccination campaigns in the 1900s. The New York City Board of Health (NYCBOH) strain and its derivative, Wyeth, were popular in the United States, whereas Copenhagen (CPN) and Lister found prominence in Europe. Historical records trace the origin of the Lister strain to Elstree, UK (1961), where the original master stock was prepared from calf lymph and distributed to centers in France, Moscow, Tokyo, and Atlanta. Early animal studies with VVL suggested a superior safety profile, particularly with regard to neurological sequelae (64-66). During the 1970s, in Japan, an attenuated Lister strain mutant, LC16m8, selected for its extremely low neurovirulence, was used to safely vaccinate more than 50,000 infants against smallpox (67).

In the past decade, the WR strain of VV, a virulent laboratory-derived NYCBOH derivative with potent tumour lytic ability, has been the most extensively studied and genetically manipulated oncolytic VV. It is currently thought to be the most superior oncolytic strain, although this assumption was made on the basis of its replication and

oncolysis in only two human cancer cell lines in an early comparative study (20). In that study, the WR strain was selected to be rationally engineered to be more tumour selective with preservation of its oncolytic potency (WRDD) by deletion of the TK and VGF genes. Despite these alterations concerns remain regarding its safety and it obviously lacks the advantage of previous clinical usage. Furthermore, we recently discovered that VVL15 (table 1.1) actually replicated in and lysed tumour cells significantly better than WRDD in 11 of the 14 tested human cancer lines, although WRDD did perform better in similar *in vitro* analyses using murine cancer cell lines (Hughes et al., in press, Gene Therapy). Despite the latter, VVL15 demonstrated significantly better antitumour potency (compared to WRDD) in several immune-competent murine cancer models (Hughes et al., unpublished data). Given the potency of WRDD against murine cancer lines *in vitro*, the improved effect of VVL15 against *in vivo* tumours must have been mediated by indirect mechanisms; for example, through modulation of host immunity or vascular compromise. The investigation of possible underlying mechanisms responsible for this effect is an ongoing focus of our group.

Many of the open reading frames (ORFs) in VV are involved in viral genome transcription, replication, structure, and assembly. These are located centrally in the viral genome and are highly conserved among all Orthopoxviruses. Peripherally located genes are responsible for modulation of host antiviral defence and are strain specific. The function and indeed expression status of many of these have yet to be delineated, but genes encoding proteins that interfere with IFN pathways seem to be over represented, indicating their significance in host defence. Although there is only an 8% difference between the genomes of Lister and other strains (68), phenotypic and functional differences between strains must be a consequence of these differences.

1.3.1 Genetic differences between Lister and other strains of VV

Garcel et al. (68) sequenced a clonal isolate of a VVL substrain. The vast majority of the 201 possible VVL ORFs (192) had more than 98% sequence homology to those previously identified in other strains, including CPN and WR strains. L172 (A53R) encodes a tumour necrosis factor (TNF) receptor homologue found in VVL but is absent

in WR. An extra interleukin (IL)-18 binding protein gene (L013) is again present in VVL but missing in the WR strain.

Genomic comparison between Lister, CPN, and WR strains conspicuously revealed a short sequence that encodes completely different proteins in the Lister genome (68). Part of this sequence (L196) bears resemblance to that encoding a transmembrane Bax (a cellular pro-apoptotic protein) inhibitor motif, found in various mammalian species and may therefore have been acquired by a historic recombination event with mammalian DNA. L196 therefore unsurprisingly encodes an apoptosis inhibitor (69). Another unique gene in this region, which is not present in CPN and WR strains encodes a TNF binding protein (L195) (70). In contrast its neighbouring gene, L194 encodes a truncated version of a type-1 IFN binding protein that appears intact in the WR strain.

Alternative sequences in the corresponding section of CPN and WR genomes include a gene encoding an IFNα/β binding protein (B19R/WR200) and a different anti-apoptotic gene, WR195 that encodes the serpin protein SPI-2 (an IL-1β converting enzyme inhibitor that ultimately inhibits Fas-mediated apoptosis).

Finally, the gene encoding a semaphorin-like protein, L156 (A39R) (which stimulates monocytes and enhances production of proinflammatory cytokines (55)) is frame-shift mutated in the WR strain. That this plays a role in the immunogenicity of VV is dramatically demonstrated by the induction of systemic inflammation and pulmonary oedema in mice administered a WR recombinant expressing this transgene.

To summarise, VVL therefore codes for at least two extra TNF binding proteins (L172 and L195) in comparison to WR and CPN strains and could thus be better armed against the host TNF response. On the other hand, it lacks at least one IFN binding protein gene (WR200). There are also qualitative differences in genes encoding anti-apoptotic proteins. How these features relate to differences between the strains of VV with regards: the generation of antiviral or antitumour immunity, host toxicity and antitumour efficacy, remains to be elucidated.

1.3.2 Differences in virulence between Lister and other VV strains

The most commonly reconstructed Lister strain variant for the purposes of antitumour therapy has been the Moscow derivative, LIVP. The WR VV is particularly neurovirulent, reflecting its origin from multiple passages through the murine brain (71). Although systemic inoculation with a VTK gene-deleted WR virus reduced viral recovery from off-target organs, titres in these organs were still significantly higher in comparison to that with LIVP (54). In one study, there was no viral recovery from the brain or ovaries of nude mice following an IV dose of 1×10^7 plaque-forming units (PFU) of VVL (54). Other organs also had a higher affinity for WR VV compared to VVL. Pulmonary titres were consistently higher at any given time-point following intranasal inoculation of similar doses of viruses (72). Indeed, as little as 5×10^5 PFU of intranasally inoculated WR caused severe signs of toxicity (including significant weight loss) and 50% death in immune-competent BALB/c mice (73). Similar toxicity was only observed with VVL if administered in doses 100-fold higher (74).

Further characterization of the expression and functional aspects of individual VV genes will enable the rational engineering of more selective, safer, and potentially more effective recombinants. Table 1.1 outlines the range of VVL constructs that we and other groups have used as potential anticancer therapeutics.

1.4 Tumour targeted Lister strain derivatives that have demonstrated antitumour efficacy

In order to enhance VVL as an anticancer therapeutic, it is necessary to review its previous successes and shortcomings.

VV, like other OVs mediates antitumour efficacy via both direct and indirect mechanisms. These include (a) direct viral oncolysis, (b) local vascular destruction, and/or (c) focusing of the effector host immune defence (both innate and adaptive) into the TME. All of these mechanisms may be augmented by incorporation of relevant therapeutic transgenes into the viral backbone.

As with other strains, VVL derivatives have demonstrated tropism for a variety of different tumour types both in cell culture and in animal models. Ascierto et al. (75) investigated whether molecular signatures within a particular tumour cell could predict permissivity of infection by the Lister strain recombinant GLV-1h68 (table 1.1). They screened the NCI 60 panel of human cancer cell lines (76), which covers a broad spectrum of human malignant cancers. Three genes were found to be consistently up-regulated in permissive versus non-permissive lines: GDF15, a member of the transforming growth factor (TGF) superfamily that regulates inflammatory and apoptotic pathways; cluster of differentiation (CD)9, a transmembrane protein that promotes cell growth, activation, and mobility; and integrin β5, which plays a role in cell movement and adhesion. In contrast, far more genes were conspicuously down-regulated. In general they included genes involved in stimulating nuclear factor (NF)-κB or IFNα/β signalling and/or the activation of the RNA polymerase complex. In other words, the most permissive cell lines to GLV-1h68 had favourably pre-dampened host cell antiviral defence and gene transcription.

Chen et al. (58) demonstrated a positive correlation between the replication efficiency of VVL derivatives in tumour cell culture and antitumour efficacy in the corresponding xenograft model. Although the latter largely reflected higher titres of replicating virus and thus oncolysis, they also postulated a significant bystander contribution from the innate immune system which should have been preserved in these animal models. Expression profile analysis post infection revealed up-regulation of characteristic "innate" cytokines, chemokines, and growth factors in tumour tissue, associated with a cellular infiltrate consisting of dendritic cells, NK cells, monocytes, and neutrophils (54, 77-79). Thus even in animal models deficient in components of adaptive immunity, mechanisms additional to viral oncolysis contribute to antitumour efficacy. It is these mechanisms that will require optimisation as viral oncolysis is likely to be rapidly curtailed in immune competent models and human patients.

Table 1.1 A list of tumour targeted oncolytic vaccinia viruses derived from the Lister Strain

Virus name	Disrupted genes	Transgene expression	References
GLV-1h68	J2R (VTK), F14.5L, A56R (haemagglutinin)	Renilla luciferase-GFP fusion protein (RLUC-GFP), β-galactosidase, β-glucoronidase	(54)
GLV-1h99	J2R (VTK), F14.5L, A56R (haemagglutinin)	Human norepinephrine transporter (into F14.5 instead of RLUC-GFP), β-galactosidase, β-glucoronidase	(80)
GLV-1h153	J2R (VTK), F14.5L, A56R (haemagglutinin)	Human sodium iodide transporter (into A56R instead of β-glucoronidase)	(81, 82)
GLV-1h107, 1h108, 1h109	J2R (VTK), F14.5L, A56R (haemagglutinin)	VEGF single-chain antibody (GLAF-1) under different promotors, RLUC-GFP fusion protein	(83)
VVL-15	J2R (VTK)	Luciferase, E. coli lacZ	(84)
VV-TK-P53	J2R (VTK)	P53, E. coli lacZ	(84)
VVhEA	F14.5L	Fused human endostatin and angiostatin	(19)
VVlacZ	F14.5L	E. coli lacZ	(19)
VVRG	F14.5L	RLUC-GFP	(85)
VV-2-12	J2R (VTK), N region	mIL-2, mIL-12, E. coli lac Z, luciferase	(53)
VV-mIL12	J2R (VTK)	mIL-12, E. coli lacZ	(53)
VV-mIL2	J2R (VTK)	mIL-2, E. coli lacZ	(53)

1.4.1 VVL as an anti-cancer gene therapeutic platform

The unique properties of VV outlined previously make it particularly appealing for use as an anticancer gene therapeutic vector. In the context of cancer, the term gene therapy has traditionally referred to the replacement of or curtailment of dysfunctional tumour suppressor or promoting genes. The tumour protein(TP)53 tumour suppressor gene is commonly mutated in solid tumours and has therefore been targeted for replacement (86). Other transgenes that have been similarly used include pro apoptotic genes including death receptors/ ligands (e.g. Fas/Fas-Ligand(L)) (86) or those coding for products (e.g. short hairpin RNAs) that disrupt overexpressed growth-factors (87).

Traditionally, replication-impaired viruses have been utilised as the delivery vehicle amid concerns of potential toxicity. A VVL recombinant in which a TP53 transgene replaced the VTK gene locus was rendered replication inactive by mild psoralen and UV treatment. It successfully infected tumour cells in culture and induced cell death mediated by apoptosis in cell lines with dysfunctional TP53 (88). However *in vivo*, it was only effective following the *ex vivo* infection of tumour cells prior to their subcutaneous (SC) implantation, a situation which has little translational validity. Its replication-competent counterpart however, demonstrated superior tumour growth inhibition compared to the control virus in a pre-established xenograft model; an affect that was further enhanced by combination treatment with radiotherapy (89). Similarly, in a syngeneic orthotopic model of bladder cancer, instillation of the same replication-competent VVL-TP53 virus decreased tumour incidence and improved survival compared to the control virus (90).

Second generation oncolytic VVs that are replication-competent are currently being investigated as oncolytic biological agents capable of delivering transgenes. However, even with a potently replicating virus such as VV, several barriers within the TME may prevent spread to and transduction of all tumour cells, which in themselves will be genetically heterogeneous (91). The latter in particular means that restoring the function of a single gene is unlikely to succeed in curbing tumour growth.

1.4.2 Combination with cytotoxic agents to enhance antitumour efficacy of VVL

A population of tumour cells is genetically heterogeneous and will often harbour cells resistant to a single treatment modality. Although VV as an antitumour therapeutic operates through multiple mechanisms (92, 93), it is unlikely that every single tumour cell will be infected and lysed. Combination with other cytotoxic modalities may be more efficacious.

For example, cisplatin and gemcitabine are commonly used for the treatment of advanced pancreatic cancer. Cisplatin binds to and cross-links double-stranded DNA. Gemcitabine is a nucleoside analogue that terminates DNA strand extension and thus replication. Both work by ultimately triggering apoptosis. These have been used in a

pancreatic xenograft model in conjunction with GLV-1h68 (94). Both demonstrated synergistic antitumour efficacy, although in the gemcitabine combination study, the final tumour size in the "virus only" group eventually caught up with that of the combination group. Possible mechanisms for this synergy include alterations in nucleotide pools, DNA repair pathways, and apoptosis. Additionally, changes in the local tumour vasculature associated with viral infection may have improved delivery of drug into the TME. Although synergism was demonstrated in this particular study, chemotherapeutics that target nucleotide production and DNA replication could adversely affect the viral life cycle (95).

Tumour targeted OVs armed with transgenes may be used to locally deliver high concentrations of the translated product into the TME. For example, they have been used to deliver enzymes that mediate the conversion of a relatively safe prodrug into a highly potent cytotoxic one (96). One advantage of doing this is that not all cells need to be infected, because the active toxic drug may spill over onto neighbouring uninfected tumour cells to cause a bystander effect. A replication-competent VV armed with the transgene for the cytosine deaminase (CTD) enzyme, which converts 5-fluorocytosine (5-FC) into the active metabolite 5-fluorouracil (5-FU), demonstrated efficacy in animal models (95). Seubert et al.(97) employed a different prodrug/enzyme system in conjunction with the GLV-1h68 recombinant. GLV-1h68 contains a lacZ transgene that encodes β-galactosidase. The prodrug in this case was derived from a seco-analogue of the highly cytotoxic natural antibiotic duocarmycin (98) which is activatable by β-galactosidase. Systemic addition of prodrug enhanced the antitumour effect of GLV-1h68 in a xenograft model of human breast cancer. Viral replication in this study was not affected by the presence of either inactive or active metabolite, in contrast to a study in which a VV CTD/5-FC system was used (95).

Similar to combination with chemotherapeutics, several preclinical studies have demonstrated mutual antitumour synergy afforded by combination of OVT with radiation (99). Most such studies, however, were conducted with adeno and herpes viruses. Timiryasova et al. (89) demonstrated that a TP53-ve glioma xenograft was more sensitive to a replication-competent VVL armed with a TP53 transgene in conjunction with radiotherapy compared to either treatment alone. As predicted, this effect was mediated by a superior level of apoptosis (89, 100).

Finally, VVL has also been armed with transgenes coding for receptors or transporters for radionuclides, to ensure their localization into tumour (101). Indeed, such a strategy could even render traditionally radio-resistant tumours more responsive. Gholami et al. (81) used a GLV-1h68 VVL backbone armed with the human sodium iodide symporter to effect uptake of radio-iodide tracer and exacerbate cell death in human anaplastic thyroid cancer cells *in vitro*. These cells are usually radio-resistant due to lack of the sodium iodide symporter on their cell membranes. The tracer concentrated in tumours in a xenograft model, although efficacy was not studied this particular experiment (102).

A further discussion of OVT in combination with chemotherapeutic agents will be continued in the discussion chapter, in the context of synergistically enhancing antitumour immunogenicity (section 4.2.1).

1.4.3 Enhancing VVL-mediated compromise of the local tumour vasculature

Tumour angiogenesis is one of the hallmarks of malignancy (47). All cells must be within 200 μm of a blood vessel (the limit of diffusion of oxygen) for survival. Solid tumours therefore need to be highly vascularized, and this is generally mediated by an imbalance between tumour-produced endogenous pro and anti-angiogenic factors (103). Soluble growth factors such as VEGF and fibroblast growth factor (FGF)β are key molecules in this regard and are overexpressed by many tumour cells. However, the resulting neovasculature within a tumour is often poorly organized, with patchy areas of collapse and leakiness. This leakiness may contribute to the tumour selectivity of the relatively large vaccinia virions. Furthermore, VV may directly interfere with the local tumour vasculature. Kirn et al. (104) demonstrated that a WR recombinant infected and destroyed tumour-associated vascular endothelial cells. Our group has also witnessed this phenomenon with a VTK gene-deleted VVL derivative (VVL15). In addition, as previously mentioned, the infectivity of VVL15 for tumour cells appeared to be enhanced by the presence of VEGF (52).

Tysome et al. (19) demonstrated that LIVP armed with a gene encoding a fusion protein comprising two potent endogenous angiogenesis inhibitors, endostatin and angiostatin (VVhEA), selectively inhibited tumour angiogenesis in a xenograft pancreatic cancer

model. This was associated with enhanced antitumour regression and animal survival, an affect that was reproduced in a similar model of head and neck cancer (105). Similarly, Frentzen et al. (83) created a recombinant Lister strain virus based on the GLV-1h68 platform in which a single-chain antibody against both human and murine VEGF (GLAF-1) replaced the VTK gene locus (GLV-1h108). This also demonstrated enhanced antitumour efficacy in xenograft models of human lung and prostate cancer; again, efficacy was associated with a significant reduction in microvessel density. Interestingly, in this study, the backbone virus GLV-1h68, when combined with the licensed monoclonal anti-VEGF-A inhibitor Avastin, demonstrated a regression pattern similar to treatment with GLV-1h108 alone. Stabilization of the haphazard tumour vasculature by independent angiogenesis inhibition may aid oncolytic viral delivery. In some circumstances, VV may in turn be mutually beneficial to drug delivery by decompressing and "normalizing" pre-existing intratumoural vessels (106, 107).

1.5 Oncolytic viruses and immunotherapy

Traditionally tumourigenesis was perceived as being consequent to the accumulation of a number of genetic misendeavours confined to the level of the cell. Clearly this was an oversimplification, with multiple mechanisms, including defects in regulatory systems external to the cell now known to be important. A relatively new addition to the "Hallmarks" of cancer is evasion of host immunity, acknowledging the significant role that immune surveillance plays in curtailing cancer ontogeny (43, 108).

Throughout the life of an organism, the host immune system is thought to play an intimate surveillance mechanism seeking out and destroying genetically and thus antigenically deviant cells (109, 110). In most cases this should result in successful and clinically covert "elimination" of such cells. However, if the tumour is not particularly immunogenic or indeed the host lacks the capacity to mount a strong immune response, a stalemate "equilibrium" state occurs with little or no tumour progression; a situation often associated with markers of chronic inflammation. Eventually host immunity may be overwhelmed or completely bypassed leading to tumour "escape" with escalation of growth and dissemination. This phase is characterized by a TME containing

immunosuppressive cells and cytokines and supported by a relatively impenetrable structural framework (111).

Although the latter picture implies a bleak outlook, the host immune system may retain the capacity to reject an "escaped" tumour. Thus reports of spontaneous cures have dotted the cancer literature and tumour infiltrating cells of both innate (e.g. NK) and adaptive (e.g. lymphocytes) immunological origin are positive prognosticators of survival (112).

1.5.1 Why host immunity is often incapable of eradicating an advanced tumour

In 1989, Janeway proposed that for the productive activation, processing and presentation of antigenic peptides, resting antigen presenting cells (APCs) require concurrent and independent binding of infectious non-self pathogen associated molecular patterns (PAMPs) to their cognate cellular pattern recognition receptors (PRRs) (113, 114). PAMPs include nucleic acid intermediates (e.g. viral DNA, dsRNA, defective viral genomes (115)) or non-self protein derivatives (including glyco and lipo-proteins that are often membrane associated (116, 117). These are recognised by a wide range of PRRs expressed in APCs and other cells and include toll-like (TLR), retinoic acid inducible gene-1 (RIG 1) like, and nucleotide oligomerisation domain (NOD) like receptors (118, 119).

Later, Matzinger modified Janeway's theory and introduced the "danger hypothesis" which proclaimed that the prime role of the immune system is to respond to cellular and tissue distress and not necessarily to non-self per. se. APCs could be stimulated by endogenously generated "danger" signals in whose presence even tolerance to self-antigens may be reversed (120). Endogenous danger signals from damaged cells may signal through PRRs in the absence of pathogen particles (121). Damage associated molecular patterns (DAMPs) include deranged host DNA or RNA, metabolic intermediates like uric acid (122), stress related proteins like high-mobility group protein B1 (HMGB1) (123, 124) and heat shock proteins (HSPs). Therefore, in the context of virotherapy, both self and pathogen (viral) related "danger" signals ultimately up-regulate genes coding for molecules that promote antigen presentation as well as

inflammatory mediators, that are designed to eliminate the offending pathogen or damaged cells (125).

Both these theories agree on the importance of favourable APC activation to initiate an immune response and both might predict the relative inadequacy of the immune system to reject an untreated tumour. According to Janeway's model (with the exception of pathogen induced tumours) there are no foreign PAMPs, whereas stably growing tumours were thought not to provide the requisite threshold of "danger signals" according to Matzinger's hypothesis. Chronic inflammation, a feature of many TMEs (126) is however associated with perpetual tissue destruction and should theoretically provide a continuous supply of "danger signals". Matzinger's hypothesis will therefore need to incorporate the notion that individual DAMPs may differ in their potency to activate APCs and/ or that immune priming may only occur if DAMP mediated APC activation can overcome regulatory forces within the TME (see later).

An obvious problem that host immunity is faced with is that tumour associated antigens (TAAs) are essentially peptides derived from variants of normal host proteins. There are of course exceptions and these include antigens associated with tumours causally linked to an infectious agent (e.g. human papilloma virus associated cervical cancer), those that are normally expressed in an immunologically privileged site such as in germ cells, or antigens that were only transiently expressed during embryogenesis (127). Furthermore, theoretically central thymic selection should have eliminated high affinity self-reacting T cell receptor (TCR) containing clones, whereas the few weakly self-reacting T cell clones that have escaped into the periphery should be curtailed from expansion by peripheral tolerance mechanisms.

There are a number of well characterized immune evasion strategies that a tumour may employ both at the level of the cell and externally. Tumour cells often down-regulate components of antigen-presenting pathways i.e. the molecular events leading to the presentation of peptide on the class I major histocompatibility complex (MHC) (128-130). In addition many tumour cells resist external cell killing strategies for example by impairing perforin or Fas binding (130). Some tumour cells secrete the stress induced ligands, MHC class I-related chains A or B (MIC A/B) whose prolonged secretion may down-regulate activating receptors on NK (NKG2D) and Cytotoxic T cells (131).

Furthermore, should a tumour antigen specific TCR bind to its cognate peptide-MHC on the tumour cell, some tumours also express inhibitory ligands (e.g. programmed death-ligand(PD-L)1) whose concurrent binding to inactivating receptors on T cells may compel them to anergise or apoptose (132).

Tumour cells may secrete non-specific immunosuppressive soluble mediators that directly inhibit cytotoxic T cells (129). These include prostaglandin E2, histamine, hydrogen peroxide and adenosine (133). Inhibitory cytokines and chemokines such as TGFβ (134) and IL10 (135) may also be expressed by many tumour cells. These directly or indirectly inhibit APCs and cytotoxic T cells; promote the development of an unfavourable T helper(Th)-2 skew in the ensuing effector immune response and play a role in the recruitment, maintenance and activation of modulatory cells. The latter include myeloid derived suppressor cells (MDSCs), T regulatory cells (T-regs), and tumour associated macrophages (TAMs) (111). These in turn may promote tumour growth through secreted growth factors and positively amplify the immunosuppressive TME (136). TMEs may also be characterised by the presence of immature APCs lacking co-stimulatory signals. Antigen presentation by these cells have been demonstrated to anergise *de novo* T cells but perhaps more importantly to induce the conversion of *infiltrating* T helper cells into regulatory ones (137).

1.5.2 Shortcomings of traditional cancer immunotherapeutic strategies

Although it is possible to vaccinate against pathogens causally linked to tumours, cancer immunotherapy, with a few notable exceptions has not yet made a successful transition into the clinic (138).

Just as with vaccination against infectious diseases, cancer immunotherapy may be classified into passive or active. The former includes administration of preformed effector molecules such as cytokines and antibodies against TAAs, but it also encompasses adoptive immune cell therapy (i.e. autologous NK and T cells that are manipulated and expanded *ex vivo* and reintroduced into the patient).

In general, such “passive” therapies are designed to act directly on the tumour cell. This means that unless they encounter every single cancer cell, complete tumour eradication can only occur through bystander killing mechanisms, a situation that is unlikely to be achieved with mono therapy. With the possible exception of adoptive T cell therapy (139), long term memory and thus tumour surveillance is not a feature of passive immunotherapy (110).

On the other hand “active” immunotherapy (often used synonymously with the term, tumour vaccination) refers to therapeutic (treating existing tumour) and prophylactic (preventing future tumours) strategies to boost host immunity to eradicate residual disease and generate tumour specific memory. Single or multiple TAAs, xenoantigens (homologous antigens derived from another species) and whole tumour cell lysates have been used in this regard. They have been delivered alone, along with various adjuvants; encoded as DNA or RNA on different vectors or delivered in autologous APCs (110).

Both modalities have suffered from being targeted to a single or relatively few tumour specific epitopes (the exception being whole cell lysates). Even within a single patient, the tumour cell population can be extremely heterogeneous with the inevitability of tumour escape if such narrowly focused therapy is used. Of course multiple tumour epitopes may be exposed following targeted tumour cell destruction, but the surrounding immunosuppressive TME, coupled with the relative paucity of co-stimulatory danger signals may hinder their ability to prime a response.

For these reasons, research has recently focused on combining existing immunotherapies with non-targeted agents designed to counter some of the aforementioned hurdles. For example, co administration of cytokines (Th-1 associated) or antibody mediated eradication of T-reg and other suppressive cells (132). Likewise, at the effector end of the immune response, the survival of those effector T cells that have been successfully stimulated can also be prolonged. Ipilimumab has proved relatively effective in malignant melanoma trials using this approach. Ipilimumab is an antibody against the CTLA4 receptor on activated T cells and prevents CTLA4 mediated T cell inactivation (140).

Systemically administered non-specific immunomodulators such as IL12 or IFNγ showed initial promise as anti-tumour immunotherapeutic agents, however, their efficacy was limited by the induction of host tolerance (141), as well as dose limiting toxicity (142).

Finally, perhaps the biggest hindrance to success in previous trials of cancer immunotherapy were the patients themselves. As with all novel treatment modalities, enrolled patients have carried advanced stage solid tumours that have likely been further selected by failed traditional treatment modalities. Additionally, patients at this stage were likely to be globally immunosuppressed, either by progression of their disease or due to therapy. Therefore, to have any chance of success, immunotherapeutics should ideally be implemented at relatively earlier stages in the disease process.

1.5.3 Hurdles for immunotherapy with OVT

Based on their potency to infect and lyse tumour cells, the developmental focus with earlier generations of replication selective OVs was to enhance their *in vivo* tumour selectivity (35). A number of recombinant platforms for this purpose were developed, culminating in the first government approved OV, H101/Oncorine (Shanghai Sunway Biotech, China), for use as adjuvant therapy in head and neck cancer (143-145). This was an attenuated adenovirus in which the E1B55K gene (encoding an anti-apoptotic protein) had been deleted and was demonstrated to be tumour selective and safe; however to date, there has been no published data demonstrating long term survival benefit.

Much preclinical and clinical data confirmed that regardless of the route of administration, OVs often infect cancers incompletely (146), a fact that would preclude the success of a therapeutic that solely relied on its ability to infect and lyse every single tumour cell. Despite being injected directly into the heart of an immunosuppressive TME (as with IT administration) an immune competent host generally retains the capacity to mount a strong antiviral immune response. Antigen presenting cells take up viral particles in the context of strong co-stimulation through PRRs. These mobilise to

local lymphoid tissue whence they are in a position to prime Th1 and 2 cells which direct the generation of effector antiviral cytotoxic T lymphocytes (CTLs) and antibodies respectively. Innate cellular (NK cells, monocytes and neutrophils) and humoral (complement) effectors are also mobilised and activated by virally infected cells or viral particles (147-149). These features are likely to lead to the relatively rapid clearance of virus.

Furthermore, cancer patients may have pre-existing immunity to many of the commonly used oncolytic viral platforms including VV. Newly generated or pre-existing antiviral immunity may be expected to preclude multiple dosing and thus efficacy, if indeed antitumour efficacy was based solely on viral oncolysis. On the other hand, it is theoretically possible that pre-existing antiviral immunity could actually aid tumour clearance. Infected tumour cells could stimulate the rapid expansion, mobilization, and infiltration of virus-specific memory CD8+ T cells into the TME to inadvertently supplement viral oncolysis. Hu et al. (150) demonstrated that IT injection of adeno or vaccinia virus in hosts pre-immunized against these, led to enhanced tumour shrinkage and greater infiltration of lymphocytes into the tumour, compared to naïve tumour bearing hosts. Our group has also observed a similar phenomenon when VVL15 was administered into a syngeneic CT26 (murine colorectal cancer) model (Chard et al. unpublished data). Unfortunately, such bystander tumour cell destruction is generally not enough to eradicate tumour, especially when aiming to treat widespread metastases that often elude systemically delivered viral infection (151). Certainly in the case of H101, clinical efficacy was partially impeded by a host antiviral response that eradicated virus at a faster rate than viral oncolysis (143, 152).

The developmental focus in OVT subsequently shifted to establishing methods of minimising the induction of antiviral immunity. Concurrent administration of global leucocyte depletors such as high dose cyclophosphamide or more focused depletion of antiviral cellular effectors e.g. clodronate liposome mediated depletion of macrophages were demonstrated to enhance tumour viral load, that in some models were paralleled by efficacy (151, 153).

However, notwithstanding the risk of fulminant viral dissemination when immunosuppressing an already immunocompromised host, other barriers within the TME exist that are likely to limit widespread permeation within the tumour. These include multiple layers of connective tissue and extracellular matrix (69-70), high intra-tumour interstitial pressure (71), poorly organized vasculature and non-cancer stromal cells that may not be permissive to viral infection (91, 111). Large tumours will also contain areas of overt necrosis or calcification (154) with patchy areas of low pH and hypoxia. These are generally not conducive to OV infection, although as previously mentioned, VVL appears to be able to replicate in hypoxic conditions (33).

Whilst, the concurrent IT administration of enzymes that degrade matrix (e.g. collagenases, matrix metalloproteinases) or antifibrinolytics or indeed arming larger OVs with transgenes encoding such enzymes (155) could aid the breakdown of components of this framework (156), the likelihood is that despite our best efforts, attempts at infecting and directly lysing every single tumour cell are likely to be futile.

Nevertheless, efficacy with OVs has been demonstrated in numerous syngeneic primary and disseminated models of tumour when intralesional virion particles were few or even absent (157). Furthermore, we and others have consistently noted the absence of tumour regrowth upon re-challenge with the same syngeneic tumour cells following successful OV mediated tumour eradication (158). That this effect was often abrogated by depletion of certain lymphocyte subsets, pointed strongly to a prominent immune effector role.

Rather than being problematic, we would therefore argue that it is the very ability of VV and other OVs to elicit a potent antiviral immune response that may ultimately be the key to their success. By virtue of their tumour selectivity, the finite immune resources of the host should theoretically be focussed into the tumour bed. Live replicating viruses should release multiple TAAs through oncolysis, against which tolerance may be reversed in the context of powerful, non-specific co-stimulatory signals, even in the face of an immunosuppressed TME (44, 159). In such a scenario infection and lysis of every single tumour cell would no longer be necessary.

1.5.4 Replication competent OVs and the induction of antitumour immunity

A virus that strongly elicits a *viral* specific CD8+ T cell response would be expected to provide the best chance to cross-prime a favourable antitumour CD8+ T cell response. In monotherapeutic regimes, highly replication-competent viruses promote better CD8+ T cell responses than their attenuated and non-replicative counterparts (74). Tumour lysis induced by replicating viruses releases multiple sequestered TAAs but it also creates greater numbers and diversity of DAMPs. Replicating viruses may also go some way to breaking down some of the physical and physiological immunosuppressive barriers previously discussed (see section 1.5.3) as well as debulking the tumour mass. APCs should therefore be able to prime the immune response against otherwise unavailable TAAs in the context of superior co-stimulation and the subsequently generated effector response might be faced with an easier task in clearing lower volume residual tumour.

In a comparison study that included Lister and NYCBOH derivatives, wild-type WR virus demonstrated the strongest level of replication in animal models and also elicited the strongest CD8+ T cell responses following both intraperitoneal and intranasal infection (74). This phenomenon was attributed to the engagement of the co-stimulatory receptors, OX40 and CD27 (both TNF receptor family members) on T cells; a phenomenon that was only observed with the more virulent strains and recombinants of VV.

There are however two potential problems with using an extremely potent replicating virus as an antitumour therapeutic. First, such viruses are likely to be dose limited by toxicity, especially in the context of the likely need to use relatively high doses in patients with advanced cancer. The wild type WR strain persisted significantly longer in off-target organs such as lungs and ovaries and afflicted considerable toxicity in both immune-competent and nude animal hosts (74). In contrast, as mentioned previously, the Lister strain was cleared more than two times faster and was 100-fold less toxic following intranasal administration. Second, although a stronger CD8+ effector response is likely with potently replicating viruses; when they are used as monotherapy (i.e. for both prime and boost phases), the *antiviral* effector response is likely to

dominate the *antitumour* response as viral antigens are likely to be vastly more immunogenic than TAAs (see section 1.5.8).

1.5.5 Oncolytic viruses and immunogenic cell death

Certain individual or combinations of "danger" signals may be more or less effective at initiating and propagating immune responses. This concept of immunogenic vs non immunogenic cell death (ICD) is a necessary modification to the "danger" model of immunity, as despite the potential release of multiple different types of endogenous damage associated molecular signals, immune tolerance clearly does not reverse every time a cell dies. There is currently intense research activity in identifying whether different modes of cell death induced by therapeutic agents including OVs, could be characterised by combinations of danger of signals that either positively or negatively favour the stimulation of an adaptive immune response (160-162).

Much work in this field has been generated by teams that have previously investigated chemotherapeutic induced ICD with the discovery that some agents like mitoxantrone appear to induce antitumour immunity independent of their direct mechanism of action (163, 164). Classically the dichotomy between apoptotic and necrotic cell death was synonymous with immune tolerant versus inflammatory/immunogenic death respectively. This we now know was an oversimplification. Certainly, other modes of death have also been described based on morphological features and activation of certain death pathways and are encompassed by terms such as necroptosis, pyroptosis and autophagy (44, 165, 166). These modes as described do not fit neatly into immunogenic versus non- immunogenic subcategories (164); thus apoptosis for example, contrary to traditional dogma may also be immunogenic.

The definition of ICD is currently in a state of flux but presently includes the surface expression of pre-apoptotic calreticulin (167), the surface translocation of uric acid (122), expression and release of HSPs (124, 164), adenosine triphosphate (ATP) and/ or the nuclear protein, HMGB1 (164, 168). Calreticulin binds to LDL receptor related protein on APCs to drive their cellular activation (169). HMGB1 is released following both apoptotic and necrotic cell death and binds to activating TLR2/ 4, receptor for

advanced glycation end products (RAGE) and T cell immunoglobulin and mucin (TIM)-3 receptors in APCs (165). ATP released from cells that die through a phase of autophagy, binds to the purinoceptor P2X7 in dendritic cells (DCs). This leads to the activation of the NLRP3-ASC (see index of abbreviations) inflammasome that drives the secretion of activated IL1β which ultimately polarises the developing adaptive immune response toward the generation of IFNγ secreting CD8+ T cells (44, 170).

OVs are capable of killing tumour and some associated stromal cells through multiple different classically defined modes of cell death, in association with some of the aforementioned immunogenic molecular markers. Often a single mode of death tends to dominate, depending on the virus, tumour and host. Thus VV has been demonstrated to kill human cancer cells through apoptosis, necrosis or necroptosis in association with HMGB1 release (59, 171-173). Autophagy (which refers to the sequestration, degradation and recycling of organelles and proteins within the antigen donor cell) associated cancer cell death has been shown to be effected by adenovirus (174), Newcastle disease virus (175), reovirus (176) and herpes simplex virus (HSV) (177) and appears to be a particularly immunogenic mode of cell death. It is associated with the release of HMGB1 (178) and uric acid (179) in addition to ATP, by which it is more commonly defined (180, 181). Interestingly, antigens from cells undergoing autophagy, may be processed through both MHC pathways in APCs (i.e. cross presented) (182-185).

Throughout the course of their evolution, cancer cells often acquire mutations in key components of apoptosis (and other death pathways). The success of an anticancer therapeutic might lie in its ability to induce death through alternative, relatively intact death modes within the cancer cell, e.g. necroptosis (186) or autophagy. This is more likely to be exploited by OVs that have plasticity in their induced modes of cell death. VV for example may kill cells by apoptosis, necroptosis or necrosis (165). Furthermore, the deliberate disruption of certain virulence genes, which inhibit strategic points in certain death pathways, could persuade the infected cell to die in a potentially greater immunogenic mode of death. Arming OVs with transgenes that promote autophagy or necroptosis for example could achieve a similar result.

1.5.6 The role of the innate immune system in mediating the antitumour effects of VV immunotherapy

Innate immunity plays a well-established and pivotal role in helping to prime and direct subsequent antigen specific adaptive immunity, but its cellular and soluble players may also contribute to tumour clearance via more direct mechanisms of action.

1.5.6.1 Antigen presentation

Following ubiquitinisation, cytosolic proteins in nearly all nucleated cells undergo proteasome mediated degradation into peptides of up to 25 amino acids in length. These are transported to the endoplasmic reticulum (ER) lumen via transporter associated with antigen processing (TAP)-1 or 2 proteins, trimmed further into 8-10 αα peptides and loaded via chaperone molecules into an MHCI molecule, before being translocated to the cell surface ready to engage CD8+ restricted T cells (187). Different components of this antigen processing machinery in tumour cells are often defective or absent (159, 188, 189).

The classic MHCII antigen presenting pathway is generally restricted to professional APCs and involves the degradation of proteins in lysosomes that have either been generated from the endocytosis of extracellular antigens or through autophagy (and thus carry intracellular antigens). MHCII molecules carrying invariant chains in their peptide binding groove (Class II-associated invariant chain peptide (CLIP)) are subsequently channelled to these endosomes where CLIP is exchanged for the epitope peptide. Peptide bound MHCII molecules are then transported to the cell surface ready to engage CD4+ restricted T-helper cells.

In general, antigens are channelled separately via these pathways, with endocytosed lysosomal antigens ultimately being presented in MHCII complexes, in contrast to proteasome degraded intra cytoplasmic epitopes that are presented in MHCI complexes. APCs are the only cells *in vivo* that retain the capacity to "cross" present antigens (190, 191) i.e. they can process and channel antigens of extracellular origin (self or non-self) through an (non-infectious) endocytic route into MHCI complexes. In this scenario,

peptides from such antigens could engage both CD4+Th cells and CD8+ CTLs to obtain maximal “help” and amplification of an effector CTL response.

TCR engagement is one of the three major signals required to prime naïve T cells into effector and memory cells, the other two being cell-cell and cytokine (paracrine) mediated co-stimulation. Key co-stimulatory pairs of molecules found on APCs and T cells respectively include CD80/86 with CD28; CD40 with CD40L and 4-1BBL with 4-1BB. Class I and II MHCs in intra-tumour DCs obtained from tumour models and patients are often down regulated along with their co-stimulatory molecules (188, 189, 192). Such APCs may also express inhibitory molecules like PD-L1 (193).

Many OVs that are currently under investigation are capable of reversing the pre-dampened state of intra-tumour APCs (159). APCs that have been isolated from the spleens of murine tumour models display lower expression of co-stimulatory molecules than their naïve counterparts, but this expression is reversed or even enhanced in some cases after OV injection into the tumour (194, 195). In the presence of OVs, APCs receive additional activation signals through engagement of their pattern recognition receptors (see section 1.5.1), which drives the production of key innate effector molecules, particularly the type-1 IFNs (159, 196, 197). Type-1 IFNs up-regulate MHC pathways in APCs and cancer cells, as well as co-stimulatory molecules like CD40, CD80 and CD86 on APCs.

Some OVs have the capacity to enhance cross presentation of viral and TAAs. Thus uninfected DCs were able to prime a CD8+ T cell response against viral and non-viral TAA following exposure to tumour cells infected with Modified vaccinia Ankara (MVA) (an attenuated strain of VV) (198, 199), reovirus (194) and measles virus (200).

1.5.6.2 Cellular innate immune effector cells

As previously described (section 1.4), the replicating VVL recombinant GLV-1h68 selectively colonized a range of human xenografts in nude mice following IV administration. In these models, gene expression profiling consistently revealed a positive correlation between tumour eradication and host expression signatures

representative of "innate defence" activation (79). These included IFN regulatory genes (e.g., signal transducers and activator of transcription(STAT)-1 and interferon regulatory factor (IRF)-7; certain chemokines and their receptors (e.g. regulated on activation, normal T cell expressed and secreted (RANTES), IFNγ induced protein-10 (IP10), monocyte chemotactic protein (MCP)-1); and cytokines: type-1 IFNs, IL1s, IL6, IL15, and IL18.

Peritumoural infiltrates of mononuclear and granulocytic cells are also a feature of virally treated tumours. In a syngeneic colorectal tumour model treated with WRDD, massive tumour necrosis occurred consequent to the influx of neutrophils interrupting tumour vascularity (157).

NK cells are directly cytotoxic to tumour cells, and infiltrating NK cells appear to be a positive prognostic factor in some tumours (201-204). Indeed in some tumour models treated with OVTs, NK cell depletion abrogated tumour clearance (153). OVs may therefore be an ideal candidate to focus an NK cell infiltrate into the TME (153, 205). Given their potential importance in the context of the current project, the next section provides a detailed description of the role of NK cells in limiting viral and tumour growth (section 1.5.6.3).

In other tumour models however, the direct antitumour contribution by innate immunity may be more modest, instead appearing to primarily limit viral replication and oncolysis. For example, cyclophosphamide depletion of leukocytes prior to the administration of GLV-1h68 into a human breast tumour xenograft model actually enhanced tumour eradication (206). We have also demonstrated enhanced uptake of IV administered VVL15 in syngeneic tumour bearing immune-competent mice following selective and temporary monocyte depletion (Ferguson, unpublished data).

1.5.6.3 The role of NK cells in controlling local tumour growth and metastasis

1.5.6.3.1 Activation of NK cells

NK cells are a key cellular component of the innate immune system and play significant roles in immune surveillance against cancer cells as well as host defence against pathogens, particularly viruses. They are of lymphoid origin but lack clonal specificity. This enables them to be activated in response to a range of non-specific stimulants. In the steady state, NK cells comprise 5-20% of peripheral blood mononuclear cells and may also be found in spleen, lymph nodes and visceral organs (207).

Traditionally, NK cells were thought to be activated solely by cells missing MHCI molecules (e.g. in tumour transformed or virally infected cells), which in healthy normal cells bind to inhibitory NK receptors and prevent the damaging consequences of their stimulation (208). However activation is now known to occur as a consequence of a complex balance of inhibitory and activating ligands. The latter include host cellular ligands that are not constitutively present, but which may be induced by cellular stress (207).

Important families of NK receptors include the murine Ly49 lectin like receptors (in mice), killer immunoglobulin like receptors (KIRs), the natural cytotoxicity receptors (NCRs) and the NKG2 family of receptors.

KIRs and the murine Ly49 receptors bind to the MHCI or components thereof and are generally inhibitory in nature (209, 210). However some members of their families are stimulatory, and are often activated by viral particles e.g. KIR2DS1 activates NK cells upon recognition of an Epstein-Barr virus (EBV) peptide loaded MHCI (211) and likewise Ly49H following recognition of the m157 ORF of murine cytomegalovirus (CMV) (212).

NCR and NKG2 receptors are generally activating in nature and important in tumour cell lysis. The NCR, NKp46 (on mice and humans) is particularly important in this context (213). NKp46 is also activated by viral derived ligands (214); for example the

vaccinia haemagluttinin protein A56 activates it, triggering NK cell mediated cellular cytotoxicity (215). NKG2D binds to stress induced ligands such as MIC-A or MIC-B, often present in tumour transformed cells and appears to be critical to the control of infection with VV (216). NKG2D ligands may also be induced on cells involved in antigen presentation (DCs, macrophages and CTLs).

Finally CD16, a receptor for the Fc portion of immunoglobulin molecules, is responsible for the antibody dependent cellular cytotoxicity (ADCC) mediated by NK cells upon binding antibody coated tumour cells. This appears to be a primary mechanism by which antibody based immunotherapy (e.g. monoclonal antibodies like trastuzumab (anti-human epidermal growth factor receptor (HER)-2) and cetuximab (anti-EGFR)) eradicates tumours (217).

1.5.6.3.2 The role of NK cells in curbing tumour growth and metastasis

NK cells employ three main strategies to kill their activating cell: the secretion of cytolytic granules, death receptor mediated apoptosis and the production of cytokines particularly IFNγ (218).

NK cells may kill through release of preformed granules containing perforin and granzymes, akin to CTLs (218-220). This is the fastest mode of cell death. Many studies have shown that perforin plays an important role in the immune surveillance of several malignancies (221).

A slower mode of death (hours) may occur through the extrinsic apoptotic pathway in target cells, following engagement of the cell death surface receptor Fas by TNF family ligands (Fas ligand (FasL) or TNF-related apoptosis-inducing ligand (TRAIL)) expressed on NK cells (222). Cancer cells are often resistant to this mode of death.

Activated NK cells secrete many cytokines including IFNγ. This cytokine may eliminate tumour cells by directly inhibiting their proliferation and/ or by the induction of antiangiogenic factors e.g. IP10 (223, 224). It can also enhance the sensitivity of neighbouring tumour cells to perforin/ granzyme or death ligand mediated cell death

(225). IFNγ may also induce DCs to produce IL12, which aids the development of antitumour cytotoxic T cells (226).

Numerous experimental studies have demonstrated that NK cells can eliminate tumour cells that either express activating ligands or lack inhibitory ligands on their surface (207, 227). Mice deficient in NK cells have higher rates of spontaneous tumour generation and accelerated growth of induced tumours (228-230). Low NK cell activity is also associated with increased cancer risk in humans and there is evidence of NK cell dysfunction in advanced cancer patients (231).

NK cells appear to play a role in the prevention of metastatic disease. Certainly in animal studies, expansion and activation of NK cells using CpG motifs (TLR agonists) or IFNγ is sufficient to prevent pulmonary and metastatic dissemination (232, 233).
These and other studies have promoted the development of therapeutic protocols designed to enhance the activity of NK cells in the context of tumour.

1.5.6.3.3 NK cells and viral infection

Cancer therapeutics that utilise a tumour selective virus platform, may exploit their additional capacity to rapidly recruit and activate NK cells within the TME. Little is known about the migration of NK cells in untreated tumours (although selectins may play a role (234)), but migration towards virally infected cells is mediated predominantly via the chemokine receptors CCR2, CCR5 and CXCR3 (235).

Virally infected cells activate NK cells through many of the same receptors used by the tumour cells, described above. In addition NK cells may also be activated by cytokines released upon viral infection (236). The major activators include type-1 IFNs, IL12, IL15 and IL18. They all enhance NK cell mediated cytotoxicity (237). Stimulation of TLRs on NK cells is another activation mechanism utilised by viruses and other infectious organisms (238-240). TLR2 stimulation on murine NK cells appear critical for the control of VV *in vivo* (216).

Intriguingly, viral mediated NK cell activation could lead to the generation of "memory" NK cells, a feature hitherto recognised as a hallmark of the adaptive immune response (227). For example, a murine CMV model of infection, gave rise to long lived memory like NK cells, with enhanced sensitivity to ligands that signal through unstimulated activating receptors (241-245). Thus NK cells that had been initially driven by a powerful non-tumour stimulant, may up regulate receptors important in tumour eradication e.g. NKp46 and NKG2D, and have demonstrated enhanced cross reactivity to tumour (227). This may be an important mechanism of OVT mediated antitumour efficacy.

1.5.6.4 Effective harnessing of innate immunity

OVs have adapted various strategies to ensure survival, replication and propagation in their hosts. These are mediated by different virulence gene products that may be classified as follows: those acting intracellularly e.g. to block apoptosis; those acting on the cell surface to enhance or supress cellular signalling cascades and those that act extracellularly to block secreted components of the antiviral immune response e.g. decoy molecules that sequester cytokines and chemokines. Vaccinia codes genes that fall into all these categories, and features genes designed to counter innate antiviral defences; namely apoptosis, IFN and TNF responses (9, 68). One way of enhancing the innate immune response against a virus in a bid to provide a backdrop for efficient antigen presentation would be by arming it with transgenes encoding innate immunomodulators like IFNs, TNFs or chemokines. For example, the IFNβ transgene was cloned into the B18R locus (which codes for an anti-interferon protein) of a WR VV recombinant (246). Antitumour efficacy was enhanced despite the anticipated enhanced clearance of virus.

An alternative way to achieve the same aim would be to disrupt one or more of the viral genes that curb antiviral immunity such as the VV N1L gene (247).

1.5.7 The VV N1L gene

The VV N1L gene (called L025 in the VVL strain) is a major virulence gene, that when disrupted, was shown to significantly reduce pulmonary toxicity following various routes of administration into animal models (248, 249). Replication of mutant virus in cultured cell lines were not however attenuated in these studies.

The WR VV was originally developed following multiple passages through murine central nervous systems (CNSs) (71). N1L gene disruption led to a significant reduction in the neurovirulence of WRDD; with reduced viral titres in the brains of mice that had been directly inoculated (250). In contrast, moderate intranasal doses of the wild type strain led to high viral loads within the CNS (251).

The improvement in neurotoxicity following N1L gene disruption may simply have reflected viral attenuation *in vivo* i.e. a diminished ability to survive and disseminate in tissues within an immune competent host. Indeed disruption of the homologue of this gene in the pox virus, ectromelia, for which mice are the natural hosts, abrogated the ability of intranasally delivered virus to travel beyond the lung into peripheral tissue (249). However the N1L gene product, a dimeric 14 kDa cytosolic protein, may specifically confer tropism of pox viruses for neural tissue. In a study designed to search for human intracellular proteins that might interact with the N1L protein, human brain originated cellular basement membrane-associated chondroitin sulfate proteoglycan (BAMACAN) (252) co-immunoprecipitated with the N1L protein and confocal microscopic analysis confirmed their co-localisation. BAMACAN is expressed at higher levels in neural versus non-neural tissue and its enhanced expression and interaction with the VV N1L protein in a neural cell line appeared to positively support its viral growth within that cell line. Mechanistic detail regarding the role of the N1L protein in the neurovirulence of VVs is currently limited, but it is of potential importance, as neurotoxicity, although an extremely rare complication when administered in vaccine doses might become more prominent with anticipated higher, prolonged dosage regimes in cancer therapy.

The N1L gene product is therefore a vitally important non redundant *in vivo* virulence protein that must enable viral survival via modulation of host innate and or adaptive antiviral immunity. Although disruption of the N1L gene did not impair VV's propensity to generate robust long term humoral or cellular antiviral immune responses in comparison to the wild type virus (247, 253, 254), it did not conclusively enhance adaptive antiviral immunity either (254). Nevertheless, in one study at least, splenocytes harvested from mice inoculated intranasally with N1L gene disrupted VV (WR in this case), demonstrated superior cytotoxicity against virally infected murine lymphoma (RMA) cells (253). Furthermore, in a similar murine model using ectromelia, the loss of virulence that occurred following disruption of the N1L gene homologue, was regained in recombination activation gene (RAG)-1 knockout mice (which lack both mature B and T cells), as well as by simultaneous depletion of CD4+ and CD8+ T cells (249).

Whilst the role of the N1L gene product as an immunomodulator of adaptive immunity remains to be further defined, more studies have focussed on its role in modulating innate antiviral immunity (247).

As with other viruses, VV induces the accumulation, activation and proliferation of NK cells at the site of infection (220, 236) and possesses numerous virulence genes that may counter their activation, often indirectly, by modulating the production of certain chemokines and cytokines (247). The N1L gene product may be one such candidate. Intranasal administration of N1L gene disrupted VV, led to an enhanced NK cell infiltrate into murine lungs in comparison to the wild type (WR) virus during the first six days post infection. Furthermore, these NK cells also demonstrated superior cytotoxicity, confirmed by their ability to lyse Yac-1 lymphoma cells. In keeping with the enhanced cellular immune response, there was a corresponding drop in lung titres of the N1L disrupted recombinant virus from day seven onwards (254).

The N1L protein is expressed within three hours after cellular infection (255). Like some other VV proteins involved in immunomodulation, part of its structure resembles a Bcl-2 like structural fold. However, unlike most other VV encoded proteins in this category, which inhibit either apoptosis or the activation of pro-inflammatory transcription factors, the N1L protein appears to inhibit both (256-258).

1.5.7.1 The VV N1L protein inhibits intracellular inflammatory pathways

The major inflammatory signalling pathways thought to be modulated by the N1L protein are the IFN and NF-κB pathways (247).

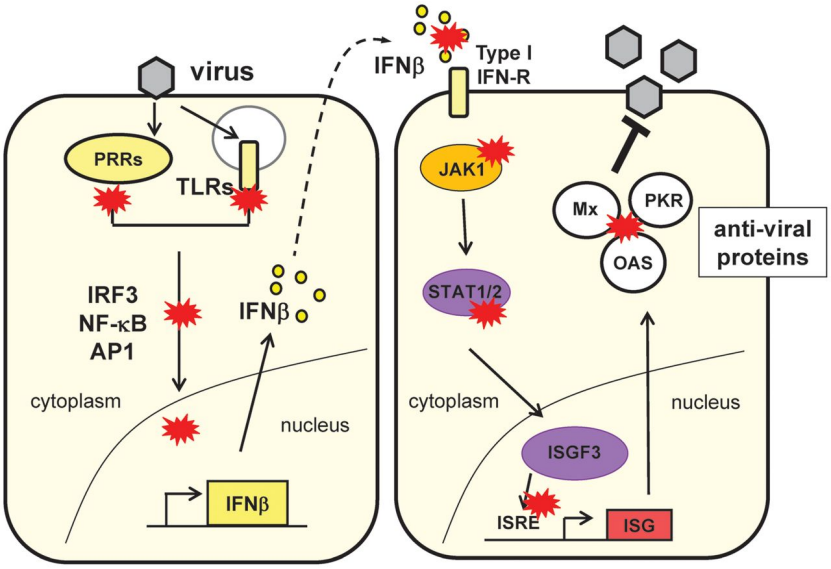

Figure 1.2 IFN signalling and its regulation by VV (247)

ISRE: IFN-stimulated response elements; ISGF3: IFN-stimulated gene factor 3 complex (see main text for other abbreviations). The positions at which viral protein products may inhibit the production or subsequent action of IFN are illustrated by the red stars.

The IFN response commences upon sensing of viral PAMPs by host cellular PRRs (figure 1.2). Upon their engagement, signalling cascades are induced leading to the activation of transcription factors such as IRF3, IRF7, NF-κB and activator protein (AP)1, that ultimately translocate into the nucleus to induce the transcription of genes encoding type-1 IFNs (notably IFNβ) and numerous other cytokines and chemokines. Secreted IFNs, through autocrine or paracrine activation of their cognate receptor, activate the Janus kinase (JAK)/ STAT signalling pathways which culminate in the co-ordinated transcription of hundreds of IFN-stimulated genes (ISGs) (259). Many of these, such as protein kinase R (PKR), 2'-5'-oligoadenylate synthase (OAS) and Mx inhibit aspects of the viral life cycle and confer an antiviral state (247). The N1L protein

has been shown to inhibit signalling through NF-κB and IRF3, possibly via inhibition of the inhibitor of κB (IκB) kinase (IKK) and TANK-binding kinase 1, upstream regulators of these pathways (258), although this mechanism is currently disputed (260).

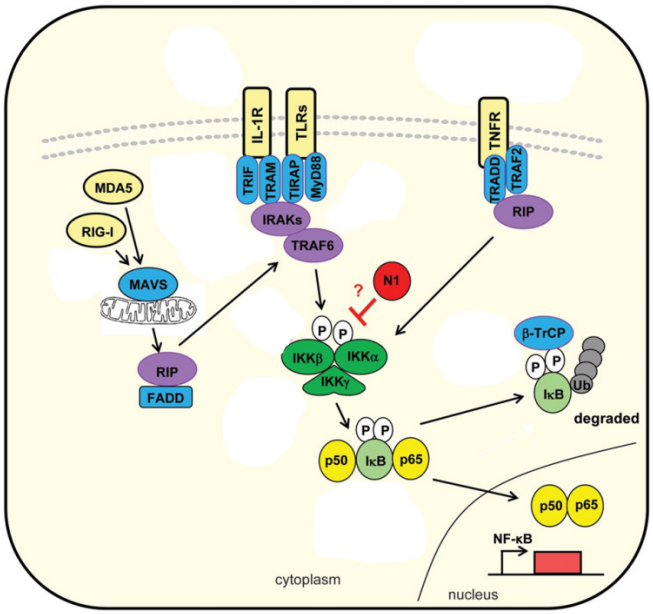

Figure 1.3 Signalling through the NFκB complex (247)

The N1L protein is thought to inhibit signalling through the NFκB cascade at the level of the IKK complex. The blue and purple boxes or ovals respectively represent adapter proteins and intermediate signalling enzymes that form complexes upon binding of PAMPs or inflammatory cytokines to their cognate receptors (beige boxes or ovals). See main text for further details.

The NF-κB complex consists of a family of transcription factors that are retained in the cytoplasm of resting cells by association with inhibitory IκB proteins (261). Signalling through this complex may be initiated by PAMPs binding to PRRs (e.g. TLRs, RIG-1) or cytokines such as IL1 or TNFα binding to their cognate receptors (IL1-R, TNFR respectively); each of which subsequently associates with specific adaptor proteins (figure 1.3). Ultimately, signalling cascades converge onto the activation of the IKK complex, which phosphorylates IκB causing its ubiquitination and degradation by the proteasome. This then frees the NF-κB subunits, p50 and p65 which translocate into the nucleus and induce the transcription of NF-κB dependent genes.

Many antiviral effector cytokines are produced by professional APCs and monocytes, in response to infectious microorganisms. N1L gene disrupted VV WR infection of peripheral human blood monocytes led to an enhancement in the secretion of the pro-inflammatory cytokines IFNα/β, TNFα and IL8 (262).

1.5.7.2 The VV N1L protein inhibits apoptosis

Apoptosis is an irreversible sequence of biochemical events that converge on the activation of caspase proteases to effect cell death. It represents an important defence mechanism against viral infection. The Bcl-2 family of proteins regulate the activation of the intrinsic pathway of apoptosis through a complex interaction of pro apoptotic and anti-apoptotic proteins (figure 1.4) (247, 263).

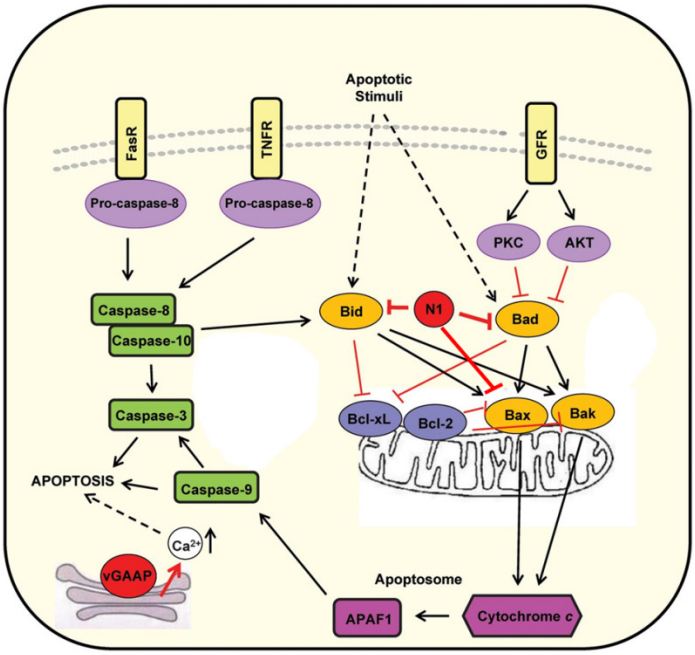

Figure 1.4 The N1L protein inhibits apoptosis (247)

The N1L protein may directly inhibit pro-apoptotic proteins as shown. See main text for further details and abbreviations.

Under steady state conditions, antiapoptotic proteins like Bcl-2 and Bcl-xl inhibit effector pro-apoptotic proteins (Bax and Bak) on the mitochondrial outer membrane. Various intrinsic death triggers, including DNA damage or viral components trigger other cytosolic pro-apoptotic proteins to bind and inhibit the anti-apoptotic Bcl-2 proteins or directly bind to and activate pro-apoptotic effector proteins (figure 1.4). Either way, these events cause the oligomerisation of Bak and Bax which permeabilises the outer mitochondrial membrane leading to the cytoplasmic release of cytochrome c and subsequent formation of the apoptosome (264). The apoptosome initiates the activation of the caspase protease cascade. The N1L protein has a groove that is structurally similar to the cellular anti-apoptotic Bcl-2 protein and may similarly bind to and inhibit pro-apoptotic intermediate proteins (57, 257).

In summary, the N1L protein product is multifunctional and appears to be able to modulate three important innate antiviral mechanisms: apoptosis, IFN and NF-κB signalling. It is therefore an ideal candidate for disruption in order to enhance and focus host innate (and possibly adaptive) anti-viral immunity to within the confines of a TME.

1.5.8 Vaccinia induced enhancement of the adaptive immune response

Optimal central thymic selection should theoretically have eliminated T cells that strongly react to self-antigens and it is therefore possible that a host organism may not possess any T cell clones that are capable of mounting an antitumour response. The heterogeneous nature of tumour cells and by implication, their TAAs makes this scenario unlikely. Certainly autoimmune disorders represent a breakdown in tolerance to autoantigens and are often characterised by strongly self-reacting T-cell clones. Furthermore, the expansion of multiple potentially weak immunogenic T cell clones could prove efficacious as demonstrated by experiments using adoptively transferred *ex vivo* expanded tumour infiltrating lymphocytes (TILs) (265).

In an attempt to enhance their ability to cross-prime antitumour immunity, VV and other OVs have been armed with transgenes coding for single or multiple (single-digit) tumour antigens (266). Their monotherapeutic use in either prophylactic or therapeutic tumour vaccination has yet to demonstrate reversal of tolerance to TAAs (266, 267).

Theoretically, single (or few) self-antigens would face stiff competition from the immunodominant antiviral response, even if they are over-expressed. Epitope spreading may not be successful for the same reason. Furthermore, even if tolerance to the target antigen(s) were to be reversed, there is a real danger of selecting out tumour cells that do not carry the antigen.

The ideal scenario would be to simultaneously vaccinate against similar frequencies of multiple tumour antigens, individualised to a specific host and tumour. This could be achieved by whole cell viral lysates either generated *ex vivo* or *in situ,* although the frequency of individual TAAs would be expected to be relatively low. In a group of pioneering experiments, Vile and colleagues recently demonstrated that systemic treatment with a pool of highly immunogenic vesicular stomatitis viruses (VSVs) engineered to express a cDNA library of xenoantigenic human cancer tissue could reject established murine tumours of a similar histological type. In their studies, which utilised prostate (268) and melanoma (269) models, there were no detectable autoimmune side effects. This demonstrated that the simultaneous presentation of a broad range of individually weak tumour antigens derived from a particular histological subtype, does indeed have the capacity to reject a histologically similar tumour. Although extremely promising, there may be logistic and quality control barriers to the translation of this highly heterogeneous biologic into the clinic. *In situ* vaccination strategies with one (or two) fully sequenced biologics should be more amenable in this regard.

Preclinical and indeed clinical data exploring the use of OVs as cancer therapeutics suggests that efficacy is significantly improved by arming viruses with immunomodulatory gene(s) designed to boost either or both of the afferent (antigen presentation) or efferent arms (effector response) of a developing adaptive antitumour immune response. Indeed two of the most clinically advanced viruses, a recombinant HSV and a Wyeth strain recombinant VV, carry the GMCSF cytokine transgene (146).

One way to enhance antigen uptake and presentation is by providing a localized boost to this phase. GMCSF has been used in multiple platforms including VV and other OVs (20, 270, 271) for cancer therapy ever since Dranoff first demonstrated its capacity to successfully generate tumour specific CTLs (272). GMCSF enhances the infiltration and differentiation of naïve APCs to mature activated ones. In similar vein, the

chemokines RANTES and FMS-like tyrosine kinase (FLT)-3 ligand, when delivered on viral vector platforms enhanced intratumoural infiltration of DCs, T and NK cells and were associated with tumour regression in the context of a tumour specific CTL response (273, 274).

A wide variety of VV recombinants incorporating various other immunomodulatory transgenes have been used in an attempt to boost the effector response and the generation of antitumour memory T cells, with variable success. These include transgenes coding for T cell co-stimulatory ligands e.g. B7.1 (275) and CD40L (276); IL-2 (53, 277, 278) and IL-12 (53, 278, 279). In the main, the goal of these therapeutic strategies were to nurture a Th-1 cytotoxic antitumour response (152).

IL12 which is mainly produced by activated APCs is a particularly important cytokine in bridging the gap between innate and adaptive immunity, skewing it in favour of a Th-1 phenotype (141, 226). It primes and activates both NK and CD8+ T cells to produce IFNγ, modulates angiogenesis and may additionally upregulate the cellular expression of both class I and II MHCs (141, 226). IL12 administered in a variety of different forms has consistently demonstrated efficacy in animal models of cancer but human trials, with predominantly systemic IL12 have been limited by toxicity (142, 226). Highly localised delivery into the TME on an OV platform could alleviate this problem.

With regards the Lister strain of VV, Chen et al. engineered a group of recombinant VVLs armed with transgenes encoding IL-2, IL-12, or both (53). Recombinants expressed high levels of cytokines *in vitro* and *in vivo* in a SC xenograft rat glioma (C6) model. Antitumour efficacy was significantly better with all constructs in comparison to the unarmed control virus following low-dose IT injection. Because nude mice were utilized, this surplus effect was likely to have been mediated by tumour-focused activation of innate immunity, evidenced by localized increases in IFN-γ and NK cells in all experimental arms.

The sequence of events in a developing immune response has been well characterised and typically takes about seven days after initial antigen exposure. Antigen loading, migration and presentation in draining lymph nodes occurs during the first half of this period, leading to the expansion of effector CTLs thereafter. Optimal enhancement of

these phases could be expected if OVs carrying transgenes designed to act primarily in one or other phase were administered in the appropriate order. For example, a virus armed with the GMCSF transgene could be administered during the first few days of treatment, followed by virus armed with IL12 in the days thereafter.

Obviously, strategies that enhance the immunogenicity of the virus are likely to enhance viral clearance in immune-competent hosts. This indeed has been observed *in vivo* with VVs armed with some of the aforementioned immunomodulatory genes (56, 280, 281). This could prove to be problematic, as secondary "booster" doses of virus are likely to be necessary in any vaccination protocol. However, only a small quantity of virus needs to be delivered into residual tumour tissue to effect killing of some, but not all, tumour cells; just enough to release enough TAAs required for boosting tumour-specific memory T cells. When administered in relatively high doses, VV colonization, replication, and transgene expression in solid tumour has been demonstrated following systemic administration in both animal models and patients, even in the face of pre-existing neutralizing antibodies (20, 282).

As previously mentioned, another potential problem with OVT is that upon administration of booster doses, the secondary immune response against viral antigens may swamp that against the much weaker tumour antigens. An alternative strategy might be to use an antigenically different OV for the secondary boost. Release and presentation of tumour antigens following administration of a second virus (to which the host is naive) should stimulate a *secondary* antitumour immune response that dominates the *primary* response to the new virus (283, 284). Bridle et al. used such a heterologous prime-boost strategy to treat an aggressive intracranial syngeneic B16-F10 murine melanoma model (266). They demonstrated that intramuscular administration of a recombinant adenovirus armed with a transgene encoding a melanoma antigen (DCT), followed later by an IV dose of recombinant VSV armed with the same gene, led to a significant increase in median survival compared to therapy with either virus alone or indeed with the same combination but with viruses lacking the DCT transgene. The heterologous regime was associated with a significantly enhanced percentage of anti-DCT CD8+ T cells. Importantly, there was a corresponding reduction in the anti-VSV CD8+ T cell response compared to that within naive mice infected with the VSV recombinant. In a similar experiment, Zhang et al. (285) used sequentially presented

Semliki Forest and vaccinia viruses to enhance antitumour efficacy against a disseminated ovarian cancer model. Again, the best results were observed when viruses were armed with a transgene encoding a common tumour antigen.

Whilst such regimes may ultimately be the future of OVT, there is evidence that single viral therapy can indeed induce a clinically significant antitumour response. A VV armed with GMCSF was used to treat a small cohort of patients with advanced disseminated malignant melanoma. Intralesional administration of virus into the primary lesion in a multidose regime led to the regression of tumour deposits at distant sites as well as the primary in four of seven patients (286). The lesions were associated with lymphocyte infiltration. Even more impressively, a HSV mutant armed with GMCSF (Talimogene laherparepvec (T-Vec)) led to complete long term cure of 8 of 50 patients with similarly advanced malignant melanoma (287).

Perhaps the success of these and other similar studies reflected a pre-existing weak level of antitumour immunity, resembling a primary response, that may have been triggered spontaneously or following prior conventional therapies. This pre-existing antitumour immunity may not have been strong enough to effect tumour eradication at first, but could have been "secondarily" boosted by presentation of tumour antigens released by initial doses of OVT. In effect, a scenario akin to the aforementioned heterologous prime boost regime.

1.5.9 Innate v adaptive immunity in OVT

The role of both innate and adaptive immunity in OV mediated antitumour clearance is therefore important but complex and is likely to vary with virus, strain, tumour type, and host. As an example, Wang et al. (246) demonstrated equivalent antitumour responses following IT administration of a VV WR recombinant into two different syngeneic SC murine lung cancer models. Viral recovery from one of the tumours (TC-1) was high. In this model, viral oncolysis played the dominant antitumour role because alteration of the immune competence of the host made little difference to antitumour efficacy. In contrast, viral recovery from the other model (LKRM2) was poor; and depletion of CD8+ T cells reversed tumour eradication.

1.6 Oncolytic viruses as a neoadjuvant treatment to surgery

The most effective means of curing a solid tumour remains surgical excision. However evidence from clinical and experimental data suggests that in many cases surgical excision with curative intent may actually promote tumour metastasis and metachronous recurrence (288-292). A major source of recurrence is from minimal residual disease (MRD) i.e. microscopic primary deposits left behind near clearance margins or micrometastases that were either pre-exisitant or potentially encouraged by surgical manipulation (288). Indeed recurrant tumour, either locoregional or disseminated is a major cause of mortality following oncologic surgery.

The growth dynamics of residual disease does appear to be altered following surgical manipulation. For example, sub-total excision of primary tumours in various experimental models causes an acceleration in the growth of residual primary tumour as well as in metastatic deposits (288, 293, 294). This phenomenon has also been observed in clinical series of cytoreduction operations and metastectomy. In one clincal study for example, novel metastasis at distant sites appeared much sooner than anticipated following lung metastectomies, and grew at much faster rates than their excised counterparts (295). Presumably therefore, they represented accelerated growth of previously dormant metastases (295, 296).

The extent of surgical manipulation can have a profound influence on subsequent tumour dissemination, as demonstrated for example by the enhanced likelihood of intra and extra peritoneal tumour dissemination following laparotomy versus laparoscopy (297-299). Direct seeding of tumour cells into the circulation or lymphatics following tissue handling is unlikely to fully explain the enhanced metastatic rates. Patients with early stage primaries often have circulating tumour cells (CTCs), but most do not develop recurrence (300). Furthermore, post operative CTC levels do not conlusively correlate with survival. Indeed only 0.01% of CTCs actually aquire the capacity to become clinically overt metastases (288).

Following surgery, there appear to be perturbations of the molecular oncology of residual cancer cells, as well as in the biological behaviour of residual and metastatic

tissue; for example, enhanced DNA sysnthesis and cellular resistance to apoptosis in addition to enhanced microvessel density (288, 301). Surgical trauma leads to elevated levels of circulating inflammatory factors such as acute phase proteins (TNFα, IL1, IL6, IL8) and VEGF, all of which may potentiate tumour growth via multiple mechanisms. VEGF for example, may promote resistance to apoptosis (by upregulating Bcl-2) as well as being proangiogenic (302). Furthermore, primary tumours may secrete soluble factors into the circulation that actively inhibit the growth of disseminated tumour (303, 304). These include inhibitors of angiogenesis e.g. angiostatin, endostatin and thrombospondin (301, 304, 305). The disinhibition of angiogenesis following excision of the primay, coupled with elevation of proangiogenic factors may kick start previously dormant metastatic deposits.

An important feature of perioperative stress is immunosuppression, which is exacerbated by anaesthesia and blood transfusions (306-309). Innate immune surveillance mechanisms, particularly NK cells, are often impaired in patients with malignancy. Numbers and function of these drop even further postoperatively (309-312); related adversely to extent and length of the operation (298, 299). Animal studies have demonstrated a correlation between post operative NK cell suppression and enhanced metastases in models of spontaneous and inoculated metastases (310-313).

Other prominent immunological changes that occur perioperatively include a reduction in DC numbers (314) and a cytokine pattern that promotes Th-2 immunological priming (288, 315, 316). Immunosupression appears to peak by post operative day three, but the restoration in the host's ability to mount an antigenic cellular response could take up to three weeks (288). These changes generate a window of opportinity for tumour to escape host immune surveillance.

At present, there are no stardard perioperative therapeutic approaches aimed at preventing post operative recurrence or metastasis from MRD and it therefore remains a signficant area of unmet clincal need. Traditional chemotherapeutic agents are too toxic to administer to patients either just prior to major surgery or in the early post operative recovery period and are likely to impair wound healing.

Cytokine therapy has been investigated in a bid to globally reverse perioperative immunosuppression. For example IL-2 (317, 318) and IFNα (319, 320) administration demonstrated early promise and reversed post-operative NK suppression; however such therapies have been hampered by substantial dose-limiting toxicities (321).

Other perioperative candidates including inhibitors of inflammation (e.g. cyclooxygenase (COX)-2 inhibitors, anti TNFα antibodies) and angiogenesis (e.g. anti VEGF antibodies), are currently being used in the context of clinical trials, but have yet to demonstrate a survival benefit (307).

OVT might be an attractive option to use in the context of neoadjuvant therapy. Intravenously active tumour selective OVs such as vaccinia may be able to directly target preexisitng, potentially dormant micrometastatic deposits (282). They are powerful stimulants of innate immunity and NK cells in particular (322). Furthermore, their ability to break down the immune suppressive TME and promote anti-tumour adaptive immunity may also aid long term immunosurveillance (44). This may be aided by utilising the ability of some OVs to locally deliver immunomodulatory proteins. IL12 for example may be an ideal candidate in the current context. It is a potent activator of both NK and CTLs and inhibits angiogenesis in an IFNγ dependent manner (141, 226).

Tai et al have recently demonstrated that a single IV dose of replicating pox virus (VV or orf virus) administered hours prior to surgery could reverese surgical stress induced NK cell suppression and enhanced metastases in experimental models of metastatic breast cancer and melanoma (310). A similar result was also obtained when inactivated influenza vaccine was used in the perioperative period; an affect that was dependent on a TNFα surge (323). These studies are certainly encouraging, but as yet lack long term survival data. In addition, a question mark remains regarding the optimum time of administration to enable adaptive antitumour priming and thus longer term immune surveillance.

An important aim of the current project is to explore the role of recombinant VVLs in the context of presurgical neoadjuvant therapy.

1.7 Safety

VV is relatively contraindicated in patients with severe immune deficiency, those who are pregnant, infants, and patients with widespread chronic dermatological conditions. Serious adverse effects are well documented and include post-vaccinial encephalitis (2–1200/10^6), eczema vaccinatum (8–80/10^6), and fulminant vaccinia (1–70/10^6) (324). The risk of death with naive vaccinations is estimated to be approximately 1/10^6, although it may be strain dependent (325). A meta-analysis based on retrospective data estimated the death rates from NYCBOH, Lister, and CPN strain-derived vaccines to be 1.5, 8, and 25 deaths per million, respectively (326). In contrast, a second-generation NYCBOH strain derivative, ACAM2000, used recently to vaccinate healthy individuals, caused an unexpectedly high incidence (5730/10^6) of cardiac complications (arrhythmias, pericarditis, myocarditis, and dilated cardiomyopathy) (327). Mild side effects of VVs include painful injection sites, skin reactions, and constitutional symptoms (e.g., headache, malaise, and fever).

Side effects attributed to VV recombinants in clinical cancer trials conducted thus far have generally been mild. It has been safely administered via SC, IV, IT, and intravesical routes. However, the combined total numbers of patients in these trials amass to only hundreds. Given the rarity of some of the more serious side effects, they would not be expected to be detected in this relatively small cohort. Furthermore, patients with advanced cancer are generally at a higher risk of suffering a severe complication due to relative immune suppression and/or comorbid conditions (328, 329); a problem that is compounded by the fact that optimum dosing regimens, which are anticipated to be much higher than that used for vaccination, have yet to be established.

To reduce the risk of serious complications, traditional vaccine strains have been attenuated. MVA (Ankara strain), NYVAC (Copenhagen strain), ACAM200 (NYCBOH), and LC16m8 (Lister) are highly attenuated VV derivatives that (aside from LC16m8) have minimal or no replication competence (330). Although they retain their immunogenicity and may be used to vaccinate against pox viruses, their use in cancer therapy is likely to be limited. As previously described, replication competence

appears to be an important characteristic for the generation of a favourable antitumour response and is necessary to mediate tumour cell oncolysis.

Toxicity may be reduced by targeted disruption of virulence genes that are not required for virus replication in tumours and/or through genetic manipulations designed to improve tumour selectivity. The tumour selectivity of the attenuated but still replication-competent VVL mutant, GLV1h68, was enhanced compared to that of its parental strain, with a significant reduction in viral toxicity (54). Upon sequencing, ORFs coding for certain non-targeted virulence genes (e.g., one encoding a TNF receptor homologue (L195) and another encoding a viral golgi-associated anti-apoptotic protein) were found to be inadvertently disrupted (55). In general, however, the extent of genetic disruption is likely to proportionately reduce the replication efficiency of VV, as indeed will the transcriptional and translational burdens imposed by multiple transgene inserts, particularly if driven by strong promoters (58).

Disruption of the VV N1L gene in the current project was a bid to enhance the safety of the virus as well its immunogenicity.

1.8 Aims

1. To engineer a set of Lister strain vaccinia viruses with deletions of the VTK and N1L gene regions, armed with either GMCSF or IL12 cytokine transgenes
2. To validate these constructs in tumour models *in vitro*
3. To explore whether these mutants are capable of cross stimulating immunity against tumour cells and tumour associated antigens
4. To develop and optimise viral treatment strategies that are capable of treating *in vivo* models of primary and metastatic cancer
5. To develop a neoadjuvant tumour vaccination strategy to prevent postoperative metastasis and long term recurrence

Chapter 2 Materials and methods

2.1 Cell lines

Immortalised tumour cells lines were derived from either murine, Syrian hamster or human hosts. They were chosen to represent a broad spectrum of solid carcinomas. All cell lines with the exception of DT6606-Ova, were maintained in stock culture medium (sCM) comprised of Dulbecco's modified Eagle's medium (DMEM) (Sigma Aldrich, Dorset, UK) supplemented with 5% heat inactivated foetal calf serum (FCS) and 1% penicillin streptomycin (Sigma Aldrich) and incubated at 37^{o}C in air with 5% carbon dioxide (CO_2). DT6606-Ova cells were maintained under similar incubation conditions in sCM which additionally contained 2 mg/ ml of the antibiotic G418 (Gibco®, Life Technologies, Paisley, UK). All human cell lines had been authenticated by short tandem repeat (STR) analysis. All cell lines were negative for mycoplasma (tested using the MycoAlert^{TM} mycoplasma detection kit, Lonza Biologics PLC, Slough, UK). Table 2.1 lists the cell lines used in this project.

Table 2.1 A list of tumour cell lines used in the current project

Cell line	Organ of origin	Histology	Host: strain
CT26	Metastatic colon	Adenocarcinoma	Mouse: BALB/c
CMT93	Rectal	Adenocarcinoma	Mouse: C57BL/6
LLC	Metastatic lung cancer	Squamous cell carcinoma	Mouse: C57BL/6
B16-F10	Metastatic melanoma	Melanoma	Mouse: C57BL/6
SCCVII	Oral cavity	Squamous cell carcinoma	Mouse: C3/HeN
DT6606	Pancreatic	Ductal adenocarcinoma	Mouse: C57BL/6 (transgenic – see text)
HPD-1NR	Pancreatic	Ductal adenocarcinoma	Syrian Hamster
HCPC-1	Oral cavity	Squamous cell carcinoma	Syrian Hamster
SUIT-2	Metastatic pancreatic	Ductal adenocarcinoma	Human
A549	Lung	Adenocarcinoma	Human
HCT-116	Colonic	Adenocarcinoma	Human
FaDu	Oral cavity	Squamous cell carcinoma	Human
A-172	Brain	Glioblastoma	Human
UW-228	Brain	Medulloblastoma	Human
CV1	Kidney (non-tumour immortalised)	Fibroblast	African green monkey

2.1.1 Murine derived carcinoma cell lines

The metastatic colon adenocarcinoma cell line CT26 originated from the BALB/c murine strain, whilst CMT93 (rectal adenocarcinoma), Lewis lung carcinoma (LLC, metastatic lung squamous cell carcinoma) and B16-F10 (metastatic melanoma) cell lines were derived from the C57BL/6 strain. These were all obtained from the Cancer Research UK central cell bank (CRUK, Clare Hall, Herts, UK)

SCCVII is a spontaneously arisen murine oral cavity squamous carcinoma cell line (C3H/HeN strain) and was a kind gift of Dr Osam Mazda (Department of Microbiology, Kyoto Prefectural University of Medicine, Kyoto City, Japan).

DT6606 (pancreatic ductal adenocarcinoma) originated from a C57BL/6 strain transgenic mouse with mutations in K-RAS and TP53 genes that were engineered to be conditionally expressed in the pancreas (331, 332). This was a kind gift of Professor David Tuveson (CRUK, Cambridge Research Institute, Cambridge, UK). DT6606-Ova was previously made by our group, whereby the plasmid, pCL-neo-cOVA (Addgene, Middlesex, UK) was stably transfected into DT6606 cells. The plasmid contains neomycin and ampicillin resistance cassettes in addition to the chicken ovalbumin transgene.

2.1.2 Syrian Hamster derived carcinoma cell lines

HPD-1NR is a pancreatic ductal adenocarcinoma cell line obtained from the German Collection of Microorganisms and Cell cultures (DSMZ; Braunschweig, Germany). HCPC-1 is a chemically induced squamous cell carcinoma of buccal pouch mucosa that was a kind gift of Professor Joel Schwartz (Department of Oral Medicine and Pathology, University of Illinois at Chicago, USA).

2.1.3 Human carcinoma cell lines

SUIT-2 (metastatic pancreatic carcinoma) and A549 (lung adenocarcinoma) were obtained from the CRUK central cell bank; whereas HCT-116 (colonic adenocarcinoma) and FaDu (buccal squamous carcinoma) were obtained from the American Type Culture Collection (ATCC; VA, USA).

The following cell lines: A-172 (adult brain glioblastoma) and UW-228 (adult medulloblastoma) were kind gifts respectively of Dr Sarah Martin at the Barts Cancer Institute and Professor Silvia Moreno at the The Blizzard Institute, Barts and The London School of Medicine and Dentistry, London, UK.

2.1.4 Non-tumour cell lines

CV1 is an African Green Monkey immortalised kidney fibroblast cell line obtained from the ATCC.

2.2 Previously constructed viruses

VVL15-LacZ (84) is a Lister strain vaccinia virus in which the VTK gene was disrupted by the insertion of firefly luciferase and E coli lacZ reporter transgenes, placed under the control of the VV P7.5 promoter and a synthetic early-late promoter respectively (figure 2.1). This was used as the backbone for all viral constructs in this project.

Figure 2.1 The transgene cassette in place of the VTK gene in VVL15-LacZ

The back to back promoters are shown in blue. P7.5: VV early-late promoter; EL: synthetic early-late promoter

VVL15-RFP was constructed by Dr Louisa Chard from our group. It is equivalent to VVL15 but contains a red fluorescent protein (RFP) transgene in place of lacZ (figure 2.2). This virus was used as the control in all experiments involving VVL15ΔN1L.

Figure 2.2 The transgene cassette in place of the VTK gene in VVL15-RFP

The back to back promoters are shown in blue. P7.5: VV early-late promoter; EL: synthetic early-late promoter

2.3 General DNA techniques used in the construction and testing of recombinant viruses

2.3.1 Agarose gel electrophoresis

Agarose gels (1%) were made using 1 g of electrophoresis grade agarose powder (Invitrogen, Life Technologies, Paisley, UK) in 100 ml of 1x Tris, acetate, EDTA (TAE) electrophoresis buffer. Ethidium bromide (EtBr) (Sigma Aldrich) was added to the molten agarose to obtain a final concentration of approximately 0.5 µg/ ml prior to casting the gel. Analytic samples were added to 5 µl of 6x blue/ orange loading dye (Promega; Southampton, UK) in distilled water (dH_2O) (made up to a total volume of 30 µl) before being loaded into the wells. For reference, a 1 kb DNA ladder (5 µl) (Promega) was also ran alongside. Electrophoresis was performed in 1x TAE buffer and bands visualised in an ultraviolet (UV) light trans-illuminator.

A 50x TAE buffer solution was made up from 242 g tris base, 57 ml of glacial acetic acid and 0.5M EDTA (pH 8.0), made up to a total volume of one litre with dH2O.

2.3.2 Low melting point gel electrophoresis

Low melting point (LMP) agarose gels were used for purification of DNA. LMP agarose gels (1%) were made using 1 g of electrophoresis grade LMP agarose powder (Invitrogen) in 100 ml 1x TAE buffer. EtBr was added to the molten agarose to obtain a final concentration of 0.5 μg/ ml prior to casting the gel. Electrophoresis was performed in 1x TAE buffer. The DNA bands were observed under low intensity UV light and appropriate gel bands excised with a knife. The DNA was purified from the gel using the GFX^{TM} PCR DNA and Gel Band purification kit, according to the manufacturer's protocol (GE Healthcare Life Sciences, Buckinghamshire, UK). DNA was eluted in 50 μl dH_2O and quantified using a NanoDrop® 1000 spectrophotometer (Thermo Scientific, DE, USA).

2.3.3 Restriction digests

5 μg of the plasmid DNA and appropriate amount of restriction enzyme(s) (all from New England Biolabs® Inc. (NEB) MA, USA), bovine serum albumin (BSA) and digestion buffer (supplied by NEB) were made up to a 50 μl volume digest with dH_2O. Digests were incubated for two hours at either 25 or 37^{o}C (depending on the optimum working temperature of the enzyme). 5 μl of the digest solution was analysed via agarose gel electrophoresis (section 2.3.1) to confirm that the desired division(s) had occurred. The simultaneous digestion of a plasmid with two different enzymes could only occur if their optimal working temperatures and buffers were identical. Where this was not the case, digests were performed in sequence, whereby DNA was extracted from buffer solution after the first digest (using the GFX^{TM} PCR DNA and Gel Band purification kit) and digested with the second restriction enzyme in a different buffer solution.

2.3.4 T4 DNA polymerase

T4 DNA polymerase was used for blunt end repair of DNA. 1 μl of T4 DNA polymerase (5 U/ μl) (NEB) was added directly to 50 μl of the restriction digest

(approximately 1U/ µg digested DNA), along with 2-3 µl of 10 mM deoxyribonucleotide triphosphates (dNTPs) (NEB). The reaction was incubated at 12^{o}C for 15 minutes and subsequently stopped by heat inactivation (75^{o}C for 20 minutes).

2.3.5 Antarctic phosphatase treatment

To remove 5' phosphate groups, 50 µl of the restriction digest was incubated for 30 minutes at 37^{o}C with 0.5 µl Antarctic phosphatase (AP) (1 U/ µl) (NEB) in 5.5 µl 10x dephosphorylation buffer (NEB).

2.3.6 Ligations

Ligations were carried out using 25-30 ng of vector with a quantified amount of purified insert at a ratio of 1:3 respectively. To this, 10 µl of 2x rapid DNA ligation buffer (Promega) and 1 µl of T4 high fidelity DNA ligase (3 U/ µl) (Promega) were added and the reaction made up to 20 µl with dH_2O. The mixture was incubated at 23^{o}C for a minimum of 30 minutes and then transformed into chemically competent E. coli cells (One Shot® TOP10, Invitrogen) (section 2.3.7). Linearised, dephosphorylated "no insert" controls were similarly processed.

2.3.7 Transformation of competent E. coli cells

5 µl of each ligation reaction (from section 2.3.6) was added to 50 µl thawed competent E. coli cells and the mixture incubated on ice for 10 minutes. Each reaction was heat shocked at 42^{o}C for 30 seconds, cooled for two minutes on ice, before adding 300 µl of standard Luria Bertani (LB) broth.

50 µl of transformed bacteria (per plate) was streaked out on LB agar plates containing 100 µg/ ml ampicillin (Sigma Aldrich) and incubated overnight at 37^{o}C.

For midi preparations, 50 µl of transformed bacteria was added to 50 ml LB media containing ampicillin (100 µg/ ml) and incubated overnight (12-16 hours) at 37°C in a flask shaker. Preparations were then pelleted by centrifugation at 5000 rpm for 15 minutes in a Beckman Coulter (High Wycombe, UK) refrigerated centrifuge. Pellets were stored at -20°C prior to purification.

2.3.8 Mini-preparation of plasmid DNA

Single colonies were picked from the LB agar plates and grown up overnight at 37°C in 5-10 ml LB broth containing ampicillin (100 µg/ ml). The culture was divided, centrifuged for three minutes at 12,000 rpm and supernatant discarded to create pellets (two pellets per 5 ml of overnight culture). Plasmid DNA was purified from the pelleted bacterial cells using the QIAprep© mini-prep kit (Qiagen, Manchester, UK) according to the manufacturer's protocol. DNA was eluted in 50 µl dH_2O and 5 µl of the sample was analysed by restriction digestion and subsequent agarose gel electrophoresis.

2.3.9 Midi-preparation of plasmid DNA

Midi-prepped DNA was obtained using the Hi-Speed Plasmid Midi Prep Kit (Qiagen) according to the manufacturer's protocol and the DNA eluted in 1 ml of dH_2O. The DNA was then precipitated for one hour at -80ºC in a solution made up by the addition of a 2x volume of 100% ethanol (EtOH) (i.e. 2 ml) and $1/10^{th}$ the original volume (100 µl) of 3M sodium hydroxyl acetate. After thawing, the DNA was pelleted following maximal speed centrifugation and washed once in 70% EtOH. The purified DNA was quantified using a NanoDrop® 1000 spectrophotometer.

2.3.10 Transfection of plasmid DNA

For the purposes of homologous recombination, CV1 cells were plated in 6-well plates (WPs) and incubated overnight to achieve 90% confluence. Each well was subsequently infected with 0.1 PFU/ cell of VVL15 in 1.5 ml of fresh sCM and incubated for a

further two hours. At this time, 0.4 µg of plasmid DNA per well was complexed with the Effectene® Transfection Reagent (Qiagen), according to the manufacturer's protocol. The transfection-complex mix (approximately 700 µl) was added drop-wise to a virally infected well. Forty eight hours later, cell lysate and supernatant were scrape-harvested and stored at -80ºC prior to plaque purification.

2.3.11 Viral DNA extraction

For the purposes of analytical polymerase chain reaction (PCR) or sequencing, viral DNA was extracted from cellular lysates or concentrated viral preparations using the QIAamp® DNA Blood Mini Kit (Qiagen), a column based extraction system, in accordance with the manufacturer's instructions. DNA was eluted in dH_2O and quantified using the Nanodrop® 1000 spectrophotometer.

2.3.12 PCR

PCR reactions were performed using primers listed in the appropriate results subsections. The following cycling conditions were applied to 25 µl reaction mixes.

Table 2.2 PCR cycle conditions

Step	Temperature	Time
1 Initial denaturation	94 °C	2 minutes
2 Denaturation	94 °C	30 seconds
3 Annealing*	52-54 °C	1 minute
4 Elongation	72 °C	1 minute
Go to 2, repeat 31 times		
5 Final elongation	72 °C	5 minutes
6 Hold	4 °C	Infinity

*The annealing temperature was adjusted according to the lowest melting temperature of each primer pair.

Each 25 µl reaction contained at least 10 ng of template DNA, 10 pmol of each primer (forward and reverse, manufactured on demand by Sigma Aldrich), 2.5 µl of 10x PCR reaction buffer (Roche, West Sussex, UK), 1 µl 10mM PCR nucleotide mix (NEB) and 0.5 µl High Fidelity PCR System (a mix of Taq DNA polymerase and a DNA polymerase with proof reading capacity) (3.5 U/ µl, Roche), with the rest made up by dH_2O. PCR cycles were performed following the program in table 2.2. PCR products were analysed via electrophoresis on a 1% agarose gel as described in section 2.3.1.

2.3.13 Homologous recombination and plaque purification

Each pUC19 (NEB) based VV super-shuttle vector was transfected, using an Effectene® based protocol (section 2.3.10), into near confluent monolayers of CV1 cells (in 6-WPs) that had been pre-infected with VVL15. Forty eight hours later, the presence of red fluorescence under green light confirmed expression of the relevant transgene cassette, either from free intracellular plasmid or from the relatively few vaccinia virions in which homologous recombination had been successful.

Cells and supernatant were harvested by scraping and freeze-thawed twice. 1 µl of this lysate was used to infect all six wells of a 6-WP containing CV1 cells grown to approximately 90% confluence. A further 48 hours later, each well was carefully scrutinized under green light, searching for those viral PFUs that fluoresced red. The colony was carefully picked by touching it with a 20 µl pipette tip after aspirating the media from the well. The tip was then submerged into a cryotube containing 250 µl of sCM. Following further freeze-thaw cycles, 5-20 µl of this virus solution was added to each well of a new 6-WP containing CV1 cells as before. This process was repeated until every PFU in a well fluoresced red; i.e. all viral colonies stemmed from novel recombinant virus. The viral lysate was then harvested and the purity of viral colonies confirmed by PCR analysis of extracted DNA.

50 µl of purified viral lysate was added to a T175 flask containing a near confluent CV1 cell monolayer. Following a further two days of incubation, cells and supernatant were scrape harvested, collected into 50 ml tubes and stored at -80ºC as a primary viral passage (PVP).

2.3.14 Mass viral production

Each PVP was rapidly freeze-thawed twice and used to infect between 36 to 40 T175 flasks containing near confluent monolayers of CV1 cells. Forty eight hours later, the infected CV1 cells were scrape harvested and through repeated rounds of centrifugation at 2000 rpm (at 4°C), collected into a single pellet. The pellet was washed in phosphate buffered saline (PBS), re-suspended in 12 ml of 10 mM Tris-HCl (pH 9.0) and stored at -80°C.

2.3.15 Viral purification

Each concentrated viral lysate suspension was freeze-thawed twice, transferred to a 40 ml Dounce homogeniser (Fisher Scientific, Loughborough, UK) and homogenised via 60 strokes. Solutions were then ultrasonicated for 30 seconds. Following centrifugation at 2000 rpm at 4°C for 5 minutes, the supernatant (containing released virion particles) was collected and diluted to a total volume of 30 ml with 10 mM Tris-HCl. The solution was divided into four; each layered gently onto 17 ml of 36% sucrose (w/v) in 10 mM Tris-HCl within a 36 ml Beckman ultracentrifuge tube (Beckman Coulter); and centrifuged at 13500 rpm at 4°C for 80 minutes. The pellets were re-suspended in 1-4 mls of viral re-suspension buffer (10% glycerol (w/v) in PBS containing 138 mM NaCl, pH 7.4). Each sample of purified virus was titrated via a TCID50 assay (see section 2.6).

2.4 The MTS cytotoxicity assay as a measure of *in vitro* oncolysis

Between 1000 and 2000 tumour cells in 90 µl of sCM were plated into individual wells of a 96-WP and incubated overnight. A starting quantity of 100 PFU/ cell in 10 µl sCM was added to the first column of wells; eight further 10-fold serial dilutions of virus were added across the plate. Wells containing sCM only, acted as positive controls i.e. 100% cell lysis, whereas wells containing uninfected cells were negative controls i.e. 0% cell lysis. The plate was incubated at 37°C in air with 5% CO_2. After six days, 20 µl

of 3-(4,5-dimethylthiazol-2-yl)-5-(3-carboxymethoxyphenyl)-2-(4-sulfophenyl)-2H-tetrazolium (MTS) (Promega) and phenazine methosulfate (PMS) (Promega) in a ratio of 20:1 respectively, was added to each well and further incubated for two to four hours. The absorbance of light at 490 nm wavelength for each well was obtained using an Opsys MR 96-WP reader (Dynex, VA, USA). Optical density (OD) comparisons with positive and negative controls enabled a viral dose-response (percentage tumour cell death) curve to be created on Prism 6 (GraphPad, CA, USA). The EC50 value was calculated as the number of PFU/ cell required to kill 50% of cells. Each virus-tumour cell experimental condition was performed in triplicate.

2.5 Viral replication

$2x10^5$ tumour cells were seeded into each well of a 6-WP (12 wells in total), in 2 ml of sCM per well. Twenty four hours later, an average live cell count/ well was calculated from harvesting and counting cells from three of the wells. Media was aspirated from the remaining wells and replaced with 2 ml of sCM containing 1 PFU/ cell of virus. Cells and supernatant were harvested from a triplicate set of wells at 24, 48 and 72 hours post infection and subjected to two freeze-thaw cycles prior to being stored at -80°C, ready to be titrated via TCID50 assays (section 2.6).

2.6 The TCID50 assay to quantify viral concentration

96-WPs were seeded with 8000 CV1 cells/ per well in 200 µl sCM and incubated overnight. A sample from each viral replicate was diluted 1000 fold in sCM and 20 µl/ well of this was mixed into the top row of the 96-WP. Ten fold serial dilutions were carried down to the penultimate row leaving the final row uninfected to act as a negative control. Plates were incubated for seven days, after which the number of infected wells per row was recorded. These values were used to calculate a viral titre in PFU/cell, using the Reed Muench method (333).

This protocol was also used to establish the concentration (PFU/ ml) of a batch of purified virus (following an initial $1x10^6$ fold dilution) and also to determine the amount of viral PFUs per gram of organ tissue following the systemic delivery of virus in bio-distribution experiments. In the latter case, each tissue homogenate was initially diluted five fold with DMEM.

2.7 Enzyme linked immunosorbent assay for the detection of viral induced chemokines and cytokines

The concentration of a cytokine/ chemokine in supernatant samples from virally infected cells or *ex vivo* cultured splenocytes was measured by enzyme linked immunosorbent assays (ELISAs), in accordance with the manufacturer's instructions. All reagents unless otherwise stated were provided by the manufacturer.

In brief, ELISAs consisted of a number of steps, between which plates were washed four times by submerging them in a large beaker of wash buffer (0.05% Tween 20® (Sigma Aldrich) in PBS). Ninety six well, flat bottomed ELISA plates were coated with 100 µl of capture antibody diluted in coat buffer, sealed and refrigerated at 4ºC overnight. Plates were washed and blocked with 200 µl per well of assay diluent (AD) (1% BSA in PBS) for one hour at room temperature (RT). Plates were washed; 100 µl of diluted (in AD) test samples/ antigen standards were added to each well and left at RT for two hours. Plates were washed; 100 µl of diluted biotinylated detection antibody was added to each well and left at RT for one hour. Plates were washed; 100 µl of diluted streptavidin horse radish peroxidase (S-HRP) was added to each well and left in the dark at RT for 30 minutes. After a final wash step, 100 µl/ well of a tetramethylbenzidine substrate solution was added and left in the dark for 15 minutes prior to the addition of 50 µl/ well of stop solution (2N H_2SO_4). Finally the absorbance of light at 450 nm wavelength for each well was obtained from an Opsys MR plate reader. Each concentration of standard or sample was performed in duplicate. Mean OD values for antigen standards were used to create curves from which sample concentrations were extrapolated. Table 2.3 lists the ELISA kits that were used during the course of this project

Table 2.3 A list of the single analyte ELISA kits used in the project

Cytokine/ Chemokine	Species	Company
GMCSF	Mouse	Biolegend®
GMCSF	Human	Biolegend®
GCSF	Mouse	R&D Systems™
IL1α	Mouse	Biolegend®
IL1β	Mouse	Biolegend®
IL4	Mouse	Biolegend®
IL12	Mouse	Biolegend®
IL12	Human	Biolegend®
IL10	Mouse	Biolegend®
IL15	Mouse	R&D Systems™
IL18	Mouse	R&D Systems™
KC (CXCL1)	Mouse	R&D Systems™
MIP-1α	Mouse	eBioscience®
IFNγ	Mouse	Biolegend®

Biolegend®, London, UK; R&D Systems™, Abingdon, UK; eBioscience®, Hatfield, UK

2.8 *Ex-vivo* stimulation of tumour-antigen specific T cells

2.8.1 Preparation of a single cell suspension of splenocytes from harvested spleens

Spleens from euthanized tumour bearing mice were harvested under sterile conditions via a midline laparotomy; mashed through 70 μm Becton Dickinson Falcon™ cell strainers (Beckton Dickinson biosciences, Oxford, UK) and flushed through with T cell culture media (tCM) (Roswell Park Memorial Institute (RPMI)-medium 1640 (Sigma Aldrich), 10% FCS, 1% streptomycin/ penicillin, 1% sodium pyruvate and 1% non-essential amino acids (Gibco®)) into 50 ml conical flasks. Splenocytes were re-suspended in 2 ml of red blood cell (RBC) lysis buffer (see below for recipe) following centrifugation at 1200 rpm and left at RT for five minutes. Following a wash, they were re-suspended with tCM to a final concentration of $5x10^6$ cells/ ml.

RBC lysis buffer was prepared as follows: 8.29 g of ammonium chloride (NH_4Cl) (0.15 M), 1 g of potassium bicarbonate ($KHCO_3$) (10 mM) and 37.2 mg of disodium ethylenediaminetetraacetate (Na_2EDTA) (0.1 mM) was dissolved dH_20 to a total volume of one litre and sterile filtered through a 0.2 μm mesh filter.

2.8.2 Preparation of growth arrested stimulator cells

Single cell suspensions of $5x10^6$ cells/ ml of stimulator tumour cells (target or control) were prepared in 50 ml conical tubes. A 1 mg/ ml solution of Mitomycin C (MMC) (Roche) was added to this suspension to achieve a final concentration of 100 μg/ ml and incubated in a humidified incubator at 37°C in air with 5% CO_2 for one hour. Cells were subsequently washed twice with 40 ml of PBS, re-suspended in 40 ml sCM and placed in the incubator until ready to seed (within 30-60 minutes). Live stimulator cells were finally re-suspended in tCM to achieve a final concentration of $5x10^5$ cells/ ml.

2.8.3 Assessment of T cell activation by measurement of IFNγ release

2.8.3.1 T cell activation by whole tumour cells

100 μl of splenocyte suspension was co-cultured with 100 μl of target stimulator cell suspension in duplicate wells of round bottomed 96-WPs (i.e. $5x10^5$ splenocytes with $5x10^4$ growth arrested tumour cells). Splenocyte only control wells contained $5x10^5$ splenocytes in 200 μl of tCM. To demonstrate tumour specificity, splenocytes were also co-cultured with 100 μl of tCM containing $5x10^4$ MHC compatible growth arrested control cells.

Plates were incubated at 37°C in air with 5% CO_2 for three days, after which they were centrifuged at 1200 rpm for five minutes. The concentration of IFNγ in supernatants taken from each of the wells was established by ELISA (Biolegend®). The final "stimulated" concentration of IFNγ per sample, averaged across duplicate wells, was

determined after deducting values from corresponding wells containing splenocytes alone.

2.8.3.2 T cell activation by peptides

Where indicated, 100 µl of splenocyte suspension was co-cultured with 100 µl of the working solution of individual peptides restricted to the H-2Kb or H-2Db Class I MHC (to which T cells from C57BL/6 mice can bind). Table 2.4 lists the peptides used in this project, all of which were obtained from Proimmune, Oxford, UK.

Table 2.4 A list of the peptides used to stimulate epitope specific T cells clones

Peptide epitope	Amino acid sequence	MHCI restriction
Chicken Ovalbumin	SIINFEKL	H-2Kb
Vaccinia WR B8R	TSYKFESV	H-2Kb
K-RAS	GADGVGKSA	H-2Kb
Mesothelin	GQKMNAQAI	H-2Db

Peptides were dissolved in dimethyl sulfoxide (DMSO) (Sigma Aldrich) to achieve a stock concentration of 5 µg/ ml. They were diluted a further 500 fold in tCM to achieve the working concentration. IFNγ concentrations following a three day incubation period were obtained by ELISA as detailed in section 2.8.3.1.

2.8.4 A non-radioactive LDH based cytotoxic T lymphocyte assay

Splenocyte suspensions were prepared from mice bearing SC tumours treated with virus or PBS (section 2.8.1) and were resuspended to $5x10^6$ cells/ ml. 1 ml aliquots of splenocytes from each experimental condition were co-cultured with 1 ml of $5x10^5$ cells/ ml of growth arrested stimulator cells (either LLC or DT6606 depending on the primary tumour model used) in each well of a 12-WP. Plates were incubated at 37°C in air with 5% CO_2 for five days.

Non adherent cells and media were carefully collected and samples from each experimental condition pooled. Cells were resuspended to a concentration of $3x10^6$ live cells/ ml in tCM. 100 µl of this suspension was added to 100 µl of live tumour cells ($5x10^4$ cells/ ml in tCM) in wells of 96 well V bottomed plates; thus establishing a top ratio of 60:1 effector (splenocyte) to tumour cell respectively.

Splenocyte cell suspensions were serially diluted by two fold and added to tumour cells in order to obtain effector: target ratios of 30:1 and 15:1. tCM containing splenocyte or tumour cells alone were similarly plated in order to calculate background signals. All samples were plated in quadruplicate. The plates were incubated at 37°C in air with 5% CO_2 for four hours. Plates were subsequently centrifuged at 250 g for one minute. 50 µl of supernatant from each well was transferred to a flat 96-WP. A non-radioactive colorimetric cytotoxicity assay kit (CytoTox 96®, Promega) was used (in accordance with the manufacturer's instructions) to measure lactate dehydrogenase (LDH) released from lysed cells. This relies on the conversion of a tetrazolium salt (INT) into a red formazon product. The mean absorbance of light at 490 nm wavelength for each well was quantified using an Opsys MR 96-WP reader.

Mean ODs (after deduction of background) from each experimental condition were divided by that derived from wells containing maximally lysed target/ control tumour cells to estimate the percentage of total lysis.

2.9 Preparation of harvested tissue for flow cytometry

1. Single cell splenocyte suspensions (section 2.8.1)

2. Single cell suspensions of blood leucocytes (section 2.9.1)

3. Single tumour cell suspensions from SC LLC or DT6606 tumours (section 2.9.2)

4. Single cell suspensions of murine bone marrow derived DCs/ monocytes (section 2.9.3)

2.9.1 Single cell suspensions of blood leucocytes

Following sacrifice of a mouse via CO_2 inhalation, a laparotomy was promptly performed; bowel and omentum were gently moved aside and blood was extracted via hepatic vein cannulation with a 23 gauge blue needle connected to a 1 ml syringe. Blood samples were added to 200 µl of heparin (50 µg/ ml) (Sigma Aldrich) in 1.5 ml microcentrifuge tubes to prevent coagulation. 0.5 to 1 ml of RBC lysis buffer (section 2.8.1) was added to each sample and left to stand for five minutes at RT. After centrifugation at 200 rpm, pellets were resuspended in 1 ml of RBC lysis buffer and left again for a similar time. Large clots or clumps of dead cells were removed by filtration of the solution through 70 µm cell strainers into 50 ml tubes. Leucocytes were resuspended to a final concentration of $1x10^6$ cells/ ml in flow cytometry buffer (FB) (1% FCS in PBS); ready to be stained by fluorophore labelled antibodies.

2.9.2 Single tumour cell suspensions from SC LLC or DT6606 tumours

A SC tumour from a sacrificed mouse was carefully dissected out, in a disinfected environment, and placed in one well of a 6-WP, in 2 ml of collagenase D (1 mg/ ml) (Roche) and DNAse I (0.1 mg/ ml) (Roche) in PBS. Debris (skin, hair, fat) was carefully removed and the remaining tumour tissue cut into fine 1-3 mm cubes. The plate was incubated at 37ºC in a shaker for up to two hours, until tissue disaggregation was complete. Homogenates were repeatedly pipetted through a 1 ml tip and then filtered through 70 µm cell strainers into 50 ml tubes. Following a PBS wash, tumour cell pellets were re-suspended to a final concentration of $1x10^6$ cells /ml in FB, ready to be stained by fluorophore labelled antibodies.

2.9.3 Single cell suspensions of murine bone marrow derived DCs/ monocytes

Murine monocyte-colony stimulating factor (M-CSF) or GMCSF (Roche) was added to bone marrow culture medium (mCM; RPMI-1640, 1% sodium pyruvate, 1% non-essential amino acids, 1% penicillin streptomycin and 0.1% β-mercaptoethanol) to obtain a stock concentration of 30 ng/ ml.

Six to seven week old C57BL/6 mice were sacrificed via CO_2 inhalation. Subsequent dissection took place in a disinfected environment. The femur and tibia of both hind legs were denuded of skin and muscle tissue, dissected out of the mouse and placed in a petri dish containing mCM. The ends of the bones were amputated to expose the red marrow which was then flushed with mCM into a mini dish using a 23G needle attached to a 3 ml syringe. The cells were homogenised further with the needle and syringe to create a uniform suspension and filtered through 70 μm cell strainers into 50 ml centrifugation tubes (one per mouse). Cells were centrifuged at 1300 rpm, resuspended in 2 mls of RBC lysis buffer and left for five minutes at RT. Following a wash cycle with RPMI-1640, cell suspensions from each mouse were split into two and each resuspended to a total volume of 50 mls with mCM containing either M-CSF (monocyte sample) or GMCSF (DC sample).

The monocyte sample was divided into five sterile, "non-culture" 10 cm petri dishes (approximately 10 ml per dish). They were incubated at 37°C in air with 5% CO_2. The media was topped up by 2.5 to 5 ml of M-CSF containing mCM every two to three days (M-CSF was added to the media to maintain an approximate concentration of 30 ng/ ml in the plate). At day seven or eight, adherent monocytes were washed with PBS, gently scraped from the plates and re-suspended in growth factor free mCM.

A similar protocol was followed for the DC sample using GMCSF containing mCM. This was divided and plated into five, 10 cm diameter sterile "culture" dishes. On day three, the supernatant and loose cells in each plate were discarded. Adherent cells were washed with PBS and replenished with mCM containing GMCSF. By day seven or eight, the non/ loosely adherent DCs were ready to use.

To confirm the purity of this enrichment process, cells were stained with fluorophore labelled antibodies that specified DCs (CD11c+MHCII+) and monocyte (CD11b+F4/80+) populations (section 2.10).

2.10 Flow cytometric analysis of cellular suspensions

Approximately $1x10^6$ cells from each suspension were plated into each well of a V bottomed 96-WP. Control samples were derived from a pool of all the different treatment conditions and were stained with fluorescence minus one (FMO) combinations of target antibodies. For the purposes of compensating for light spill over from neighbouring channels in the flow cytometer, control samples were also singly stained with antibodies attached to each of the different fluorophores used.

Plated cells were washed twice with 150 µl FB; each plate was centrifuged at 1500 rpm at 4°C for three to five minutes per wash cycle. All antibodies were acquired from eBioscience® and were diluted 200 fold in FB. After discarding the supernatant, cells were re-suspended in 100 µl Fc block (anti-CD16/32) and incubated for 15 minutes at 4°C in the dark. After a wash cycle with FB, each pellet from experimental wells was resuspended in 100 µl of the diluted antibody master mix solution. The plate was left on ice for 45 minutes in the dark. Antibody stained cells were washed a further three times with FB, re-suspended in 200 µl 2% formaldehyde (in PBS) and transferred into 1.2 ml cluster tubes (Qiagen). These were stored at 4°C in the dark for less than 24 hours and analysed in an LSRFortessa™ multichannel flow cytometer (Becton Dickinson). The raw data was analysed using FloJo v10 (FloJo, LLC. Or, USA).

Table 2.5 Fluorophore labelled antibodies used for flow cytometry

Antibody (anti-mouse)	Species	Clone	Labelled fluorophore	Dilution (from X mg/ml)
Fc Block				
CD16/32	Rat	93	Unlabelled	1:200 (0.5mg/ml)
The common leukocyte antigen				
CD45	Rat	30-F11	eFluor® 450	1:200 (0.2mg/ml)
CD45	Rat	30-F11	FITC	1:200 (0.5mg/ml)
CD45	Rat	30-F11	APC-eFluor® 780	1:200 (0.2mg/ml)
Lymphocyte markers				
CD3e	Rat	145-2C11	PerCP-Cy5.5	1:200 (0.2mg/ml)
CD3	Rat	17A2	FITC	1:200 (0.5mg/ml)
CD8a	Rat	53-6.7	FITC	1:200 (0.5mg/ml)
CD8a	Rat	53-6.7	APC	1:200 (0.2mg/ml)
CD44	Rat	IM7	APC	1:200 (0.2mg/ml)
CD44	Rat	IM7	eFluor® 450	1:200 (0.2mg/ml)
CD62L	Rat	MEL-14	PE-Cy7	1:200 (0.2mg/ml)
CD49b	Rat	DX5	PE	1:200 (0.2mg/ml)
Myeloid cell markers				
CD11b	Rat	M1/70	PerCP-Cy5.5	1:200 (0.2mg/ml)
Gr1 (Ly-6G)	Rat	RB6-8C5	Alexa Fluor® 700	1:200 (0.2mg/ml)
F4/80	Rat	BM8	PE-Cy7	1:200 (0.2mg/ml)
Antigen presenting cells (APCs)				
CD11c	Armenian Hamster	N418	PE	1:200 (0.2mg/ml)
CD11c	Armenian Hamster	N418	Alexa Fluor® 700	1:200 (0.2mg/ml)
MHCII	Rat	M5/114.15.2	FITC	1:200 (0.5mg/ml)
CD80 (B7-1)	Armenian Hamster	16-10A1	PE	1:200 (0.2mg/ml)
CD86 (B7-2)	Rat	GL1	APC	1:200 (0.2mg/ml)

2.10.1 Pentamer staining of mesothelin epitope specific CD8+ T cell clones.

A custom built pentamer consisting of phycoerythrin (PE) labelled Pro5® H-2Db class I MHC complexed to the mesothelin epitope, GQKMNAQAI (Proimmune©) was used to identify its complementary clone of CD8+ T cells. The staining protocol was identical to that with the fluorophore labelled antibodies outlined above, with an additional step. 5 µl of pentamer, made up to 100 µl in FB, was used to resuspend the relevant pellet of splenocytes after the initial wash and was left at RT for 10 minutes. Cells were subsequently treated as described in section 2.10 with Fc block and stained with the other antibodies.

2.11 Measurement of activation of virus infected bone marrow derived monocytes and DCs.

Monocytes/ DCs were stained with fluorophore labelled antibodies against class II MHC and/ or CD80 and CD86 cell surface co stimulator molecules, at various times post viral infection (see the relevant results sections for details).

$1x10^6$ cells of monocytes or DCs in 2 ml mCM/ well were plated in triplicate wells of a 6-WP. Following a two hour incubation period 1 PFU/ cell of virus in 500 µl of mCM was added to each well. At each time point, cells were gently scrape-harvested, washed in FB, stained with the relevant antibody cocktail and analysed as described in section 2.10.

2.12 A screen of chemokines/ cytokines secreted within viral treated LLC tumours

A stock solution of tissue extraction buffer (TEB) containing a proteinase inhibitor cocktail solution and EDTA (inhibits metalloproteinases) was prepared by dissolving one cOmplete ULTRA mini tablet (Roche) into 10 mls of 50 mM Tris-HCl at pH 7.4. Tumours from euthanized mice were carefully harvested from flanks, leaving behind as

much skin as possible and placed into 2 ml cryotubes. Following the addition of a small volume of TEB they were homogenised with an Ultra-Turrax® (IKA®, Staufen, Germany) homogeniser (at 12000 rpm) for 30 seconds, diluted 10 fold w/v in 15 ml centrifuge tubes and finally centrifuged at high speed (6000 rpm) for 5 minutes. Supernatants were carefully removed without disturbing the pellet and their total protein concentration (g/ ml) was obtained using the NanoDrop® 1000 Spectrophotometer.

Each sample was diluted in 1% BSA in PBS and simultaneously screened for a panel of 12 chemokines or cytokines using Qiagen® Multi-analyte ELISArray kits: inflammatory cytokines or common chemokines. These consisted of 96 well plates, comprised of eight, 12-well strips that were pre-coated with 12 different capture antibodies against the different chemokines or cytokines. All reagents including standards and wash buffer were provided by the manufacturer. Each experimental sample was plated in triplicate. A standard protocol for a sandwich ELISA was performed as per the manufacturer's instructions.

The absorbance of light at 450 nm wavelength for each well was obtained from an Opsys MR plate reader; an arbitrary OD value per gram of tumour protein was calculated and subsequently normalised to the corresponding mean value of the VVL15 treatment group.

If there were any consistent differences between the levels of a particular cytokine or chemokine across time, then further quantitative analyses were performed on supernatants taken from *in vitro* infected tumour cells or APCs (see below) using the relevant single analyte ELISA kit.

2.13 Cytokine release from monocytes, DCs and tumour cells following infection with recombinant virus

$1x10^5$ bone marrow derived monocytes or DCs and murine tumour cell lines (LLC or DT6606) were plated (in 200 µl of tCM or sCM per well respectively) in triplicate, into flat bottomed 96-WPs and incubated at 37ºC in air with 5% CO_2. Two hours later, 1

PFU/ cell of virus in 50 µl of the appropriate CM or CM alone was added to each well. At 24 and 48 hours post infection, single analyte ELISAs were performed on the supernatant to determine the concentration of the specific cytokines as indicated in the results subsections (see also section 2.7).

2.14 Histological analysis of virally infected tumours

All histology including immunohistochemistry was performed by George Elliah (Pathology department, BCI, QMUL). This included the processing of formaldehyde fixed and snap frozen samples and the optimisation of all primary antibodies used for immunohistochemistry (IHC). All slides were subsequently reviewed by Jahangir Ahmed (JA) or Yaohe Wang (YW).

Specimens that had been fixed with 4% formaldehyde (for at least 24 hours) were washed with 70% EtOH, paraffin embedded and cut into 4 µm sections with a Leica EG1160 microtome (Leica Microsystems UK Ltd, Milton Keynes, UK). Cut sections were stained with haematoxylin and eosin (H&E) in accordance with standard protocols on a Leica autostainer XL.

Snap frozen specimens were cut to widths of 6 µm, air dried at RT and fixed in neutral buffered formalin. IHC staining was performed using the Ventana® Discovery staining system (Ventana Medical Systems Inc. Az, USA). All primary antibodies were rat antimouse antibodies and had been previously optimised using frozen sections of mouse spleen. They are listed in table 2.6. The staining layer comprised of secondary biotinylated rabbit anti rat antibody (AI 4001, Vector laboratories UK, Peterborough, UK) to which S-HRP (Omnimap, Roche) could conjugate. The latter catalyses the oxidation of the chromogenic substrate, 3, 3' diaminobenzidine tetrahydrochloride (DAB) (Roche) by hydrogen peroxide to produce a dark brown stain, visible on light microscopy.

Light microscopy was performed using an Olympus BX-51 microscope (Olympus, Southend on Sea, UK) in conjunction with a digital camera (Pixera, Bourne End, UK).

Images were acquired under a 20x objective (200x overall magnification) and visualised on a PC through the Pixera viewfinder. Quantification of cells positive for a particular surface antigen was performed by averaging independent manual cell counts from 10 to 15 randomly selected high power fields (HPFs) depending on the size of the histological section.

Table 2.6 Antibodies used for purposes of immunohistochemistry

Antibody against	Species	clone	Optimised dilution (from 0.5mg/ml)	Company
CD4	Rat	GK 1.5	1:200	Biolegend®
CD8a	Rat	53-6.7	1:300	Biolegend®
NK1.1	Rat	PK 136	1:50	Biolegend®
F4/80	Rat	CI:A3-1	1:2000	AbD Serotec®

2.15 Establishment of *in vivo* models

Unless otherwise specified, studies with live animals were conducted at the biological services unit (BSU), BCI by JA. All other experiments were conducted at the Sino-British Research Centre for Molecular Oncology (SBRCMO), Zhengzhou University, Henan Province, China, according to protocols designed by JA. All animals were treated in accordance with UK home office regulations (334). Tumour volumes were calculated as $w^2 \times l \times \pi/6$, where w is the maximal width at 90 degrees to the maximal length l.

The following syngeneic murine models were used:
CT26 (colon cancer) cells in BALB/c mice
SCCVII (head and neck squamous cancer) cells in C3/HeN mice
4T1 (metastatic breast cancer) cells in BALB/c mice (performed at the SBRCMO)
DT6606/ DT6606-Ova (pancreatic cancer), CMT93 (rectal cancer) and LLC (lung cancer) cells in C57BL/6 mice

2.15.1 Establishment and IT treatment of subcutaneous syngeneic tumour models

The relevant number of tumour cells (see table 2.7 and table 2.8) in 100 µl of serum free DMEM were injected subcutaneously into the shaved right flanks of six to seven week old BALB/c, C3/HeN or C57BL/6 mice. When tumours were approximately 100 mm^3 in volume, mice were randomized into treatment groups. Doses of $1x10^8$ PFU of virus in 50 µl of PBS were injected IT using a 1 ml insulin syringe attached to a 29 gauge needle (dosing schedules varied depending on the experiment). The needle was passed a number of times in different directions throughout the tumour prior to virus deployment for broad dissemination. Control groups were injected with the equivalent volume of vehicle buffer i.e. 50 µl of PBS.

Tumour volumes were monitored via twice weekly calliper measurement when mice were also weighed. Animal models were euthanized via CO_2 inhalation at appropriate time points post-infection (see specific experiments) or when the tumour volume exceeded that stipulated by UK home office guidance.

Table 2.7 Biological time-point experiments

See text for details, n=3-4 mice per treatment group per time-point.

No.	Model	Mouse	Cell no./route	Definition of day 0	One dose	Schedule (day/ route)	Additional procedures	Time-point (s) (day)
1	LLC	C57BL/6	$1x10^6$ SC	Tumour 100 mm^3	$1x10^8$ PFU Virus/ 50µl PBS	0/ IT		1, 3, 5, 7, 14 (depending on experiment)
2	DT6606	C57BL/6	$3x10^6$ SC	Tumour 100 mm^3	$1x10^8$ PFU Virus/ 50µl PBS	0/ IT		7, 14, 21 (depending on experiment)
3	DT6606-Ova	C57BL/6	$3x10^6$ SC	Tumour 100 mm^3	$1x10^8$ PFU Virus/ 50µl PBS	0/ IT		14
4	DT6606	C57BL/6	$3x10^6$ SC	Tumour 100 mm^3	$1x10^8$ PFU Virus/ 50µl PBS	0,1,2,3,4/ IT		14
5	LLC	C57BL/6	$1x10^6$ SC	IV virus injection	$1x10^8$ PFU Virus/ 50µl PBS	0/ IV		1, 3, 5, 8, 11
6	CT26	BALB/c	$2x10^6$ SC	IV virus injection	$1x10^8$ PFU Virus/ 50µl PBS Virus/	0/ IV		1, 3, 7, 10
7	LLC	C57BL/6	$1x10^6$ SC	Tumour 100 mm^3	$1x10^8$ PFU Virus/ 50µl PBS	0,1,2,3,4/ IT		Sacrificial endpoint
8	LLC	C57BL/6	$1x10^6$ SC	Tumour 100 mm^3	$1x10^8$ PFU Virus/ 50µl PBS	0,1,2,3,4/ IT	Day 11: Tumour excision	18

Table 2.8 Intratumourally treated syngeneic flank tumour models to demonstrate efficacy

See text for details, n=5-7 mice per treatment group

No.	Model	Mouse	Cell no./ route	Definition of day 0	One dose	Schedule (day/ route)	Additional procedures	End-point
1	LLC	C57BL/6	$1x10^6$ SC	Tumour 100 mm^3	$1x10^8$ PFU Virus/ 50µl PBS	0,1,2,3,4/ IT	Thoracotomy	Tumour >1200 mm^3
2	SCCVII	C3/HeN	$2x10^6$ SC	Tumour 100 mm^3	$1x10^8$ PFU Virus/ 50µl PBS	0,1,2,3,4/ IT		Tumour >1200 mm^3
3	CMT93	C57BL/6	$5x10^6$ SC	Tumour 100 mm^3	$1x10^8$ PFU Virus/ 50µl PBS	0,1,2,3,4/ IT		Tumour >1200 mm^3
4	CT26	BALB/c	$2x10^6$ SC	Tumour 100 mm^3	$1x10^8$ PFU Virus/ 50µl PBS	0,1,2,3,4/ IT		Tumour >1200 mm^3
5	DT6606	C57BL/6	$3x10^6$ SC	Tumour 100 mm^3	$1x10^8$ PFU Virus/ 50µl PBS	0,1,2,3,4/ IT		Tumour >1200 mm^3
6	DT6606 (Sequential virus)	C57BL/6	$3x10^6$ SC	Tumour 100 mm^3	$1x10^8$ PFU Virus/ 50µl PBS	Virus A: 0,1,2/ IT Virus B: 4,5,6/ IT (see text)		Tumour >1200 mm^3

2.15.2 Assessment of viral biological distribution following IV virus into tumour bearing mice

Following the establishment of SC CT26 or LLC syngeneic flank tumours, $1x10^8$ PFU (in 50 µl PBS) of either VVL15 or VVL15ΔN1L was injected via tail vein. At various times post virus injection (table 2.7, experiments 5 and 6), three mice from each group were sacrificed via CO_2 inhalation. The following organs were harvested: tumour, brain, lung, liver, spleen, kidneys and ovaries. They were immediately snap-frozen in precooled (to -80°C) isopentane. Samples were subsequently thawed, weighed and homogenised using an Ultra-Turrax® homogeniser (at 12000 rpm) in a small volume of serum-free DMEM. Samples were diluted five fold w/v (i.e. 5 µl DMEM per mg). After a further freeze-thaw cycle, tissue homogenates were titrated for live viral PFUs using the TCID50 assay described in section 2.6.

2.15.3 Efficacy of VVL recombinants against an orthotopic lung cancer model

$5x10^5$ LLC cells in 100 µl PBS were injected into the tail veins of seven week old C57BL/6 mice. Repeated, non-contrast CT scans of the lungs were used to assess lung volumes of individual mice over a period of 21 days and any reduction used to extrapolate tumour burden. When tumour was initially present on CT, the first of three IV doses of virus/ PBS was administered as outlined in table 2.9, experiment 3. Mice were weighed twice weekly and were sacrificed if they showed signs of distress or if weight loss exceeded 20% of their maximal weight.

Table 2.9 Viral treatment of syngeneic orthotopic and surgical models of cancer. See text for details, n=7-10 mice per treatment group.

.No.	Model	Mouse	Cell no./ route	Definition of day 0	One dose	Schedule (day/ route)	Additional procedures	End-point
1	LLC (IT neoadjuvant)	C57BL/6	$1x10^6$ SC	Tumour 100 mm^3	$1x10^8$ PFU Virus/ 50µl PBS	0,1,2,3,4/ IT	Day 11: Tumour excision Thoracotomy	Weight loss >20% Tumour regrowth Signs of distress
2	4T1 (Orthotopic breast)	BALB/c	$1x10^5$ SC (into mammary fat pad)	Tumour 50 mm^3	$1x10^8$ PFU Virus/ 50µl PBS	0, 2, 4/ IT	Day 9: Tumour excision Thoracotomy	Weight loss >20% Tumour regrowth
3	LLC (Orthotopic lung)	C57BL/6	$5x10^5$ IV	LLC cell injection	$1x10^8$ PFU Virus/ 50µl PBS	5, 7, 9/ IV	CT lungs Thoracotomy	Weight loss >20% Signs of distress

Table 2.10 Schedule of treatment of tumour models with immune cell subset depletion. See text for details, n=7-10 per treatment group. IP: intraperitoneal.

No.	Model	Mouse	Cell no./ route	Definition of day 0	Treatment	Schedule (day/ route)	Additional procedures	End-point
1	DT6606	C57BL/6	$3x10^6$ SC	Tumour 100 mm^3	$1x10^8$ PFU VVL15ΔN1L	0,1,2,3,4/ IT	IP 200 µg cell depleting antibody or control IgG: Day: -1, 3, 7, 11...end of experiment	Tumour >1200 mm^3
2	LLC	C57BL/6	$1x10^6$ SC	Tumour 100 mm^3	$1x10^8$ PFU VVL15ΔN1L	0,1,2,3,4/ IT	IP 200 µg cell depleting antibody or control IgG: Day: -1, 3, 7, 11...end of experiment Day 11: Tumour excision Thoracotomy	Weight loss >20% Tumour regrowth Signs of distress

2.15.4 Efficacy of VVL recombinants against a spontaneously metastatic lung cancer model

Syngeneic flank LLC tumours were established and randomised into the appropriate number of treatment groups (section 2.15.1). Injections of recombinant virus/ PBS were administered IT as per the treatment schedule in table 2.7, experiment 7. Tumours were monitored via calliper until a group reached the sacrificial end point. All animals were euthanized at the same time; their lungs were harvested and any gross tumour deposits noted. Lung lobes were separated and fixed in 4% formaldehyde. They were subsequently embedded in paraffin, sectioned through the largest cross sectional dimension and stained with H&E (performed by George Elliah in the BCI pathology unit). For each lobe, slices were also performed above and below the largest cross section. All three sections were scrutinized for tumour deposits by an experienced pathologist (YW) who was blinded to the treatment schedule.

2.15.5 Efficacy of pre-surgical neoadjuvant recombinant VVL treatment against spontaneously metastatic tumour models

Syngeneic LLC lung or 4T1 breast tumour models were established in the flanks or mammary glands of seven week old female mice respectively (table 2.9, experiments 1 and 2). The latter experiment was performed at the SBRCMO, China. Following randomisation into treatment groups, the tumour bearing mice were treated with IT virus/ PBS (see table 2.9).

Five or seven days after the final dose of virus as indicated (table 2.9), tumours were carefully excised under general anaesthetic (continuous isofluorane and nitrous oxide via nose cone) and wounds were closed primarily with interrupted 4-0 monocryl absorbable sutures (Ethicon, Livingston, UK). Mice that suffered from surgical complications e.g. wound infection/ dehiscence were excluded. To capture regrowth from minimal microscopic residual disease, any tumour that clinically regrew within a week of the operation were also excluded. Mice were followed up via twice weekly

weight measurements and assessment of general well-being. All sacrificed mice had thoracotomies to confirm whether their likely cause of demise was due to overt lung metastases.

At the end point of the experiment with LLC tumours (day 60 post op), surviving animals were re-challenged with a subcutaneous injection of $2x10^6$ LLC cells in 100 µl serum free DMEM and assessed for tumour regrowth. A further 14 days later all mice were sacrificed and harvested splenocytes were tested for the presence of antitumour memory T cells using the IFNγ immunoassay described in section 2.8.3.1.

In a separate biological time-point experiment, syngeneic LLC tumour bearing mice were established and treated as above with similar criteria for exclusion. Mice were sacrificed seven days after resection (approximately 14 days following the final dose of IT virus) (table 2.7, experiment 8). Harvested splenocytes were tested for the presence of antitumour T cells using the IFNγ immunoassay described in section 2.8.3.1.

2.15.6 Immune cell subset depletion protocol

These experiments were conducted at the SBRCMO, China. The VVL15ΔN1L treatment arms of experiment 5 in table 2.8 (IT therapy of DT6606 flank tumours) and experiment 1 in table 2.9 (IT neoadjuvant therapy prior to surgical resection of LLC flank tumours) were repeated under the following conditions: depletion of NK, CD4+ or CD8+ cells. Table 2.11 lists the IgG clones of antibodies used. All antibodies were derived from in-house cultured hybridomas.

A single 200 µg intraperitoneal dose of cell depleting antibody caused a reduction of over 90% of the relevant splenic cell population (measured 48 hours later), when compared to mice treated with IgG control antibody (data not shown).

Intraperitoneal antibody was commenced when tumour growth approached 100 mm^3, a day prior to the initial dose of VVL15ΔN1L. Control rat IgG and PBS treatment (no antibody) groups were also included (see table 2.10 for treatment schedules).

Table 2.11 Antibodies used for *in vivo* immune cell subset depletion

Antibody against cell	Species	IgG clone	Volume per dose (1 mg/ ml)
CD4	Rat	GK 1.5	200 µl
CD8	Rat	TIB210	200 µl
NK	Rat	PK 136	200 µl

2.16 Statistical Analysis

GraphPad Prism 6 was used for comparative statistical analysis. Dual condition comparisons were made using the unpaired student t-test. For more than one condition or for an additional variable such as time, one or two-way ANOVAs respectively were performed. A post hoc Tukey test compared pairs of conditions. For the purpose of comparing specific treatment pairs when data was categorical, the Fisher's exact test was used following sub-classification into multiple 2x2 tables. Survival data was represented as a Kaplan-Meier plot with log rank analyses to delineate whether any differences between specific treatment pairs were statistically significant.

Key to significance level characters used in the thesis:

* $P \leq 0.05$

** $P \leq 0.01$

*** $P \leq 0.001$

**** $P \leq 0.0001$

Chapter 3 Results

3.1 Construction and *in vitro* validation of N1L(L025) deleted and cytokine-armed VVL15 recombinant viruses

3.1.1 Creation of pUC19 based VV super-shuttle vectors -summary

Murine and human cytokine transgenes were incorporated into the VVL15 (luciferase) backbone via homologous recombination. This process involved creating plasmid super-shuttle vectors containing the relevant transgene(s), straddled on either side by short sequences homologous to those flanking the insert position within the virus. Recombination with virus would effectively delete the intervening viral DNA between these "left" and "right" arm sequences, replacing it with the transgene(s).

Specifically, transgene cassettes designed to replace the L025 (N1L) coding region were constructed via standard cloning techniques (see below) and incorporated into VV specific super-shuttle vectors, based on the pUC19 plasmid vector (NEB, figure 3.2). RFP plus/ minus cytokine transgenes were designed to be individually driven by the constitutively stimulated VV H5 transcription factor promoter (335). Each transgene cassette was straddled on either side by sequences homologous to that on the extreme left and right of the L025 gene and included code belonging to the L024 and L026 ORFs respectively.

The following murine transgene super-shuttle vectors had already been constructed by Dr Ming Yuan in our group:

pUC19-LA-H5-mGMCSF-H5-RFP-H5-RA

pUC19-LA-H5-H5-RFP-H5-mIL12-RA

Three further super-shuttle vectors were constructed as part of the current project by JA:

pUC19- LA-H5-H5-RFP-H5- RA

pUC19- LA-H5-H5-RFP-H5-hGMCSF- RA

pUC19- LA-H5-H5-RFP-H5-hIL12- RA

Key:

LA: left arm sequence of L025

RA: right arm sequence of L025

RFP: ORF sequence of DSRed Express 2 (Clontech labs Inc. CA, USA)

H5: the VV H5 transcription factor promoter

mGMCSF/ hGMCSF: murine or human GMCSF transgenes respectively

mIL12/ hIL12: murine or human IL12 transgenes respectively

3.1.2 Detailed steps in the construction of VVL15ΔN1L and the human cytokine transgene armed N1L gene deleted viruses

The following shuttle vectors had previously been constructed by Dr Ming Yuan:

pGEM-T-H5-RFP- H5 (figure 3.1)

pGEM-T-LA-H5 (figure 3.1)

pUC19-RA (figure 3.2)

See figure 3.1 and figure 3.2 for maps of the parent pGEM-T Easy (Promega) and pUC19 cloning vectors respectively.

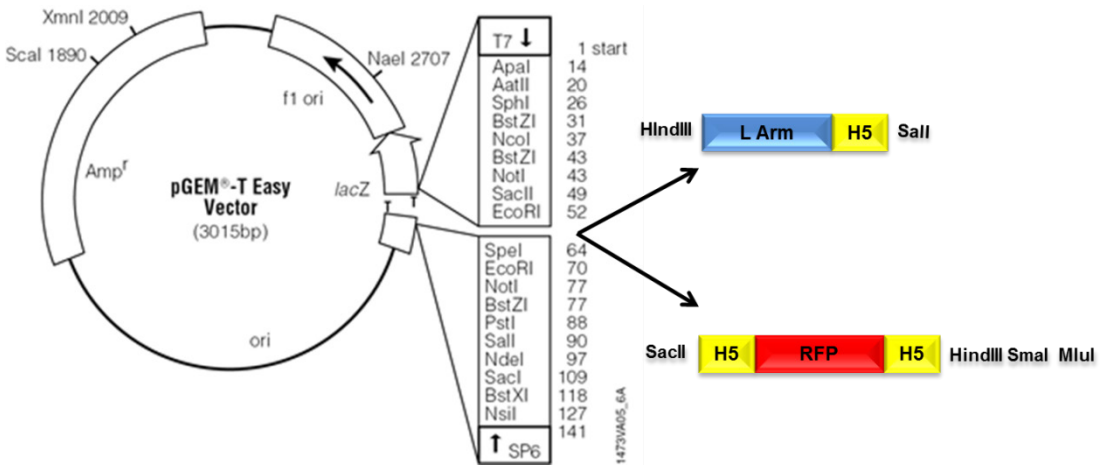

Figure 3.1 pGEM®-T Easy based shuttle vectors

The left arm sequence of the L025 gene (L Arm) and the RFP coding sequence had previously been cloned into the pGEM®-T Easy platform. Note relevant restriction sites on either side of the transgene insert. See text for further details and abbreviations.

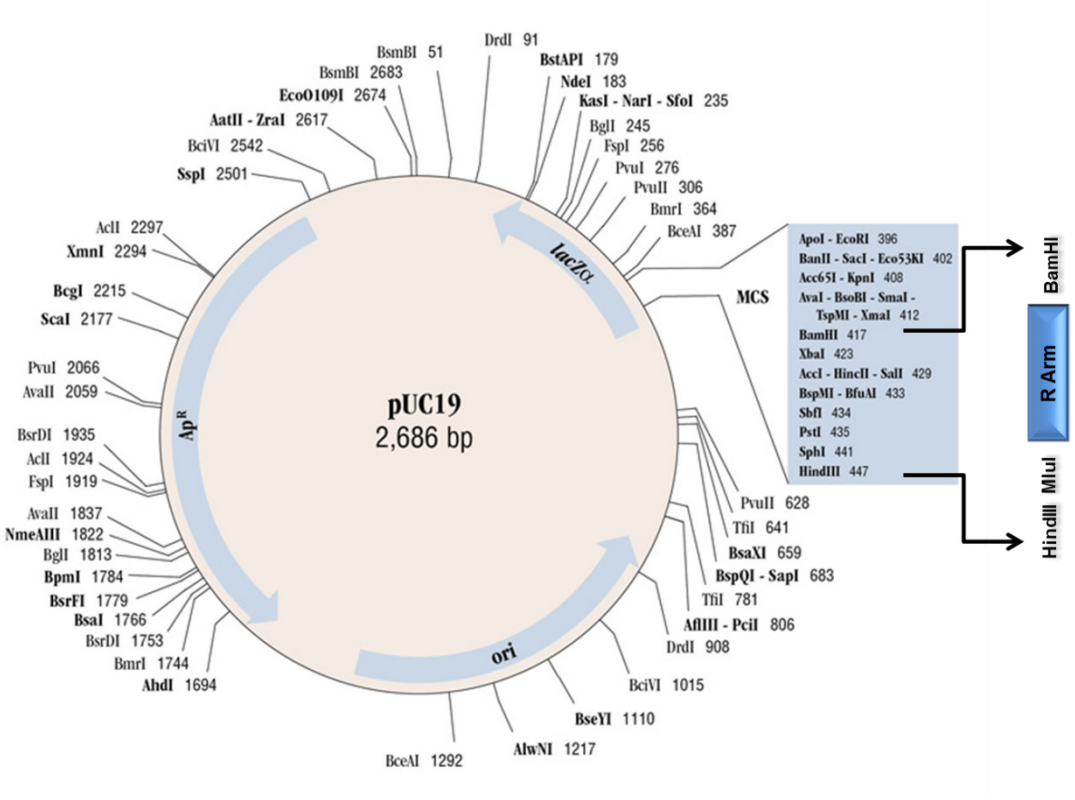

Figure 3.2 Right arm sequence of the L025 gene within the pUC19 (NEB®) vector

Note the relevant restriction enzymes used to clone the transgene into the multiple cloning site (MCS) of the plasmid. See text for details.

Further plasmids were purchased from the companies indicated:

pORF-hGMCSF (InvivoGen, Toulouse, France)

pORF-hIL12 (InvivoGen)

pCMV-DsRed-Express 2 (Clontech labs Inc.)

3.1.2.1 Step 1. Construction of the shuttle vector: pGEM-T-H5-RFP-H5-hGMCSF

The following plasmid vectors were amplified and purified as described in the methods (sections 2.3.7, 2.3.8 and 2.3.9):

1. pGEM-T *(SacII)*-H5-RFP-H5-*(HindIII SmaI MluI)*
2. pORF-*(HindIII)*-hGMCSF-(*SwaI*)

Note the relevant restriction sites used for cloning in brackets. All restriction enzymes were purchased from New England Biolabs® Inc. (NEB).

Vector 1 above was opened by sequential digestion with *HindIII* and *SmaI* enzymes (section 2.3.3, figure 3.3). *SmaI* digestion leaves blunt ended cuts. The final linearised DNA was 5' de-phosphorylated (with Antarctic phosphatase) to prevent re-annealing. Following electrophoresis in a LMW agarose gel, the DNA was cut out, extracted from the gel and quantified (section 2.3.2).

The hGMCSF insert fragment was similarly extracted from its parent plasmid (vector 2, above and figure 3.3) by sequential digestion with *HindIII* and *SwaI* enzymes. The latter enzyme also leaves blunt ends. It was subsequently ligated to the open vector 1, in a ratio of 3:1 (insert: vector), using T4 high fidelity ligase.

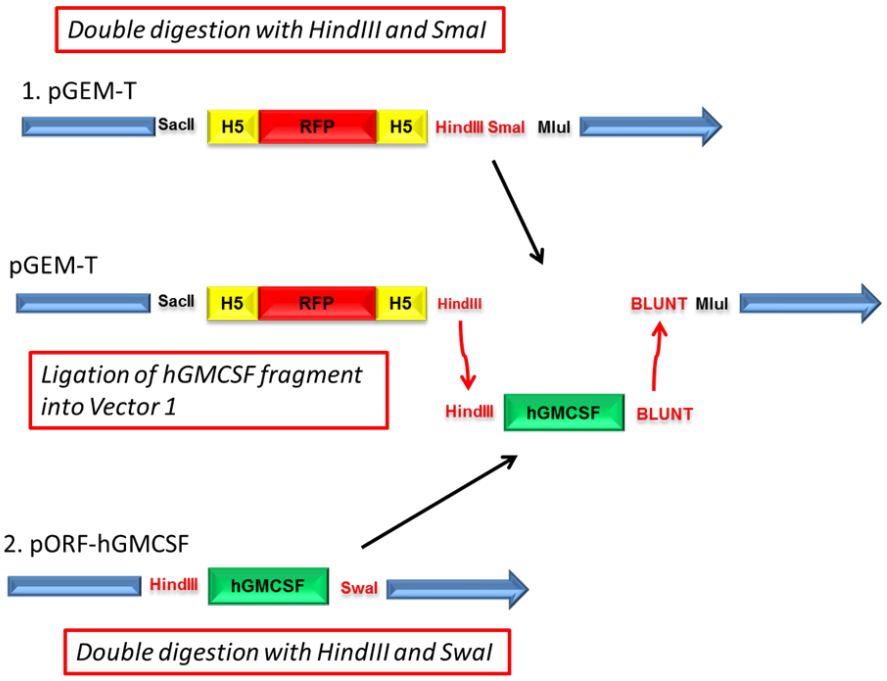

Figure 3.3 Creation of the pGEM-T based hGMCSF shuttle vector

See text for abbreviations and details.

The newly constructed pGEM-T based hGMCSF shuttle vector was then transformed into competent E. coli cells and plated on ampicillin containing agar plates (as was the linearised vector 1 as a control). Only the circularized hGMCSF shuttle vectors produced colonies and these were picked, amplified and purified as described in sections 2.3.7 and 2.3.8.

3.1.2.2 Step 2. Creation of super-shuttle vectors: pUC19-LA-H5-H5-RFP-H5-RA and pUC19-LA-H5-H5-RFP-H5-hGMCSF-RA

The shuttle vectors below were initially singly digested with *SacII* and the resulting "stepped" ends were blunted with T4 polymerase (see figure 3.4):

1. pGEM-T-*(SacII)*-H5-RFP-H5-hGMCSF-*(MluI)* (from step 1)
2. pGEM-T-*(SacII)*-H5-RFP-H5-*(MluI)*

Following DNA extraction after gel electrophoretic separation, the linearized vectors were subsequently digested with *MluI* freeing up the insert fragments:

3. (blunt end)- H5-RFP-H5-hGMCSF-*(MluI)*
4. (blunt end)- H5-RFP-H5-*(MluI)*

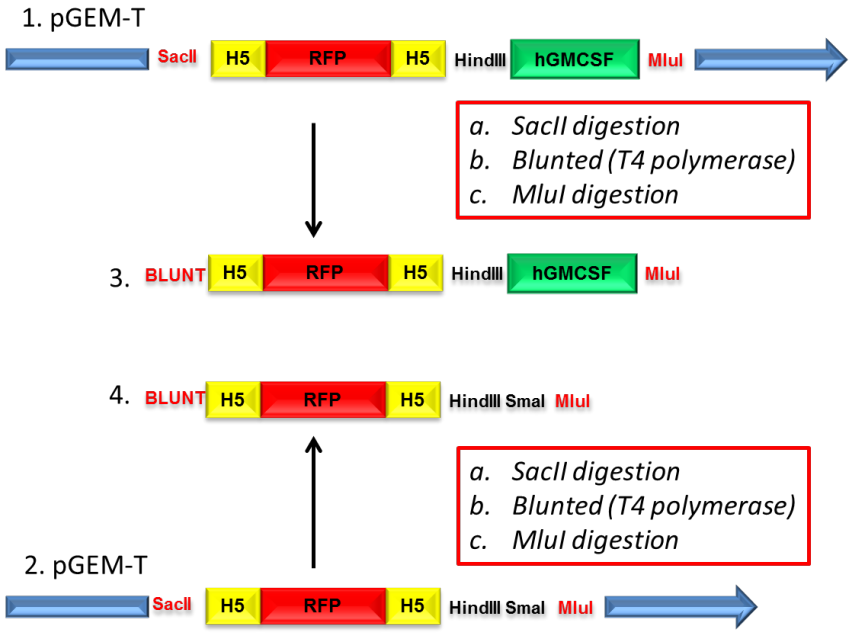

Figure 3.4 Blunting and release of the RFP and RFP-hGMCSF transgene fragments from their respective pGEM-T shuttle vectors

See text for abbreviations and details.

pGEM-T-*(HindIII)*-LA-H5 *(SalI)* was digested initially with *SalI* and the free ends were blunted with T4 polymerase. A *HindIII* digest released the LA-H5 insert fragment from the linearised pGEM-T-*(HindIII)*- LA-H5-*(blunt end)* plasmid (figure 3.5).

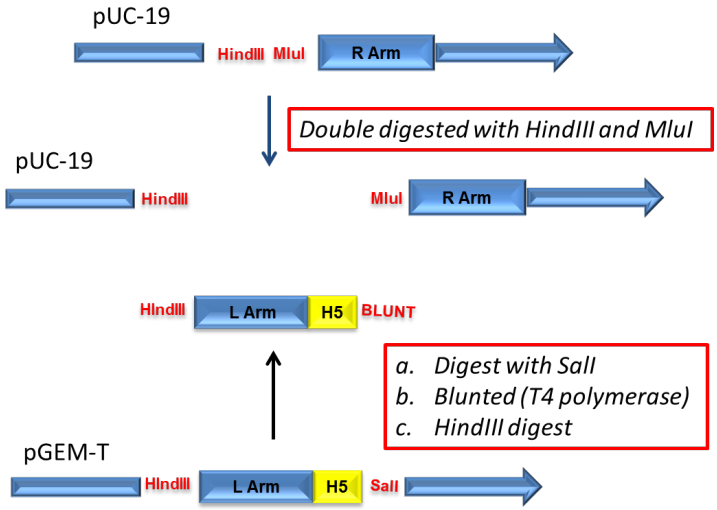

Figure 3.5 Blunting and release of the left arm transgene fragment from its pGEM-T shuttle vector. See text for abbreviations and details.

The shuttle vector pUC19-(*HindIII MluI*)-RA was simultaneously digested with *HindIII* and *MluI* to linearise the vector (figure 3.5). It was then 5' phosphorylated. The open vector was ligated to the insert fragment, *(HindIII)*-LA-H5-*(blunt end)* in tandem with either fragment 3. or 4. above, to produce the following VV "super-shuttle" vectors (figure 3.6):

pUC19-*(HindIII)*-LA-H5-(blunt ligation)- H5-RFP-H5-hGMCSF-*(MluI)* RA

pUC19-*(HindIII)*-LA-H5-(blunt ligation)- H5-RFP-H5-*(MluI)* RA

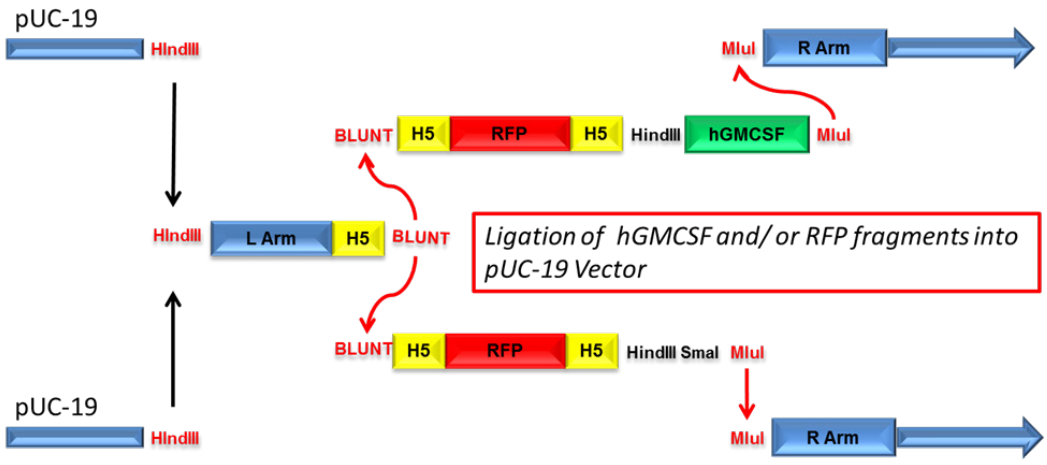

Figure 3.6 Final steps in the creation of the pUC19 based RFP and RFP-hGMCSF VV super shuttle vectors. See text for abbreviations and details.

These VV super-shuttle vectors were transformed into competent E. coli cells, amplified and column purified (sections 2.3.7, 2.3.8 and 2.3.9). For ease of constructing other similar transgene cassettes, numerous single-digestion sites were retained from the parental pORF plasmid on either side of the hGMCSF sequence.

3.1.2.3 Step 3. Using the super-shuttle vector: pUC19-LA-H5-H5-RFP-H5-hGMCSF-RA to create the equivalent human IL12 cytokine transgene vector

The hGMCSF fragment was digested out from its super shuttle vector, pUC19- LA-H5-H5-RFP-H5-*(AfeI)*- hGMCSF-*(NheI)*-RA, using the enzymes indicated in brackets and replaced with an insert from a similarly digested sequence (hIL12) from the pORF-*(AfeI)*-hIL12-*(NheI)* plasmid (figure 3.7). This was followed by the same amplification and column purification steps previously described.

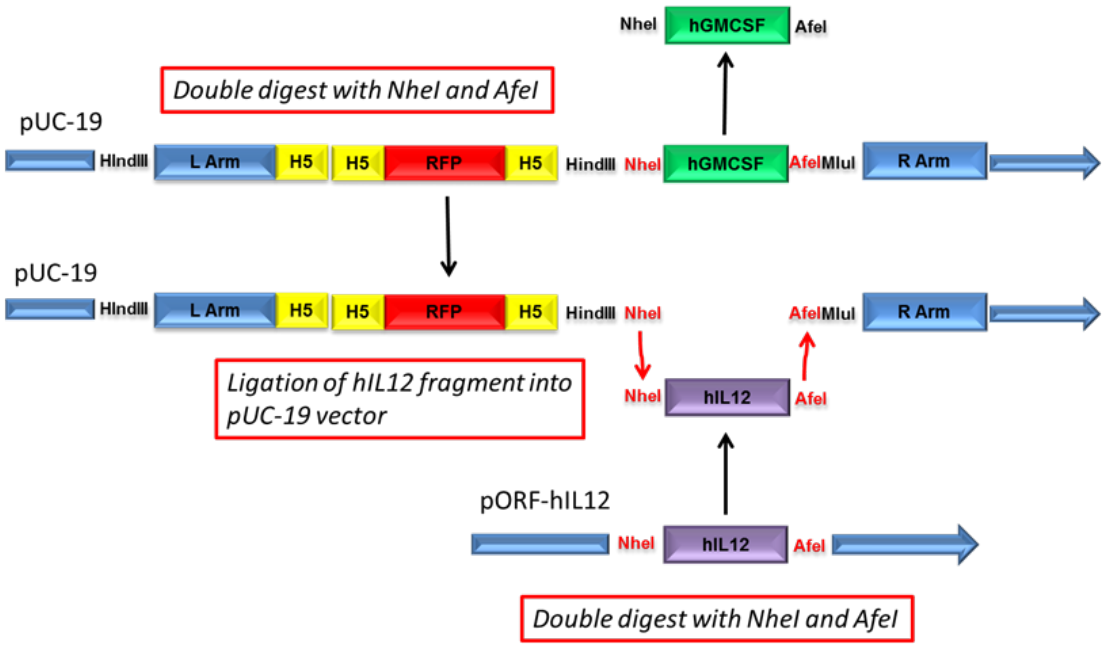

Figure 3.7 Creation of the pUC19 based hIL12 VV super-shuttle vector. See text for abbreviations and details.

We had now collectively created the following five pUC19 based VV super-shuttle vector plasmids:

1. pUC19- LA-H5- mGMCSF -H5- RFP –H5 RA
2. pUC19-LA-H5-H5-RFP-H5-mIL12- RA

3. pUC19- LA-H5-H5-RFP-H5- RA
4. pUC19- LA-H5-H5-RFP-H5-hGMCSF- RA
5. pUC19- LA-H5-H5-RFP-H5-hIL12-RA

They were fully sequenced (The Genome Centre, BCI) (see Appendix).

3.1.2.4 Each VV pUC19 based super-shuttle vector expressed its relevant cytokine transgene product

To validate the production of functional VV super-shuttle vectors, each vector was transfected into VVL15 infected CV1 cells. Forty eight hours later, microscopic inspection revealed scattered red fluorescent dots (figure 3.8).

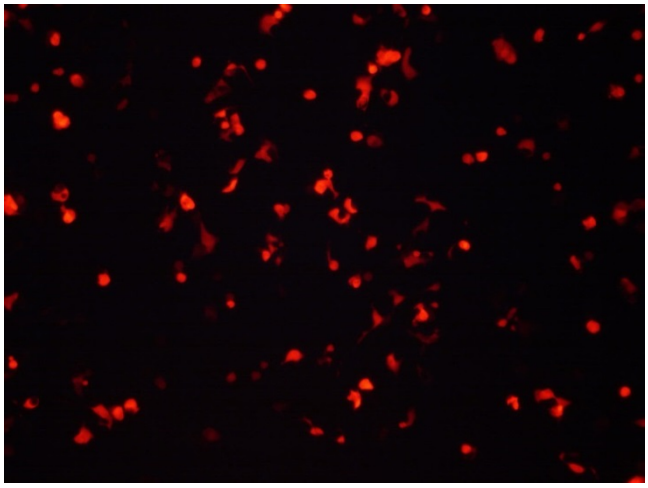

Figure 3.8 Confirmation of the successful transfection of VV super-shuttle vectors into VVL15 infected CV1 cells

The red dots under fluorescent microscopy indicated expression of RFP driven by the VV H5 promoter (400x magnification).

This indicated viral activation of the H5 promoter, which drove the RFP portion of the super-shuttle cassettes. ELISA assays were subsequently performed on supernatant samples taken from the wells at this time to confirm that the relevant cytokine transgene was also expressed (figure 3.9).

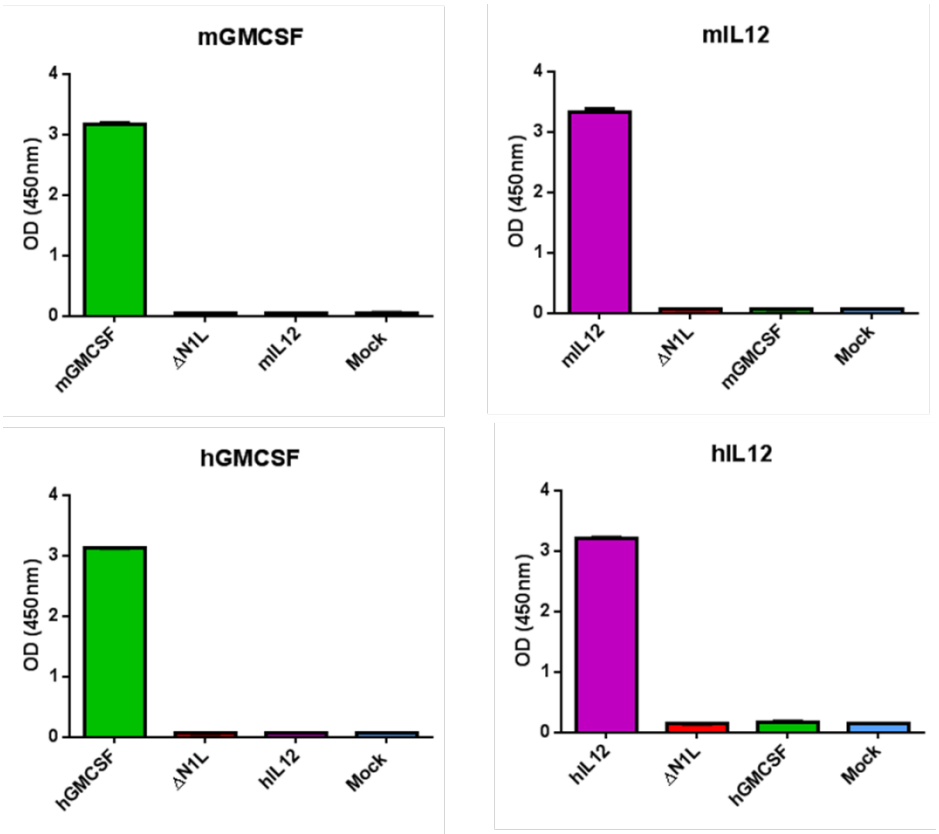

Figure 3.9 Cytokine transgene containing super-shuttle vectors successfully expressed their cytokine insert

Supernatant samples at 48 hours post infection were taken from wells containing VVL15 infected CV1 cells that had been transfected with super-shuttle vectors, or mock infected. These were analysed by the relevant ELISAs (corresponding to the title of each graph). X axis: mGMCSF/ hGMCSF**:** super-shuttle vectors containing mouse/ human GMCSF transgenes respectively; mIL12/ hIL12: super-shuttle vectors containing mouse/ human IL12 transgenes respectively; ΔN1L: super-shuttle vector containing RFP only; Y axis. OD (450nm): optical density for light at 450 nm wavelength.

3.1.2.5 Confirmation of the deletion of the N1L gene in novel VVL15 recombinant viruses

To replace the N1L region of VV with our cytokines, VVL15 (in which the VTK gene deletion had previously been confirmed by our lab) infected cells were transfected with each super-shuttle vector separately and the recombinant virus plaque purified as detailed in section 2.3.13). For each novel virus, visual inspection, under green fluorescent light, of the final round of plaque purification confirmed that all colonies within a well expressed RFP (figure 3.10).

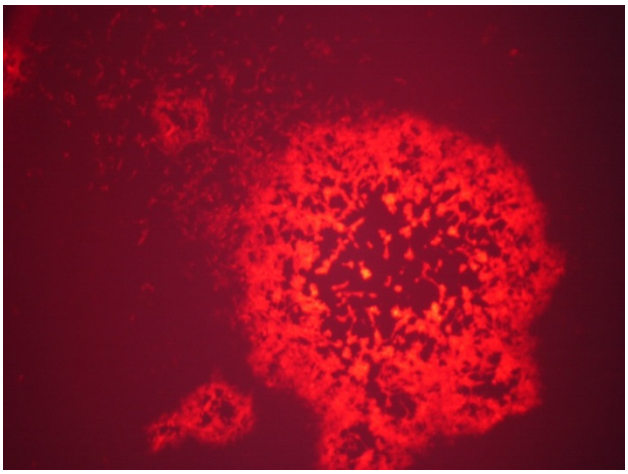

Figure 3.10 An example of colonies formed by an RFP expressing recombinant virus

A near confluent monolayer of CV1 cells was infected with a viral MOI of 0.1 PFU/ cell and analysed 48 hours later by fluorescence microscopy under green fluorescent light (400x magnification).

Viral DNA was subsequently extracted from infected CV1 cells (section 2.3.11) and the L025 (N1L) primer pairs listed in table 3.1 (sequences 1 and 2) used to PCR amplify any virions containing the N1L gene. The N1L gene was expected to be absent if homologous recombination had been successful. As a positive control, the VV A52R gene was also PCR amplified using the primer pairs listed in table 3.1 (sequences 5 and 6). All novel constructs were negative for L025 (N1L) (figure 3.11) and positive for A52R (figure 3.12). Sequencing of the junctions between L024/25 and L025/26 (using primers 3 and 4 respectively in table 3.1) confirmed that the ORFs of the neighbouring L024 and 26 genes remained intact**.**

Table 3.1 Primer sequences used for PCR and sequencing

See text for details

	Lies in Gene/ORF	Sense/Antisense	Primer Sequence 5'→ 3'
1	L025 (N1L)	Sense	CAATCTATCTAGCAATGGACC
2	L026 (N2L)	Antisense	CCGAAGGTAGTAGCATGGA
3	L024 (C1L)	Sense	CATCCGGATATTCTTCTACGA
4	L026 (N2L)	Antisense	GTTACGTCCTGTACGAGAACG
5	L170 (A52R)	Sense	ATGATGCGGAAGAACAAT
6	L172 (A56R)	Antisense	TTGCGGTATATGTATGAGGTG

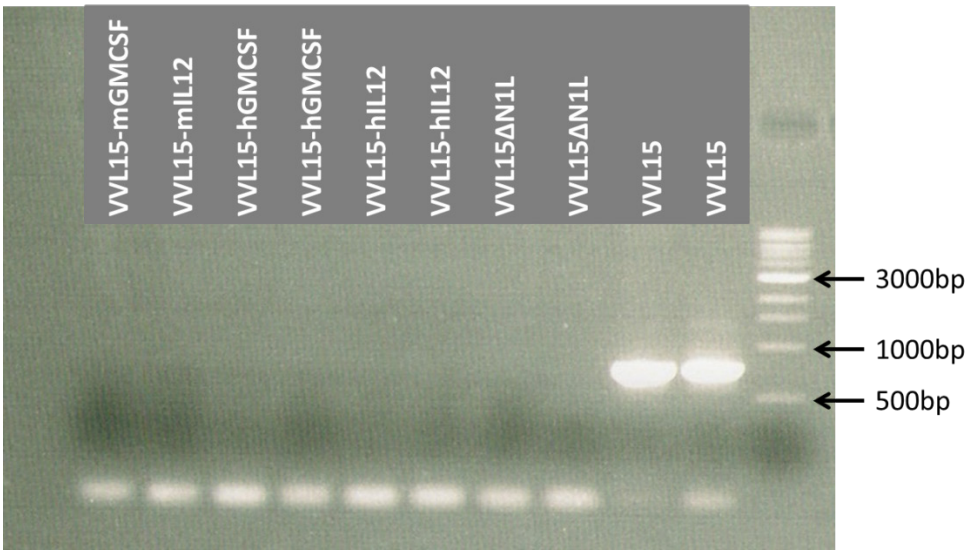

Figure 3.11 The N1L gene was deleted in all novel VVL recombinants

Sense and anti-sense N1L gene primers were used to amplify this locus via PCR, from viral DNA that had been extracted from infected CV1 cells. Each lane is representative of a recombinant virus, plaque purified from a single PFU following homologous recombination. The VVL15 DNA samples were extracted from VVL15-LacZ (left) and VVL15-RFP (right) infected CV1 cells (see figures 2.1 and 2.2). The parent platform, VVL15 contained the gene. The gene segment spanning the primer pair was expected to be approximately 750 bp.

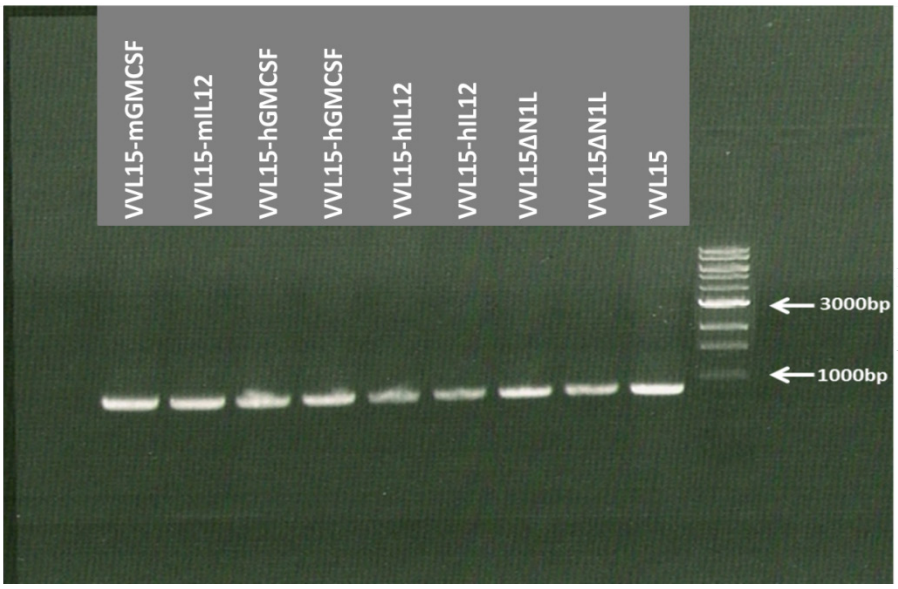

Figure 3.12 The A52R gene was present in all VVL recombinants

Sense and anti-sense A52R gene primers were used to PCR amplify this locus from viral DNA extracted from virally infected CV1 cells. Each lane is representative of a recombinant virus, plaque purified from a single PFU following homologous recombination. The VVL15 DNA sample was extracted from VVL15-RFP infected CV1 cells (see figure 2.2). The A52R gene segment spanning the primer pair was expected to be approximately 880 bp.

3.1.3 Validation of the cytotoxic ability of novel recombinant VVL viruses against tumour cells *in vitro*

Using the MTS cytotoxicity assay outlined in section 2.4, the cytotoxic capacity of VVL15ΔN1L was compared with the parental virus VVL15 against a range of murine cancer cell lines *in vitro*. Based on the EC50 values, i.e. the PFU required to kill 50% of cells, there was no significant difference in cytotoxicity between the two viruses against CT26 (colon) or DT6606 (pancreatic ductal) cells. In contrast VVL15ΔN1L was significantly more potent at killing CMT93 (rectal), LLC (lung), SCCVII (head and neck) and B16-F10 (metastatic melanoma) cells (figure 3.13).

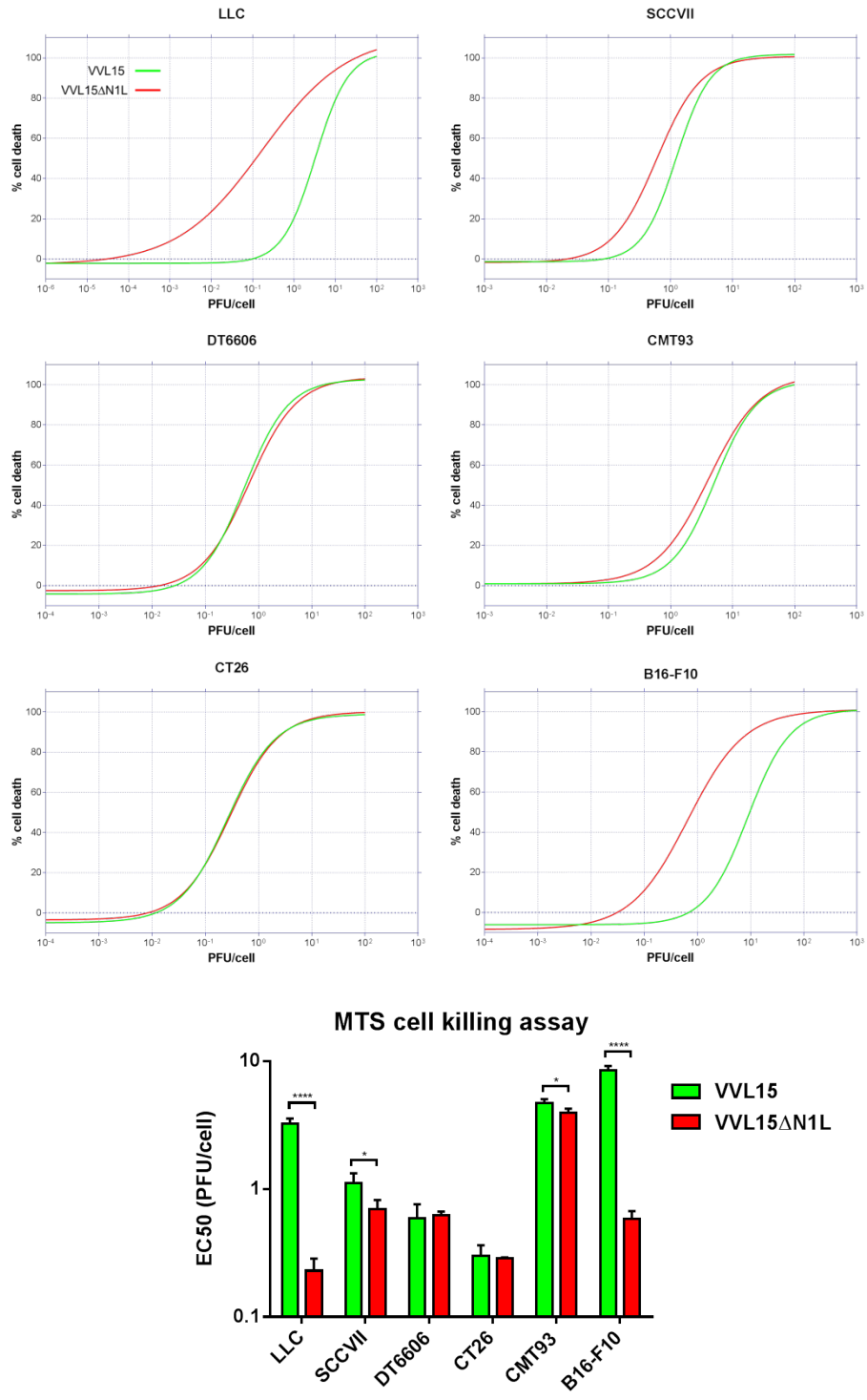

Figure 3.13 The oncolytic potency of VVL15ΔN1L against murine tumour cell lines

MTS based assays were performed to measure the cytotoxicity of viruses against the indicated tumour cell lines. The line graphs represent typical viral dose-response curves with percentage cell death (Y axis) plotted against increasing viral concentration (X axis). From these, the corresponding EC50 values (i.e. the number of PFUs/cell required to kill 50% of cells) were calculated and plotted on a bar chart. Unpaired t-tests were used to compare means of EC50s.

In anticipation of testing our recombinant viruses in immune competent Syrian hamster *in vivo* models, cytotoxicity was assessed against two Syrian hamster cell lines: HCPC-1 (cheek pouch) and HPD-1NR (pancreatic). The cytotoxicity of VVL15ΔN1L was at least as potent as VVL15 against these two cell lines (figure 3.14).

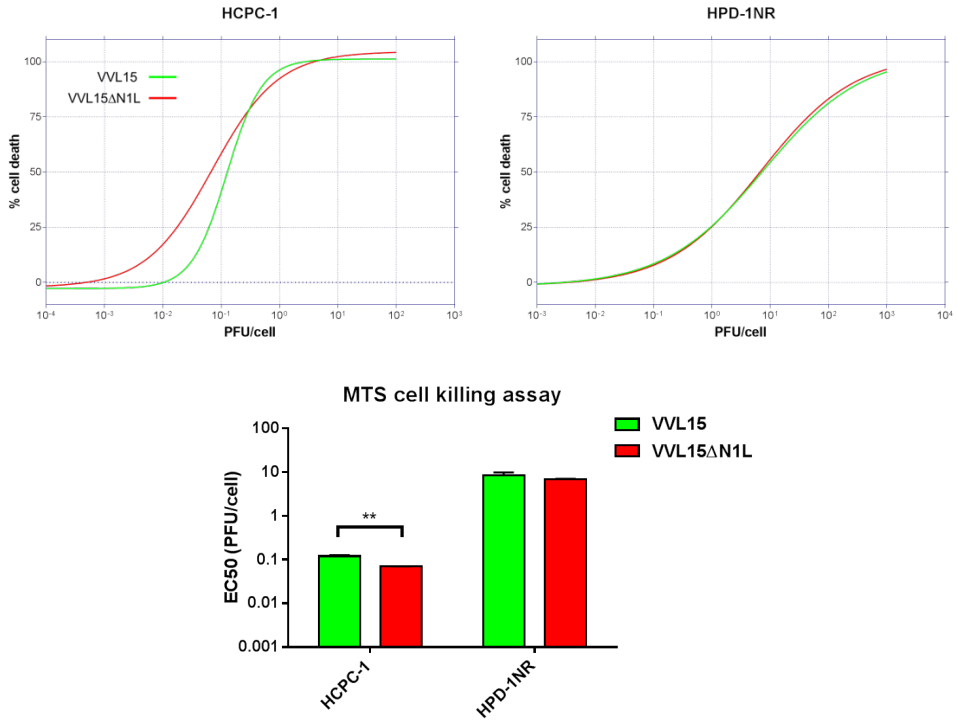

Figure 3.14 The oncolytic potency of VVL15ΔN1L against Syrian hamster tumour cell lines

MTS based assays were performed to measure the cytotoxicity of viruses against the indicated tumour cell lines. The line graphs represent typical viral dose-response curves with percentage cell death (Y axis) plotted against increasing viral concentration (X axis). From these, the corresponding EC50 values (i.e. the number of PFUs/cell required to kill 50% of cells) were calculated and plotted on a bar chart. Unpaired t-tests were used to compare means of EC50s.

To assess the cytotoxic potency of VVL15ΔN1L against human tumour cells, a panel of human tumour cell lines were also infected and analysed using MTS assays. All human cell lines were exquisitely sensitive to the cytotoxic effects of both viruses, and exhibited very low EC50 values. In contrast to the rodent cell lines, VVL15 was however significantly more cytotoxic than VVL15ΔN1L against three of the six human cell lines tested: SUIT-2 (pancreatic), FaDu (buccal) and HCT-116 (colon) (figure 3.15).

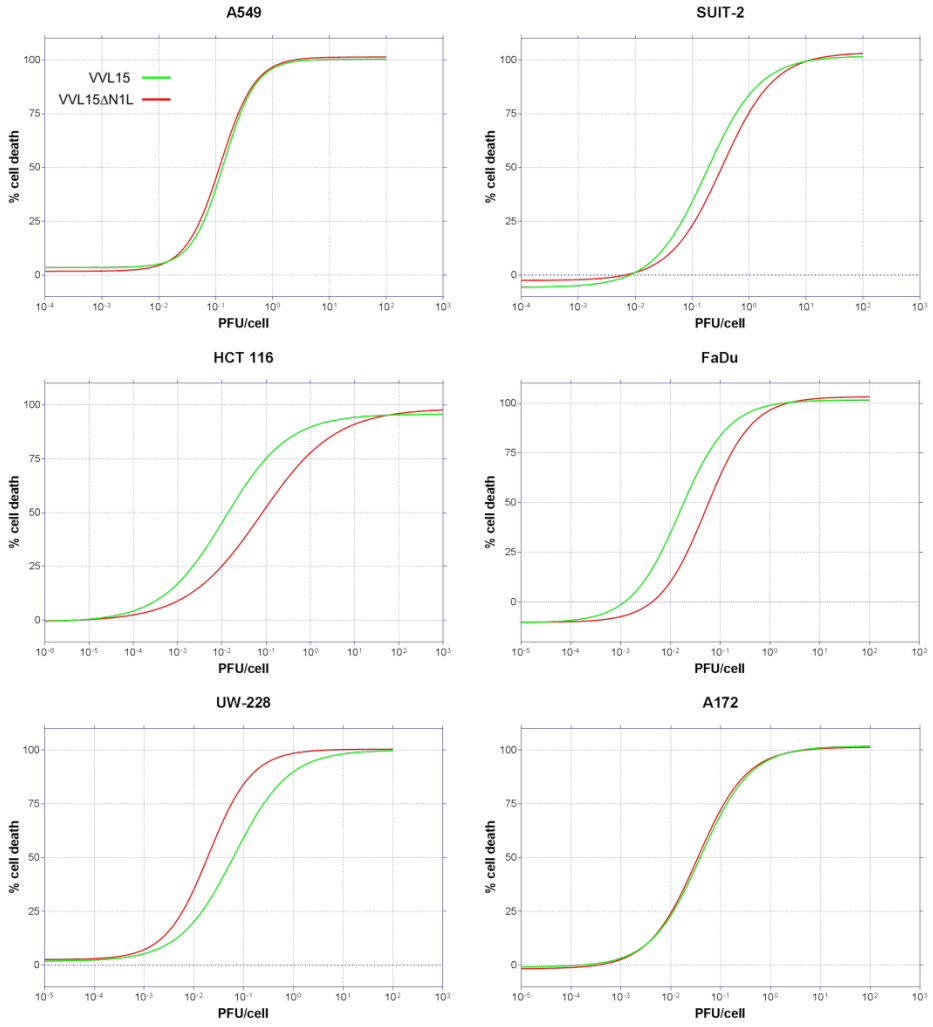

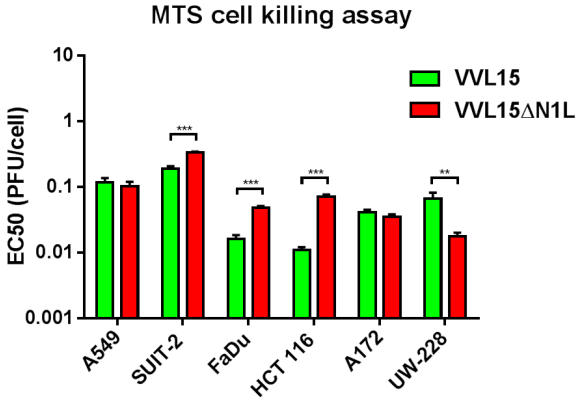

Figure 3.15 The oncolytic potency of VVL15ΔN1L against human tumour cell lines

MTS based assays were performed to measure the cytotoxicity of viruses against the indicated tumour cell lines. The line graphs represent typical viral dose-response curves with percentage cell death (Y axis) plotted against increasing viral concentration (X axis). From these, the corresponding EC50 values (i.e. the number of PFUs/cell required to kill 50% of cells) were calculated and plotted on a bar chart. Unpaired t-tests were used to compare means of EC50s.

Following confirmation that deletion of the N1L gene had not ablated the cytotoxicity of VVL15, the cytotoxic potency of murine transgene (mIL12 and mGMCSF) armed viruses against murine tumour cell lines were compared to VVL15ΔN1L. In general, the EC50 values following infection with transgene-armed viruses were significantly higher than VVL15ΔN1L, i.e. they were worse than VVL15ΔN1L at killing the relevant cell line (except against LLC and CMT93 cells). The VVL15ΔN1L-mIL12 recombinant appeared to be more potent at cell killing than VVL15ΔN1L-mGMCSF (figure 3.16).

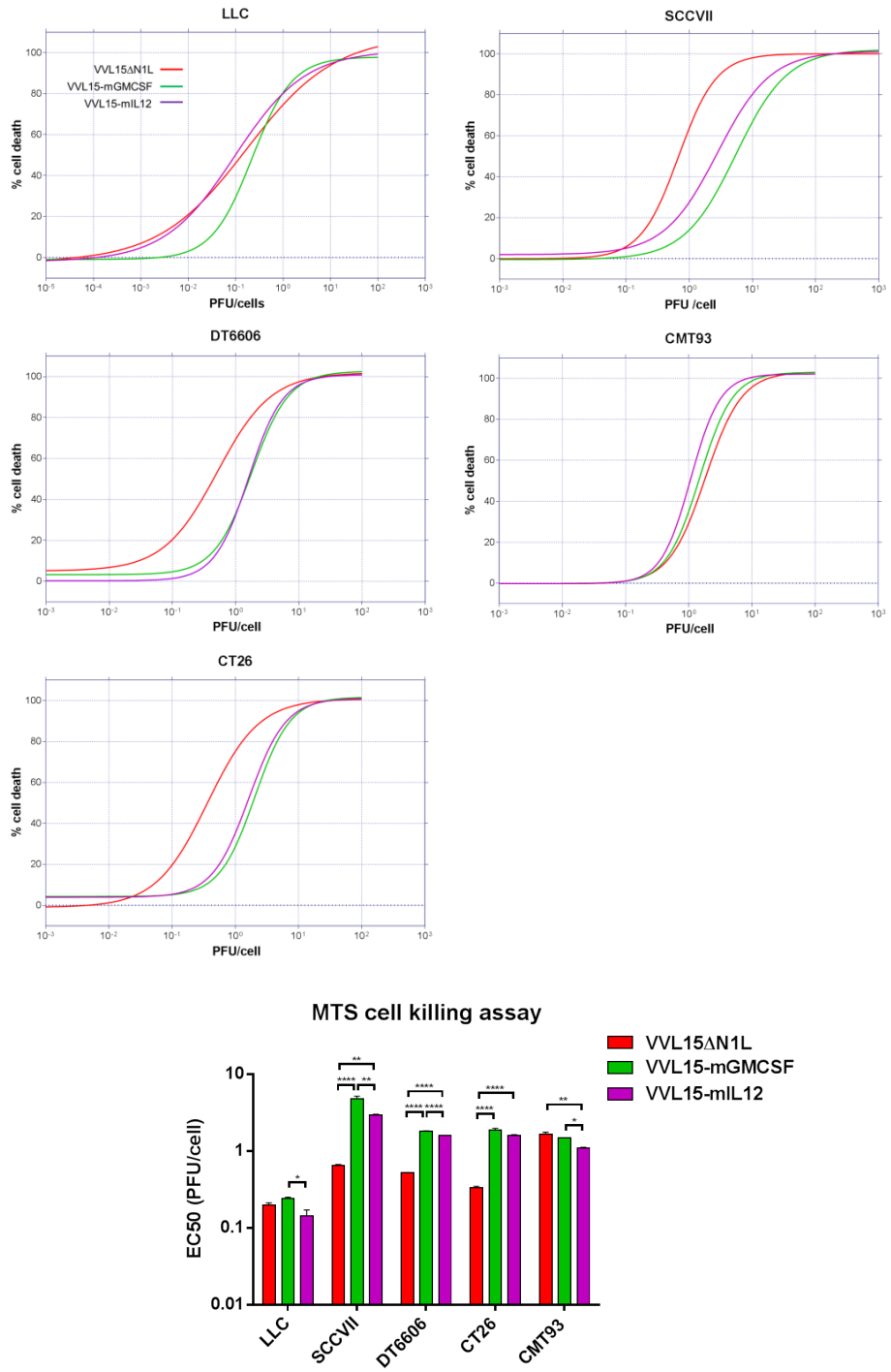

Figure 3.16 The oncolytic potency of murine cytokine transgene armed viruses against murine tumour cell lines

MTS based assays were performed to measure the cytotoxicity of viruses against the indicated tumour cell lines. The line graphs represent typical viral dose-response curves with percentage cell death (Y axis) plotted against increasing viral concentration (X axis). From these, the corresponding EC50 values (i.e. the number of PFUs/cell required to kill 50% of cells) were calculated and plotted on a bar chart. One way ANOVAs with post hoc Tukey tests were used to compare means of EC50s.

The cytotoxic potencies of human transgene-armed viruses were also compared to VVL15ΔN1L against both Syrian hamster (figure 3.17) and human (figure 3.18) cell lines. In general, the results reflected a similar pattern to that observed against murine cells i.e. VVL15ΔN1L was a more potent cytotoxic agent than the transgene-armed recombinants, although VVL15-hIL12 demonstrated the best cytotoxic potency against HPD-1NR and HCT-116 cell lines. Just like its murine counterpart, VVL15-hGMCSF fared the worst against all tested cell lines.

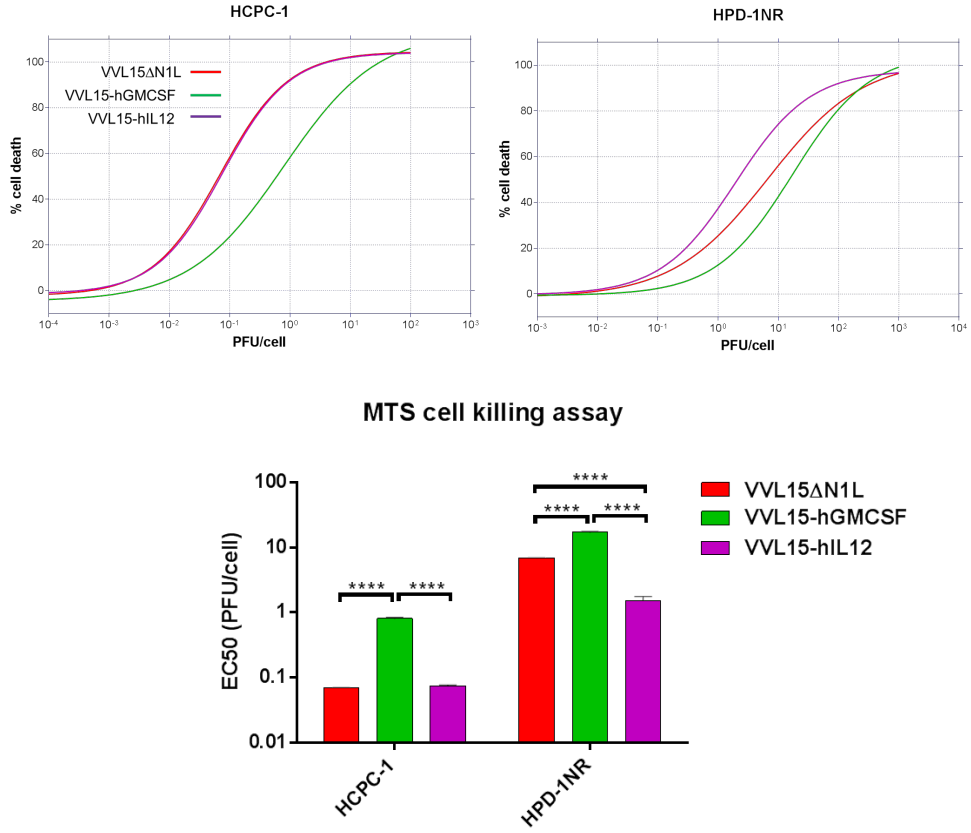

Figure 3.17 The oncolytic potency of human cytokine transgene armed viruses against Syrian hamster tumour cell lines

MTS based assays were performed to measure the cytotoxicity of viruses against the indicated tumour cell lines. The line graphs represent typical viral dose-response curves with percentage cell death (Y axis) plotted against increasing viral concentration (X axis). From these, the corresponding EC50 values (i.e. the number of PFUs/cell required to kill 50% of cells) were calculated and plotted on a bar chart. One way ANOVAs with post hoc Tukey tests were used to compare means of EC50s.

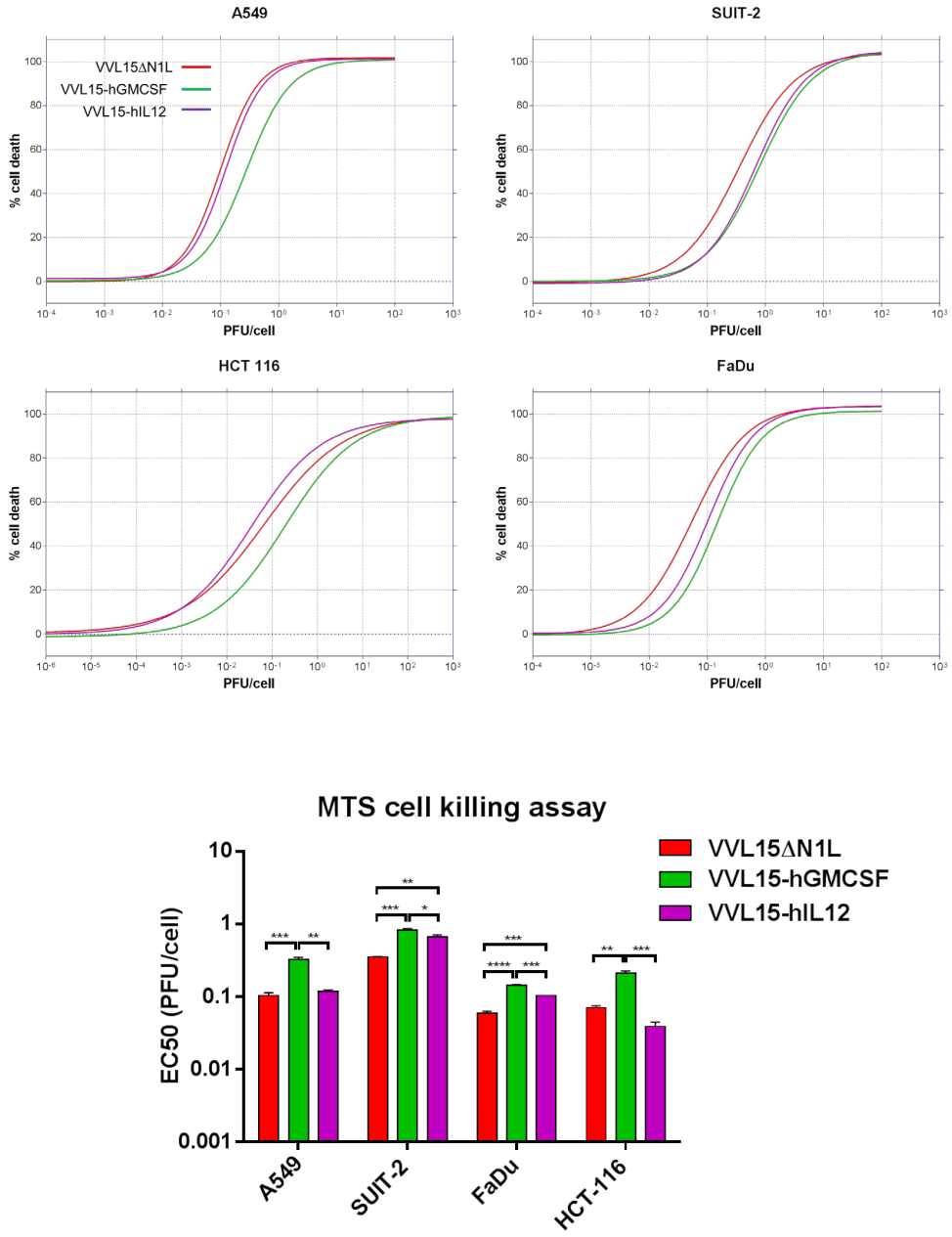

Figure 3.18 The oncolytic potency of human cytokine transgene armed viruses against human tumour cell lines.

MTS based assays were performed to measure the cytotoxicity of viruses against the indicated tumour cell lines. The line graphs represent typical viral dose-response curves with percentage cell death (Y axis) plotted against increasing viral concentration (X axis). From these, the corresponding EC50 values (i.e. the number of PFUs/cell required to kill 50% of cells) were calculated and plotted on a bar chart. One way ANOVAs with post hoc Tukey tests were used to compare means of EC50s.

3.1.4 Validation of novel recombinant viral replication in a panel of murine, Syrian hamster and human tumour cell lines.

Replication assays were performed by infection of relevant cell lines with either VVL15 or VVL15ΔN1L at a multiplicity of infection (MOI) of 1 PFU/ cell. After 24, 48 or 72 hours, viral titres were quantified using TCID50 assays on CV1 indicator cells (sections 2.5 and 2.6).

Viral titres plateaued by 72 hours in most cell lines. This was likely to reflect the slower turnover of uninfected cells in comparison to viral replication; with virions effectively running out of cells to infect. Toxic proteases, nucleases and acids released from lysed cells may have also suppressed the elevation in viral titre.

In general, there appeared to be a trend for attenuated replication of VVL15ΔN1L in comparison to VVL15 (figure 3.19).

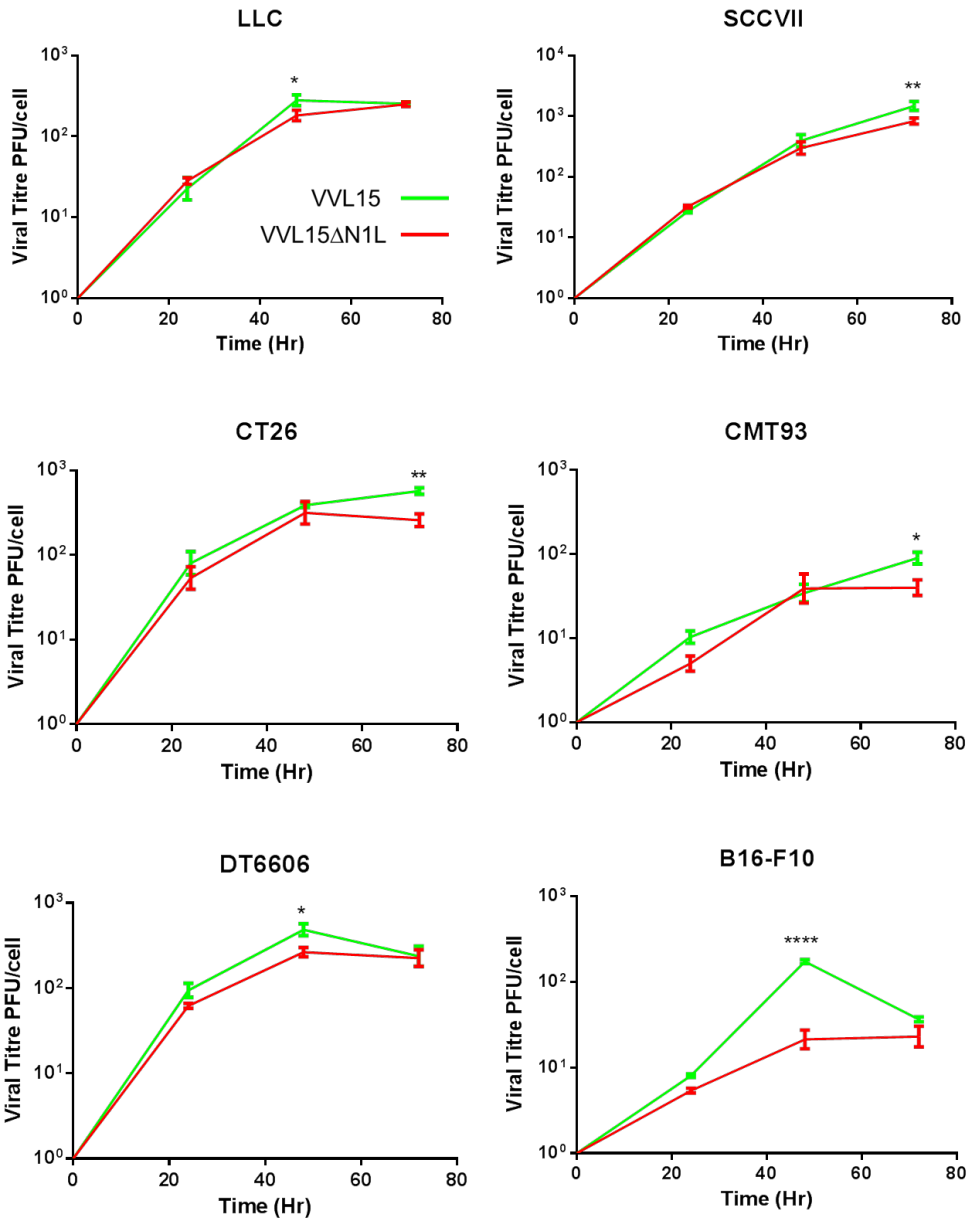

Figure 3.19 Replication of VVL15ΔN1L in murine tumour cell lines

Viral titres in PFU/ tumour cell were determined by performing TCID50 assays on viral lysates collected at 24, 48 and 72 hours after infection with an MOI of 1 PFU/ tumour cell (the relevant cell line indicated by the title). Two-way ANOVAs with post hoc Tukey tests were used to compare mean titres.

Syrian hamster and human tumour cell lines were also assessed for their ability to support replication of VVL15ΔN1L. All cells were permissive to infection, but both viruses replicated relatively poorly in SUIT-2, HCT-116 and HPD-1NR cell lines (figure 3.20 and figure 3.21). Again, there was a general tendency for VVL15ΔN1L to replicate inferiorly in comparison to VVL15. This reached statistical significance in HCPC-1, SUIT-2 and FaDu cell lines by 72 hours post infection.

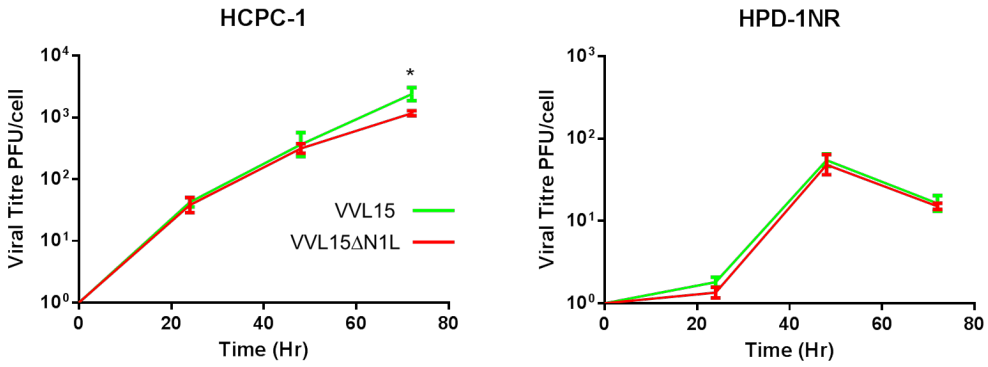

Figure 3.20 Replication of VVL15ΔN1L in Syrian hamster tumour cell lines

Viral titres in PFU/ tumour cell were determined by performing TCID50 assays on viral lysates collected at 24, 48 and 72 hours after infection with an MOI of 1 PFU/ tumour cell (the relevant cell line indicated by the title). Two-way ANOVAs with post hoc Tukey tests were used to compare mean titres.

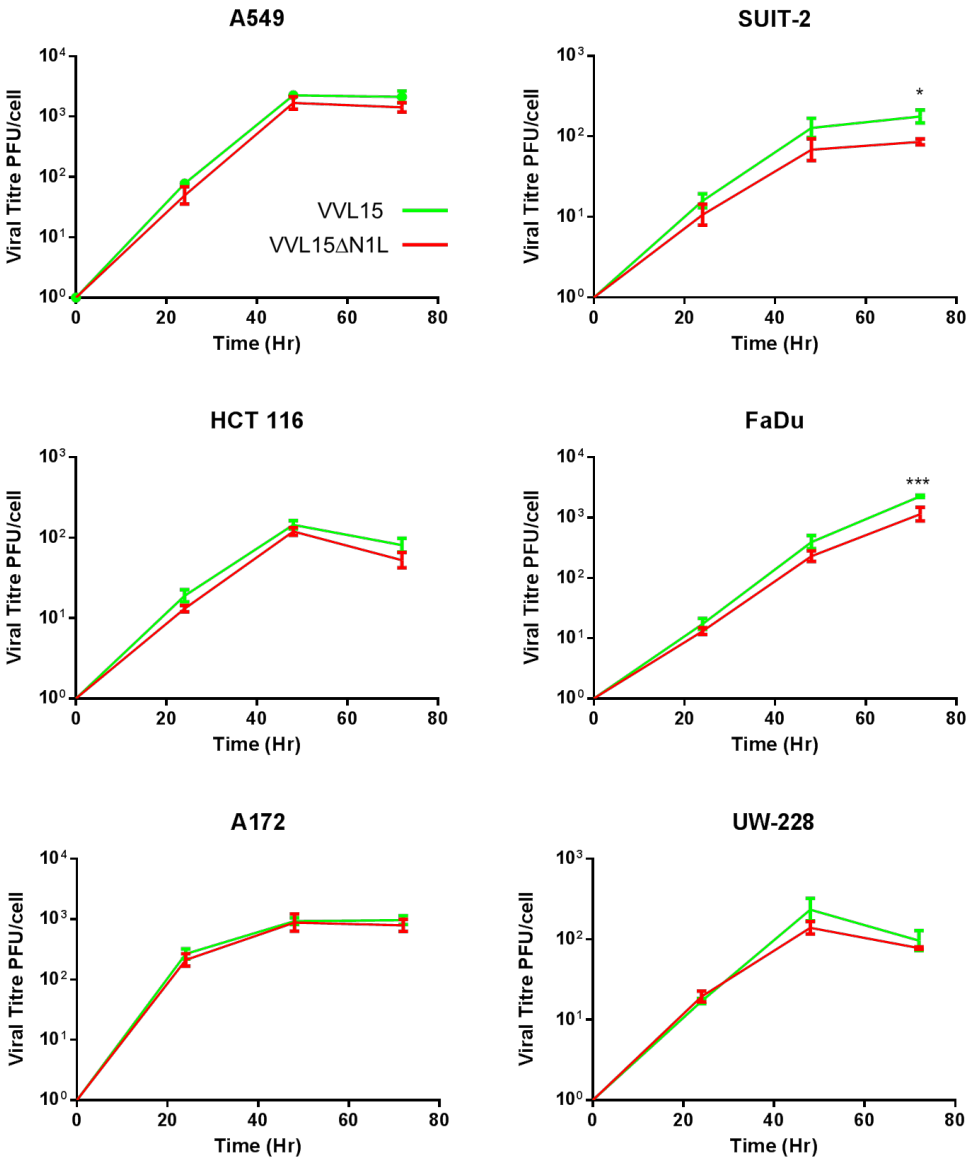

Figure 3.21 Replication of VVL15ΔN1L in human tumour cell lines

Viral titres in PFU/ tumour cell were determined by performing TCID50 assays on viral lysates collected at 24, 48 and 72 hours after infection with an MOI of 1 PFU/ tumour cell (the relevant cell line indicated by the title). Two-way ANOVAs with post hoc Tukey tests were used to compare mean titres.

To assess whether insertion of IL12 or GMCSF transgenes into the N1L region affected the ability of recombinant viruses to replicate, they were compared to VVL15ΔN1L.

Both murine GMCSF and IL12 transgene-armed viruses were attenuated in their ability to replicate in all murine cell lines except CMT93 (figure 3.22). A similar trend was seen in experiments assessing the replication of human cytokine transgene-armed viruses in hamster and human cell lines (figure 3.23 and figure 3.24).

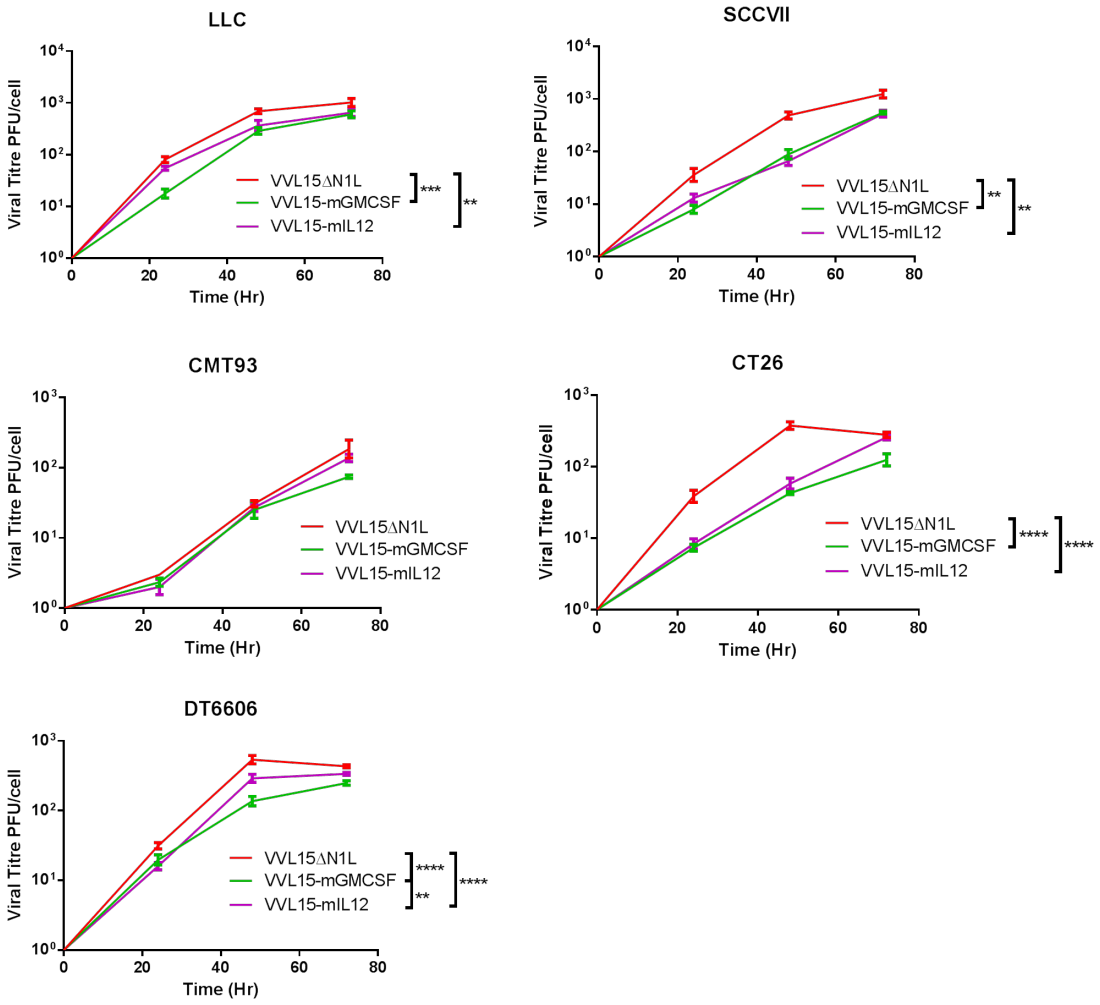

Figure 3.22 Replication of murine cytokine transgene armed recombinant VVL viruses in murine tumour cell lines

Viral titres in PFU/ tumour cell were determined by performing TCID50 assays on viral lysates collected at 24, 48 and 72 hours after infection with an MOI of 1 PFU/ tumour cell (the relevant cell line indicated by the title). One way ANOVAs with post hoc Tukey tests were used to compare mean titres at the 48 hour time-point.

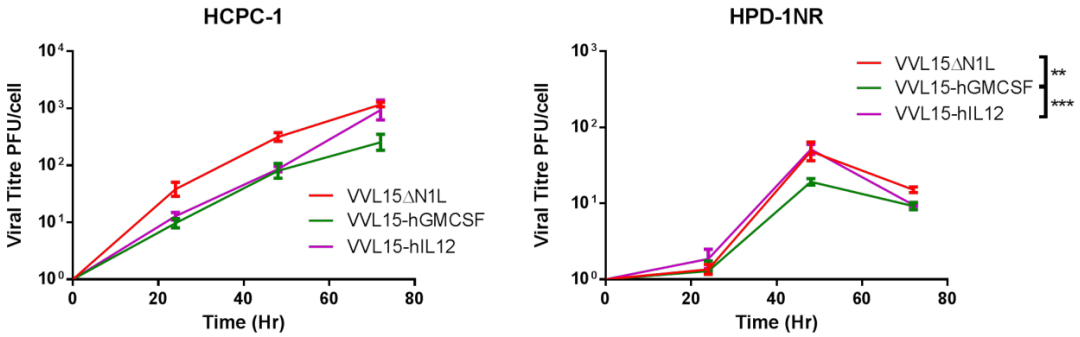

Figure 3.23 Replication of human cytokine transgene armed recombinant VVL viruses in Syrian hamster tumour cell lines

Viral titres in PFU/ tumour cell were determined by performing TCID50 assays on viral lysates collected at 24, 48 and 72 hours after infection with an MOI of 1 PFU/ tumour cell (the relevant cell line indicated by the title). One way ANOVAs with post hoc Tukey tests were used to compare mean titres at the 48 hour time-point.

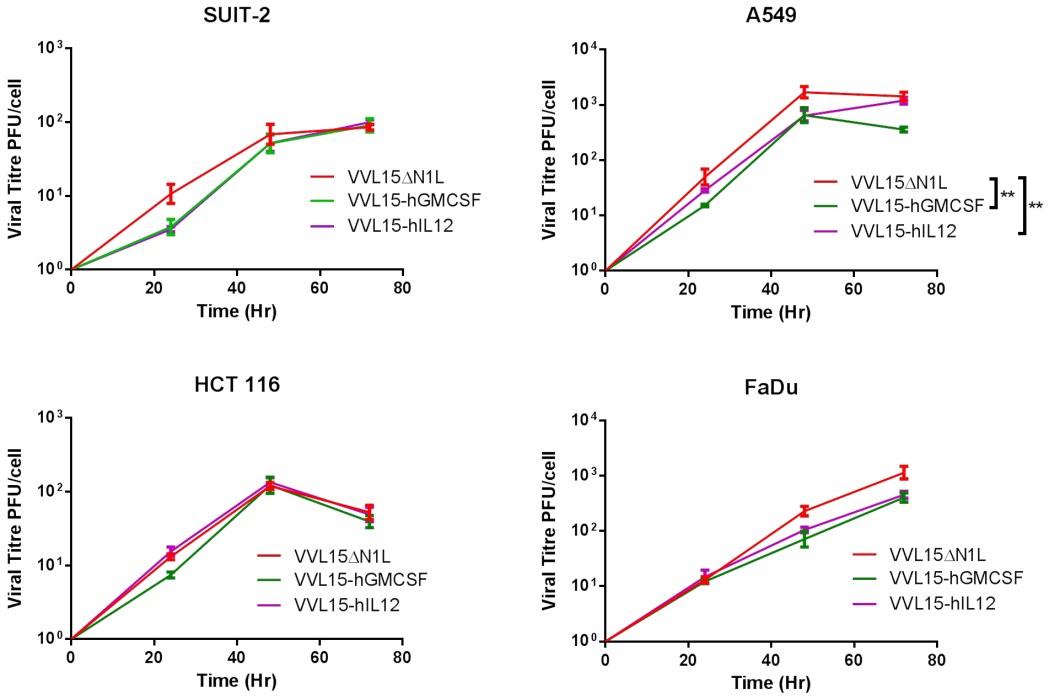

Figure 3.24 Replication of human cytokine transgene armed recombinant VVL viruses in human tumour cell lines

Viral titres in PFU/ tumour cell were determined by performing TCID50 assays on viral lysates collected at 24, 48 and 72 hours after infection with an MOI of 1 PFU/ tumour cell (the relevant cell line indicated by the title). One way ANOVAs with post hoc Tukey tests were used to compare mean titres at the 48 hour time-point.

3.1.5 Cytokine transgene expression in tumour cell lines following infection with novel recombinant VVL viruses

The expression of transgenes from VVL15-IL12 (murine and human) and VVL15-GMSCF (murine and human) was confirmed over a 72 hour time course in the same cell lines used to assess their replication (figure 3.25).

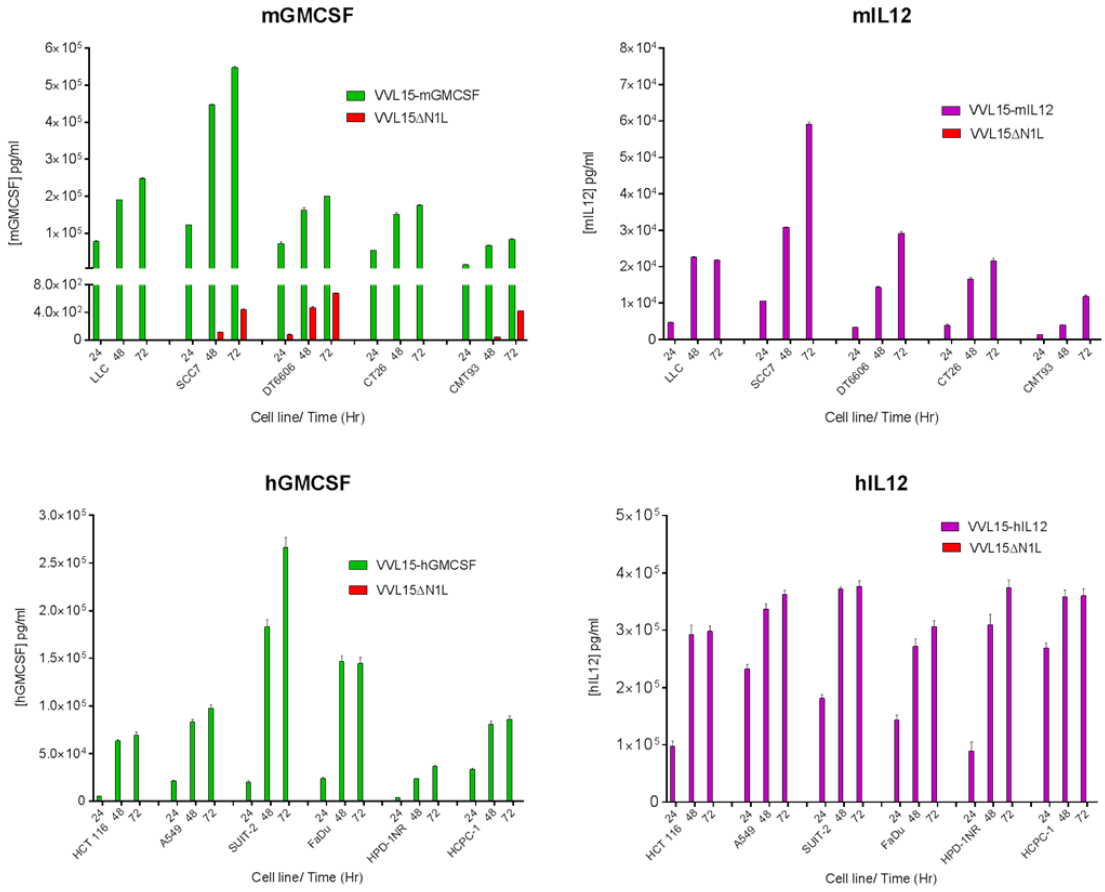

Figure 3.25 Expression of human and murine cytokine transgenes in tumour cell lines

Supernatant samples from wells containing murine, Syrian hamster or human tumour cells (as indicated on the X axes) infected with recombinant cytokine transgene-armed virus (murine or human as indicated) or VVL15ΔN1L, were taken at 24, 48 and 72 hours following infection with an MOI of 1 PFU/ tumour cell. Concentrations (in pg/ml) of the relevant cytokines in supernatant samples were determined by ELISAs (corresponding to the title of each graph). mGMCSF/ hGMCSF refers to mouse/ human GMCSF respectively; mIL12/ hIL12 refers to mouse/ human IL12 respectively.

Of note, certain murine cell lines, namely SCCVII, CMT93 and in particular DT6606, appeared to secrete a background level of murine GMCSF. Figure 3.26 illustrates the variation of mGMCSF concentration in supernatant samples with time from both mock and VVL15ΔN1L infected tumour cell lines. The levels were lower following VVL15ΔN1L infection, presumably due to viral cell destruction; this also excluded the possibility that viral infection per se. led to the up regulation of cellular mGMCSF.

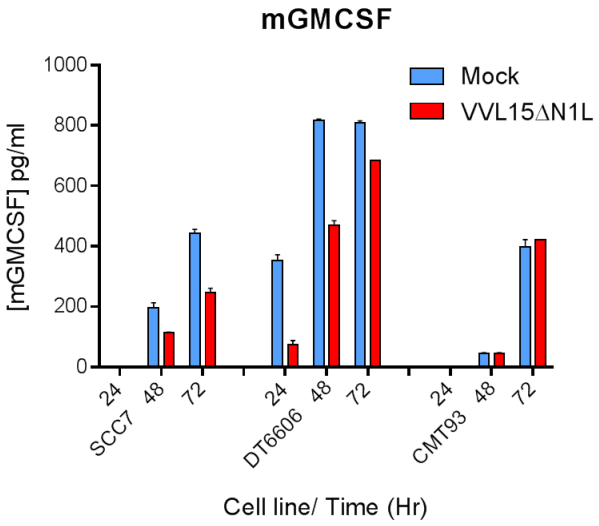

Figure 3.26 Some tumour cell lines endogenously secrete GMCSF

Supernatant was collected from wells containing murine tumour cells (as indicated on the X axis) infected with VVL15ΔN1L or mock infected at 24, 48 and 72 hours following infection with an MOI of 1 PFU/ tumour cell**.** The concentration (in pg/ml) of murine GMCSF [mGMCSF] in the supernatant was determined by ELISA.

3.1.6 Summary of results chapter 3.1

We have successfully cloned a set of recombinant N1L deleted VVL15 viruses, armed with either murine or human versions of transgenes encoding the cytokines GMCSF or IL12. Viral genes down and upstream of the N1L ORF were intact upon sequencing. The novel recombinant viruses were all able to infect cell panels of hamster, human and/ or murine cancer cell lines and express detectable quantities of their cytokine transgene.

There are multiple mechanisms by which a tumour cell may be killed by VVs. These include the triggering of apoptosis, death from virus mediated cellular burst and host immunological defence mechanisms. If a virus is excessively cytotoxic to a cell, it may not generate enough progeny to self-propagate throughout a tumour. Furthermore its ability to replicate might also be hampered if it has been subject to significant genetic manipulation.

In general, the replication of VVL15ΔN1L was moderately attenuated across most tested cell lines. However, its ability to kill cells, particularly murine cell lines appeared to be enhanced. This may have reflected the anti-apoptotic function of the N1L gene product, which upon deletion may have enhanced viral induced cellular apoptosis (section 1.5.7.2).

As might have been expected, the replication and cytotoxic potency of the cytokine transgene armed viruses appeared to be further attenuated in comparison to VVL15ΔN1L; but despite this they were all able to express detectable levels of their transgene following infection of all tested cell lines. GMCSF armed recombinants (both murine and human) appeared to be less cytotoxic to cell lines in comparison to their IL12 armed counterparts. A partial explanation for this could relate to that fact that some murine cell lines appear to naturally secrete GMCSF and for those cells this GMCSF may have acted as a growth factor.

3.2 VVL15ΔN1L is capable of enhancing adaptive antitumour immunity

The major rational for deleting the VV N1L gene was to create an oncolytic viral backbone with enhanced antitumour immunogenic potential. Syngeneic immune competent animal models would thus be required to explore whether this was indeed the case.

In this section, three syngeneic *in vivo* models were used:
DT6606 (pancreatic) or DT6606-Ova tumours in C57BL/6 strain mice
LLC (lung) tumours in C57BL/6 strain mice

3.2.1 VVL15ΔN1L enhanced adaptive antitumour immunity against LLC (lung) and DT6606 (pancreatic) cancer models

Subcutaneous syngeneic LLC and DT6606 tumours were established and treated with a single dose of virus or PBS (table 2.7, experiments 1 and 2). Upon co-culture with growth arrested LLC or DT6606 cells respectively, splenocytes from VVL15ΔN1L treated groups produced higher levels of IFNγ than those from VVL15 or PBS groups (figure 3.27). IFNγ levels from VVL15ΔN1L treated mice were higher at day seven in comparison to day 14 in both models.

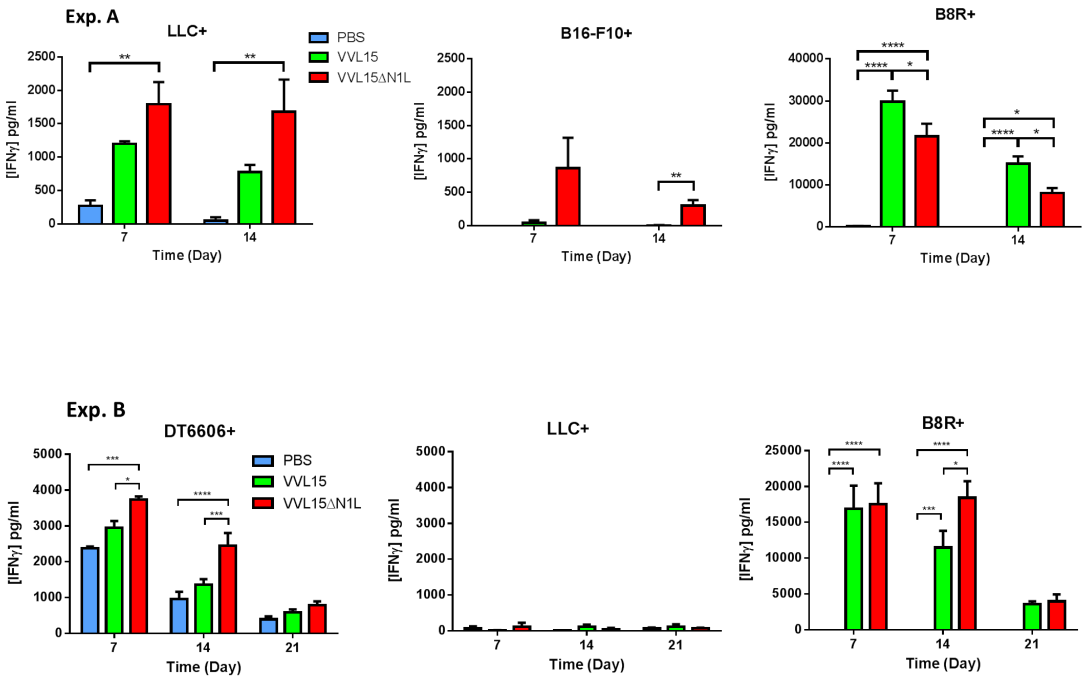

Figure 3.27 Intratumoural VVL15ΔN1L enhanced tumour specific IFNγ release from *ex vivo* cultured splenocytes

LLC (Exp. A) or DT6606 (Exp. B) flank tumours in C57BL/6 strain mice were treated with $1x10^8$ PFUs of IT virus or the equivalent volume of PBS (n= 3-4/ group). Seven, 14 or 21 days later, splenocyte suspensions were co-cultured with either growth arrested target (LLC or DT6606) or control (B16-F10 or LLC in respective experiments) cells or VV B8R peptide as indicated. IFNγ concentrations (in pg/ ml, Y axes) of supernatants were measured by ELISA. Two-way ANOVAs with post hoc Tukey tests were used to compare means.

Interestingly, in the LLC tumour model, the antiviral (anti B8R) response appeared to be attenuated by deletion of the N1L gene, although this was not the case in the DT6606 tumour model (figure 3.27).

To demonstrate anti-tumour specificity, splenocytes from both experiments were also co-cultured with an MHC haplotype compatible control tumour cell line: B16-F10 cells for the LLC tumour model and LLC cells for the DT6606 tumour model.

For LLC tumour bearing mice, splenocytes from the VVL15ΔN1L treatment group, that were co-cultured with B16-F10 cells also released significant levels of IFNγ (figure 3.27 Exp.A). It is certainly likely that a number of tumour epitopes are shared between these and other solid tumour cell lines; CTLs generated against these could have been stimulated and expanded by the B16-F10 cells. In contrast, when control LLC cells were co-cultured with splenocytes derived from virally treated DT6606 tumour models, very little IFNγ was produced.

For both tumour models, IFNγ levels waned with time post virus injection, with levels approaching the PBS group by day 21 in the DT6606 model. The highest levels in both experiments occurred at day seven. In addition, although inter experimental results cannot be statistically compared, splenocytes from mice bearing DT6606 tumours (in contrast to those bearing LLC tumours) consistently produced higher levels of IFNγ upon co-culture with their respective target cell line. The generation of an antitumour immune response is likely to be influenced by the suppressive nature of the TME; perhaps the TME of LLC tumours are more suppressive in this regard than DT6606 tumours. It should however be noted, that the generation of a strong antiviral (anti B8R) immune response was not hampered in LLC tumour bearing mice. Indeed IFNγ levels following co-culture with the B8R antigen were comparable in the two experimental models.

3.2.2 VVL15ΔN1L enhanced immunity against a surrogate tumour antigen

The TAA profile of the DT6606 cell line has yet to be fully defined. In a bid to demonstrate the generation of an antigen specific immune response, DT6606-Ova, which stably expresses the foreign antigen, chicken ovalbumin was used to create a syngeneic subcutaneous flank model (table 2.7, experiment 3). At 14 days post IT injection of virus, IFNγ levels following splenocyte co-culture with growth arrested DT6606-Ova cells or Ova peptide were highest in the VVL15ΔN1L injected group (figure 3.28).

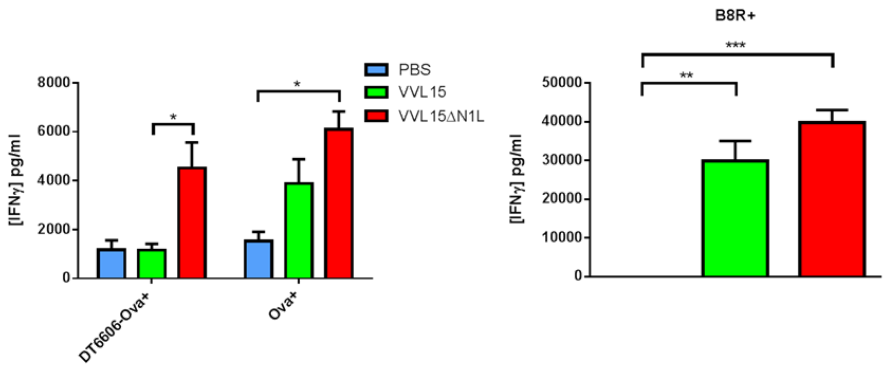

Figure 3.28 Intratumoural VVL15ΔN1L enhanced the adaptive immune response against an artificial TAA

DT6606-Ova flank tumours in C57BL/6 strain mice were treated with $1x10^8$ PFUs of IT virus or the equivalent volume of PBS (n=4/group). Fourteen days later, splenocyte suspensions were co-cultured with DT6606-Ova cells**,** Ova peptide or B8R peptide, as indicated. IFNγ concentrations (in pg/ ml, Y axes) of supernatants were measured by ELISA. One way ANOVAs with post hoc Tukey tests were used to compare means.

IFNγ production in PBS groups appeared to be no different than from VVL15 treatment arms. This probably reflected the ability of the "foreign" chicken ovalbumin to induce a significant immunogenic response even in untreated tumours; a response that was further exacerbated by VVL15ΔN1L administration but not VVL15 (figure 3.28).

The antiviral (anti B8R) immune response was not significantly different between the two viral treatment arms.

3.2.3 VVL15ΔN1L enhanced immunity against a natural tumour-antigen

Mesothelin is a 40 kDa protein present in normal mesothelial cells and overexpressed in several human tumours, including mesothelioma, ovarian and pancreatic adenocarcinoma (336). Following on from the DT6606-Ova experiment above, our group established by Western blot that DT6606 cells also express a murine mesothelin homologue. We therefore explored the possibility that this might be a candidate protein against which a natural TAA specific immune response may be generated. A nonamer

peptide was created by Proimmune™ (section 2.8.3.2). This nonamer was predicted to be the best fit into the H-2Db MHCI binding groove, and thereby potentially the most immunogenic. Splenocytes from VVL15ΔN1L injected DT6606 tumour bearing mice produced the highest levels of IFNγ upon co-culture with this mesothelin peptide. As might be expected, the response generated against this solitary peptide antigen was less than that generated against whole tumour cells carrying multiple TAAs.

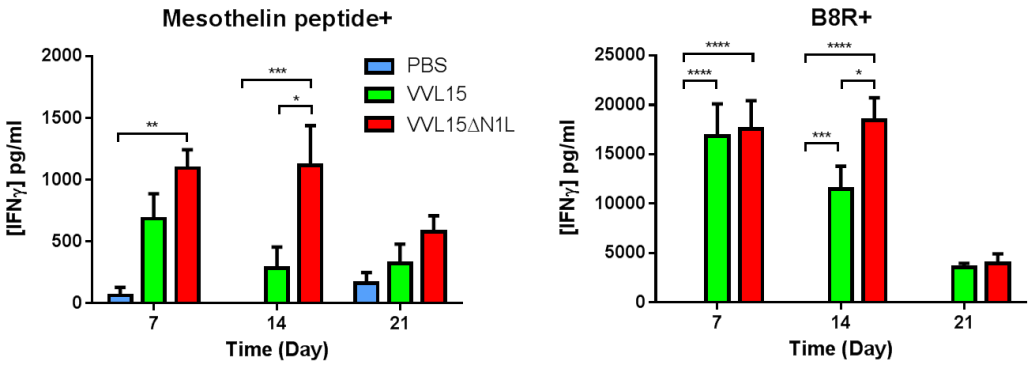

Figure 3.29 Intratumoural VVL15ΔN1L enhanced the adaptive immune response against a natural TAA

Syngeneic DT6606 flank tumours were treated with $1x10^8$ PFUs of IT virus or the equivalent volume of PBS (n=3-4/group). Fourteen days later, splenocyte suspensions were co-cultured with murine mesothelin peptide or B8R peptide as indicated. IFNγ concentrations (in pg/ ml, Y axes) of supernatants were measured by ELISA. Two way ANOVAs with post hoc Tukey tests were used to compare means. The B8R+ stimulated graph is identical to that from figure 3.27 (Exp. B)

3.2.4 VVL15ΔN1L administration enhanced the generation of an effector CD8+ T cell population

The ultimate goal of any antitumour immunotherapeutic is to enhance the pool of tumour specific CTLs. Although debate exists as to which type of CTL memory pool (central or effector) is relatively important (section 4.1), clearance of tumour in the periphery at any time will necessarily rely on a significant proportion of effector CTLs. We therefore explored by fluorescence cytometry, whether VVL15ΔN1L treatment could alter the immunological profile of CD8+ T cells in this regard. The CD62L surface antigen (a central lymphoid homing integrin) is lost in both primary effector and effector memory T cells, allowing them to circulate into the periphery in order to mediate their cytotoxic effects (section 4.1). Activated memory T cells also upregulate CD44, a cell adhesion molecule. Thus CD8+ effector memory T cells were defined as CD44hiCD62Llo. Splenocytes from experimental groups were stained with the following combinations of fluorophore labelled antibodies (for gating strategy see figure 3.30): anti CD45-eFluor® 450, anti CD3e-PerCP-Cy5.5, anti CD8a-FITC and anti CD62L-PE-Cy7.

Figure 3.31 depicts the percentage of CD8+ T cells that were CD44hiCD62Llo amongst splenocytes taken from treated LLC or DT6606 tumour bearing mice. In both tumour models, there was an enhancement of this population following treatment with VVL15ΔN1L. This enhancement declined with time, dropping to levels comparable to the PBS group by day 21 in DT6606 tumour bearing mice. Given the absence of any significant enhancement of antiviral (anti B8R) immunity following IT VVL15ΔN1L (figure 3.27), any differences in the overall percentage of effector memory CD8+ T cells may have reflected differences within the tumour specific CTL subset.

Note the relatively higher percentages of effector memory CD8+ T cells in mice bearing DT6606 tumours in comparison to those bearing LLC tumours. Coupled with the previous IFNγ immunoassays, these results further strengthened the impression that DT6606 tumours in comparison to LLC tumours were more likely to be sensitive to immunotherapy with oncolytic VV.

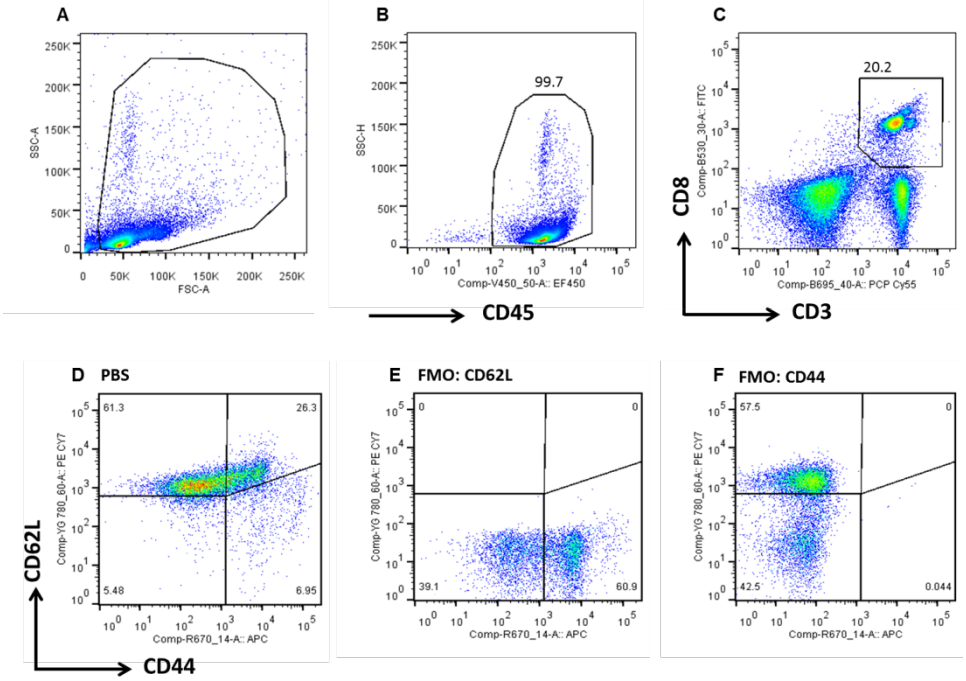

Figure 3.30 Gating the effector memory (CD44hiCD62Llo) percentage of CD8+ T cells

Following the selection of CD3+CD8+ cells (C), an experimental sample from the PBS group was used to set the CD62L lo/hi and CD44 lo/hi boundaries as shown (D). Dot plots from samples stained with all except anti CD62L (E) or anti CD44 (F) (fluorescence minus one (FMO) samples, section 2.10) confirmed the appropriateness of these gaits.

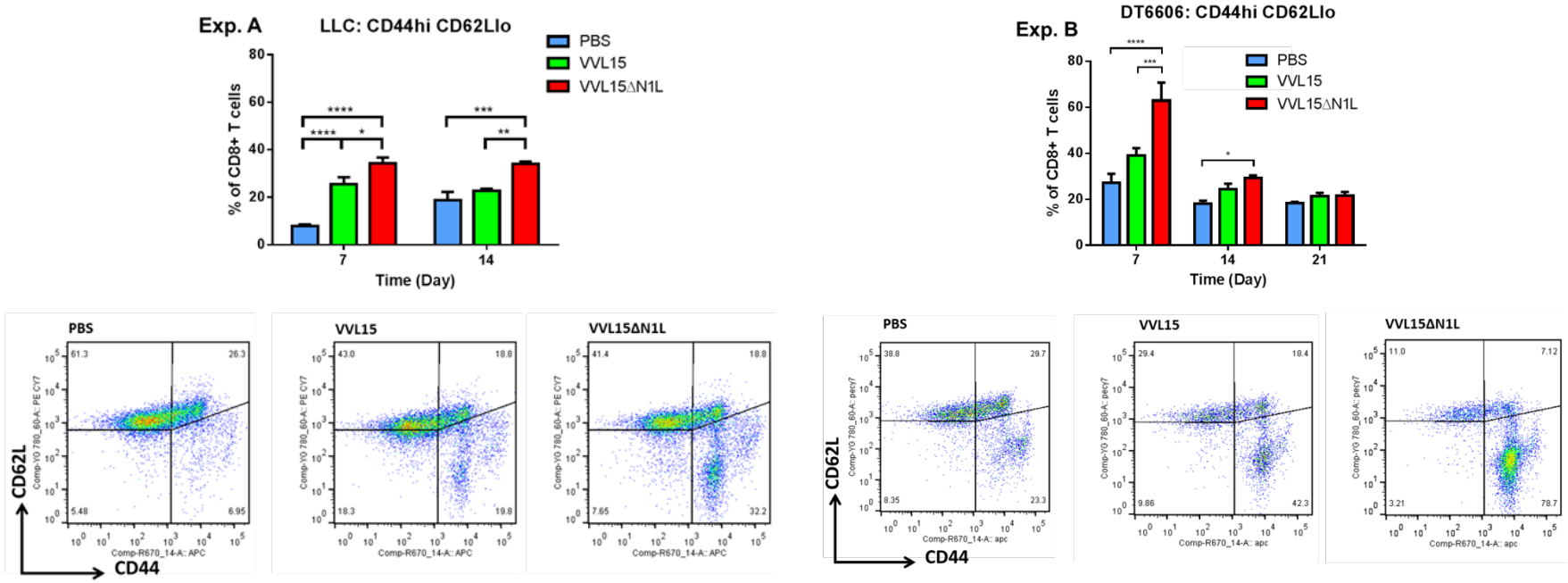

Figure 3.31 Intratumoural VVL15ΔN1L enhanced the generation of an effector memory CD8+ T cell population

Syngeneic LLC (Exp. A) or DT6606 (Exp. B) flank tumours were treated with $1x10^8$ PFUs of IT virus or the equivalent volume of PBS (n=3- 4/group). Seven, 14 or 21 days later as indicated, splenocyte suspensions were stained with fluorophore labelled antibodies against CD45, CD3, CD8, CD44 and CD62L surface antigens and analysed in a multichannel flow cytometer. The bar charts depict the effector memory (CD44hiCD62Llo) percentage of CD8+ T cells. Two-way ANOVAs with post hoc Tukey tests were used to compare means.

3.2.5 IT VVL15ΔN1L viral treatment invoked a higher intratumoural infiltrate of CD8+ cells in comparison to VVL15

LLC and DT6606 flank tumours were harvested at 14 days following a single IT dose of virus/ PBS. Tumours were snap frozen in precooled isopentane, sectioned and stained with anti CD4 and CD8 antibodies. Slides were scrutinised for the presence of the relevant marker as described in section 2.14. Although VVL15ΔN1L administration (in comparison to VVL15 or PBS) appeared to enhance the number of CD8+ cells that infiltrated LLC tumours, absolute counts per high power field (HPF) were relative low; certainly when compared to CD8+ T cell infiltration within similarly treated DT6606 tumours (see figure 3.32 and figure 3.33).

Note all IHC slides in this project were also stained with anti NK1.1 and F4/80 antibodies. However, positively stained NK cells were too sparse to count, whereas the numbers of anti F4/80 stained macrophages were contrastingly too substantial to quantify by manual counting (see figure 4.1); hence these data are not presented.

IHC cell counts in this project were performed by JA who was not blinded to group allocation. To minimise inadvertant error, 10-15 randomly selected HPFs were counted and averaged per sample. To verify JA's mean counts, randomly selected slides were independently counted by YW who was blinded to treatment arms.

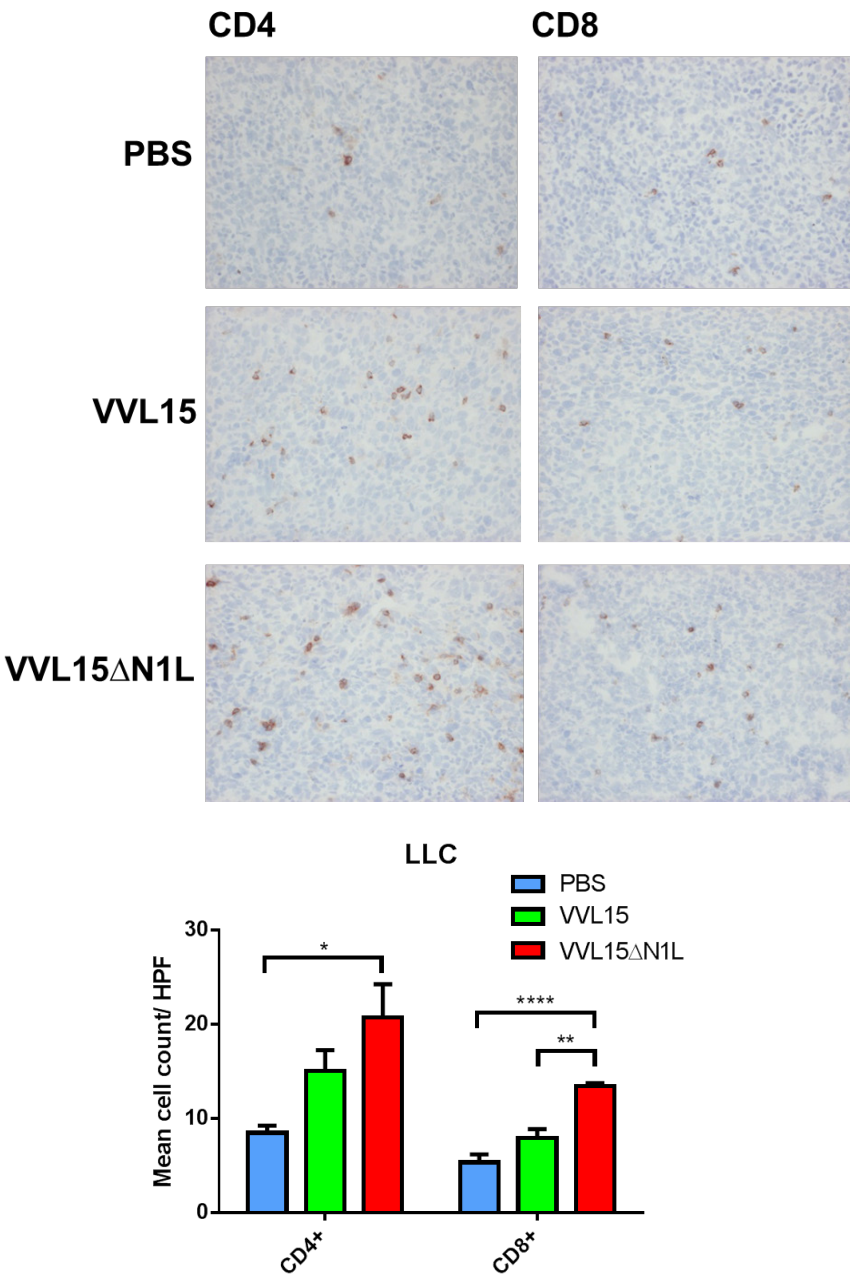

Figure 3.32 Intratumoural VVL15ΔN1L enhanced the infiltration of CD8+ cells into LLC tumours

Syngeneic LLC flank tumours were treated with $1x10^8$ PFUs of IT virus or the equivalent volume of PBS (n=3- 4/group). Fourteen days later, frozen sections of harvested tumour were immunostained with either anti CD4, CD8, NK1.1 or F4/80 antibodies. The bar chart depicts the mean manual cell count per HPF from 10-15 HPFs (x200 magnification). One way ANOVAs with post hoc Tukey tests were used to compare means.

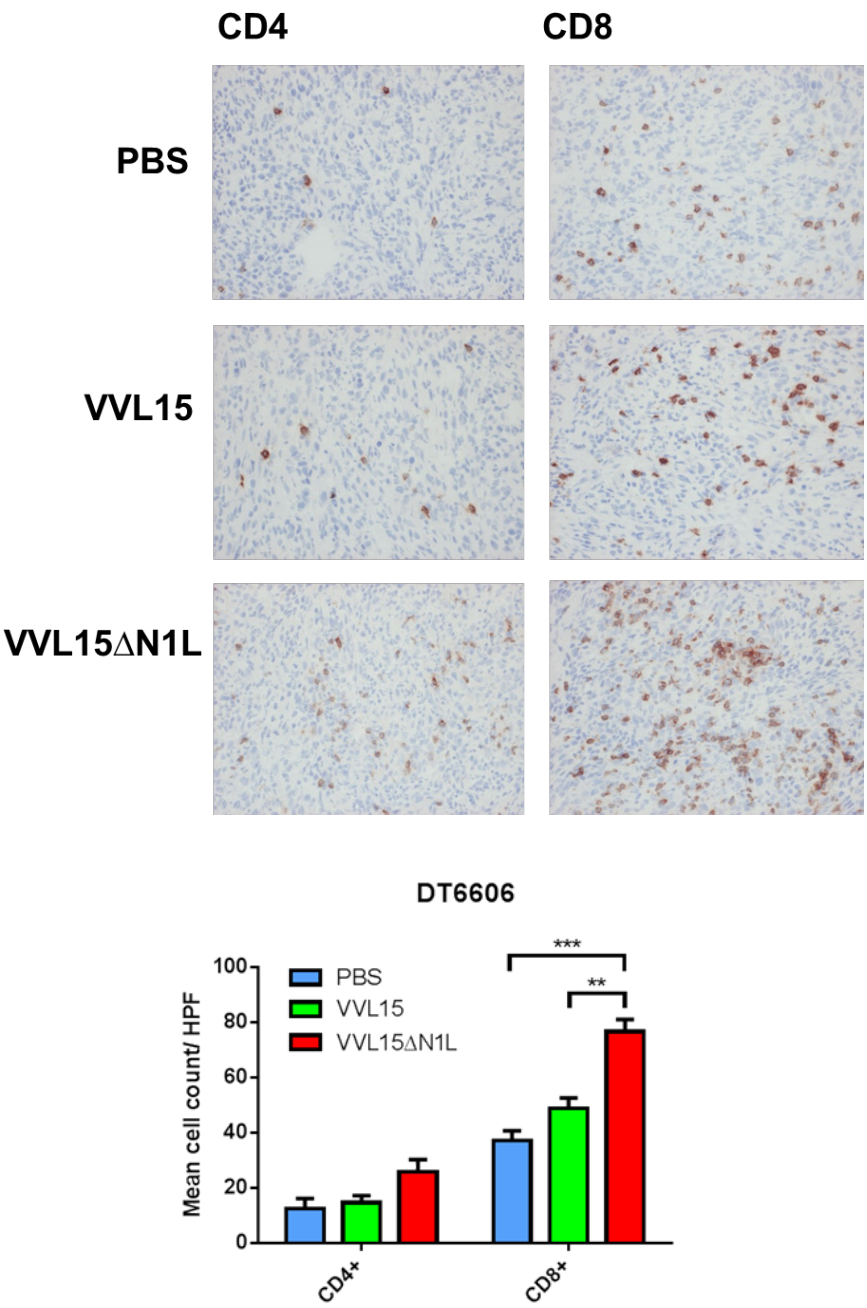

Figure 3.33 Intratumoural VVL15ΔN1L enhanced the infiltration of CD8+ cells into DT6606 tumours

Syngeneic DT6606 flank tumours were treated with $1x10^8$ PFUs of IT virus or the equivalent volume of PBS (n=3- 4/group). Fourteen days later, frozen sections of harvested tumour were immunostained with either anti CD4, CD8, NK1.1 or F4/80 antibodies. The bar chart depicts the mean manual cell count per HPF from 10-15 HPFs (x200 magnification). One way ANOVAs with post hoc Tukey tests were used to compare means.

3.2.6 VVL15ΔN1L treated LLC and DT6606 tumours produced higher levels of tumour-specific cytotoxic lymphocytes

IFNγ production from splenocytes in response to tumour cell or antigen challenge is an indirect measure of a CTL response (the major IFNγ producing adaptive immune cell), with the magnitude of response likely to be proportional to the number of CTLs generated. ELISPOT assays measuring secreted IFNγ or granzyme B for example could quantify the numbers of potential CTLs, nevertheless such assays will not be able to demonstrate the ability of antigen specific CTLs to actually lyse their target containing cells. To demonstrate this, we performed a non-radioactive CTL assay, based on the release of the enzyme LDH from lysed cells (section 2.8.4).

As illustrated in figure 3.34, at the effector to target ratio of 60:1, splenocytes from VVL15ΔN1L treated groups from both models were able to lyse a higher percentage of target tumour cells in comparison to those harvested from the other treatment arms. The specificity of response was demonstrated by the inability of these effector splenocytes to lyse MHC compatible control tumour cells. Splenocytes from all mice within each treatment group were pooled to produce a solitary mean value per time point and was therefore not amenable to statistical analysis.

In keeping with the previous experiments in this section, VVL15ΔN1L treatment induced a more potent cytolytic response against DT6606 (in comparison to LLC) tumour cells.

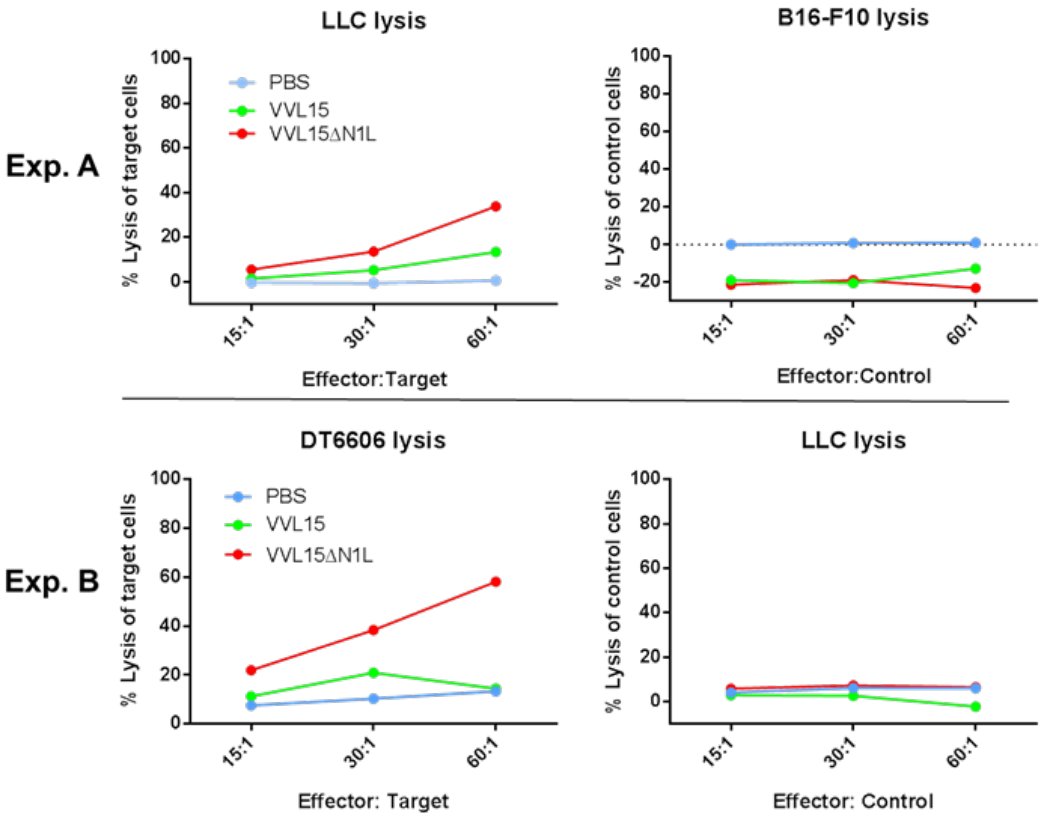

Figure 3.34 VVL15ΔN1L enhanced the generation of tumour specific cytolytic splenocytes

Syngeneic LLC (Exp. A) or DT6606 (Exp. B) flank tumours were treated with $1x10^8$ PFUs of IT virus or the equivalent volume of PBS (n=3- 4/group). Fourteen days later splenocyte suspensions were co-cultured with growth arrested target (LLC or DT6606) tumour cells. Five days later splenocytes from each treatment group were pooled and further co-cultured with 5000 target or control (B16-F10 or LLC) tumour cells in ratios of 15:1, 30:1, and 60:1. A non-radioactive lymphocyte cytotoxicity assay based on LDH release from lysed cells, was used to estimate percentage tumour cell lysis (Y axes).

3.2.7 Summary of results chapter 3.2

IT VVL15ΔN1L led to significantly higher levels of IFNγ from tumour cell/ TAA stimulated splenocytes in comparison to VVL15. Interestingly there was no such enhancement in the antiviral response (as measured by the anti B8R antigen response).

Flow cytometric profiling of CD8+ T cells within splenocytes, suggested the generation of a higher proportion of effector memory CD8+ T cells in response to IT VVL15ΔN1L, which in parallel to the IFNγ assays peaked at around day seven post infection then waned to control levels by day 21.

The magnitude of adaptive antitumour immunity evoked by VVL15ΔN1L appeared to be much higher in DT6606 tumour bearing mice in comparison to their LLC counterparts. Evoked anti-tumour IFNγ levels, percentage effector memory CD8+ T cells and counts of intratumoural CD8+ cells were all higher in the former group. Indeed splenocyte mediated tumour cell lysis in a CTL assay was also superior. The DT6606 tumour model appears to be more immunogenic than the LLC model and thereby potentially more responsive to immunotherapeutic strategies with VV.

3.3 *In vivo* efficacy of VVL15ΔN1L

3.3.1 VVL15ΔN1L was more efficacious than VVL15 against a model of pancreatic cancer.

In order to establish the broad antitumour utility of VVL15ΔN1L, SCCVII, LLC, CT26, CMT93 and DT6606 syngeneic subcutaneous flank models were established (table 2.8) and treated with five daily IT doses of virus or PBS. For SCCVII, LLC and CMT93 models, there were no statistically significant differences in tumour growth rates between the two viral treatment groups (figure 3.35). VVL15ΔN1L did however significantly slow the growth of CT26 and DT6606 tumours (figure 3.35).

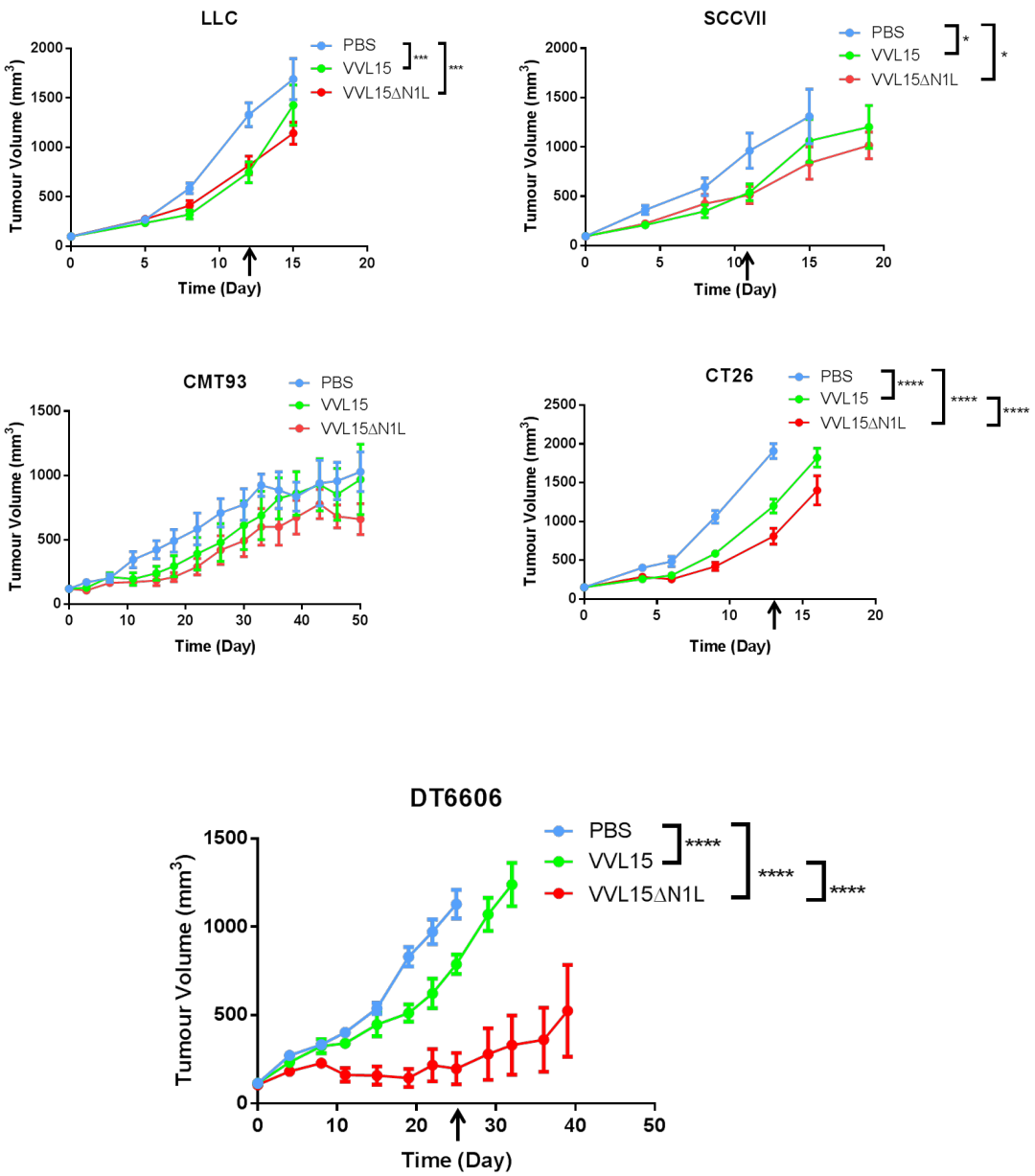

Figure 3.35 Intratumoural VVL15ΔN1L slowed tumour growth in models of pancreatic and colorectal cancer

Syngeneic DT6606, CMT93, LLC, SCCVII and CT26 flank models (as indicated) were treated with five, daily IT doses of $1x10^8$ PFUs of virus or the equivalent volume of PBS (n=5-7 per group). The first dose was injected at day 0. Tumour growth was followed up via twice weekly calliper measurement. Two way ANOVAs with post hoc Tukey tests were used to compare mean tumour volumes. The arrow depicts the time point to which the comparative statistical figures on each graph relate to.

3.3.2 CD8+ T cells play a pivotal role in the efficacy demonstrated by VVL15ΔN1L treated DT6606 subcutaneous tumours

The DT6606 flank tumour model was the most sensitive to treatment with VVL15ΔN1L as might have been predicted by the results from chapter 3.2. In order to explore this further, the VVL15ΔN1L arm of the experiment was repeated in mice that had been depleted of key immune effector cells (section 2.15.6 and table 2.10, experiment 1). Figure 3.36 demonstrates that the efficacy of IT VVL15ΔN1L was abrogated when CD8+ cells were depleted for the duration of the experiment; similar depletion of NK or CD4+ cells made no difference.

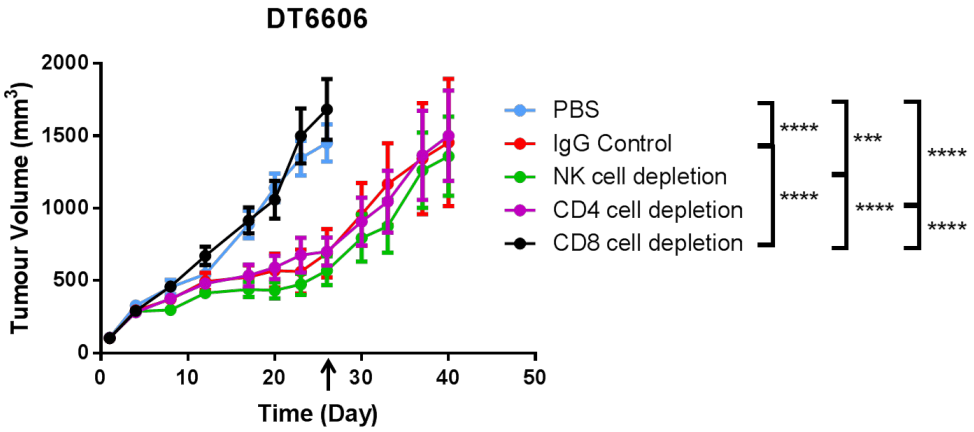

Figure 3.36 CD8+ cells play a pivotal role in mediating the efficacy of VVL15ΔN1L against subcutaneously implanted DT6606 tumours

Cell depleting or IgG control antibodies were commenced intraperitoneally in mice bearing syngeneic DT6606 flank tumours, a day prior to the initial dose of IT treatment with VVL15ΔN1L (n=8-10 per group) (see table 2.10, experiment 1). Tumour growth was followed up via twice weekly calliper measurement. Two way ANOVAs with post hoc Tukey tests were used to compare mean tumour volumes. The arrow depicts the time point to which the comparative statistical figures on each graph relate to.

3.3.3 Confirmation of antitumour immunogenicity following a multidose regime of IT VVL15ΔN1L in DT6606 tumours

Immunoassays were repeated after DT6606 tumour bearing mice were treated with multiple doses of IT virus (section 2.15.1 and table 2.7, experiment 4). This served a) to confirm the reproducibility of the previous immunoassay experiments, and b) to enhance the likelihood of detecting the presence of *in vivo* generated mesothelin specific CD8+ T cells.

Another way of demonstrating an enhancement in tumour specific immunity is to confirm the elevation of tumour epitope specific clones of CD8+ T cells. A pentamer of H-2Db MHCI complexed to a murine mesothelin epitope (section 2.10.1) had recently been created by Proimmune© and could be utilised for this purpose. Unlike the IFNγ and CTL assays, where splenocytes were selectively expanded *ex vivo*, for up to five days, antigen specific T cells were measured at the point of animal sacrifice. Therefore in order to maximise the chances of detecting this likely small pool of cells, the experiment was conducted following multiple doses of virus.

IFNγ assays were set up as previously described, using splenocytes harvested at day 14 after the initial dose of virus. The level of IFNγ produced from splenocytes co-cultured with growth arrested DT6606 cells was highest following treatment with VVL15ΔN1L. Splenocytes were also co-cultured with a mesothelin peptide, a peptide derived from a mutated K-RAS proto-oncogene (an activating mutation of K-RAS may be a critical step in the initiation of pancreatic and other cancers (331)) or an artificial ovalbumin peptide (Ova) as a control (table 2.4). The mesothelin and K-RAS peptides evoked IFNγ production from splenocytes harvested from VVL15ΔN1L treated mice.

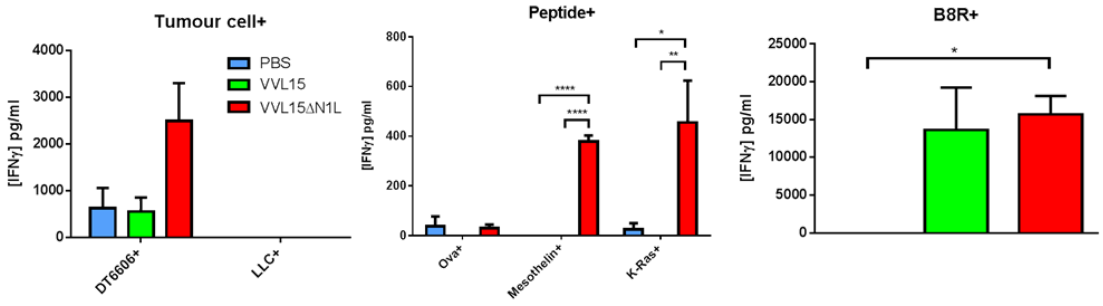

Figure 3.37 Multiple doses of intratumoural VVL15ΔN1L enhanced antitumour adaptive immunity

Syngeneic DT6606-flank tumours were treated with five daily IT doses of $1x10^8$ PFUs or the equivalent volume of PBS (n=3-4/group). Fourteen days after the first dose, splenocyte suspensions were co-cultured with growth arrested whole tumour cells (Tumour cell+), tumour peptides (Peptide+) or the VV B8R peptide (B8R+). IFNγ concentrations (in pg/ ml, Y axes) of supernatants were measured by ELISA. One way ANOVAs with post hoc Tukey tests were used to compare means.

Immunohistochemical staining of frozen sections of DT6606 tumour confirmed the previously demonstrated enhanced infiltration of both CD4+ and in particular CD8+ cells into the tumour.

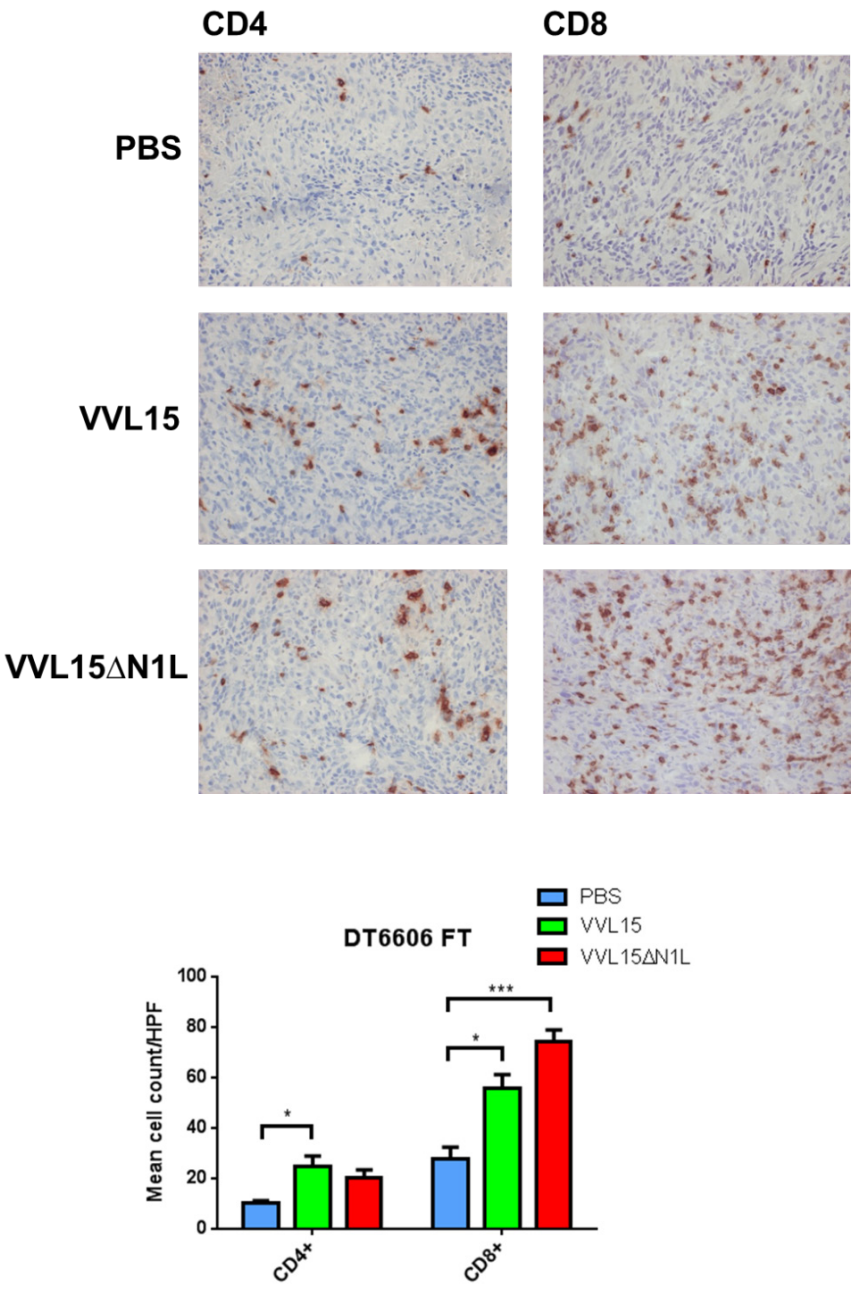

Figure 3.38 Multiple doses of IT VVL15ΔN1L enhanced the infiltration of CD8+ cells into DT6606 tumours

Syngeneic DT6606 flank tumours were treated with five daily IT doses of virus ($1x10^8$ PFUs per dose) or the equivalent volume of vehicle buffer (n=3-4/group). Fourteen days after the first dose, frozen sections of harvested tumour were immunostained with either anti CD4, CD8, NK1.1 or F4/80 antibodies. The bar chart depicts the mean manual cell count per HPF from 10-15 HPFs (x200 magnification). One way ANOVAs with post hoc Tukey tests were used to compare means.

Flow cytometric analysis of splenocytes harvested at day 14 post initial viral injection also confirmed the previously demonstrated enhancement of effector memory (CD44hiCD62Llo) CD8+ T cells in the VVL15ΔN1L treated group (figure 3.39). The following fluorophore labelled antibodies were used to stain splenocytes, with a similar gating strategy to that shown in figure 3.30: anti CD45-FITC, anti CD3e-PerCP-Cy5.5, anti CD8a-APC, anti CD62L-PE-cy7 and anti CD44-eFluor® 450.

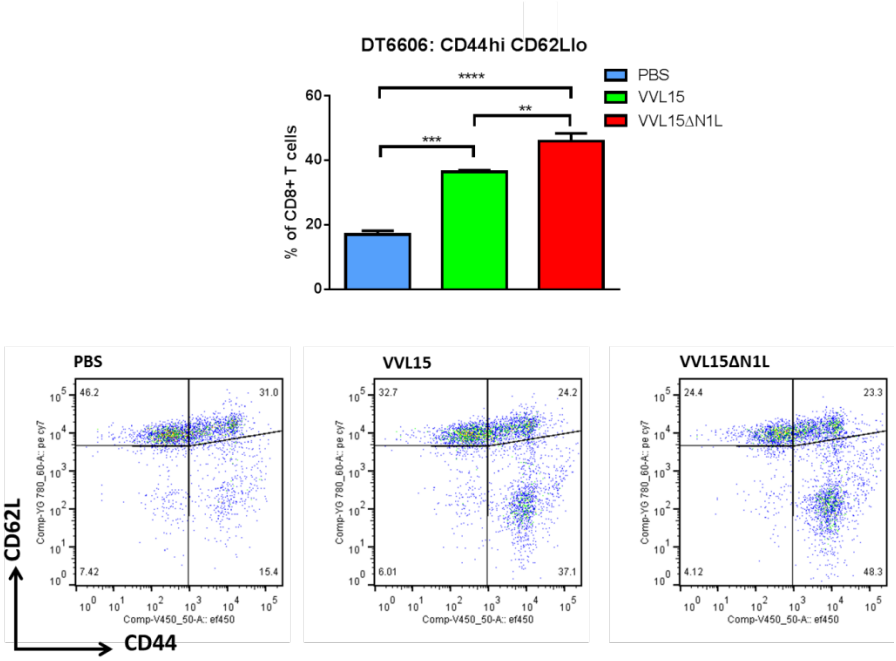

Figure 3.39 Multiple doses of IT VVL15ΔN1L enhanced the generation of an effector memory CD8+ T cell population

Syngeneic DT6606 flank tumours were treated with five daily IT doses of virus ($1x10^8$ PFUs per dose) or the equivalent volume of vehicle buffer (n=3- 4/group). Fourteen days after the first dose, splenocyte suspensions were stained with fluorophore labelled antibodies against CD45, CD3, CD8, CD44 and CD62L cell surface antigens and analysed in a multichannel flow cytometer. The bar chart depicts the effector memory (CD44hiCD62Llo) percentage of CD8+ T cells. A one-way ANOVA with post hoc Tukey tests was used to compare mean values.

Finally, the following fluorophore labelled antibodies and mesothelin pentamer (MesoPent) were used to stain splenocytes as described in section 2.10: anti CD3-FITC, anti CD8a-APC and MesoPent-PE.

There was a significant elevation in the mesothelin epitope specific clone of CD8+ T cells following VVL15ΔN1L treatment (figure 3.40 and figure 3.41). Although statistically significant, this enhancement was relatively modest.

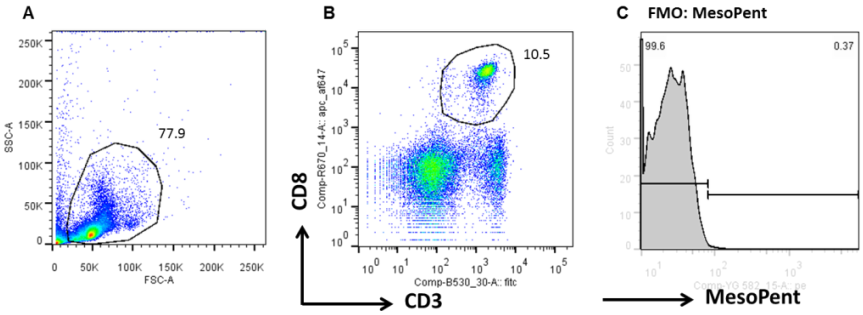

Figure 3.40 Gating the mesothelin pentamer stained population of T cells

Following the selection of CD3+CD8+ cells (B), the histogram from the MesoPent FMO sample (stained with all antibodies but no MesoPent) was used to set the gate for MesoPent positive clones (C).

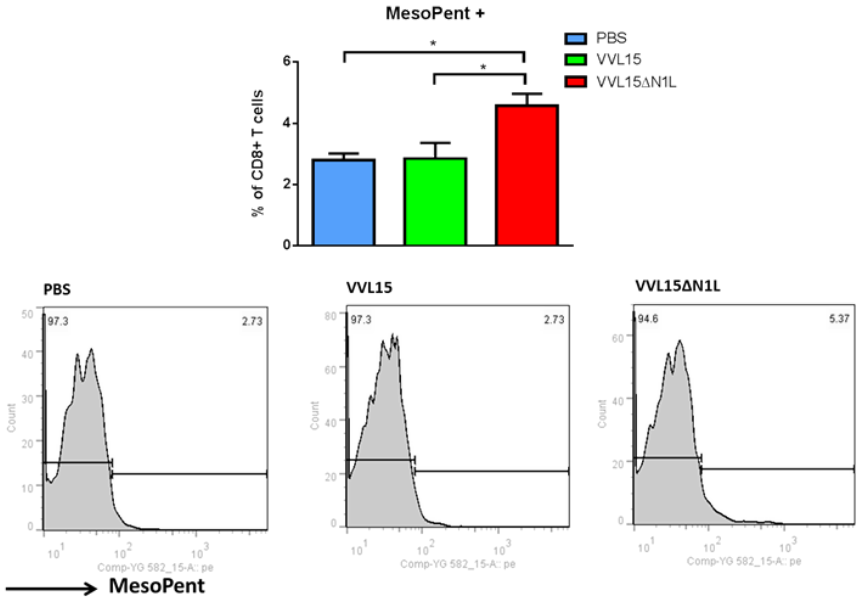

Figure 3.41 Multiple doses of IT VVL15ΔN1L enhanced the *in vivo* expansion of a mesothelin specific clone of T cells

Syngeneic DT6606 flank tumours were treated with five daily IT doses of virus ($1x10^8$ PFUs per dose) or the equivalent volume of PBS (n=3- 4/group). Fourteen days after the first dose, splenocyte suspensions were stained with fluorophore labelled mesothelin pentamer as well as with antibodies against CD3 and CD8 cell surface antigens and analysed in a multichannel flow cytometer. The bar chart depicts the mesothelin peptide specific clone of CD8+ T cells. A one way ANOVA with post hoc Tukey tests was used to compare means.

3.3.4 Replication of intravenous VVL15 in off-target organs was reduced by the deletion of its N1L gene

A biological distribution experiment was performed to establish whether IV delivered virus could disseminate to subcutaneous tumour and importantly to determine any off target infection and replication. LLC and CT26 subcutaneous flank models were utilised, being representative of two syngeneic models from different strains of mice (C57BL/6 and BALB/c respectively) (section 2.15.1 and table 2.7, experiments five and six)

Following tail vein injection, live, replication competent viruses could be recovered from tumour tissue until at least 10 days post injection in both models (figure 3.42). The peak titre appeared to lie between three and seven days. Titres in general were much higher with the LLC model in comparison to the CT26 model. This probably reflected differences in vascularity between tumours or indeed the potency of viral clearance between strains. Whilst there was no difference in viral recovery from tumours between groups with the CT26 model; with the LLC model VVL15ΔN1L titres were significantly lower from day three onwards (figure 3.43).

With the exception of lung tissue, virus was not recovered from any organ beyond 24 hours post injection (figure 3.43). At 24 hours, VVL15ΔN1L titres were significantly lower than VVL15 from liver and spleen in the CT26 model and liver in the LLC model. In the CT26 model there was no viral recovery from brain. Brain titres were significantly lower following IV VVL15ΔN1L injection into the LLC model. Neither virus was recovered from ovaries. In contrast, virus persisted in the lungs until at least three days in the CT26 model and five days in the LLC model. In both models, VVL15ΔN1L titres in lungs were lower than VVL15.

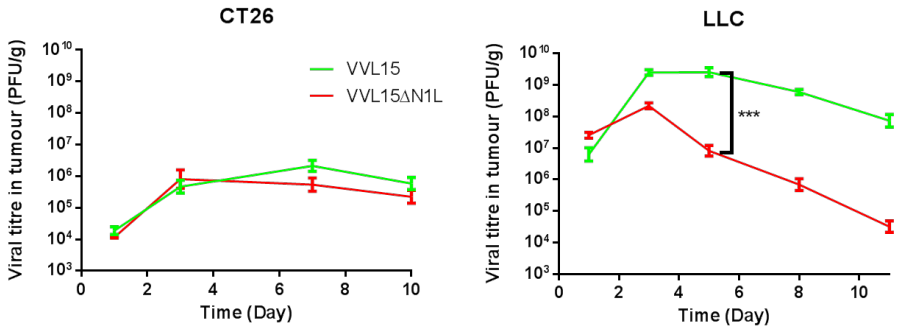

Figure 3.42 Systemic viral delivery to flank tumours

Mice bearing syngeneic LLC or CT26 flank tumours (in C57BL/6 or BALB/c mice respectively) as indicated were administered tail vein injections of $1x10^8$ PFU of either VVL15 or VVL15ΔN1L. At the depicted time-points post virus injection (X axis), mice (n=3 per group) were euthanized and tumours were harvested. Viral titres in PFU/ gram weight of tumour tissue (Y axes) were estimated using TCID50 assays on tumour homogenates. Two-way ANOVAs with post hoc Tukey tests were used to compare mean viral titres.

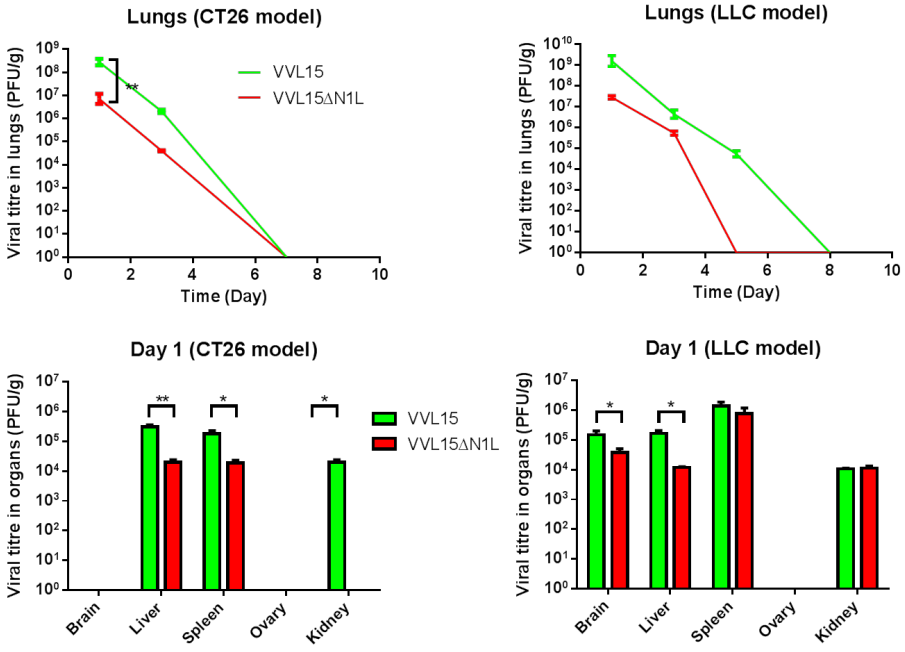

Figure 3.43 N1L gene deletion reduced the off-target viral replication of VVL15

Mice bearing syngeneic LLC or CT26 flank tumours (in C57BL/6 or BALB/c mice respectively) as indicated were administered tail vein injections of $1x10^8$ PFU of either VVL15 or VVL15ΔN1L. At the depicted time-points post virus injection (X axis), mice (n=3 per group) were euthanized and lungs and other organs were harvested. Viral titres in PFU/ gram weight of organ tissue (Y axes) were estimated using TCID50 assays on tissue homogenates. Viral titres were detectable only on day one post injection for non-lung organs. For lungs, two-way ANOVAs with post hoc Tukey tests were used to compare mean viral titres; whereas unpaired t-tests were used likewise for other organs.

3.3.5 Intravenous delivered virus maintained the capacity to generate antitumour immunity

In the LLC model, viral titres within tumour tissue diminished at a faster rate following IV VVL15ΔN1L administration in comparison to VVL15. This may have been due to enhanced innate as opposed to adaptive antiviral clearance mechanisms. Innate defences mobilise within hours to days following pathogen exposure and viral titres from tumours and lungs started to deviate between groups from day three in the current experiment.

Despite the enhanced clearance of virus from tumour, could IV delivered VVL15ΔN1L retain its ability to enhance antitumour adaptive immunity? To answer this question, splenocyte IFNγ assays were performed on days eight and 11 following the IV administration of virus or PBS into LLC tumours (table 2.7, experiment 5). IFNγ levels were significantly higher from splenocytes derived from VVL15ΔN1L injected tumour bearing mice at both time points following co-culture with growth arrested LLC cells. As previously demonstrated, this enhancement was not paralleled by an enhanced antiviral (anti B8R) adaptive immune response.

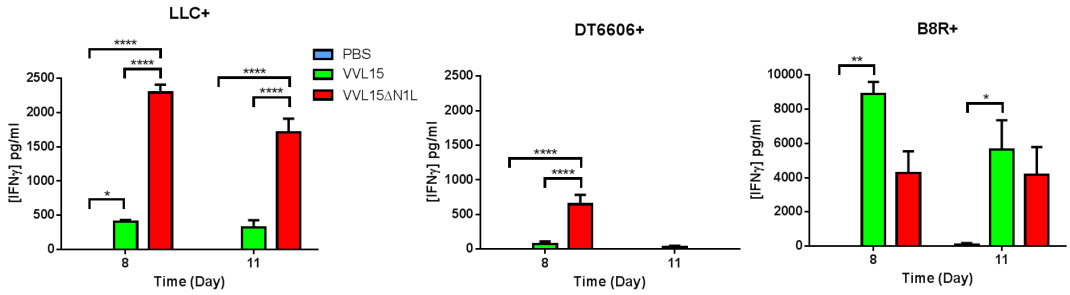

Figure 3.44 Intravenous VVL15ΔN1L also enhanced antitumour adaptive immunity against LLC tumours

Mice bearing syngeneic LLC flank tumours were treated with a single IV dose ($1x10^8$ PFU) of virus. At days eight and 11 post injection (X axes), splenocyte suspensions were co-cultured with either growth arrested LLC (target) or DT6606 (control) cells and VV B8R peptide, as indicated. IFNγ concentrations (in pg/ml, Y axes) of supernatants were measured by ELISA. Two-way ANOVAs with post hoc Tukey tests were used to compare means.

3.3.6 IV administered VVL15 and VVL15ΔN1L prolonged survival in an orthotopic lung cancer model

The orthotopic LLC lung tumour model is very reliable; in our experience almost all animals establish tumour foci within their lungs following the tail vein injection of a relatively low number of LLC cells. $5x10^5$ LLC cells were injected into the tail veins of seven C57BL/6 mice. CT imaging was used to assess their lung volumes over time; the reduction of which was used as a surrogate marker for tumour volume (figure 3.45). All mice developed tumour, with deaths occurring between 14 to 21 days, at which time thoracotomy confirmed extensive lung tumour. CT detectable tumour volumes arose between four and seven days, thus the first dose of viral therapy in a subsequent efficacy study was commenced at day five post-LLC cell injection.

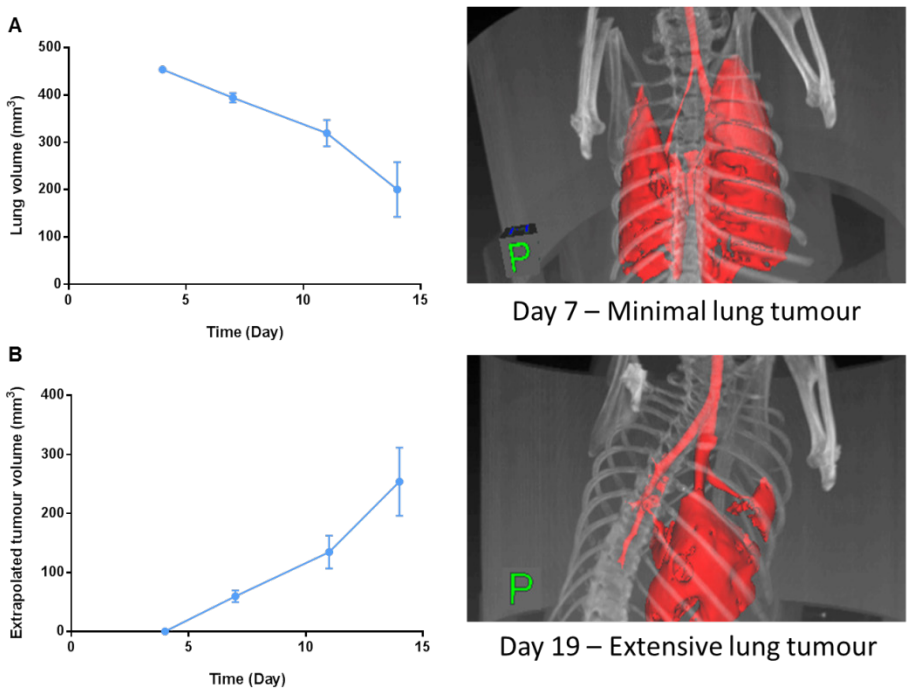

Figure 3.45 The CT lung profile of an orthotopic lung cancer model

C57BL/6 mice were injected with $5x10^5$ LLC cells via tail vein (n=7). Their lungs were monitored by regular non contrast CT scans. Graph A. depicts the reduction in lung volume with time after cell injection and was used as a surrogate marker for lung tumour burden (B). Note the CT scans of the same mouse at different days following tumour cell injection. These figures and images were constructed with the help of Dr Mark Ferguson in our group.

Twenty one mice were administered tail vein injections of $5x10^5$ LLC cells in 100 µl serum-free DMEM. They were randomised into three groups (table 2.9, experiment 3) and treatment was commenced from day five. All mice in the PBS treatment group were symptomatic after 10 days post LLC cell injection as evidenced by weight loss, and all had died or needed to be culled by 21 days (figure 3.46). The median survival was enhanced by 5 and 6.5 days following VVL15 and VVL15ΔN1L viral treatment respectively (the median survival for the PBS group was 19 days). There was no statistically significant difference in survival between viral groups.

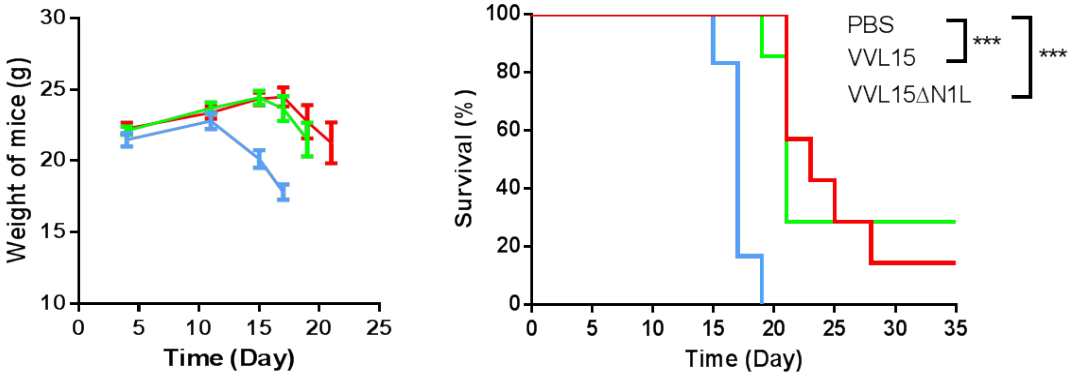

Figure 3.46 Intravenous recombinant VVL15 viruses prolonged survival in an orthotopic lung cancer model

C57BL/6 mice were injected with $5x10^5$ LLC cells via tail vein (n=7). Five, seven and nine days later they were treated with $1x10^8$ PFUs of virus administered via tail vein or the equivalent volume of vehicle buffer (n=7 per group). The left graph demonstrates the mean weight of mice in each group as a function of time after LLC cell injection (X axes); the right graph is the corresponding Kaplan Meier survival analysis. Log rank analyses were used to compare treatment pairs.

3.3.7 Summary of results chapter 3.3

Multiple doses of IT VVL15ΔN1L reduced the tumour growth rate in some murine syngeneic flank tumour models. DT6606 tumours were the most responsive, whilst the least responsive were the aggressively growing LLC tumours. If the generation of adaptive antitumour immunity was indeed mechanistically important in the efficacy of VVL15ΔN1L against primary tumour models, then this data was consistent with the conclusion of chapter 3.2; namely that IT VVL15ΔN1L evoked a stronger tumour specific immune response in DT6606 tumour bearing mice, in comparison to the LLC counterpart.

VVL15ΔN1L treated DT6606 tumour bearing mice, generated elevated numbers of mesothelin specific CD8+ T cells in comparison to treatment with VVL15. Indeed the critical role of CTLs in mediating the efficacy of VVL15ΔN1L in this model was confirmed by the complete abrogation of efficacy in tumour bearing mice that lacked CD8+ cells.

VVL15 recombinant viruses were able to localise to syngeneic flank tumours in two different genetic strains of mice following a single IV dose of virus. Their presence in tumour tissue was maintained for at least 10 days, peaking between three and seven days post injection. Off-target replication of VVL15 was reduced by the deletion of its N1L gene, although this also appeared to enhance viral clearance from LLC tumour tissue. Despite this, IV VVL15ΔN1L retained its ability to enhance (in comparison to VVL15) the generation of adaptive antitumour immunity.

IV VVL recombinant viral treatment of established LLC orthotopic tumours led to significantly prolonged short term survival of mice in comparison to those treated with vehicle buffer alone. There was however, no difference in survival between viral treatment groups.

3.4 The neoadjuvant potential of VVL15ΔN1L

LLC is an aggressively growing murine lung carcinoma that has the propensity to metastasize to the lungs following primary establishment in the flank. Indeed surgical excision of subcutaneously grown LLC tumour has been shown to enhance the rate of lung metastases, perhaps via removal of an angiogenesis inhibitor secreted by the primary (304, 337). This would be an ideal animal model to mimic the potentially enhanced rate of micro-metastases secondary to surgical manipulation of relatively advanced solid tumours.

We sought to answer two questions with this model. First, even though IT VVL15ΔN1L had no impact on the growth of primary LLC tumours (figure 3.35), could it reduce seeding of metastases from the primary? Second, could IT virus administered prior to surgical excision of the primary tumour, prolong post-operative survival of mice?

3.4.1 Intratumoural VVL15ΔN1L reduced dissemination of lung metastases from primary flank LLC tumours

Subcutaneous LLC tumours were established in female C57BL/6 mice as previously described. Intratumoural injections of PBS and treatment viruses ($1x10^8$ PFUs per dose) were commenced for a total of five daily doses (table 2.7, experiment 7). All animals were euthanized when the first group reached the criteria for sacrifice (mean volume $>1200mm^3$) and their lungs were scrutinized macroscopically and microscopically for tumour metastases as described in the methods (2.15.4).

There were no significant differences between groups with regards to tumour volumes at sacrifice. However the percentage of mice with lung metastases at the end point of the experiment was 14, 43 and 71% for VVL15ΔN1L, VVL15 and PBS groups respectively (figure 3.47).

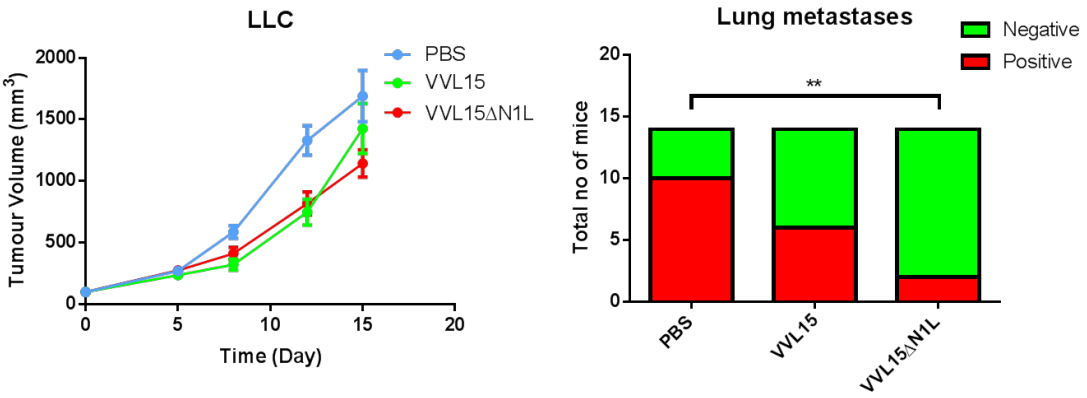

Figure 3.47 Intratumoural VVL15ΔN1L reduced metastatic dissemination from LLC flank tumours

Syngeneic LLC flank tumours were treated with five daily IT doses of virus ($1x10^8$ PFUs per dose) or the equivalent volume of PBS (n=14/ group). Tumour volumes were tracked via twice weekly calliper measurement (left). At day 15 post injection of the first dose of virus (X axis), mice were euthanized and lung sections were stained with H&E. The slides were scrutinized for the presence or absence of lung metastases by a pathologist (YW) who was blinded to the treatment groups (right hand graph). Fisher's exact tests were performed on 2x2 tables comparing specific pairs of conditions.

3.4.2 Pre-surgical treatment with VVL15ΔN1L prolonged post-operative survival in models of metastatic cancer

Given the possibility of reducing metastatic spread from the primary tumour, we explored the use of VVL15ΔN1L as a neoadjuvant alongside surgical excision of tumour. Many patients die post "curative" surgery as a consequence of either metastasis or regrowth of minimal residual local disease. The subcutaneous syngeneic LLC flank model would be ideal to model this scenario. First, as demonstrated it has a propensity to metastasise to lung from flank implants and second these tumours grow rapidly, infiltrating underlying tissue so even the cleanest surgical excision is likely to leave foci of residual disease. The model, pre-operative treatment schedule and surgical technique are described in detail in section 2.15.5.

Of note, surgical excision took place seven days following the final dose of viral treatment, a) to allow the mouse to recover from the effects of a protracted course of

viral therapy and importantly b) to provide adequate time for the development of an antitumour adaptive immune response. The results are shown in figure 3.48A.

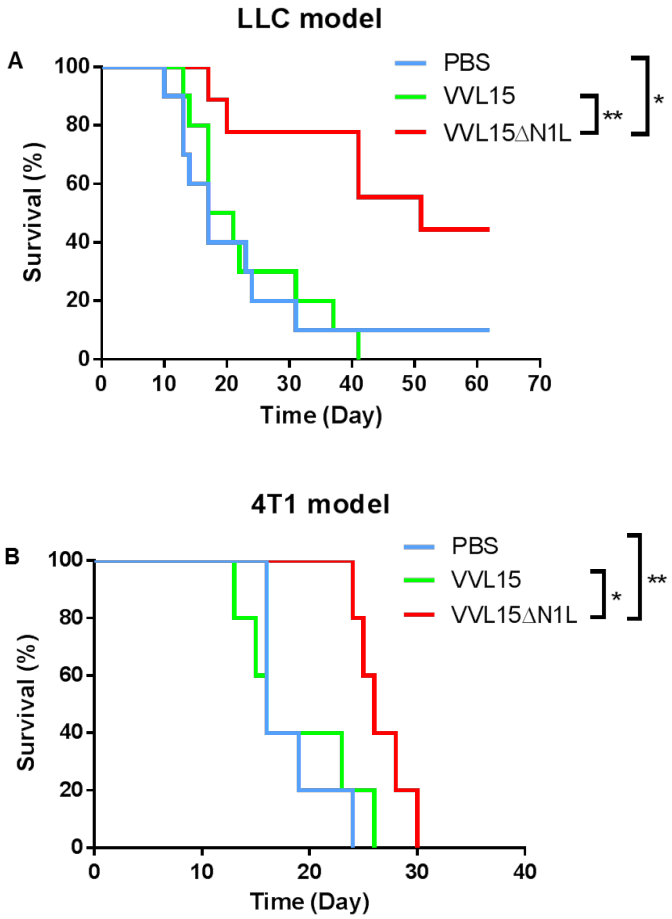

Figure 3.48 Pre-surgical IT treatment with VVL15ΔN1L prolonged post-operative survival in models of metastatic cancer

Syngeneic 4T1 (orthotopic) or LLC flank tumours, as indicated, were treated IT with three or five doses respectively of virus ($1x10^8$ PFUs per dose) or the equivalent volume of PBS (n=7-10/ group). Tumours were surgically resected five or seven days after the final dose of virus respectively. The X axes represent day's post-surgical excision. Log rank analyses were used to delineate any significant differences between specific treatment pairs.

There was no significant difference in tumour volumes between groups prior to surgical excision. The end points of this experiment were cure, death from lung metastasis or significant local regrowth from MRD. After exclusions, the numbers of mice in each

group were 9-10. There was a statistically significant short term survival advantage favouring treatment with VVL15ΔN1L.

In another syngeneic model of metastatic cancer, 4T1 breast cancer cells were orthotopically implanted into BALB/c mouse mammary glands (2.15.5). Tumours were treated with a similar schedule of recombinant virus or PBS prior to surgical excision. A significant prolongation of short term survival following treatment with VVL15ΔN1L virus was also observed with this model (figure 3.48B).

3.4.3 Surgery abolished the VVL15ΔN1L mediated enhancement of adaptive antitumour immunity

To assess whether general anaesthesia or operative stress per se. could impede the development of an adaptive immune response against either tumour or virus, subcutaneous LLC tumour bearing mice were treated as above with multiple doses of IT virus/ PBS (table 2.7, experiment 8). Seven days after tumour resection, mice were sacrificed and their harvested splenocytes were co-cultured with growth arrested LLC cells or VV B8R peptide. Splenocytes from three of four mice in each viral treatment group produced detectable levels of IFNγ upon co-culture with LLC cells. The mean values of these positive responders are shown in the graph (figure 3.49). Although the study contained a limited number of mice, the fact that one in four showed no evidence of antitumour immunity following viral treatment and that the enhancement of IFNγ secretion from stimulated lymphocytes (consequent to VV N1L gene deletion) was abolished, implied that surgical excision did indeed impair the generation of adaptive antitumour immunity. As further confirmation, splenocytes from LLC tumour bearing mice lost the ability to lyse LLC cells in a non-radioactive CTL assay (see section 2.8.4) (compare figure 3.49 with figure 3.34).

In contrast, an anti-viral (anti B8R) IFNγ response was present in all virally treated mice with values comparable to previous non-surgical experiments.

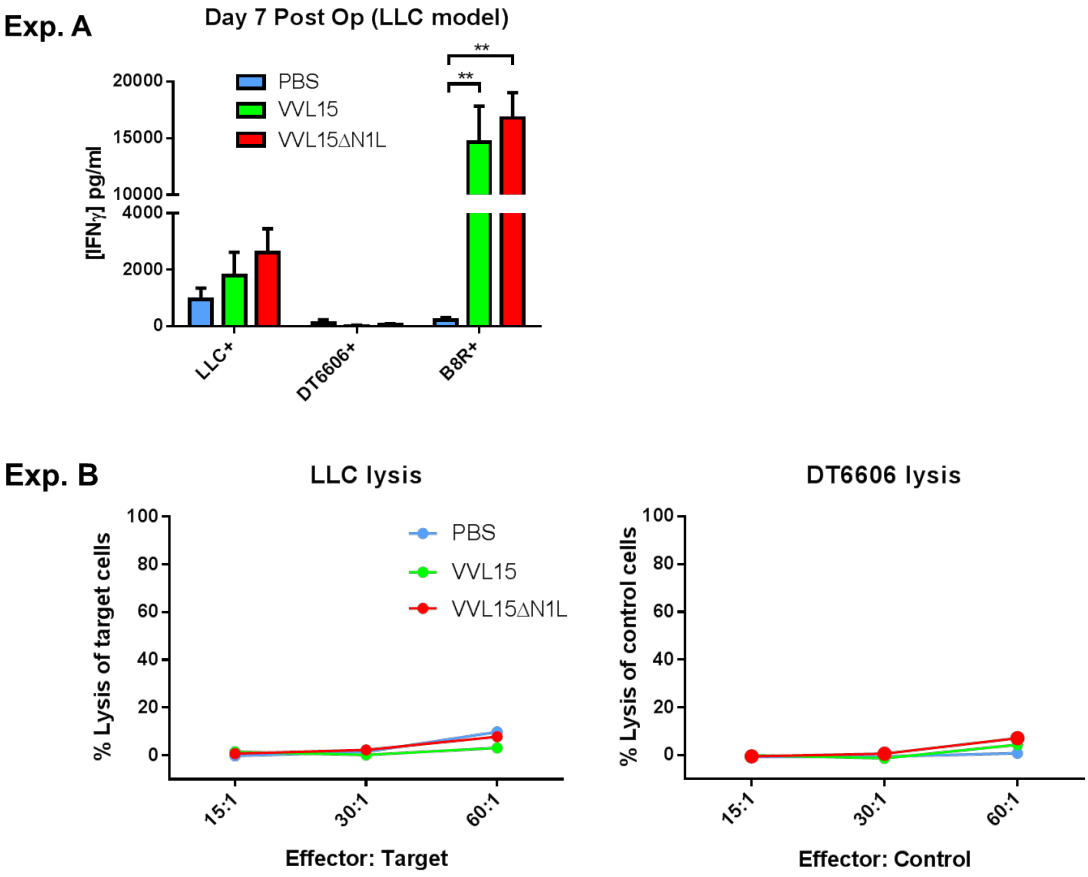

Figure 3.49 Surgery impaired VVL15ΔN1L mediated enhancement of adaptive antitumour immunity

Fourteen days after the final dose of IT virus (i.e. seven days after surgical resection of tumours), splenocyte suspensions were co-cultured with growth arrested target (LLC) or control (DT6606) tumour cells or the VV B8R peptide. IFNγ concentrations (in pg/ml, Y axis) of supernatants were measured by ELISA three days later. One-way ANOVAs with post hoc Tukey tests were used to compare means (Exp. A). In a second experiment, five days following co-culture with tumour cells, the splenocytes from each treatment group were pooled and further co-cultured with 5000 target or control tumour cells in ratios of 15:1, 30:1, and 60:1. A non-radioactive lymphocyte cytotoxicity assay based on LDH release from lysed cells, was used to estimate percentage tumour cell lysis (Exp. B).

Finally, of the 4 of 10 mice in the VVL15ΔN1L group that were apparently cured (figure 3.48A), two did not demonstrate tumour re-growth following re-challenge with a relatively high dose ($2x10^6$) of subcutaneously implanted LLC cells. The sole survivor of the PBS group regrew a tumour upon LLC cell implantation. IFNγ assays using

splenocytes isolated from surviving mice confirmed that tumour re-growth was associated with a low anti-LLC immune response (figure 3.50). Due to the low numbers of surviving mice, statistical calculations could not be performed.

The VVL15ΔN1L platform appeared to enhance short term survival of neoadjuvantly treated animal models (perhaps by enhancing innate immune surveillance – see later). It also had the potential to enhance long term immune surveillance. However, the latter certainly was not universal, as only 20% of the original number of mice treated developed the ability to prevent tumour regrowth. There remained significant room therefore to improve this therapeutic platform.

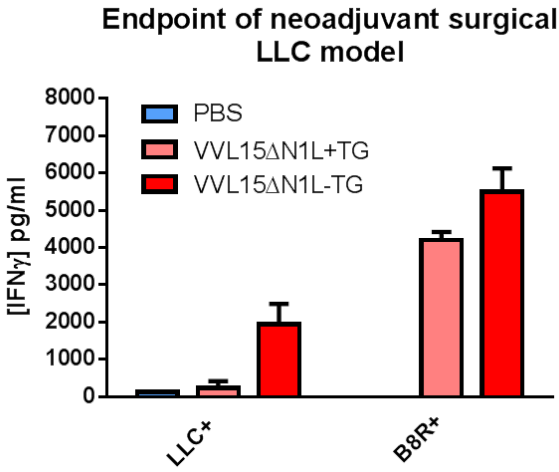

Figure 3.50 Neoadjuvant IT VVL15ΔN1L induced long term post-surgical antitumour immunity in only 20% of treated mice

Splenocyte suspensions from mice that had reached the end point of the LLC neoadjuvant experiment (section 3.4.2) were co-cultured with either growth arrested LLC cells or the VV B8R peptide. The IFNγ concentration of supernatants was measured by ELISA. VVL15ΔN1L+TG: splenocytes isolated from VVL15ΔN1L treated mice in which tumour regrew following re-challenge with LLC cells; VVL15ΔN1L–TG: likewise for the two mice in which tumour did not regrow.

3.4.4 VVL15ΔN1L treated tumours attracted a disproportionate amount of neutrophils with a reciprocal reduction in the monocyte/ macrophage population

In order to explore why pre-treatment with VVL15ΔN1L led to a reduction in metastatic dissemination from the primary tumour in the LLC flank model, a biological time-point study was set up to look at cellular players that were attracted to the TME at relatively early time points following IT virus administration (table 2.7, experiment 1). We initially sought to establish the relative intra-tumour proportions of the main cellular innate (neutrophils, macrophages, NK and DCs) and adaptive (T cell) effector cells.

Table 3.2 lists the fluorophore labelled antibodies used to stain single cell suspensions of tumour.

Table 3.2 Fluorophore labelled antibodies used to stain intra-tumour leucocytes

Antibodies against myeloid antigens	Antibodies against lymphoid antigens
CD45 APC-eFluor® 780	CD45 eFluor® 450
CD11b PerCP-Cy5.5	CD3e PerCP-Cy5.5
CD11c PE	CD8a FITC or APC
MHCII FITC or APC	CD49b PE
Gr1 Alexa Fluor® 700	
F4/80 Pe-Cy7	

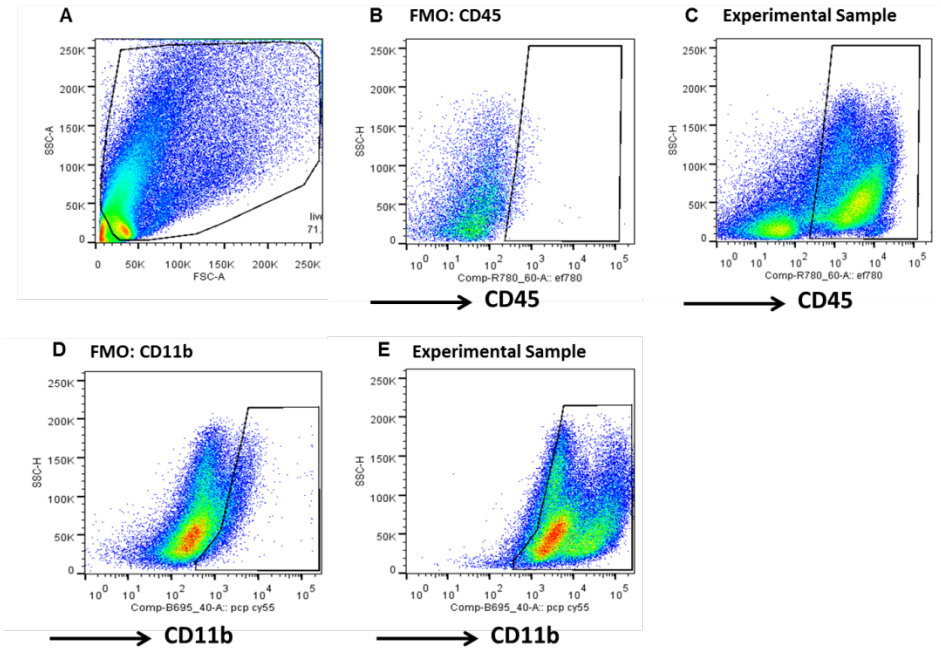

Figure 3.51 Selection of CD45+CD11b+ cells

Samples that were stained with all antibodies except anti CD45 or anti CD11b antibodies (B and D) were used to set gates for the sequential selection of CD45+CD11b+ cells as shown.

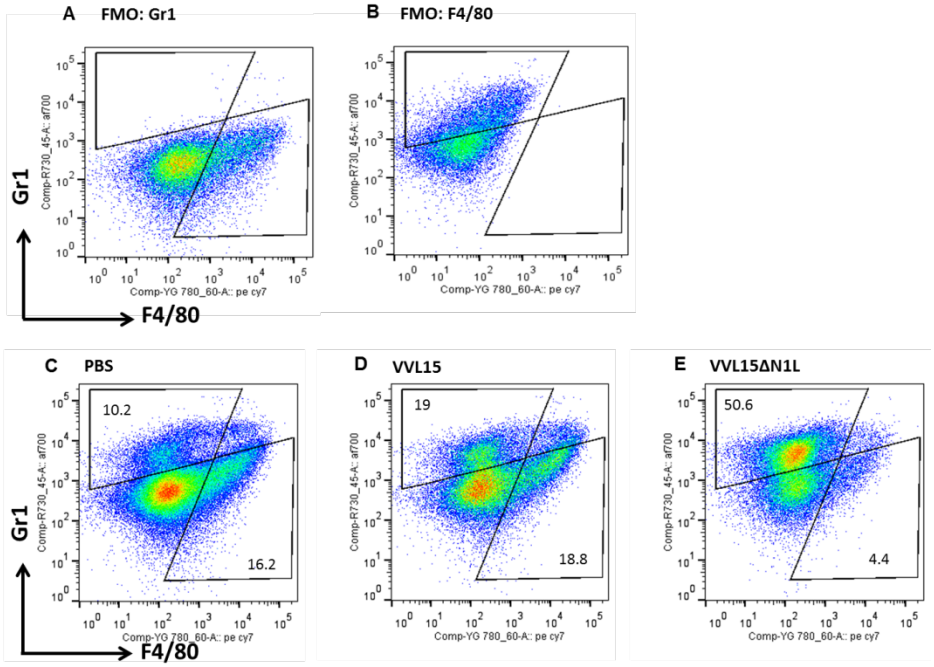

Figure 3.52 Gating for Neutrophils (CD11b+Gr1+) and Macrophage/monocytes (CD11b+F4/80+)

Following the selection of CD45+CD11b+ cells (figure 3.51), FMO stained samples that excluded either anti Gr1 (A) or anti F4/80 (B) were used to set their respective gates as shown.

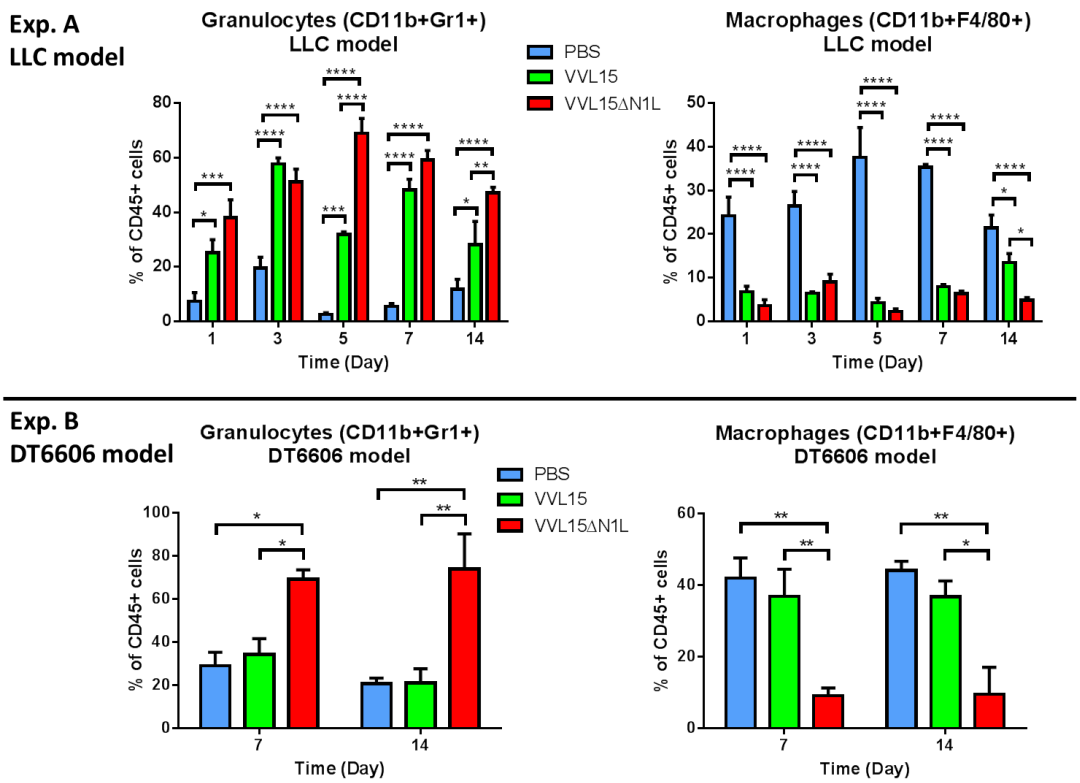

Figure 3.53 Intratumoural VVL15ΔN1L enhanced the infiltration of neutrophils into LLC and DT6606 flank tumours

Syngeneic LLC (Exp. A) and DT6606 (Exp. B) flank tumours (as indicated) were treated with $1x10^8$ PFUs of virus or the equivalent volume of PBS (n=3- 4/group). At one, three, five, seven and 14 days after virus injection, tumour cell suspensions were stained with fluorophore labelled anti CD45, CD11b, F4/80 and Gr-1 and analysed in a multichannel flow cytometer. The bar charts depict granulocytes or macrophages as a percentage of intratumoural CD45+ cells. Two-way ANOVAs with post hoc Tukey tests were used to compare mean values.

Figure 3.51 and figure 3.52 depict the gating strategy used to identify neutrophils (defined as CD11b+Gr1+) and monocytes/macrophages (defined as CD11b+ F4/80+).

Figure 3.53 shows that following a single dose of IT virus into LLC tumour bearing mice, there was a sustained enhancement of tumour infiltrating neutrophils with a reciprocal percentage decrease in the monocyte/macrophage pool. This pattern was exaggerated following treatment with VVL15ΔN1L in comparison to VVL15. All other cell populations (NK, T cells) were miniscule (i.e. less than 3% of CD45+ leucocytes)

in comparison to CD11b+ cells, at all time-points and therefore could not be accurately quantified using this method. A similar experiment was conducted on DT6606 flank tumour models, although tumours on this occasion were analysed at only two time-points, days seven and 14 post IT virus. Once again the granulocyte pool, as a percentage of CD45+ leucocytes, was markedly enhanced at both these times especially following IT VVL15ΔN1L, with a marked decline in intra-tumour monocyte/ macrophages.

3.4.5 IT VVL15ΔN1L enhanced the systemic NK cell response

As described in the introduction, NK cells are major innate antiviral and antitumour effectors. The systemic NK response is often elevated following viral infection, a fact that might have accounted for the beneficial effects of VVL15ΔN1L on limiting dissemination from primary LLC tumours.

Blood and spleen were harvested from IT injected LLC tumour bearing mice (as described in section 2.15.1) at days one, three, seven and 14 post treatment. They were processed to obtain single cell suspensions; stained with anti CD45-eFluor® 450 , CD3e-PerCP-Cy5.5 and CD49b-PE (a murine pan NK cell marker) and analysed in a multichannel flow cytometer. NK cells were defined as CD3-CD49+ and were expressed as a percentage of CD45+ leucocytes (see figure 3.54 and figure 3.55). There was a significicant increase in circulating NK cells following VVL15ΔN1L treatment in comparison to VVL15. This had occurred by 24 hours of treatment and was sustained throughout the timecourse of the experiment. At day three, for example nearly 50% of circulating leucocytes were NK cells. A non-significant trend for enhanced numbers of NK cells within spleen was also seen after day seven post infection.

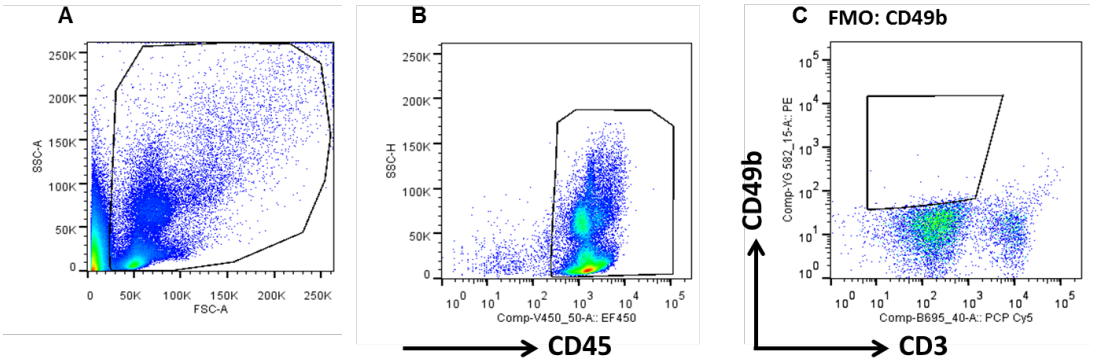

Figure 3.54 Gating for NK cells (CD3-CD49+)

Following the selection of CD45+ cells (B), the CD49b FMO sample (C) was used to define the CD3-CD49+ gate as shown.

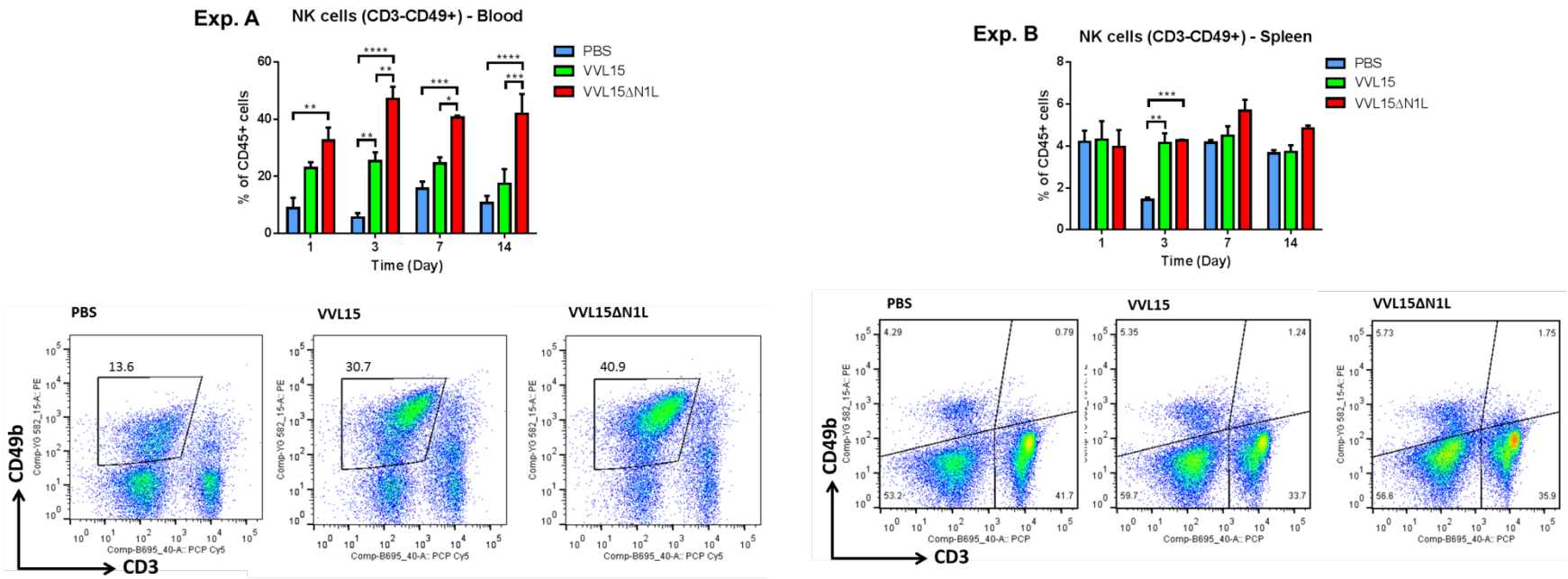

Figure 3.55 VVL15ΔN1L enhanced systemic NK cell numbers

Syngeneic LLC flank tumours were treated with $1x10^8$ PFUs of virus or the equivalent volume of PBS (n=3- 4/group). At one, three, seven and 14 days post virus injection, blood leucocyte (Exp. A) and splenocyte (Exp. B) suspensions were stained with fluorophore labelled anti CD45, CD3 and CD49b and analysed in a multichannel flow cytometer. The bar charts depict NK cells (defined as CD3-CD49b+) as a percentage of CD45+ cells. Two-way ANOVAs with post hoc Tukey tests were used to compare mean values.

3.4.6 NK cell depletion abrogated the survival benefit of VVL15ΔN1L in a neoadjuvant surgical lung cancer model

It was conceivable that the systemic rise in NK cells upon IT injection of VVL15ΔN1L was responsible for the reduction in the growth of MRD and perioperative dissemination of tumour metastases and thus responsible for the prolonged survival in the neoadjuvant surgical experiments described earlier. The VVL15ΔN1L treatment arm was thus repeated in mice in which NK and T cells were selectively depleted (section 2.15.6 and table 2.10, experiment 2). The efficacy of VVL15ΔN1L was abrogated when NK cells were concurrently depleted for the duration of the experiment; whereas depletion of CD4+ or CD8+ cells made no difference (figure 3.56).

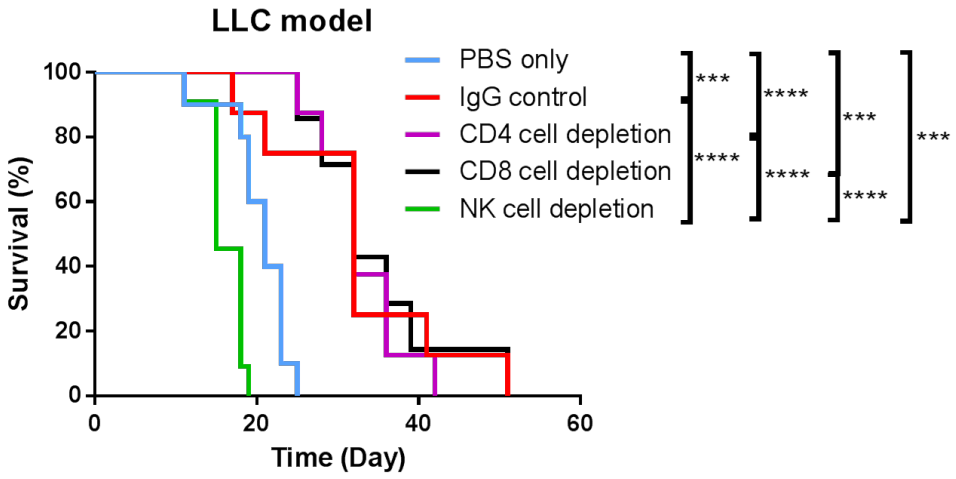

Figure 3.56 NK cells play a pivotal role in mediating the efficacy of VVL15ΔN1L in the context of neoadjuvant therapy prior to surgical excision

Cell depleting or IgG control antibodies were commenced intraperitoneally in mice bearing syngeneic LLC flank tumours a day prior to the first dose of IT treatment with VVL15ΔN1L or PBS (n=7 per group). Tumours were surgically resected seven days after the final dose of virus. The X axis represents day's post-surgical excision. Log rank analyses were used to delineate any significant differences between specific treatment pairs.

This result therefore revealed a different mechanistic picture to that responsible for the reduction in the growth of primary syngeneic DT6606 flank tumours treated with VVL15ΔN1L in which CD8+ T cells were the apparent major player.

3.4.7 Summary of results chapter 3.4

The syngeneic LLC flank tumour model is extremely aggressive and metastasises to the lung if untreated. Dissemination appears to be enhanced upon surgical excision of the primary. It would thus serve as an effective, accelerated model of perioperative tumour dissemination and post-operative tumour recurrence.

Although multiple IT doses of VVL15ΔN1L did not slow the growth of primary LLC tumours, it did reduce metastatic dissemination to the lung (in comparison to treatment with VVL15). A similar treatment schedule administered seven days prior to surgical excision of tumour prolonged short term post-operative survival. The heightened adaptive antitumour immune response following IT VVL15ΔN1L in comparison to VVL15 appeared to be dampened by operative or perioperative stress; confirmed by the fact that only 2/10 mice developed the ability to reject implanted LLC tumour cells.

Contrastingly, the efficacy of VVL15ΔN1L in the surgical neoadjuvant setting appeared to be dependent on its ability to stimulate innate immunity. Flow cytometric analysis of tumour infiltrating leucocytes demonstrated heightened neutrophil infiltration, with concurrently diminished monocyte populations. Most tellingly of all, IT VVL15ΔN1L enhanced the numbers of circulating NK cells; an effect that was sustained for at least 14 days post injection of a single dose of virus. The proliferation and mobilisation of these cells were a critical component of the efficacy of VVL15ΔN1L in this neoadjuvant model; demonstrated by the complete abrogation of efficacy in mice lacking NK cells.

3.5 Preliminary investigations into mechanisms responsible for VVL15ΔN1L mediated enhancement of innate and adaptive immunity

3.5.1 The splenic pool of DCs was elevated following IT VVL15ΔN1L injection of LLC tumours

As has been discussed in the introduction, professional APCs play an important bridging role between innate and adaptive immunity. In terms of antitumour immunity, a rational for the deletion of the VV N1L gene was to enhance the cocktail of innate signals that might ultimately lead to the favourable activation of APCs.

Before this hypothesis was explicitly tested, we sought to establish whether IT treatment with VVL15ΔN1L enhanced the recruitment of DCs. Peripheral murine DCs drain through local lymph nodes and will also channel through the spleen. Differences in splenic DCs should reflect similar changes in tissue DCs, which are difficult to quantify within murine tumours.

Splenocytes harvested at different times post IT viral injection of LLC flank tumours were stained with the following fluorophore labelled antibodies and analysed in a multichannel flow cytometer: anti CD45-eFluor® 450, anti CD11c-PE and anti MHCII-FITC.

The DC population was defined as CD11c+MHCII+ and expressed as a percentage of CD45+ splenocytes (figure 3.57). Although there was no statistically significant difference between treatment groups, there was a trend for enhanced splenic DC numbers following IT VVL15ΔN1L, which was maintained until day seven post injection.

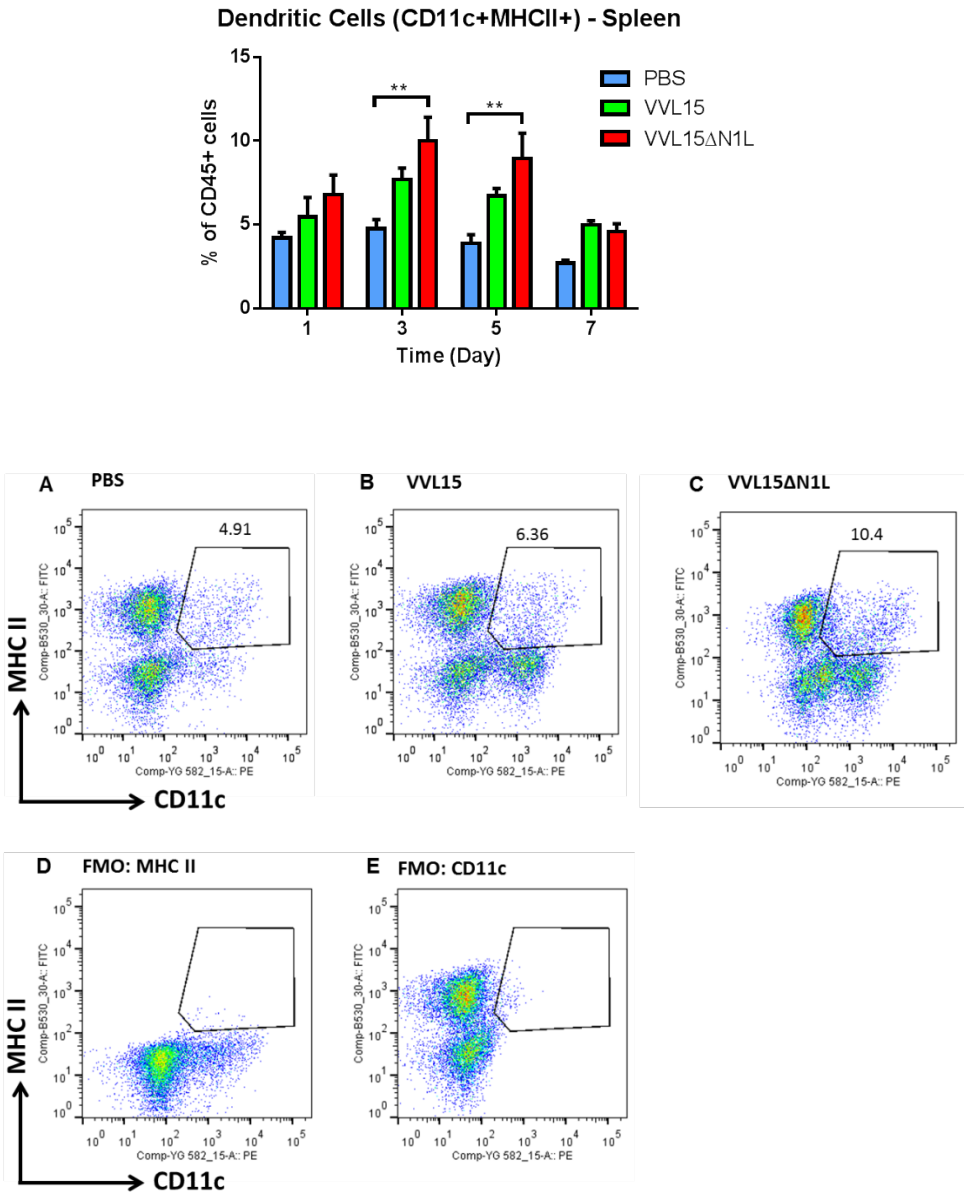

Figure 3.57 VVL15ΔN1L enhanced DCs in the spleen

Syngeneic LLC flank tumours were treated with $1x10^8$ PFUs of virus or the equivalent volume of PBS (n=3- 4/group). At one, three, seven and 14 days post virus injection splenocyte suspensions were stained with fluorophore labelled antibodies against CD45, CD11c and MHCII surface antigens and analysed in a multichannel flow cytometer. The CD11c and MHCII FMO samples were used to set their respective boundaries as shown (D and E respectively). The bar chart depicts DC cells (defined as CD11c+ MHCII+) as a percentage of CD45+ splenocytes. Two-way ANOVAs with post hoc Tukey tests were used to compare mean values.

3.5.2 .Infection with VVL15ΔN1L enhanced the activation of murine antigen presenting cells.

In the previous section IT VVL15ΔN1L appeared to enhance DCs in murine spleen. Could this novel virus also enhance their activation?

This question was addressed *in vitro*. Bone marrow, containing naïve myeloid precursors of DCs and monocytes from C57BL/6 mice was harvested as described in section 2.9.3. DCs and monocytes were enriched in mCM containing GMCSF and M-CSF respectively. Phenotypic confirmation of the desired pool of cells (i.e. DC or monocytes) was achieved by staining each group with the following antibodies prior to analysis in a multichannel flow cytometer: anti CD11b-PerCP-Cy5.5, anti F4/80-Pe-Cy7, anti CD11c-Alexa Fluor® 700 and anti MHCII-FITC.

The vast majority of GMCSF enriched cells were CD11c+MHCII+, whereas over 90% of cells enriched with M-CSF were CD11b+F4/80+ (figure 3.58).

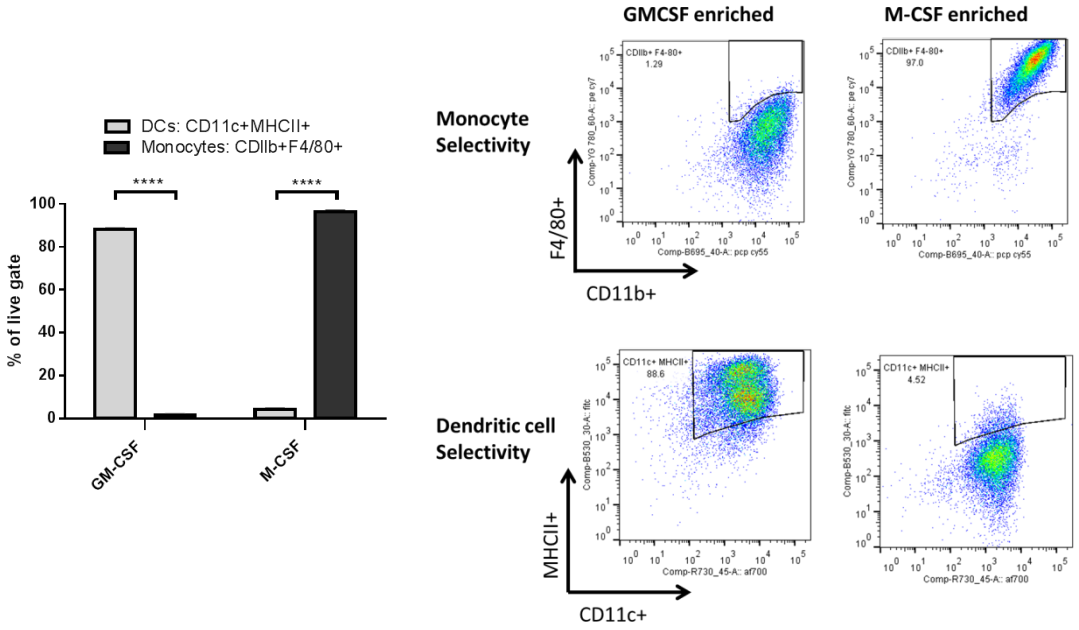

Figure 3.58 Enrichment of mature DCs and monocytes from murine bone marrow

Single cell suspensions of murine bone marrow were cultured for up to eight days in media containing GMCSF and M-CSF to selectively grow and mature DCs and monocytes respectively. For confirmation, at the end of the maturation period, suspensions were stained with fluorophore labelled antibodies against CD11b, CD11c, F4/80 and MHCII surface markers and analysed on a multichannel flow cytometer. Monocytes were defined as CDllb+F4/80+, whereas DCs as CD11c+MHCII+. Unpaired t tests were used to compare mean values

VVL recombinants successfully infected APC populations *in vitro*, as demonstrated by the presence of the RFP marker when examined under green fluorescent light. At different early time points following infection, cells were harvested and stained with the following fluorophore labelled antibodies prior to analysis in a multichannel flow cytometer: anti CD11b-PerCP-Cy5.5, anti F4/80-Pe-Cy7, anti CD11c-Alexa Fluor® 700, anti MHCII-FITC, anti CD80-PE and anti CD86-APC.

CD80 and 86 are co-receptors to the MHCII-TCR "immunological synapse" and are upregulated upon activation of the APC. The presence of MHC class II molecules on the surface of monocytes enables them to take on the role of "professional" antigen presentation.

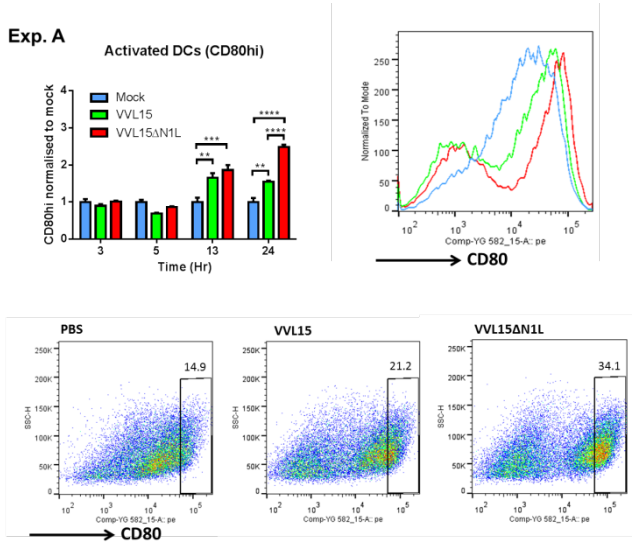
Exp. A
Activated DCs (CD80hi)
CD80hi normalised to mock
Mock
VVL15
VVL15ΔN1L
Time (Hr)
Normalized To Mode
Comp-YG 582_15-A:: pe
CD80
PBS
VVL15
VVL15ΔN1L
14.9
21.2
34.1
SSC-H
CD80

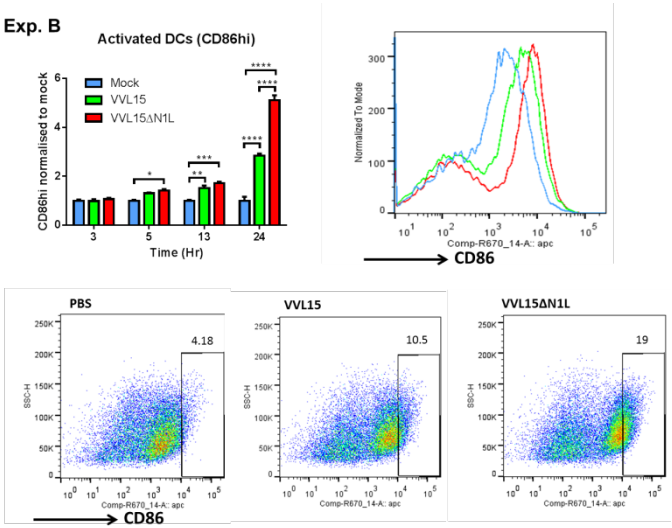
Exp. B
Activated DCs (CD86hi)
CD86hi normalised to mock
Mock
VVL15
VVL15ΔN1L
Time (Hr)
Normalized To Mode
Comp-R670_14-A:: apc
CD86
PBS
VVL15
VVL15ΔN1L
4.18
10.5
19
SSC-H
CD86

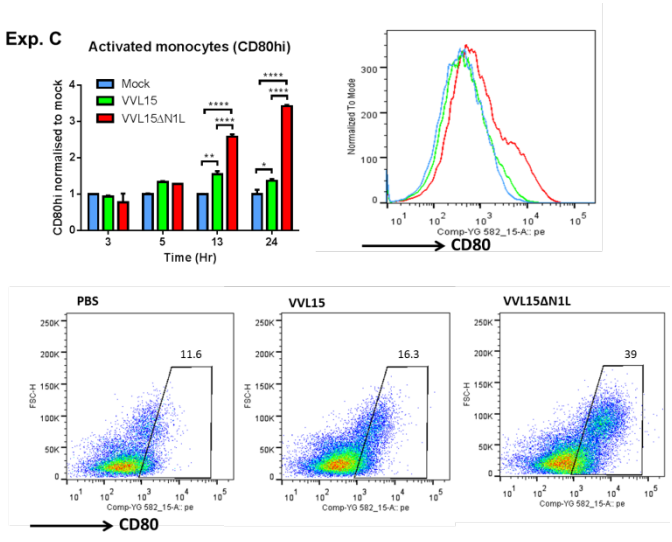
Exp. C
Activated monocytes (CD80hi)
CD80hi normalised to mock
Mock
VVL15
VVL15ΔN1L
Time (Hr)
Normalized To Mode
Comp-YG 582_15-A:: pe
CD80
PBS
VVL15
VVL15ΔN1L
11.6
16.3
39
FSC-H
CD80

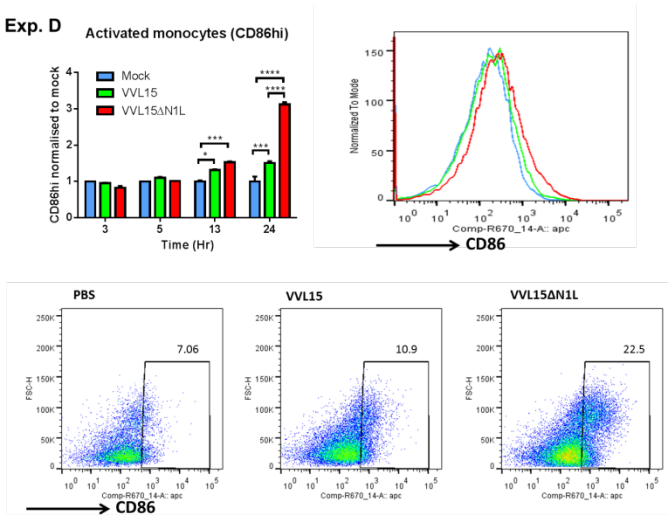
Exp. D
Activated monocytes (CD86hi)
CD86hi normalised to mock
Mock
VVL15
VVL15ΔN1L
Time (Hr)
Normalized To Mode
Comp-R670_14-A:: apc
CD86
PBS
VVL15
VVL15ΔN1L
7.06
10.9
22.5
FSC-H
CD86

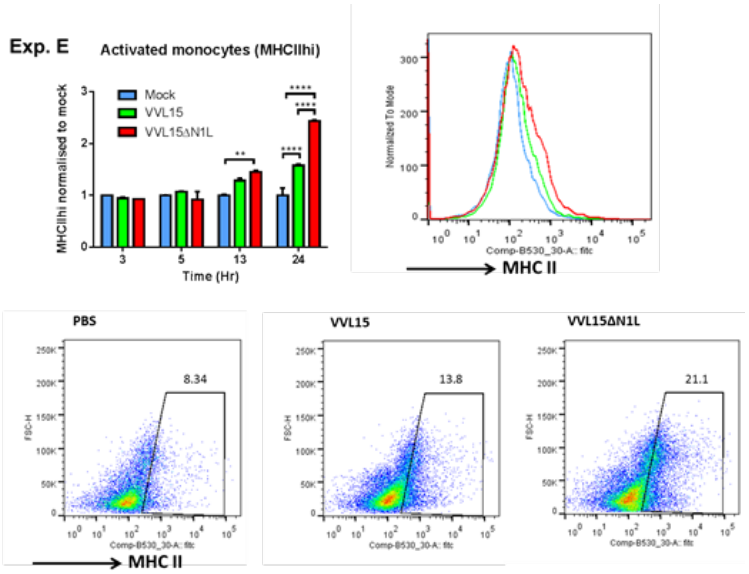

Figure 3.59 VVL15ΔN1L infection of DCs and monocytes enhanced their activation

At the time-points indicated following viral infection (MOI of 1 PFU/ cell) of enriched DCs and monocytes, cells were harvested and stained with fluorophore labelled antibodies against CD80, CD86 and MHCII surface antigens. The "hi/lo" boundaries of these markers were set at the upper border of the densest population of mock treated cells (the bottom left dot plot in each experimental set of graphs/plots). Activation marker levels were normalised to the mean value for mock infected cells. Two-way ANOVAs with post hoc Tukey tests were used to compare mean values.

The graphs in figure 3.59 demonstrate that from 13 hours post infection and certainly by 24 hours, surface expression of CD80 and CD86 and thereby activation of both DCs and monocytes were significantly higher following infection with VVL15ΔN1L in comparison to VVL15. In addition there appeared to be an enhanced shift of the monocyte pool into "professional" APCs as evidenced by the significantly enhanced elevation in MHCII positivity following infection with VVL15ΔN1L.

3.5.3 The cytokine profile of VVL15ΔN1L infected DCs and monocytes was conspicuous for enhanced IL10 expression

Amongst other factors, the cytokine milieu peri-antigen presentation, plays an important role in the type of antigen specific adaptive immunity that develops. Many of these

cytokines are secreted by the APCs themselves. IL12 or IL15 for example may drive the development of a Th1 CTL immune response (338). In contrast IL10 production from APCs has traditionally been associated with local immune suppression and the development of Th2 CD4+ T cells (339, 340).

There was no detectable murine IL4, IL12 or IL15 (measured by ELISA) in the supernatants from plates of virally infected DCs or monocytes. Surprisingly, there was an enhanced level of murine IL10 in the supernatant of wells containing VVL15ΔN1L treated DCs and monocytes. The magnitude of response was higher following monocyte infection figure 3.60.

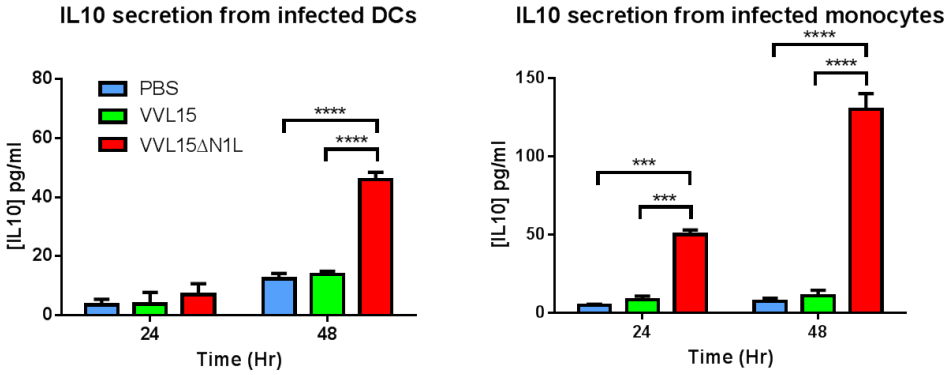

Figure 3.60 VVL15ΔN1L infection of DCs and monocytes enhanced their production of IL10

Supernatant samples taken at 24 and 48 hours were removed from wells containing virally infected DCs or monocytes (MOI of 1 PFU/cell). Concentrations of murine IL4, IL12, IL15 (not shown) and IL10 were measured by ELISA. Two-way ANOVAs with post hoc Tukey tests were used to compare mean values.

3.5.4 An analysis of the intratumoural chemokine/ cytokine milieu following infection with VVL15ΔN1L

In order to establish how VVL15ΔN1L was able to effect the innate cellular changes demonstrated intratumourally and systemically, a further biological time-point experiment was set up using the syngeneic LLC flank model. Animals were euthanized at relatively early time points (one, three, five and seven days) following the IT injection of virus/ PBS and tumours were carefully harvested. These early time-points

were chosen in acknowledgement of the role of the early mobilisation of innate immune cells (NK cells, neutrophils and monocytes).

Tumour tissue was processed as described in section 2.9.2 to separate the supernatant phase from solid cellular debris. The supernatant was screened for common inflammatory cytokines and chemokines via multianalyte ELISAs.

The levels of cytokines/ chemokines within each tumour were normalised to the mean arbitrary value of VVL15 infected tumours (figure 3.61 and figure 3.62). By day seven, IL1α, β and GCSF cytokines were consistently and significantly elevated in VVL15ΔN1L (as compared to VVL15) infected tumours and likewise the chemokines macrophage inflammatory protein(MIP)1α and keratinocyte chemoattractant (KC) (at later time-points).

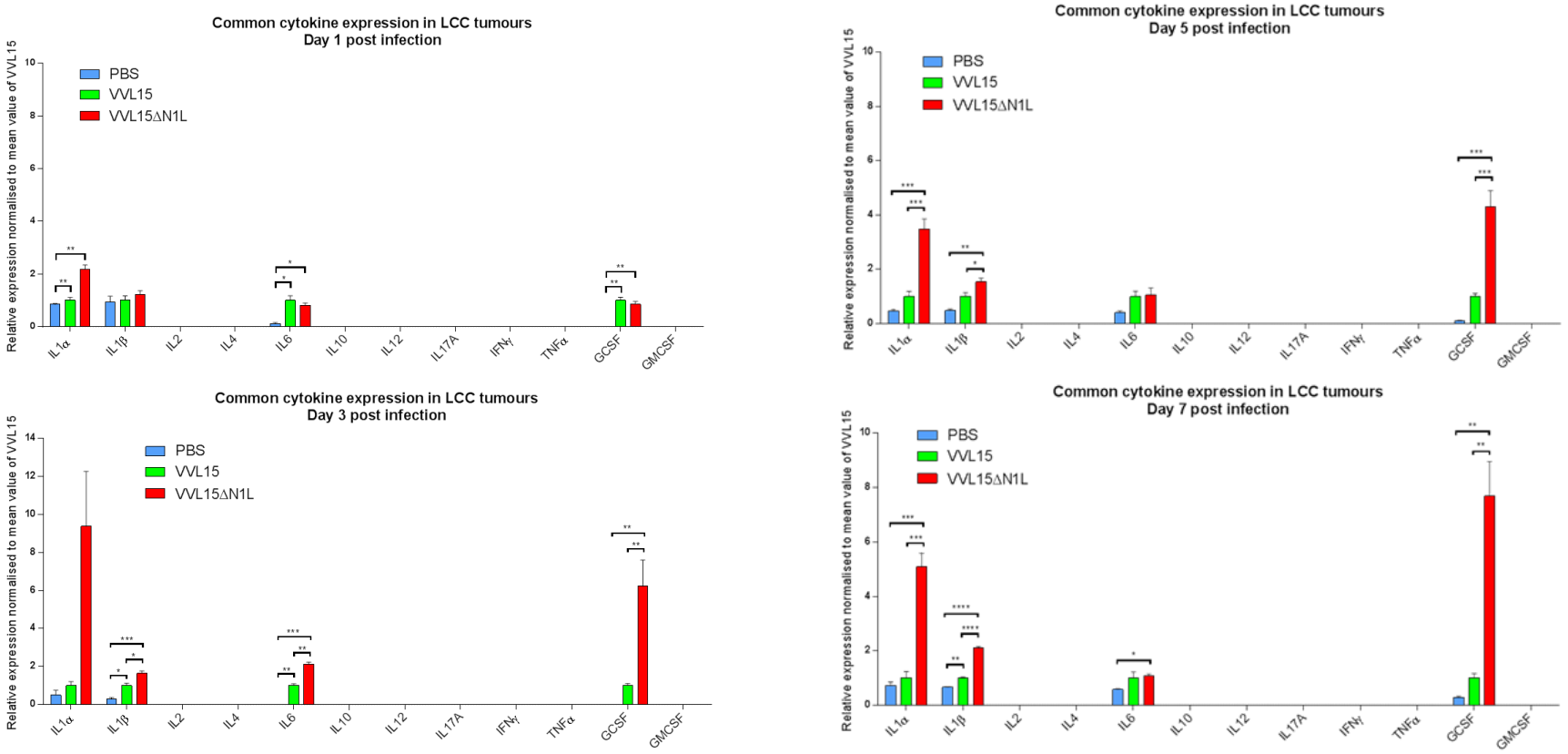

Figure 3.61 Intratumoural expression of inflammatory cytokines following viral infection of LLC flank tumours

Syngeneic LLC tumours were treated with $1x10^8$ PFUs of virus or the equivalent volume of vehicle buffer (n=3- 4/group). At one, three, five and seven days post infection, harvested tumours were homogenised and centrifuged. Their supernatants were analysed for the presence of 12 common inflammatory cytokines by multi-analyte ELISA. For comparison, arbitrary units of OD/ total gram of tumour protein were normalised to their corresponding mean values from VVL15 infected tumours. One-way ANOVAs with post hoc Tukey tests were used to compare means.

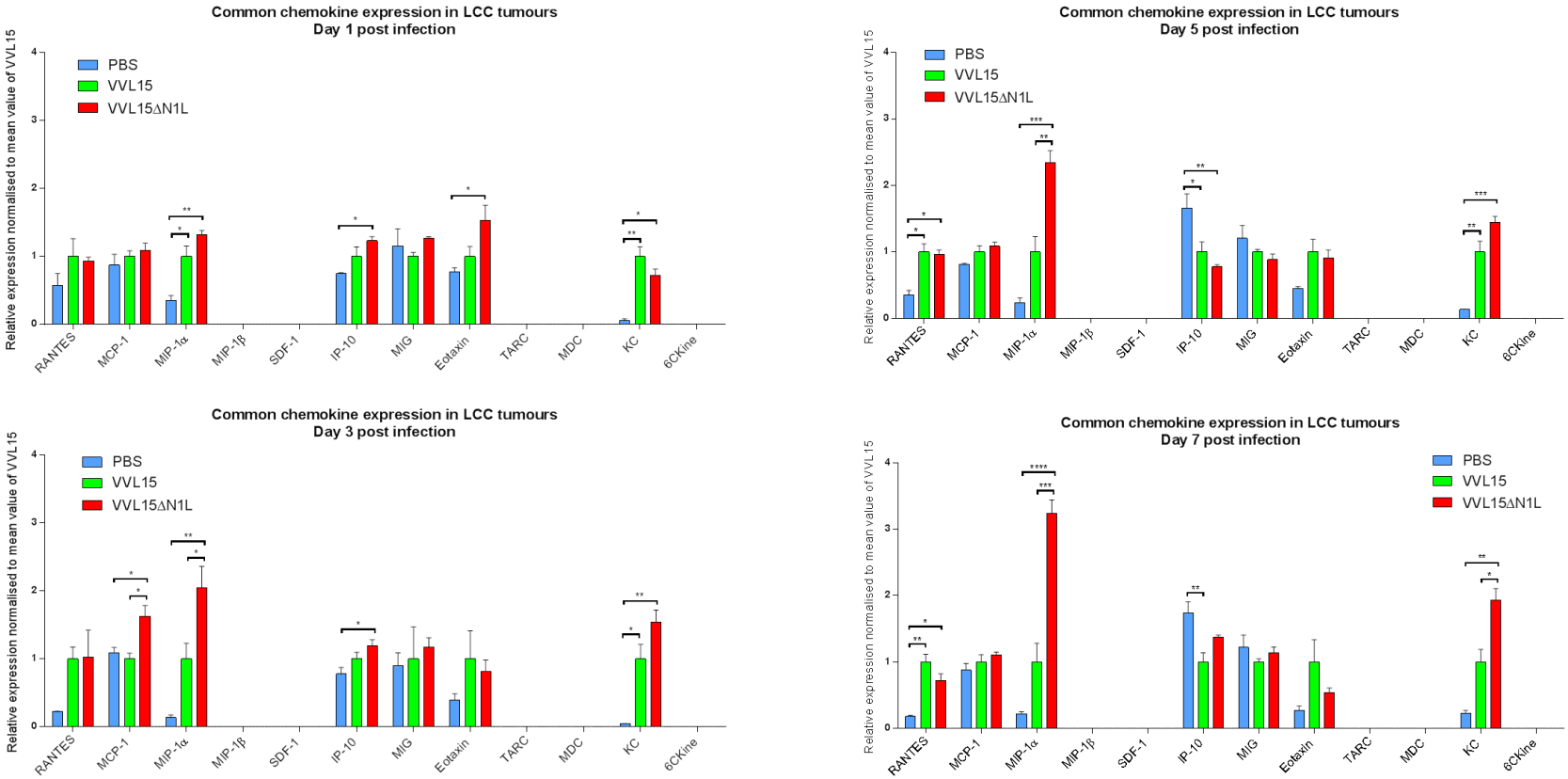

Figure 3.62 Intratumoural expression of inflammatory chemokines following viral infection of LLC flank tumours

Syngeneic LLC tumours were treated with $1x10^8$ PFUs of virus or the equivalent volume of vehicle buffer (n=3- 4/group). At one, three, five and seven days post infection, harvested tumours were homogenised and centrifuged. Their supernatants were analysed for the presence of 12 common inflammatory chemokines by multi-analyte ELISA. For comparison, arbitrary units of OD/ total gram tumour protein were normalised to their corresponding mean values from VVL15 infected tumours. One way ANOVAs with post hoc Tukey tests were used to compare means.

3.5.4.1 Establishment of the source of the VVL15ΔN1L enhanced chemokines and cytokines

Major sources of cytokines or chemokines during the early stages in the development of an antigenic immune response include the professional APCs and monocytes/ macrophages. To test whether they were responsible for the chemokine/ cytokine profile observed above, supernatants of virally infected bone marrow derived DCs and monocytes were analysed for the presence of IL1α/ β, GCSF, KC and MIP1α using single analyte ELISAs. The supernatants of similarly infected LLC and DT6606 tumour cells were also analysed as other potential sources.

3.5.4.1.1 KC (CXCL1)

The murine chemokine KC (CXCL1) is a functional homologue of human IL8 and thus plays an important role in the recruitment of neutrophils. Its secretion was much higher from virally infected tumour cells (especially DT6606) than DCs or monocytes. Infection with VVL15ΔN1L led to higher levels of KC in comparison to infection with VVL15 (figure 3.63). Note uninfected tumours produced significant basal levels of KC.

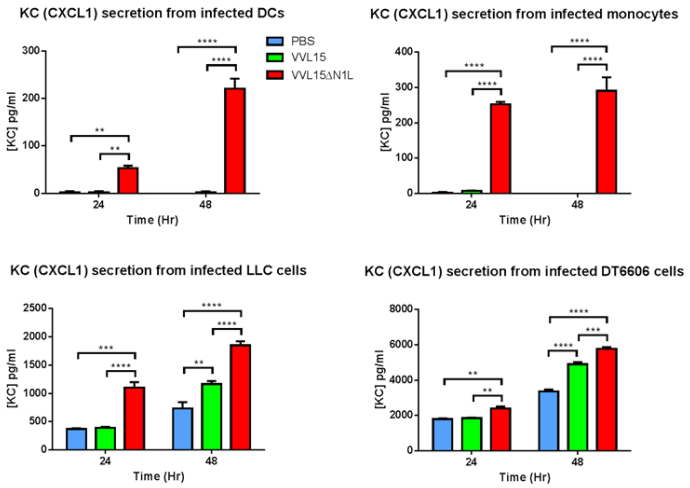

Figure 3.63 KC expression following VVL15ΔN1L infection of DCs, monocytes, LLC and DT6606 cells

Supernatant samples at 24 and 48 hours post infection, were removed from wells containing viral or mock infected DCs, monocytes, LLC or DTT6606 cells (MOI of 1 PFU/ cell). Concentrations of KC were measured by ELISA. Two way ANOVAs with post hoc Tukey tests were used to compare mean values.

3.5.4.1.2 GCSF

GCSF is a cytokine that also aids the recruitment and maturation of neutrophils as well as other myeloid derived cells. Its output was induced in an almost all or none fashion by VVL15ΔN1L (in comparison to VVL15) from DCs and monocytes; with much higher levels from monocytes. VVL15ΔN1L also induced production of this cytokine from DT6606 cells, but not from LLC cells (figure 3.64).

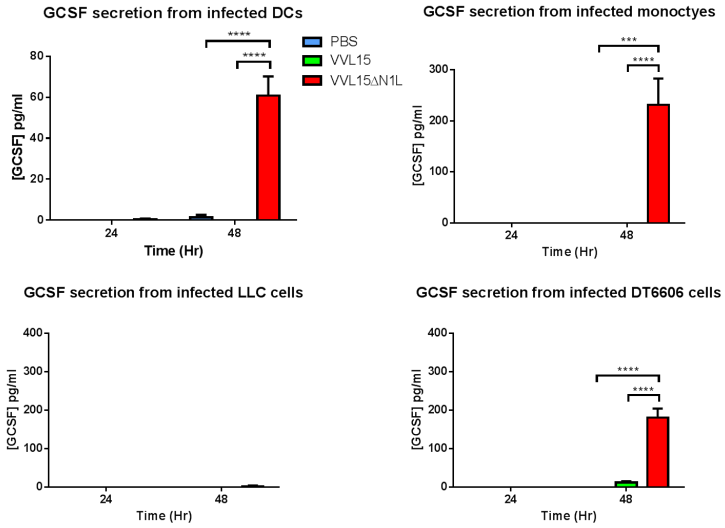

Figure 3.64 GCSF expression following VVL15ΔN1L infection of DCs, monocytes, LLC and DT6606 cells

Supernatant samples at 24 and 48 hours post infection, were removed from wells containing viral or mock infected DCs, monocytes, LLC or DTT6606 cells (MOI of 1 PFU/ cell). Concentrations of GCSF were measured by ELISA. Two-way ANOVAs with post hoc Tukey tests were used to compare mean values.

3.5.4.1.3 MIP1α (CCL3)

MIP1α is a chemokine with multiple functions that encompass both innate and adaptive immune cellular recruitment. It facilitates the recruitment and activation of myeloid derived cells involved in antigen presentation, for example immature DCs, monocytes and macrophages (341). It also encourages NK cell migration and may aid the generation of a CD8+ CTL memory response (190, 342, 343). In the current experiment, MIP1α was only secreted from DCs and monocytes. VVL15ΔN1L infection markedly increased output from both these cells (figure 3.65).

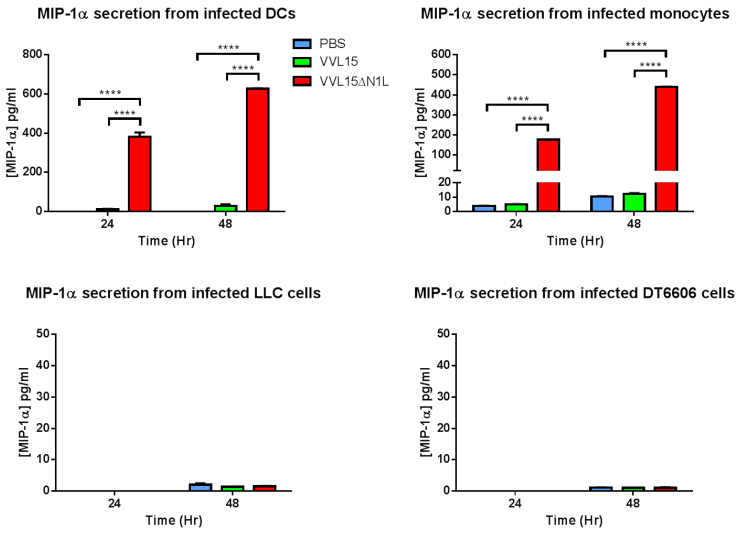

Figure 3.65 MIP1α expression following VVL15ΔN1L infection of DCs, monocytes, LLC and DT6606 cells

Supernatant samples at 24 and 48 hours post infection, were removed from wells containing viral or mock infected DCs, monocytes, LLC or DTT6606 cells (MOI of 1 PFU/ cell). Concentrations of MIP1α were measured by ELISA. Two way ANOVAs with post hoc Tukey tests were used to compare mean values.

3.5.4.1.4 IL1α/ IL1β

The classic acute phase reactant cytokines, IL1α and IL1β in the current context play a major role in the recruitment and activation of myeloid derived cells like macrophages and neutrophils as well as lymphocytes. IL1β may also drive a Th1 type antigen specific CTL response (344). The IL1 family of cytokines have been implicated in tumour progression via propagation of chronic inflammation, but may also enhance anticancer immunity, particularly in the context of chemotherapeutic and possibly virotherapeutic induced cell death (344). Both these cytokines were secreted from DCs and monocytes almost exclusively in response to VVL15ΔN1L. Levels of IL1α were however very low. IL1β secretion especially from DCs, was significantly enhanced by infection with VVL15ΔN1L (figure 3.66 and figure 3.67). Tumour cells did not secrete these cytokines upon viral infection.

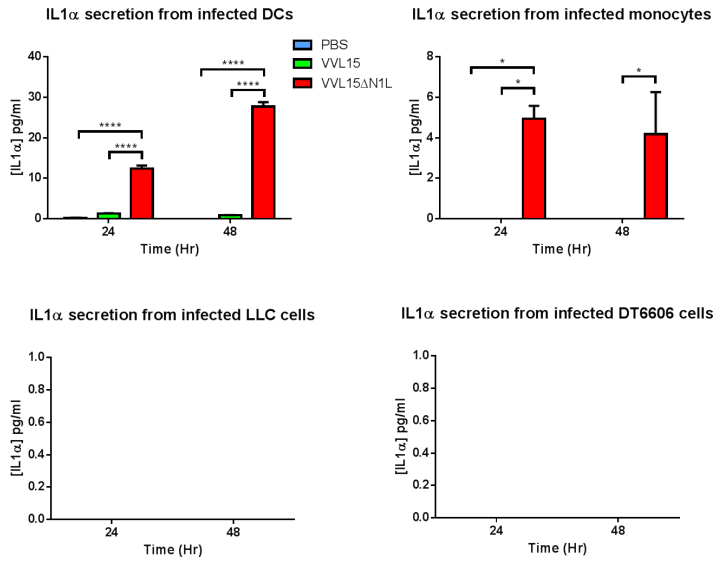

Figure 3.66 IL1α expression following VVL15ΔN1L infection of DCs, monocytes, LLC and DT6606 cells

Supernatant samples at 24 and 48 hours post infection, were removed from wells containing viral or mock infected DCs, monocytes, LLC or DTT6606 cells (MOI of 1 PFU/ cell). Concentrations of IL1α were measured by ELISA. Two-way ANOVAs with post hoc Tukey tests were used to compare mean values.

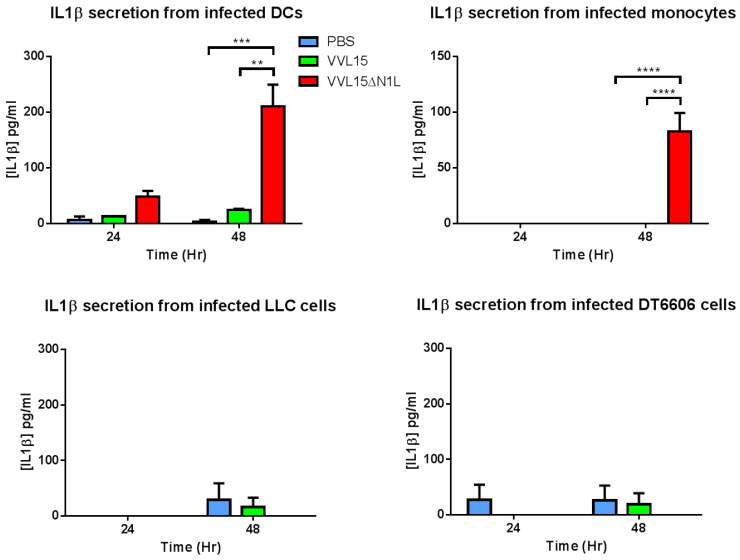

Figure 3.67 IL1β expression following VVL15ΔN1L infection of DCs, monocytes, LLC and DT6606 cells

Supernatant samples at 24 and 48 hours post infection, were removed from wells containing viral or mock infected DCs, monocytes, LLC or DTT6606 cells (MOI of 1 PFU/ cell). Concentrations of IL1β were measured by ELISA. Two-way ANOVAs with post hoc Tukey tests were used to compare mean values.

3.5.5 VVL15ΔN1L also enhanced IL18 production from infected DCs and monocytes

Transcription and post translational processing of IL1β is regulated by NF-κB and inflammasome signalling pathways respectively. As discussed in the introduction, the N1L protein is an inhibitor of NF-κB signalling, and the enhancement of IL1β may have been a consequence of disinhibition of this signalling pathway. However, it is possible that the N1L protein, indeed like the F1L protein (345) may also modulate signalling through inflammasome platforms. As a prelude to exploring this in detail, levels of IL18, another member of the IL1 family of cytokines (that is also post translationally activated by inflammasomes), was measured by ELISA in supernatants of virally infected DCs and Monocytes. IL18 is constitutively produced by certain cells and unlike IL1β its further up-regulation appears not to be regulated by NF-κB signalling (346).

As can be seen in figure 3.68, IL18 levels were significantly enhanced following VVL15ΔN1L infection of both DCs and monocytes. IL18 was not expressed by tumour cells.

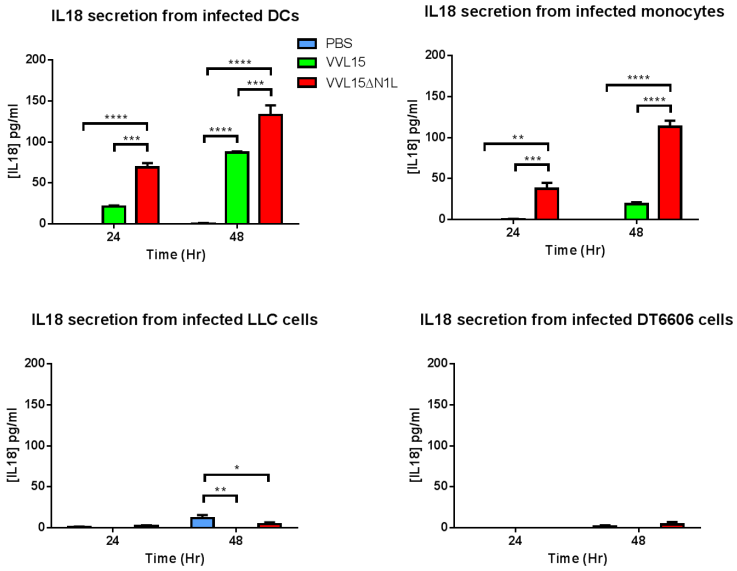

Figure 3.68 IL18 expression following VVL15ΔN1L infection of DCs, monocytes, LLC and DT6606 cells

Supernatant samples at 24 and 48 hours post infection, were removed from wells containing viral or mock infected DCs, monocytes, LLC or DTT6606 cells (MOI of 1 PFU/ cell). Concentrations of IL18 were measured by ELISA. Two-way ANOVAs with post hoc Tukey tests were used to compare mean values.

3.5.6 Summary of Results Chapter 3.5

Intratumoural VVL15ΔN1L appeared to enhance DCs in murine spleens. In comparison to VVL15, VVL15ΔN1L infection enhanced the activation of DCs and monocytes and in the latter also enhanced the up-regulation of MHCII, effectively transforming them into professional APCs. This may have mechanistic implications for its ability to enhance adaptive immunity in the LLC and DT6606 syngeneic tumour models. Interestingly, infection of APCs with VVL15ΔN1L also led to enhanced IL10 production from these cells. As will be further discussed in section 4.1; this may not be detrimental to the development of adaptive antitumour immunity.

Multi-analyte ELISAs performed on LLC tumour homogenates at relatively early time-points following IT virus administration confirmed enhanced levels of IL1α, IL1β, GCSF, KC and MIP1α levels within VVL15ΔN1L treated tumours. These have multiple functions including the recruitment and activation of neutrophils (GCSF, KC, IL1β) and NK cells (MIP1α). The IL1 family and MIP1α may play additional roles in promoting a Th1 driven antigen specific CTL response. *In vitro* analyses confirmed the enhanced production of these cytokines and chemokines by VVL15ΔN1L infected DCs and monocytes, although KC was most likely to have been produced by infected tumour cells.

Finally, the production of IL18 (another IL1 family member) was also enhanced from DCs and particularly monocytes following infection with VVL15ΔN1L. The apparent dampening of both IL1β and IL18, suggests that the N1L protein may regulate signalling through inflammasome platforms, a potentially novel mechanism of action.

3.6 Efficacy with the cytokine armed recombinant viruses

The syngeneic DT6606 flank tumour model was sensitive to IT administered VVL15ΔN1L monotherapy; however, efficacy was either limited or modest in other similar models. Even in the DT6606 tumour cohort many mice were not cured. In addition, neoadjuvant treatment with VVL15ΔN1L appeared to only enhance short term survival of mice following resection of LLC tumours. There thus remained significant scope to try and improve upon this novel VVL recombinant platform. VVL15-mGMCSF and VVL15- mIL12 recombinant viruses were constructed with this premise in mind.

3.6.1 VVL15-mIL12 further enhanced the antitumour immunity induced by VVL15ΔN1L but VVL15-mGMCSF did not

Stimulated splenocyte IFNγ immunoassays were utilised as markers of antitumour and antiviral adaptive immunity. Splenocytes were co-cultured with growth arrested DT6606 cells, the murine mesothelin peptide or the VV B8R peptide (table 2.4). The VVL15ΔN1L treatment arm was the control group in this and all subsequent experiments in this chapter.

Figure 3.69 demonstrates that splenocytes from VVL15-mIL12 infected tumour bearing mice produced the highest levels of IFNγ upon co-culture with growth arrested DT6606 cells as well as with the mesothelin peptide. Absolute levels of IFNγ diminished with time and any differences between groups had disappeared by day 21.

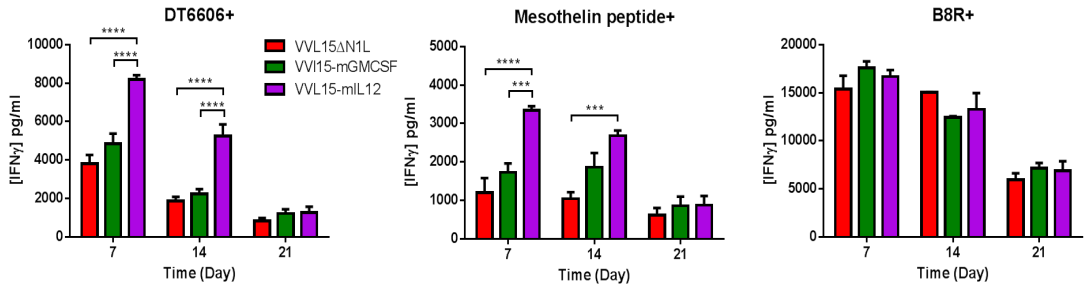

Figure 3.69 VVL15-mIL12 enhanced the adaptive antitumour immune response afforded by VVL15ΔN1L

Syngeneic DT6606 flank tumours were treated with $1x10^8$ PFUs of IT virus or the equivalent volume of PBS (n=3- 4/group). Seven, 14 or 21 days later, splenocyte suspensions were co-cultured with either growth arrested target DT6606 cells, mesothelin peptide or VV B8R peptide. IFNγ concentrations (pg/ml, Y axes) of supernatants were measured by ELISA. Two-way ANOVAs with post hoc Tukey tests were used to compare mean values.

3.6.2 Splenic CD8+ effector memory cells were further enhanced by VVL15-mIL12 but not by VVL15-mGMCSF

Splenocyte suspensions from days 14 and 21 post viral injection were stained with a panel of fluorophore labelled antibodies and analysed via multi-channel flow cytometry. The following antibodies were used: anti CD45-eFluor® 450, anti CD3e-PerCP-Cy5.5, anti CD8a-FITC, anti CD62L-PE Cy7 and anti CD44-APC.

Previously we demonstrated that IT VVL15ΔN1L enhanced the generation of effector memory CD8+ T cells above that stimulated by IT VVL15. A similar experiment was conducted to establish whether either of the two cytokine armed viruses could improve upon this response.

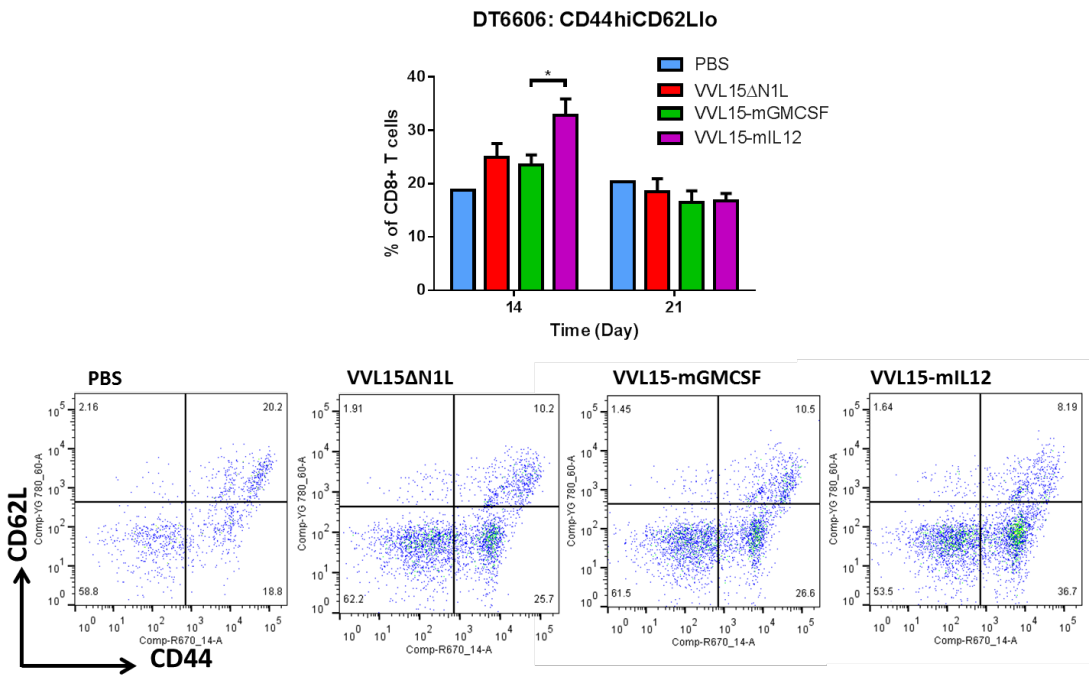

Figure 3.70 Intratumoural VVL15-mIL12 enhanced the generation of CD8+ effector memory T cells

Syngeneic DT6606 flank tumours were treated with $1x10^8$ PFUs of IT virus or the equivalent volume of PBS (n=3- 4/group). Fourteen or 21 days later, splenocyte suspensions were stained with fluorophore labelled antibodies against CD45, CD3, CD8, CD44 and CD62L cell surface antigens and analysed in a multichannel flow cytometer. The bar chart depicts the effector memory (CD44hiCD62Llo) percentage of CD8+ T cells. The result from a single mouse treated with PBS is also included for reference. Two-way ANOVAs with post hoc Tukey tests were used to compare mean values.

Effector memory CD8+ T cells were defined as CD44hiCD62Llo. Gating was performed with FMO stained samples that excluded either anti CD44 or CD62L antibodies with a similar strategy to that illustrated in figure 3.30. At day 14 post IT virus, there was an enhancement of CD8+ effector memory T cells in the spleens of mice treated with VVL15-mIL12 (in comparison to the other two viral groups (figure 3.70)). This enhancement had diminished by day 21.

3.6.3 Splenic DCs were enhanced by infection with VVL15-GMCSF but not by VVL15-mIL12

GMCSF is a chemoattractant and growth factor for the mobilisation, differentiation and maturation of professional APCs. A number of OVTs have been armed with this transgene in a bid to reverse tolerance to TAAs (see section 4.1).

We sought to establish whether splenic DCs could be altered by VVL15-mGMCSF treatment. Splenocytes were stained with the following antibodies prior to analysis in a multichannel flow cytometer: anti CD45-eFluor® 450, anti CD11c-PE and anti MHCII-FITC.

DCs were defined as CD11c+MHCII+ and expressed as a percentage of CD45+ cells. At day 14 post treatment there was a statistically significant increase in the splenic DC pool following IT VVL15-mGMCSF, in comparison to the other two viruses (figure 3.71). This difference had diminished by day 21.

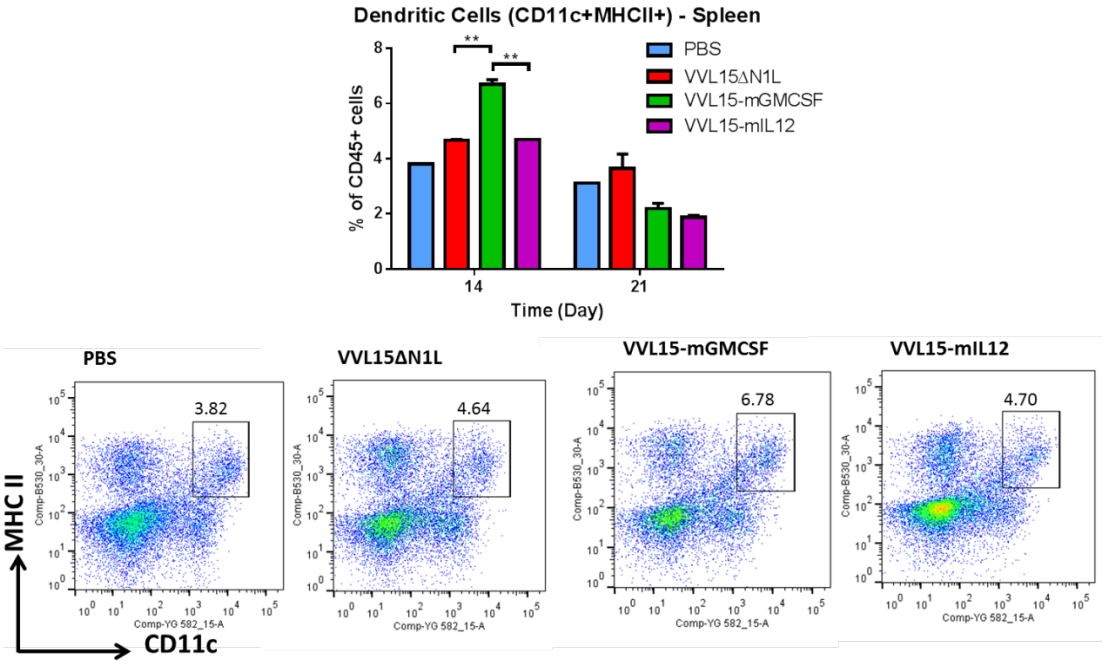

Figure 3.71 Intratumoural VVL15-mGMCSF enhanced the DC pool within murine spleens

Syngeneic DT6606 flank tumours were treated with $1x10^8$ PFUs of IT virus or the equivalent volume of PBS (n=3- 4/group). Fourteen or 21 days later splenocyte suspensions were stained with fluorophore labelled antibodies against CD45, CD11c and MHCII cell surface antigens and analysed in a multichannel

flow cytometer. The bar chart depicts splenic DCs (CD11c+MHCII+) as a percentage of CD45+ splenocytes. The result from a single mouse treated with PBS is also included for reference. Two way ANOVAs with post hoc Tukey tests were used to compare mean values.

3.6.4 Bone marrow derived DCs were highly activated by VVL15-mGMCSF in comparison to VVL15-mIL12

Given the enhancement in numbers of *in vivo* DCs following treatment with VVL15-mGMCSF, we attempted to establish if this recombinant virus was also capable of activating them to a greater degree. DCs were harvested from the bone marrow of naïve C57BL/6 mice as described in section 2.9.3, validated by flow cytometry and infected with the cytokine armed viruses. Cells were harvested 24 hours later and stained for the presence of CD80 and CD86 surface antigens.

In comparison to treatment with the other viral groups, the proportion of DCs positive for these markers (in particular CD86) was highest following infection with VVL15-mGMCSF (figure 3.72).

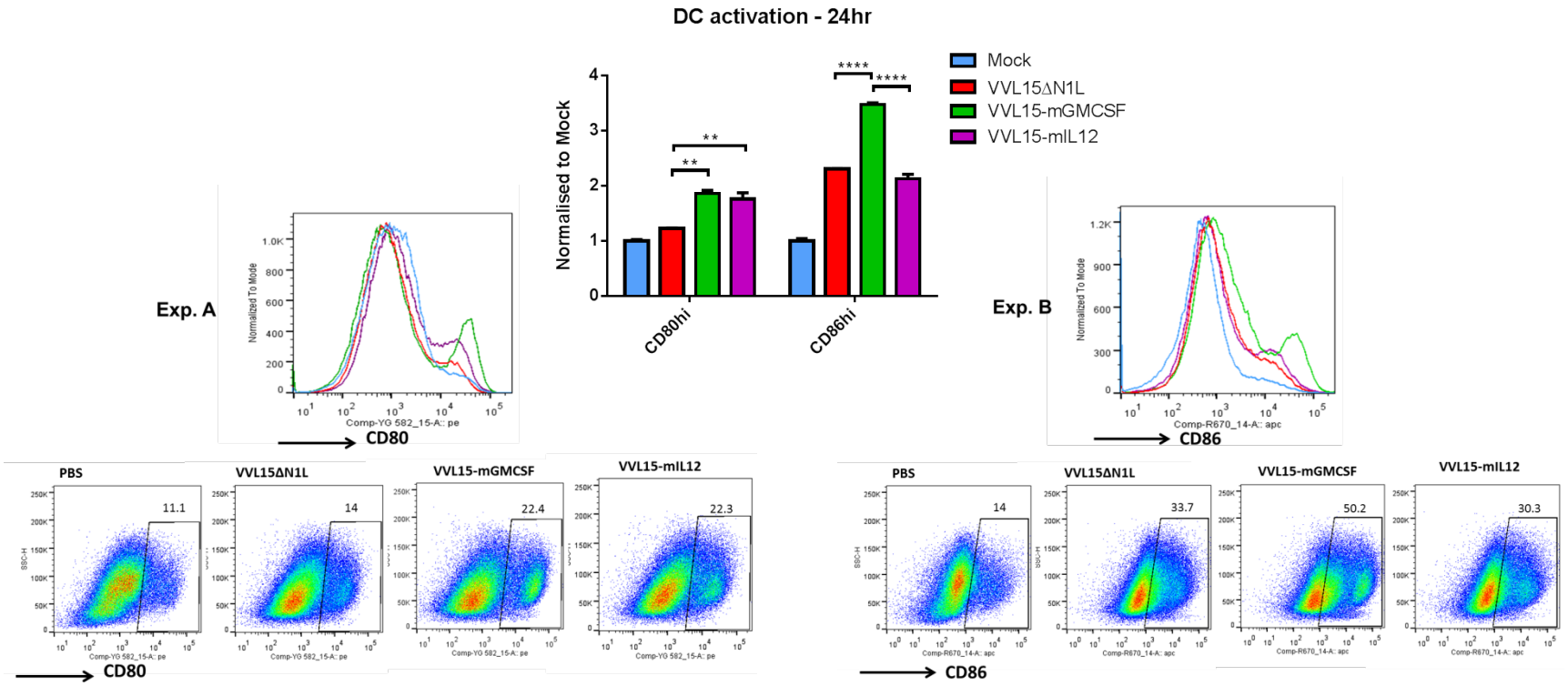

Figure 3.72 VVL15-mGMCSF infection of DCs enhanced their activation in comparison to VVL15ΔN1L and VVL15-mIL12

Twenty four hours after viral infection of enriched DCs (MOI of 1 PFU/cell), cells were harvested and stained with fluorophore labelled antibodies against CD80 (Exp. A) and CD86 (Exp. B) surface markers. The "hi/lo" boundaries of these markers were set at the upper border of the densest population of mock treated cells (left most dot plot). "Hi" values were normalised to the mean for mock infected cells. One way ANOVAs with post hoc Tukey tests were used to compare means.

We had now demonstrated that VVL15-mGMCSF could enhance splenic DCs *in vivo*, as well their activation (and by implication, their ability to present antigen); whereas VVL15-mIL12 greatly enhanced the tumour specific adaptive antitumour immune response in at least one tumour model.

3.6.5 Antigen presenting cells were hijacked into expressing the relevant cytokine transgene following infection with VVL15ΔN1L recombinant viruses

Cytokine transgene armed viruses could infect, replicate and express their transgenes in a number of different tumour cell lines derived from murine, hamster and human hosts *in vitro* (sections 3.1.3, 3.1.4 and 3.1.5). Could they also do so in DCs and macrophages; in effect forcing them into expressing strong Th1 promoting cytokines?

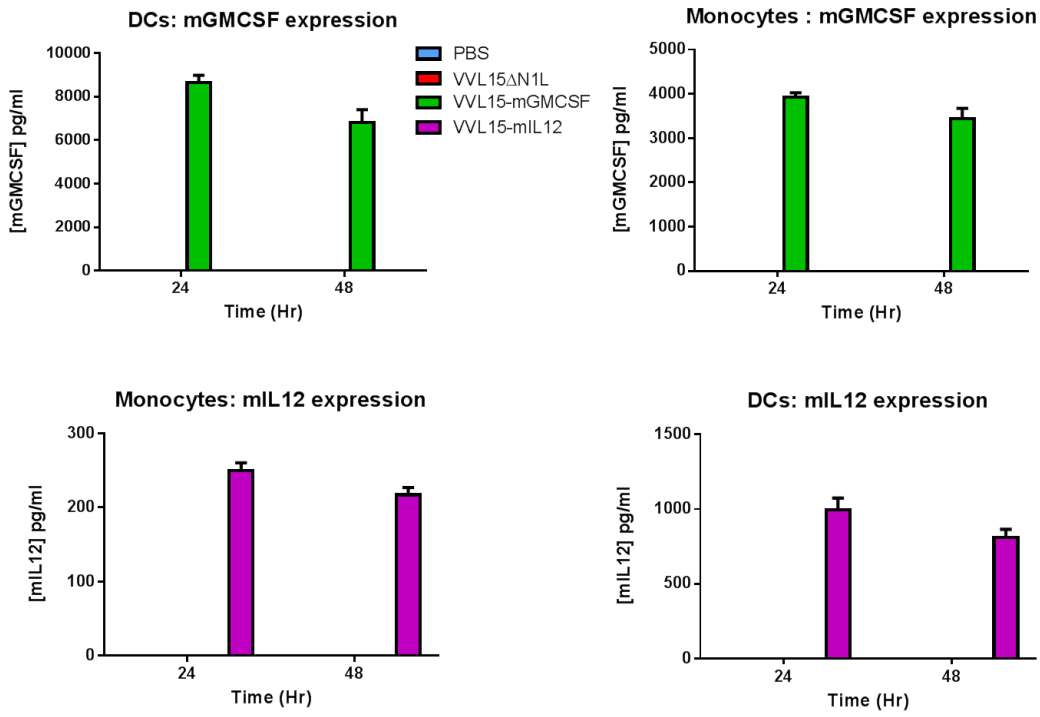

Figure 3.73 VVL15-mGMCSF and VVL15-mIL12 were able to express their respective cytokines upon infection of DCs and monocytes

Supernatant samples at 24 and 48 hours, were removed from triplicate wells containing virally infected DCs or monocytes (MOI of 1 PFU/cell). Murine GMCSF and IL12 concentrations (as indicated) were measured by ELISA. Two-way ANOVAs with post hoc Tukey tests were used to compare means.

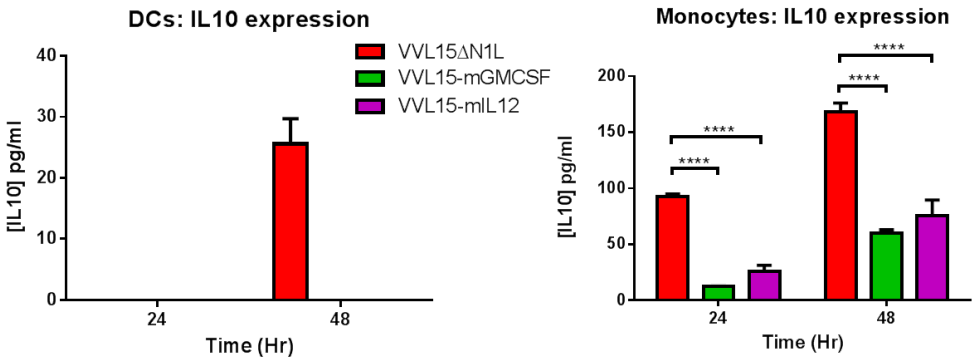

Figure 3.74 Infection with cytokine armed viruses dampened down the VVL15ΔN1L induced production of IL10 from DCs and monocytes

Supernatant samples at 24 and 48 hours, were removed from triplicate wells containing virally infected DCs or monocytes (1 PFU/cell). Murine IL10 concentrations were measured by ELISA. Two-way ANOVAs with post hoc Tukey tests were used to compare mean values.

Figure 3.73 shows that the cytokine transgene armed viruses were able to infect both DCs and monocytes and express detectable quantities of either cytokine; mGMCSF or mIL12. In terms of IL10 production, this experiment replicated the ability of VVL15ΔN1L to induce the production of this cytokine from DCs and monocytes in particular. Whilst not abrogating output from monocytes completely, levels of IL10 were significantly diminished following infection with either cytokine transgene armed virus (figure 3.74).

3.6.6 *In vivo* efficacy with cytokine armed viruses

3.6.6.1 Early administration of VVL15-mIL12 virus led to superior efficacy against syngeneic flank DT6606 tumours.

The data thus far illustrated that our cytokine armed recombinant VVs had the potential to selectively enhance different components of a developing immune response. It might therefore have been logical to treat a tumour with a combination of these viruses to take advantage of their respective functions i.e. sequential treatment with VVL15-mGMCSF

followed by VVL15-mIL12 virus in order to boost TAA presentation and antitumour effector responses respectively.

To test this, DT6606 syngeneic flank models were established as described in 2.15.1 and mice were randomised into five treatment arms (table 2.8, experiment 6). Contrary to expectation, initial treatment with IT VVL15-mIL12, regardless of whether it was followed by further doses of VVL15-mIL12 or VVL15-mGMCSF produced the most efficacious reduction in tumour growth (figure 3.75). Surprisingly the efficacy of the reverse combination of virus treatment (i.e. initial treatment with VVL15-mGMCSF), in this tumour model was relatively poor.

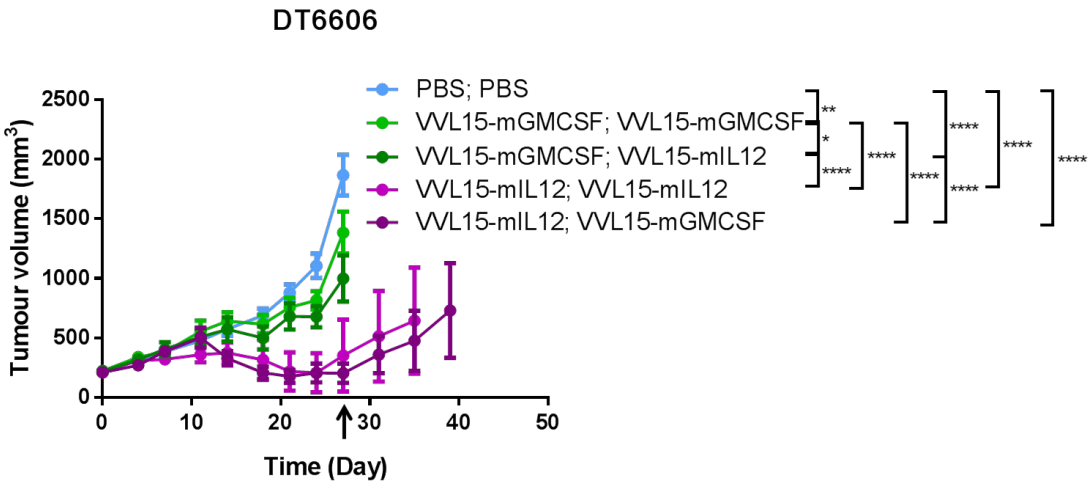

Figure 3.75 Early IT treatment with VVL15-mIL12 led to the most efficacious reduction in tumour growth

Syngeneic DT6606 flank tumour models were treated with a total of six doses ($1x10^8$ PFUs of virus per dose) of different combinations of recombinant viruses as shown (three single daily doses of virus A followed by three single daily doses of virus B (see table 2.8, experiment 6)) or the equivalent volume of PBS (n=7 per group). The first dose was injected at day 0 on the X axis. Two-way ANOVAs with post hoc Tukey tests were used to compare mean tumour volumes. The arrow depicts the time point to which the comparative statistical figures on the graph relate to.

Given the success of VVL15-mIL12 in the previous experiment, a repeat was conducted on syngeneic flank models of DT6606 and other solid tumours, using a monotherapeutic schedule. There was a dramatic reduction in the growth rate of DT6606 tumours following treatment with VVL15-mIL12, with long term cure of six out of seven tumour bearing mice (figure 3.76). Furthermore, even the more aggressive tumours, i.e. LLC and CT26 that were previously resistant to VVL15ΔN1L, were significantly more responsive to treatment with VVL15-mIL12 monotherapy, although notably, there were no complete cures.

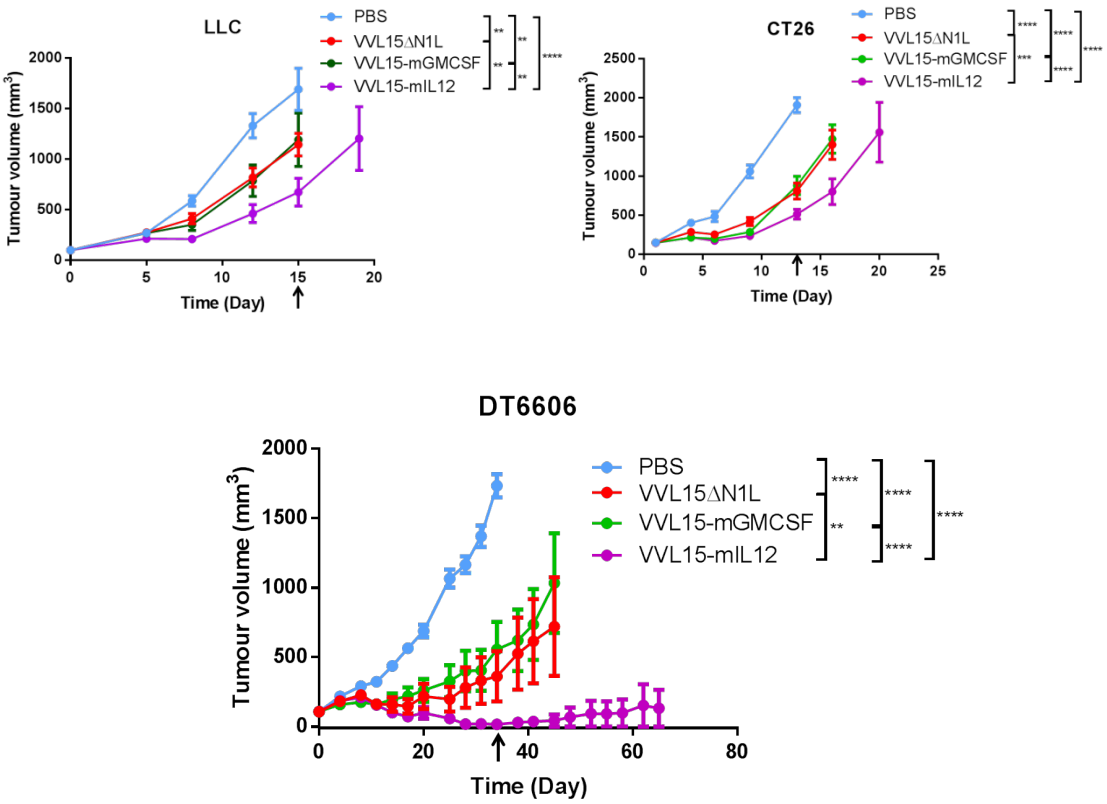

Figure 3.76 VVL15-mIL12 was the most efficacious recombinant ΔN1L virus against syngeneic flank tumour models

Syngeneic DT6606, LLC and CT26 flank models were treated with five daily IT doses of $1x10^8$ PFUs of virus or the equivalent volume of PBS (n=5-7 per group). The first dose was injected at day 0. Two way ANOVAs with post hoc Tukey tests were used to compare mean tumour volumes. The arrows depict the time point to which the comparative statistical figures on each graph relate to.

.

3.6.6.2 Confirmation of the enhancement of antitumour immunity after multiple doses of cytokine armed viruses

Further splenocyte IFNγ immunoassays were conducted following the administration of multiple doses of virus into DT6606 tumour bearing mice. This again served dual purposes of confirming the reliability of the immunological data obtained following single dose IT virus as well has enhancing the prospect of detecting *in vivo* generated mesothelin epitope specific CD8+ T cells.

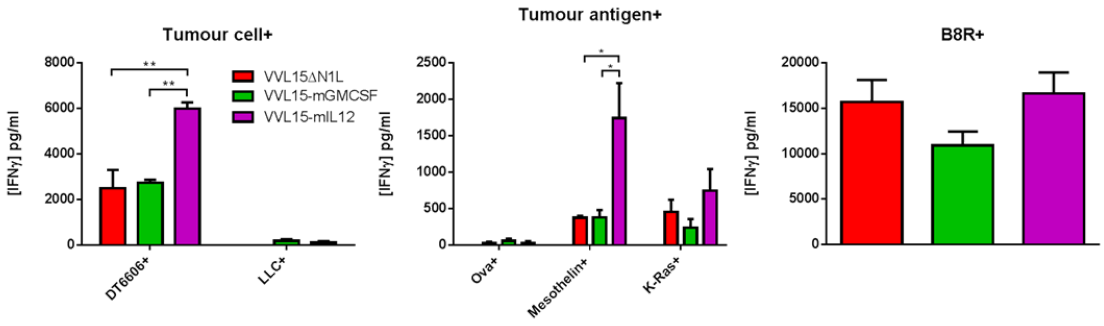

Figure 3.77 Multiple doses of IT VVL15-mIL12 enhanced the antitumour adaptive immunity afforded by VVL15ΔN1L

Syngeneic DT6606-flank tumours were treated with five daily IT doses of $1x10^8$ PFUs or the equivalent volume of PBS (n=3-4/group). Fourteen days after the first dose, splenocyte suspensions were co-cultured with growth arrested whole target (DT6606) or control (LLC) tumour cells, tumour peptides or the VV B8R peptide as indicated. The IFNγ concentrations (pg/ml, Y axis) of supernatants were measured by ELISA. One-way ANOVAs with post hoc Tukey tests were used to compare means values.

As previously demonstrated, the highest concentrations of IFNγ were obtained following co culture of splenocytes from VVL15-mIL12 treated tumour bearing mice (figure 3.77). This pattern was also seen following co-culture with the murine mesothelin peptide, although not with the K-RAS peptide. The anti-B8R responses from all three groups were predictably high although the VVL15-mGMCSF group appeared to fare worse than the other two. Interestingly the antiviral immune response was not enhanced by the presence of mIL12.

The percentage of splenic CD8+ T cells was highest following treatment with VVL15-mIl12 (figure 3.78). Of these, the effector memory (CD44hiCD62Llo) pool was also elevated in the VVL15-mIL12 treated group (figure 3.78).

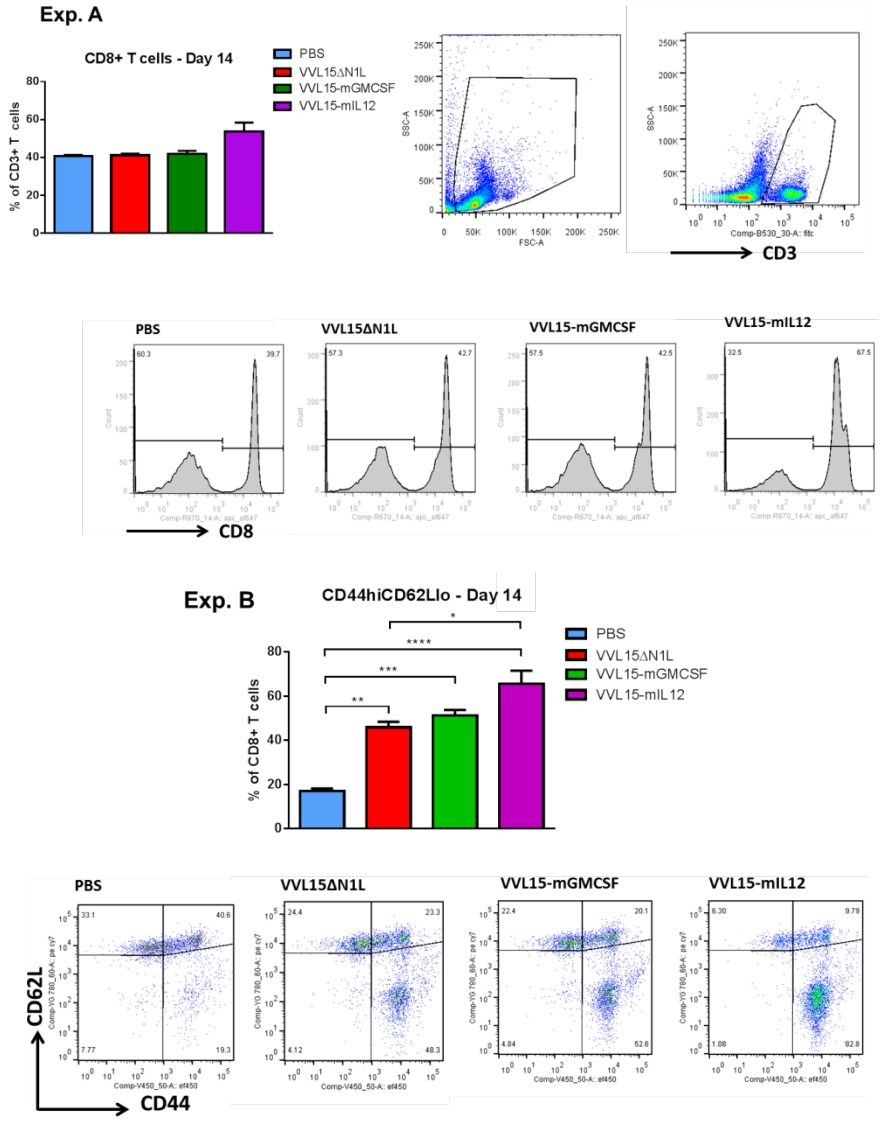

Figure 3.78 Multiple doses of IT VVL15-mIL12 enhanced the generation of effector CD8+ T cells afforded by VVL15ΔN1L

Syngeneic DT6606 flank tumours were treated with five daily IT doses of virus ($1x10^8$ PFUs per dose) or the equivalent volume of PBS (n=3- 4/group). Fourteen days after the first dose, splenocyte suspensions were stained with fluorophore labelled antibodies against CD45, CD3, CD8, CD44 and CD62L cell surface antigens and analysed in a multichannel flow cytometer. Exp. A depicts the gating strategy used to isolate the CD8+CD3+ population. Exp. B represents the effector memory (CD44hiCD62Llo) percentage of CD8+ T cells. One-way ANOVAs with post hoc Tukey tests were used to compare mean values.

Immunohistological analysis of snap frozen tumour sections, 14 days after the first dose of virus confirmed the enhanced intratumoural infiltration of both CD8+ and CD4+ cells following VVL15-mIL12 administration (figure 3.79).

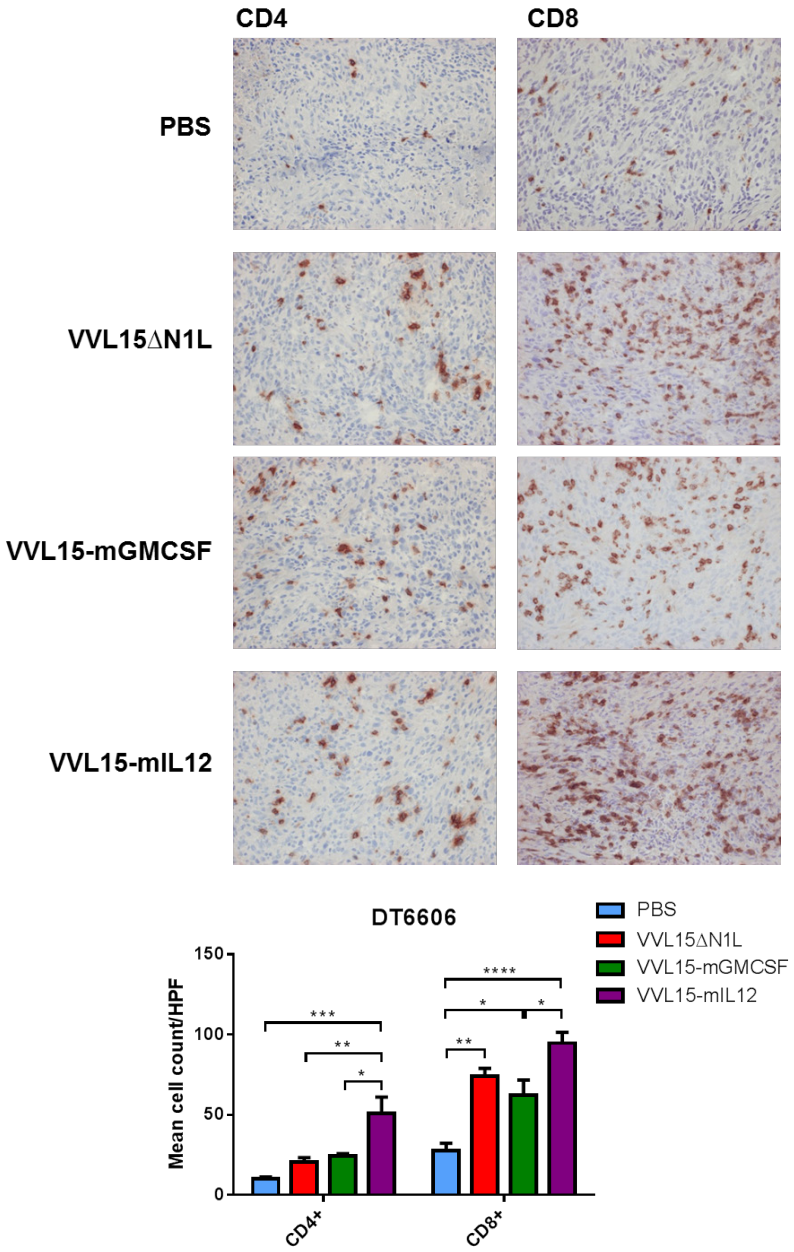

Figure 3.79 Multiple doses of IT VVL15-mIL12 enhanced the VVL15ΔN1L mediated infiltration of CD8+ cells into DT6606 tumours

Syngeneic DT6606 flank tumours were treated with five daily IT doses of virus ($1x10^8$ PFUs per dose) or the equivalent volume of vehicle buffer (n=3-4/group). Fourteen days after the first dose, frozen sections of harvested tumour were immunostained with either anti CD4, CD8, NK1.1 or F4/80 antibodies. The bar chart depicts the mean manual cell count per HPF from 10-15 HPFs (x200 magnification). One-way ANOVAs with post hoc Tukey tests were used to compare pairs of means.

In order to control for the relatively expanded population of CD8+ splenic T cells, Mesothelin epitope specific CD8+ T cells were expressed as a percentage of CD3+ T cells (i.e. total T cells). There was no significant enhancement in this clone of anti-tumour T cells in comparison to that obtained from the VVL15ΔN1L treated group (figure 3.80).

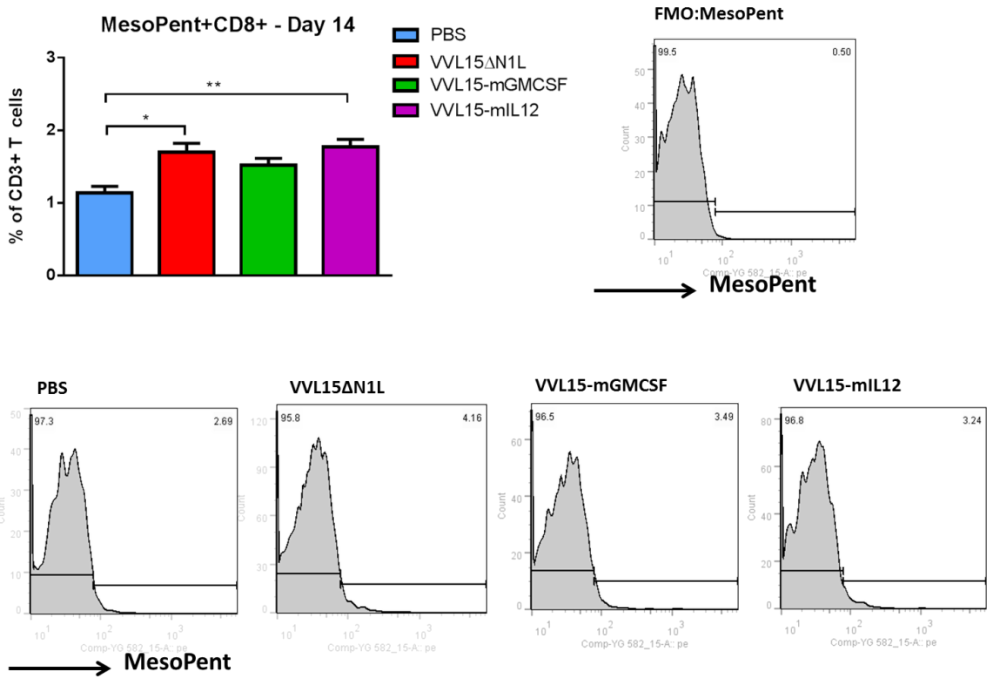

Figure 3.80 Multiple doses of IT cytokine armed recombinant viruses did not enhance the *in vivo* expansion of a mesothelin TCR specific clone of T cells

Syngeneic DT6606 flank tumours were treated with five daily IT doses of virus ($1x10^8$ PFUs per dose) or the equivalent volume of PBS (n=3- 4/group). Fourteen days after the first dose, splenocyte suspensions were stained with PE labelled mesothelin pentamer as well as with anti CD3-FITC and anti CD8a-APC and analysed in a multichannel flow cytometer. The bar chart depicts the mesothelin epitope specific clone of CD8+ T cells, expressed as a percentage of total CD3+ T splenocytes. An FMO stained sample that excluded the MesoPent-PE was used to set the gate for pentamer positivity (top right graph). A one-way ANOVA with post hoc Tukey tests was used to compare pairs of means.

3.6.6.3 Efficacy of cytokine armed VVL15ΔN1L with neoadjuvant surgical models of lung cancer.

Recall that:

1. Multiple doses of IT VVL15ΔN1L, appeared to significantly reduce the lung metastatic rate from syngeneic LLC flank tumours. There was no difference between viral treatment groups in terms of the growth restriction of primary tumours.

2. Neoadjuvant treatment with multiple doses of IT VVL15ΔN1L prior to the surgical excision of the primary flank LLC tumour led to significantly enhanced short term survival in comparison to treatment with VVL15. This appeared to be dependent on the enhancement of circulating NK cells.

These experiments were repeated with the cytokine armed viruses

1. Following the establishment of syngeneic LLC flank tumours, mice were randomly divided into treatment groups (section 2.15.1). Five doses of IT virus/ PBS were administered.

Figure 3.76 demonstrated that the growth of the primary LLC tumour was slowed by IT administration of VVL15-mIL12 in comparison to the other viruses. All animals were euthanized when the first group achieved criteria for sacrifice. Their lungs were scrutinized macroscopically and microscopically for tumour metastases. All three N1L deleted recombinant viruses appeared to reduce lung metastases in comparison to treatment with PBS, with 0/7 positive in VVL15ΔN1L and VVL15-mIL12 groups and 1/7 in the VVL15-mGMCSF group (figure 3.81). In contrast 6/7 PBS treated mice had lung tumours at sacrifice.

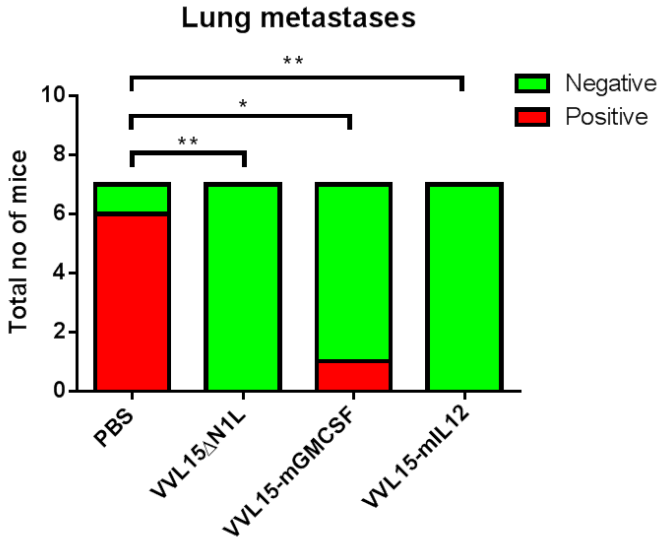

Figure 3.81 Metastatic dissemination from LLC flank tumours following intratumoural cytokine armed recombinant viral administration

Syngeneic LLC flank tumours were treated with five daily IT doses of virus ($1x10^8$ PFUs per dose) or the equivalent volume of PBS (n=7/ group). Tumour volumes were tracked via twice weekly calliper measurement. Mice were euthanized when the first group of tumours reached the criteria for sacrifice. Lung sections were stained with H&E and slides were scrutinized for the presence or absence of lung metastases by a pathologist (YW) who was blinded to the treatment groups. Fisher's exact tests were performed on 2x2 tables comparing specific pairs of conditions.

2. Finally, LLC flank tumour models were again established with a view to neoadjuvant treatment prior to surgical excision of the primary tumour (section 2.15.5). There was a dramatic enhancement of long-term survival following neoadjuvant treatment with VVL15-mIL12. Seven of eight mice were apparently cured, as dictated by long term health and accumulation of weight (figure 3.82).

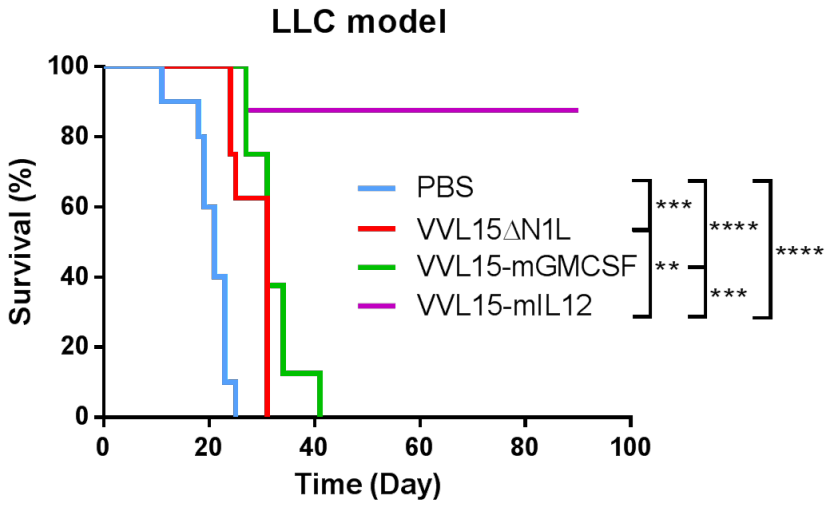

Figure 3.82 Pre-surgical IT treatment with VVL15-mIL12 prolonged long term post-operative survival of LLC tumour bearing mice

Syngeneic LLC flank tumours were treated with five daily IT doses of virus ($1x10^8$ PFU per dose) or the equivalent volume of vehicle buffer (n=8-10/group). Tumours were surgically resected seven days after the final dose of virus. The X axis represents days post-surgical excision. Log rank analyses were used to delineate any significant differences between specific treatment pairs.

In addition to its effects on adaptive immunity IL12 is known to enhance the proliferation and activation of NK cells and may have simply potentiated the already enhanced antitumour NK response following treatment with VVL15ΔN1L. It remains to be determined whether VVL15-mIL12 recruited additional "adaptive" immune effectors to mediate the long term survival benefit seen here post-operatively.

3.6.7 Summary of Results Chapter 3.6

In a bid to improve upon the efficacy of VVL15ΔN1L, mGMCSF and mIL12 cytokine transgenes were cloned into this platform. *In vitro*, these viruses were able to infect and express their respective transgenes in murine bone marrow derived DCs and monocytes. In addition, IL10 production from both cell types was reduced following infection by either virus.

IT injection of VVL15-mIL12 into DT6606 tumour bearing mice further enhanced adaptive antitumour immunity in comparison to either VVL15ΔN1L or VVL15-mGMCSF. As predicted by the function of its cytokine transgene, treatment with VVL15-mGMCSF stimulated the highest splenic DCs *in vivo* as well as their activation *in vitro*.

Given these results, it was initially hypothesised that sequential treatment with VVL15-mGMCSF followed by VVL15-mIL12 might have been the most efficacious combination. However, monotherapy with VVL15-mIL12 produced a far superior growth reduction across all tested primary tumour models, especially against DT6606 syngeneic tumours.

As with VVL15ΔN1L, multiple doses of IT VVL15-mIL12 or VVL15-mGMCSF also reduced metastatic dissemination to the lungs from LLC flank primaries. Intratumoural administration of VVL15-mIL12 as a neoadjuvant to surgical resection of LLC tumours, appeared to prolong long term survival. It remains to be determined whether this effect was due to the recruitment of adaptive immune effectors, as opposed to potentiation of an already enhanced antitumour innate immune response.

Chapter 4 Discussion

4.1 Analysis of results and outline of future work

During the past eight years, our research group has developed the Lister strain recombinant backbone, VVL15 for use in the therapy of solid tumours. We have been able to demonstrate that VVL15 has superior oncolytic potency against a large panel of human cancer cell lines, in comparison to more virulent platforms such as WRDD (Hughes et al., in press, Gene Therapy). Its antitumour efficacy in immunocompetent syngeneic murine cancer models was also superior. Nevertheless, monotherapy with VVL15 could not accomplish complete cancer cure and so there remained scope for further development.

Appropriate activation of the innate immune system is a prerequisite to effective priming of adaptive immune responses against both foreign and self-antigens, including TAAs (347-349). Deletion of the N1L gene of VVL15 served two purposes: a) to locally enhance the cellular and cytokine responses consequent to viral oncolysis (i.e. innate immunity) and thus augment the quantity of PAMPs and DAMPs and b) to enhance the safety of the viral backbone. If indeed VVL15ΔN1L was deemed to be superior to VVL15 in these regards, regardless of efficacy per se. then we could confidently start to explore the effects of arming it with immunomodulatory transgenes.

The homologous recombination strategy used in this project was designed to replace almost the entirety of the coding sequence of the L025 (N1L) locus. Sequence analysis at the junctions of L024/25 and L025/26 (using primers 3 and 4 in table 3.1 respectively) confirmed that the ORFs upstream and downstream of L025 remained intact (data not shown). In the wild type virus, there is a 14 bp overlap of the L024 ORF with that of L025 and this was unaltered.

VVL15ΔN1L was at least as potent, if not more so than VVL15 at killing murine and hamster derived cancer cells *in vitro*. The N1L gene product is a Bcl-2 structural homologue (57) and one of its functions is postulated to be inhibition of cellular

apoptosis. Infection with VVL15ΔN1L could have accelerated apoptosis in these cells. Although, given that multiple anti-apoptotic mutations are already likely to be present in cancer cells, this explanation may be an over-simplification. Indeed, the cytotoxicity in human cell lines was more variable; VVL15ΔN1L was statistically superior at killing only one of six human cancer cell lines tested (UW-228). Furthermore, the anti-apoptotic function of the N1L protein has been questioned in at least one study (350).

VVL15ΔN1L demonstrated superior cytotoxicity against murine cancer cells lines in comparison to its cytokine transgene armed recombinants (VVL15-mGMCSF, VVL15-mIL12), despite these viruses also lacking the N1L gene. A major mechanism of viral cell killing is by cellular burst once a threshold level of intracellular viral progeny has been achieved. One explanation for the observed results could be that the transcription machinery and indeed cellular energy resources were diverted away from the production of virion particles and towards cytokine expression and translation.

Interestingly, the cytotoxic potencies of the IL12 transgene armed viruses were superior to their GMCSF armed counterparts (both murine and human). IL12, acting through its cognate cell surface receptor may be directly cytotoxic to certain cancer cells, of both haematogenous and epithelial origin (351-354). It would certainly be of translational significance to establish whether the cell lines used in this project constitutively express surface IL12 receptors.

Contrary to its original premise as an anticancer immune modulator, there is an accumulating body of evidence that GMCSF may promote tumour growth under certain circumstances. A number of murine and human cancers express GMCSF as well as its receptor (355-357). In head and neck squamous carcinoma for example, intratumoural GMCSF (as well as VEGF and PDGF) expression correlated with poor prognosis in one cohort of patients (357). GMCSF can stimulate the growth, migration and metastases of tumour models both *in vitro* and *in vivo* (358-360), often indirectly via activation of stromal components (360-362).

Thus differences in cytotoxicity between the cytokine armed viruses may have reflected differences in the responsiveness of the tested tumour cells to the expressed cytokines.

Disruption of the N1L gene in vaccinia was previously shown not to attenuate replication *in vitro* (248). Our experiments however, revealed that in comparison to VVL15, the replication of VVL15ΔN1L was modestly but significantly attenuated in over half of the panel of cell lines tested, with an inferior trend in the others. This is unsurprising as viral replication has been inversely correlated to the extent to which it has been genetically manipulated (58). A feature confirmed by the fact that there was a further attenuation of the replication of cytokine transgene armed recombinants. Despite this, all novel recombinant viruses remained replication competent and were able to detectably express their relevant transgene.

Effective immunotherapeutics are likely to be those that generate a response against multiple TAAs. A logistically simple way to do this would be to try and enhance the simultaneous presentation of different TAAs within an *in situ* syngeneic tumour. Intratumoural injections of virus into a syngeneic flank tumour would theoretically release multiple TAAs (through oncolysis), the combination of which would be unique to the host and tumour at that particular time.

The generation of an adaptive antitumour immune response was initially investigated by comparing IFNγ release from *ex vivo* stimulated splenocytes. IFNγ production *in vivo* occurs mainly from cells of lymphoid origin; namely T and NK cells. The contribution from the former would be expected to be relatively high particularly after *ex vivo* selection with whole tumour cells or immunodominant T cell stimulating epitopes. Using these assays, we have shown that VVL15ΔN1L was superior to VVL15 at priming adaptive tumour specific immunity. In contrast, antiviral immunity (measured by the response to an immunogenic VV B8R epitope) was not significantly altered. As expected, after a single dose of IT virus, both antitumour and antiviral responses in LLC and DT6606 tumour bearing mice waned with time, so that by day 21 there were no significant differences between treatment groups. Unsurprisingly therefore, boosting strategies will be required for more prolonged antitumour responses.

IFNγ released from splenocytes harvested from virally treated DT6606 tumour bearing mice were consistently higher than from their LLC bearing counterparts. This may again reflect differences in immunogenicity between the oncolysed TAAs or the ease with which tolerance to TAAs may be reversed. Thus the TME of LLC tumours may be more immunosuppressive than DT6606 tumours. There were higher numbers of CD4+ (in comparison to CD8+) cells in histological sections of LLC tumours post treatment; the reverse was true in DT6606 tumour sections. T regulatory cells of the CD4+ subset are naturally more abundant and have been more extensively studied than those of a CD8+ phenotype (363, 364). It is tempting to think that LLC tumours may therefore contain a higher ratio of T-regs to CTLs than DT6606 tumours, but this assumption would need to be confirmed by formal investigation. Furthermore, it is unclear from this explanation why the strength of the antiviral (anti VV B8R) response in LLC tumour bearing mice was not lower than in DT6606 tumour bearing mice.

At the time of testing, the immunodominant TAA profile of DT6606 pancreatic tumour cells (331, 332) had not been established. An "artificial" TAA, like chicken ovalbumin is foreign to the host in this context and likely to be highly immunogenic; but we felt it should suffice in a comparative study. Intratumoural VVL15ΔN1L enhanced anti-Ova immunity in comparison to VVL15. Once again, the relatively high IFNγ levels upon splenocyte co-culture with the B8R epitope was not statistically different between groups treated with either viral platform.

Fluorescence cytometric analysis of splenic T cells following IT viral administration into tumour bearing mice provided some preliminary data on the nature of the T cell response. At relatively early time points i.e. seven and 14 days post injection, VVL15ΔN1L generated significantly higher levels of CD44+CD62Llo, CD8+ T cells in comparison to VVL15 or PBS.

Memory T cells, both CD4+ and CD8+ may be categorised into at least two different functional groups: effector and central memory (reviewed in (365)). Whilst both subsets are positive for CD44 (a hyaluronate receptor that has been associated with "activated" memory cells), effector memory cells lose the lymphoid homing receptors CCR7 and

CD62L; they are thought to circulate throughout the periphery, being capable of rapidly maturing into IFNγ producing cells and in the case of CD8+ T cells, immediately effecting target cell cytotoxicity. Central memory T cells are CCR7 and CD62Lhi and remain within lymphoid tissue, producing mainly IL2 in their native state. Although they are capable of proliferation upon meeting their cognate antigen, they can only do so in lymphoid tissue and therefore rely on APCs for delivery of antigen. In addition, they take longer than effector memory T cells to differentiate into an activated effector phenotype. As the surface expression of CCR7 mirrors that of CD62L, our chosen definitions of effector or central memory T cells were CD44+ and CD62Llo or hi respectively. Based on this definition, in both LLC and DT6606 tumour bearing mice, VVL15ΔN1L (in comparison to the other treatment arms) enhanced splenic effector memory CD8+ T cells at early time points following infection. As previous IFNγ immunoassays revealed non-significant differences in antiviral adaptive immunity between viral groups, it was possible that the enhanced number of CD8+ effector memory cells reflected an enhanced antitumour memory pool. The enhanced generation of mesothelin pentamer specific CD8+ T cells following treatment of DT6606 tumour bearing mice with multiple doses of VVL15ΔN1L corroborated this notion.

Measurement of IFNγ levels from *ex-vivo* activated T cells can only act as a surrogate marker for the potency of a tumour specific cytotoxic response. A demonstration of direct T cell mediated cytotoxicity would be desirable. To this effect, a non-radioactive CTL assay, based on LDH release from lysed cells, confirmed the ability of VVL15ΔN1L (in comparison to VVL15) to induce a greater number of tumour specific cytotoxic splenocytes. In parallel to the previous results, antitumour cytotoxicity was superior following viral treatment of DT6606 as opposed to LLC tumour bearing mice.

A number of SC syngeneic flank models were used to assess whether the induced adaptive antitumour immunity translated into efficacy. Treatment with VVL15ΔN1L slowed tumour growth to a significant degree in DT6606 and CT26 tumour bearing mice. The replication and cellular cytotoxicity of VVL15ΔN1L in DT6606 and CT26 cells *in vitro* were not enhanced in comparison to VVL15, so viral oncolysis must have been augmented, probably by a boost in antitumour immunity *in vivo*. Indeed the

complete abrogation of the efficacy of VVL15ΔN1L against DT6606 tumours in mice depleted of CD8+ cells confirmed the critical role of antitumour CTLs. Surprisingly, depletion of NK or CD4+ cells made little difference in this regard.

The next group of experiments were designed to establish whether VVL15ΔN1L could be delivered to tumours following IV administration, as well as its off-target infectivity. The use of two syngeneic flank models derived from different strains of mice, C57BL/6 (LLC) and BALB/c (CT26) would confirm the validity of any conclusions. Note that although non-invasive imaging (measuring luminescence and fluorescence) was available and from previous studies was capable of detecting viral replication within tumour, this investigative modality was not sensitive enough to detect virus in organs other than the lungs (Ferguson, unpublished data).

Following a single IV dose of either VVL15 or VVL15ΔN1L ($1x10^8$ PFUs), live virus could be recovered from tumour for at least 10 days. In mice carrying CT26 tumours, there was no significant difference between viral tires at any time point, although there did appear to be a trend for the enhanced clearance of VVL15ΔN1L. VVL15ΔN1L titres in the LLC model were significantly worse after day three. Viral titres rose and peaked between three and seven days post injection implying that virus was able to amplify within tumours. Significant titres of live virus were recovered from filtering organs (lungs, liver, spleen and kidneys) during the first 24 hours. The highest titre outside of tumour was seen in the lungs, with live virus present for at least three days. Importantly, VVL15ΔN1L was cleared by the host to a greater extent than VVL15 in off-target organs. There was no live virus in the brains of CT26 tumour bearing mice and although live virus was demonstrated in the brains of LLC bearing animals, deletion of the N1L gene appeared to moderately reduce titres as expected from the literature (see section 1.5.7)

Despite enhanced host clearance of live VVL15ΔN1L virus from LLC tumours, IV delivery did retain the capacity to stimulate a superior antitumour immune response in comparison VVL15. However, as with the IT treatment of flank LLC tumour bearing mice, this enhancement did not translate into superior efficacy upon IV treatment of its

orthotopic counterpart. The LLC model is extremely aggressive and the time needed to generate an efficacious effector immune response is likely to far exceed that required to cause the demise of the animal by tumour dissemination. Nonetheless, given the reduced off-target replication of VVL15ΔN1L it may be possible to safely administer higher IV doses compared to VVL15. LD50 (dose for lethality in 50% of animals) experiments using escalating doses of IV virus will need to be performed in order to establish a safe dosage window; which could then be extrapolated to the first in-human trials.

One of the "hallmarks" of cancer is their ability to metastasize (47). The next experiment demonstrated that although IT VVL15ΔN1L was unable to restrict the growth of primary tumour, it did reduce metastases from the primary. Histological examination of murine lungs at the end point of the experiment, demonstrated a higher proportion of tumour free lungs following treatment with VVL15ΔN1L. Explanations could include blockage of peritumour vasculature by leucocyte (granulocyte in particular) infiltrates, enhanced numbers and activity of circulating NK cells and/ or indeed enhanced adaptive anti-tumour surveillance. Regardless of the mechanisms, given the above result, we postulated that VVL15ΔN1L might be a good neoadjuvant to conventional antitumour therapy, including surgery.

Interestingly, numerous animal studies have demonstrated that surgical manipulation can enhance post-operative metastases (288, 307). As detailed in the introduction, there may be a number of reasons for this including intraoperative seeding, enhanced secretion of pro-metastatic growth factors and immune suppression. Surgical damage is inflammatory and should theoretically release cellular "danger signals", but other sub-components of the innate immune response may be dampened e.g. the NK response (288, 307, 310). Neoadjuvant virotherapy could tip the balance into one that favours eradication of *in situ* microscopic disease. In one study the concurrent administration of WRDD, reversed the dampened NK response associated with major surgery and was able to reduce metastatic dissemination (310). In that experiment virus was administered just a few hours prior to surgery. This may cause two problems upon translation to human patients: a) systemic high dose virotherapy may be hazardous in

the setting of prolonged surgery under general anaesthesia, and b) excision of the tumour bed (and thus virally released TAAs) so soon following OVT may preclude the priming of long term tumour specific adaptive immunity.

Our preliminary results demonstrated a significant short term survival benefit for mice pre-treated with VVL15ΔN1L prior to surgical excision of their primary tumour. This effect was mediated by the elevation of circulating NK cells as demonstrated by the complete abrogation of response when the experiment was repeated in mice in which NK cells were depleted. A further important experiment that should be performed is to test whether VVL15ΔN1L treatment also enhances the activation of NK cells.

Tumour regrowth after re-implantation of primary cancer cells in survivors from the neoadjuvant surgical cohort was positively associated with diminished antitumour immunity. Indeed only 20% of total mice treated with VVL15ΔN1L could overturn the immune dampening effect of surgery (see figure 3.49) and developed the ability to reject a novel tumour challenge, so there remained significant room for improvement.

In a bid to explore some of the mechanisms responsible for the efficacy of VVL15ΔN1L, biological time-point experiments were performed following the IT injection of syngeneic flank LLC tumour models. Intratumoural neutrophil infiltration following virotherapy was not unexpected from the literature and VVL15ΔN1L appeared to enhance this response (see below). The prolonged presence of neutrophils within TMEs have been associated with tumour progression via multiple mechanisms (366) and it is interesting to note that KC, a murine neutrophil chemoattractant was constitutively secreted by LLC and DT6606 tumour cells *in vitro*. Analogous to GMCSF, in the resting state KC may act as an autocrine growth factor in these models. In contrast, hyper recruitment and stimulation of neutrophils, as occurs following virotherapy, has been associated with tumour cell cytotoxicity and suppression (367). The latter has been attributed to mechanisms such the mechanical blockage of tumour vessels, excess release of cytotoxic agents, enhanced antigen dependent cellular cytotoxicity (ADCC) in the presence of antitumour antibodies, or indeed through a phenotypic switch of neutrophils to being able to present antigens (368-370).

Interestingly there was a reciprocal reduction in the IT macrophage pool following administration of VVL15ΔN1L (and to a lesser extent VVL15) in DT6606 tumours. This may have been an artefactual consequence of the flow cytometric gating strategy used to quantify intra-tumour leucocytes. The monocyte pool, expressed as a percentage of CD45+ cells may have been artificially lowered by the disproportionately large neutrophil response following VVL15ΔN1L administration. Immunohistochemical scrutiny of tumour sections following VVL15ΔN1L treatment did confirm substantial infiltration by (F4/80+) macrophages (figure 4.1) although qualitatively less so in comparison to other treatment groups.

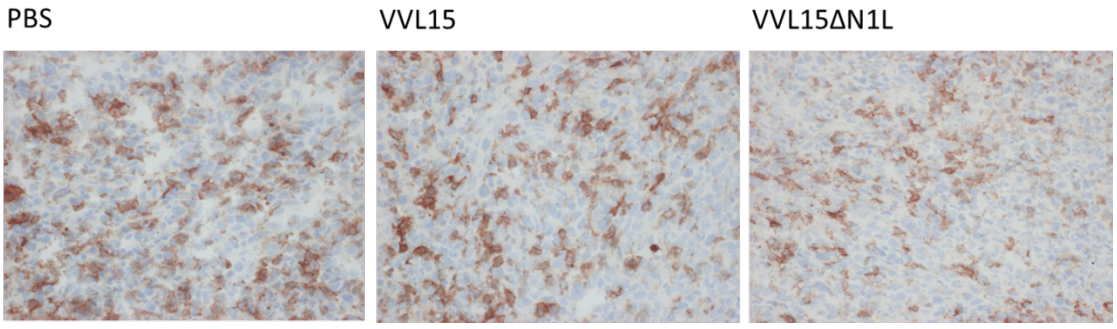

Figure 4.1 Qualitative reduction of IT macrophages following IT VVL15ΔN1L

Syngeneic LLC flank tumours were treated with $1x10^8$ PFUs of IT virus or the equivalent volume of PBS. Fourteen days later, frozen sections of harvested tumour were immunostained with anti F4/80 antibodies (x200 magnification).

Until recently it was thought that monocytes, macrophages and DCs could not support VV replication, although early genes like N1L could still be expressed (262, 371-374). However Byrd et al. (375) recently confirmed that tissue macrophages may indeed be a significant source of viral load *in vivo* and that VV can in fact replicate in and lyse monocytes and macrophages, particularly those of the tumour promoting M2 phenotype. There is an abundance of literature documenting the role of these macrophages in tumour progression (376). A relatively select reduction of this pool through infection with VVL15ΔN1L might have been an additional mechanism

responsible for the efficacy seen with VVL15ΔN1L in this project. This hypothesis will obviously require formal investigation.

Thus far, IT administered VVL15ΔN1L appeared to enhance the stimulation of anti-tumour adaptive immunity without altering antiviral immunity. One explanation might be that presentation of TAAs in this context is predominantly mediated by activated DCs, whereas viral epitopes could additionally be presented by monocytes/ macrophages. In our studies, VVL15ΔN1L enhanced splenic DCs *in vivo* as well as their activation *in vitro*. *In vivo*, the consequent rise in viral epitope presentation may have been offset by the reduction in viral antigen presentation by the reduced pool of monocytes/ macrophages. Again further detailed studies will be required to test this hypothesis; although it should be noted that some groups have contrastingly demonstrated the importance of CD169+ intra-nodal macrophages in the presentation of TAAs from dead tumour cells, albeit in a non-viral context (377, 378).

Another explanation for the selective enhancement of antitumour immunity might relate to the expression of IL10. IL10 is widely regarded as an immunosuppressive cytokine and in the current context may supress the potentially toxic antiviral immune response, ensuring host and therefore viral survival. Infection with VVL15ΔN1L enhanced IL10 production from DCs and monocytes in particular, a result that was originally reported with a WR strain of VV (262). Furthermore, we have recently shown that IT administration of a different (N1L intact) VVL15 recombinant, armed with an IL10 transgene similarly enhanced the generation of antitumour adaptive immunity at the expense of antiviral immunity (379). The rise in local IL10, associated with deletion of the N1L gene may therefore have caused a relative dampening of the vastly immunodominant antiviral immune response.

A screen of inflammatory cytokines and chemokines within virally infected LLC flank tumours revealed the selective enhancement of KC, GCSF, IL1α/β and MIP1α. These are all regulated by NF-κB transcription factors and their expression might have been expected to be enhanced given the suppressive effect of the N1L protein on this pathway (247).

Based on their well characterised functions, enhanced production of KC (mainly from infected tumour cells) and GCSF were most likely to be responsible for the enhanced infiltration of intratumoural neutrophils seen *in vivo* following VVL15ΔN1L infection. MIP1α is a chemo attractant produced mainly by infected/ activated monocytes, macrophages and dendritic cells. In addition to DCs and monocytes, it also recruits NK and T cells (190, 342). It is possible that that this cytokine may have been responsible for the elevation of circulating NK cells following IT VVL15ΔN1L. Further studies using inhibitory molecules, mRNA silencing techniques and/or transgenic mice will be required to confirm this.

Interestingly, VVL15ΔN1L infection upregulated the expression of the IL1 family of cytokines from both DCs and APCs: IL1α, IL1β and IL18. The latter two are surrogate markers for the activation of inflammasome platforms. Inflammasomes are a group of multimeric protein complexes (consisting of a pattern recognition receptor molecule, the adaptor protein ASC and caspase-1, that form in response to a range of exogenous and endogenously generated pathogen or damage associated molecules (247, 346). Activated caspase-1, in turn cleaves and activates IL1β and IL18 precursor molecules which are subsequently secreted. Interestingly, hyperactivation of inflammasome complexes may lead to a particularly immunogenic form of cell death called pyroptosis (344). On the other hand, chronic signalling through both NF-κB pathways and inflammasome complexes have been associated with perpetuation and growth of tumour (344).

Although transcription of the precursor, pro IL1β gene is under the control of NF-κB transcription factors, pro-IL18 mRNA is constitutively expressed and appears to have different regulatory controls (346). The fact that in our studies IL18 was also upregulated by VVL15ΔN1L infection, suggests that the N1L protein may additionally regulate inflammasome signalling. Interestingly, the F1L protein, another VV antiapoptotic Bcl-2 structural homologue, has recently been shown to specifically inhibit the NLRP1 inflammasome complex (345). In the defining study, the authors utilised a re-constituted *in vitro* model to isolate the activity this particular inflammasome complex. They also noted the inability of the N1L protein to alter

signalling through this complex. However there are numerous other candidate inflammasomes; for example the largest inflammasome (NLRP3) is oligomerised by a wide range of stimuli including viruses and bacteria and would be a good starting point for further functional studies of the N1L protein. It would also be intriguing to investigate whether VVL15ΔN1L could induce pyroptotic cell death, an established form of ICD.

To summarize, thus far VVL15ΔN1L retained its ability to replicate in and lyse a range of tumour cells and has the potential to convert an immunosuppressive TME into one that favours the generation of an antitumour immune response (both innate and adaptive). This translated into tumour growth reduction in a primary model of pancreatic cancer and a prolongation of post-operative survival when used as neoadjuvant therapy to surgery in a spontaneously metastasising lung cancer model. The former was mediated by CD8+ cells whereas the latter by enhanced circulating NK cells.

The data obtained has recently encouraged a switch by our research group from the use of VVL15 to the VVL15ΔN1L platform, upon which other VVL based therapeutics will be constructed in the future.

The final results chapter included some preliminary experiments with murine GMCSF or IL12 transgene armed VVL15ΔN1L viruses. Intratumoural injection of VVL15-mIL12 into syngeneic DT6606 flank models boosted tumour specific adaptive immunity above that afforded by VVL15-mGMCSF and VVL15ΔN1L. IFNγ production from whole DT6606 cell/ mesothelin peptide stimulated splenocytes was enhanced, as was the percentage of effector memory CD8+ T cells following both single and multiple doses of VVL15-mIL12. VVL15-mIL12 appeared to globally enhance the CD8+ pool of T cells.

As with previous experiments, there was no enhancement of the antiviral (anti B8R) immune response. Given the dramatic elevation in IFNγ following splenocyte stimulation with growth arrested DT6606 cells, it is likely therefore that a significant

proportion of elevated CD8+ effector memory T cells were clones with specificity for tumour epitopes, although on this occasion, flow cytometric analysis did not reveal a significant enhancement in a mesothelin peptide specific pool of CD8+ T cells. Assuming this was a true result, it may have reflected the disproportionate expansion of other more immunogenic TAA specific CD8+ T cells.

The percentage of *in vivo* splenic DCs, as well as their *in vitro* activation was enhanced by treatment with VVL15-mGMCSF, which also expressed its transgene following the *in vitro* infection of DCs and monocytes. Theoretically, early treatment of tumours with VVL15-mGMCSF followed by the sequential administration of VVL15-mIL12 should have provided optimal boosts to afferent and efferent arms of a developing immune response respectively. Such a sequence of administration into syngeneic flank DT6606 tumours surprisingly did not translate into the most efficacious regime. Instead, early and prolonged administration of VVL15-mIL12 was most efficacious. The effects of IL12 on enhancing innate as well as adaptive immunity are well established, i.e. the cytokine has been shown to enhance APC activation and the proliferation and activation of NK cells (141, 226).

Of note, VVL15-mGMCSF was unable to enhance antitumour immunity or efficacy above that due to VVL15ΔN1L. Its replication in DT6606 tumour cells was comparable to VVL15-mIL12 and it was able to express its cytokine armed transgene in this cell line to even greater levels than its IL12 armed counterpart. mGMCSF was functional as demonstrated by its ability to enhance DC or monocyte activation *in vitro* as well as enhance the splenic pool of DCs *in vivo*.

Cytotoxicity assays however, revealed that VVL15-mGMCSF was significantly worse than VVL15-mIL12 at killing murine tumour cell lines *in vitro* and this may have been a contributing factor to its poorer response. A reduction in oncolysis implies a reduced burden of TAAs and danger signals. Additionally, DT6606 cells constitutively secrete low levels of mGMCSF and in the corresponding *in vivo* tumour model this cytokine may play a role in promoting tumour growth (380, 381). This is of translational

significance given the fact that some of the most clinically advanced viral therapeutics (i.e. T-Vec (287), JX-594 (92)) carry the human version of this transgene.

VVL15-mIL12 retained its parent platform's capacity to reduce metastatic dissemination from primary flank LLC tumours. However, unlike VVL15ΔN1L or VVL15-mGMCSF, it was also able to slow the growth of the primary tumour. Furthermore, its use in a neoadjuvant setting appeared to prolong the long term survival of mice following surgical resection of the primary. Seven out of eight mice were alive at 90 days post-operatively. Although not explicitly tested, the latter result could have either been due to a vastly enhanced NK response and/or the generation of longer term antitumour T cell mediated immune surveillance. These fundamentally different mechanisms of action will be imminently investigated by our group; in the first instance through biological time-point and immune cell subset depletion experiments analogous to those already performed in this project.

A note of caution must be made with regards the systemic administration of VVL15ΔN1L based recombinant viruses. Although substantial efficacy was seen following IT delivered VVL15ΔN1L, particularly against the DT6606 pancreatic tumour model, IV delivered virus however was not able to slow tumour growth (data not shown). The IV dosage however in the latter experiment was limited to only three alternate-daily doses. We found that daily administration of $1x10^8$ PFUs of virus was too toxic for the mice (especially with the cytokine transgene armed recombinants) and more practically, mouse tail veins were completely thrombosed after the third IV dose.

The current project and previous work by our group revealed that a substantial quantity of VV virion is sequestered upon "first-pass" in the reticuloendothelial system following IV administration. Splenic macrophages in particular appeared to be a significant barrier for delivery to peripherally located tumours (Ferguson et al. unpublished data). Interestingly, temporary inhibition of macrophage function (through selective PI3Kinase inhibition) enhanced tumour uptake of IV administered VVL15 and slowed tumour growth (Ferguson et. al. unpublished data). Intravenous VVL15ΔN1L based viruses will be incorporated into a similar protocol in the near future.

Although systemic administration has yet to be optimised, VVL15-mIL12 when administered via the IT route was the most promising of all the VVL platforms tested in this project. Before conducting human trials with its human cytokine armed counterpart, further animal studies will be required. Indeed, using data from this project, our group has recently secured a Developmental Pathway Funding Scheme grant from the Medical Research Council, to further evaluate and optimise vaccination strategies using these and other recombinant viruses in a neoadjuvant surgical setting. We plan to use a syngeneic subcutaneous mouse model of a spontaneously metastasising head and neck cancer (SCCVII) as a prelude to treating a histologically similar orthotopic model in Syrian hamsters. The HCPC-1 cell line is a Syrian hamster cheek pouch derived epidermoid carcinoma that can metastasise to lungs following its orthotopic implantation (382, 383). These oral tumours are morphologically closer to their human counterparts than the equivalent mouse or rat alternatives (383). Hamster immunity is also functionally closer to humans than rodent species and importantly is able to respond to some human cytokines like GMCSF (384, 385). Indeed we have recently demonstrated that human IL12 is capable of inducing antitumour immunity in a syngeneic Syrian hamster pancreatic cancer model but not in a murine counterpart (Wang et al., unpublished data).

It is hoped that the above will lead to an investigational new drug (IND) application followed by early phase clinical trials, which in the first instance, due to our group's strong collaboration with local and regional head and neck cancer units, will likely involve this patient population.

4.2 Future strategies to realise the anticancer potential of oncolytic viruses

Waning optimism for OVT has recently been re-ignited by novel strategies to realise their potential to cross stimulate an antitumour effector immune response.

Two notable GMCSF cytokine transgene armed viruses are amongst the most advanced in stages of clinical testing.

T-Vec is a $\gamma_1$34.5 gene deficient HSV (386). Monotherapeutic treatment of advanced malignant melanoma led to complete remission of primary and distant metastatic nodules in eight of 50 patients (287). This led to a phase three trial of advanced malignant melanoma patients, which demonstrated a six-month response rate of 16% (compared to 2% for patients treated with GMCSF alone) (387). A phase one/two trial with ipilimumab (an anti-CTLA4 inhibitory antibody) in patients with malignant melanoma was underway at the time of writing (146). In head and neck cancer, an uncontrolled phase two trial of T-Vec in combination with chemo-radiotherapy led to a 93% complete pathological response (388).

The vaccinia viral platform has also shown promise as an anticancer therapeutic in clinical trials (6). JX-594, a Wyeth strain recombinant, armed with a human GMCSF transgene, is the most advanced of these (92). It has recently demonstrated a dose dependent survival advantage following IT injection into hepatocellular carcinomas (HCC) in a randomised phase two, dose finding trial (median survival 14.1 months in the high dose, versus 6.7 months in the low dose group) (389). Additionally, it also demonstrated tumour-targeted replication following IV administration (282). This occurred in some cases despite the pre-existence of neutralizing antibodies. In these trials efficacious responses were only consequent to very high doses of viruses and long term survival data have yet to be accrued.

Wild type reovirus (serotype 3-Dearing, Reolysin® Oncolytics Biotech), a dsRNA virus is another promising platform that features prominently in the literature. Its selectivity is based on defects in the RAS pathway in tumour cells. Its segmental dsRNA genome

does not lend itself to genetic manipulation, although it is systemically active and can promote protective antitumour immunity (194). An important phase three trial involving IV Reolysin® in combination with paclitaxel and carboplatin for patients with platinum refractory head and neck cancers has just been completed according to the Oncolytics Biotech website (http://www.oncolyticsbiotech.com/clinical-trials/default.aspx). The data has yet to be publically released.

GL-ONC1 (GLV-1h68) is the first recombinant Lister strain virus to enter clinical trials. At the time of writing recruitment was ongoing for four dose escalating phase one trials. Two were designed to examine the effect of IV administered virus in patients with either advanced disseminated solid tumours of various types (http://www.clinicaltrials.gov; trial identifier: NCT00794131) or in combination with cisplatin and radiotherapy of head and neck cancer (http://www.clinicaltrials.gov; trial identifier: NCT01584284). Early reports from both trials indicated that IV virus was well tolerated, with some evidence of viral delivery to tumour (390, 391). The other two were aimed at treating patients with malignant pleural or peritoneal carcinomatosis via intrapleural (http://www.clinicaltrials.gov; trial identifier: NCT01766739) and intraperitoneal (http://www.clinicaltrials.gov; trial identifier: NCT01443260) routes respectively.

Although some clinical trials with OVT have produced exciting results, many have ultimately disappointed and indeed none of the viral platforms have yet to achieve United States Food and Drug Administration (FDA) approval. OVs as monotherapy are unlikely to cure advanced tumours, but may find a role in the potentiation of existing therapeutic agents or be one component of novel immunotherapeutic strategies; some of which are discussed below.

4.2.1 Combination with chemotherapeutic agents

In many clinical trials, OVTs have been introduced in conjunction with the current standard of care in advanced cancers: usually chemotherapeutic agents. We introduced a discussion of the use of VVL derivatives in conjunction with chemotherapeutic agents

in section 1.4.2. This section elaborates that discussion in an attempt to stimulate further avenues of investigation to improve the therapeutic potential of our novel recombinant viruses.

Chemotherapeutic agents inhibit mitosis, damage DNA, and ultimately cause cell death via a multitude of mechanisms. Given they may directly damage the viral genome or prematurely eliminate the host cell; combination with OVs should theoretically not be synergistic. However, the efficacy of such combinations may not solely be due to the potentiation of cellular cytotoxicity (99, 392). In some situations chemotherapeutics may remove barriers to successful viral infection, weaken immunosuppressive forces or even enhance antitumour immune priming.

Chemotherapeutics may inadvertently supress antiviral immunity and therefore enhance viral spread. For example, histone deacetylase inhibitors (HDACIs), as well as enhancing histone acetylation and thus chromatin modulation, often cause the acetylation and inhibition of proteins involved in key antiviral pathways, for example the type 1 IFN response (393). In one study their concurrent use with HSV reduced the infiltration and activation of NK cells (394). Cyclophosphamide, a DNA alkylating agent induces apoptotic cell death. At high doses, for example it was shown to limit host antiviral immunity (especially neutralising antiviral antibodies) and enhanced the persistence, dissemination and therapeutic benefit of a recombinant VV (395).

Chemotherapeutic agents may also enhance the ability of OVs to reverse immune tolerance to TAAs. One mechanism might operate through the selective inhibition of immune suppressive cells within the TME. Thus cyclophosphamide, paclitaxel and temozolomide can successfully reduce T-regs when delivered in repeated low doses (396-398), which in the case of cyclophosphamide mitigates the toxic effects of global immunosuppression following high solitary doses. Low repeated dosing of cyclophosphamide has also been shown to restore T and NK cell effector function in advanced cancer patients (399). In the context of OVT, preconditioning of mice with either cyclophosphamide or anti-CD25 monoclonal antibodies to deplete T-regs, enhanced the efficacy of reovirus, VSV and adenovirus therapy (400-402).

In healthy tissue, MDSCs protect the host by dampening the inflammatory response to pathogens; but in the TME they are tumour promoting and may supress induced antitumour effector T cells (403). Furthermore, they may promote the expansion of T-regs and M2 macrophages (404, 405). MDSCs can be depleted by treatment with chemotherapeutic agents such as gemcitabine, sunitinib, 5-FU and docetaxel (392) which if administered concurrently with OVT appears to enhance the survival of preclinical animal models (406).

Some chemotherapy drugs may have multiple non-canonical effects within the transformed cell that may benefit concurrent OVT e.g. paclitaxel treatment causes the up regulation of class I MHC and indeed other components of the antigen presentation pathway (407) and may reduce the threshold for immune activation. Interestingly, others such as doxorubicin may decrease the expression of immune checkpoint ligands PD-L1, reducing their inhibition of TILs (408).

Like OVTs, certain chemotherapeutics (e.g. anthracyclines and platinum based drugs) may induce a state of "pre mortem" cellular stress, associated with the surface expression of and release of DAMPs characteristic of immunogenic cell death (see section 1.5.5) (409) and may ultimately lead to the generation of potent tumour specific immunity (410). The combination of such drugs with OVT may synergistically boost antitumour immunogenicity (411).

Although appealing, combination therapy with OVTs may not be beneficial in all circumstances. For example, low dose CPA may clear T-regs, but this may promote antiviral immunity leading to viral clearance. Conversely, high dose cyclophosphamide mediated immunosuppression may prolong viral survival and thus oncolysis, but may impair the development of antitumour immunity (125, 166).

Although potentially exciting a great deal of translational research needs to be performed in order to determine the optimal combination(s) of chemo-OVT and in particular chemo-VVL recombinant viral therapy. This is certainly one line of investigation that our group intends to perform in the near future.

4.2.2 Other immunomodulatory strategies

As previously discussed, a potential problem with using a single viral platform in both prime and boost phases of a tumour vaccination regime, even with a loaded autoantigen (that would be expressed at high levels within the TME), is that the secondary antitumour immune response may be swamped by an even greater magnitude antiviral response (44). The use of different viral vectors in priming and booster phases of therapy has been previously discussed in the context of generating an immune response to a single tumour antigen and remains a very promising strategy. Our group has recently demonstrated the complete eradication of a syngeneic subcutaneous pancreatic tumour model in a hamster host using a heterologous prime-boost regime with a recombinant adenovirus followed by VVL15 (412). Antitumour immune memory was generated as evidenced by no tumour regrowth following subsequent tumour cell re-challenge, whilst immune cell subset depletion experiments confirmed the critical role of T cells. Unlike other similar studies, these viruses were not armed with a tumour antigen-encoding transgene and therefore illustrated for the first time that a heterologous prime-boost regime tailored to whole tumour cells (as opposed to a single tumour antigen) was indeed possible in the face of two antigenically different but strongly immunogenic OVs, administered in a favourable sequence. Although similar results were obtained by our group in other syngeneic murine and hamster tumour models, complete abrogation of tumour was not universal. The therapeutic regime being developed in the current project might ideally fit into the "vaccinia" slot of this heterologous prime boost strategy.

The relative clinical success of immune checkpoint inhibition, confirmed the curative potential of tumour immunotherapy. Thus a CTLA4 blocking antibody ipilimumab demonstrated promise in a phase three trial in patients with advanced malignant melanoma (413) and was the first in class to obtain FDA approval. A small proportion of patients were completely cured. CTLA4 on the surface of T cells acts as an "off switch" upon binding the costimulatory molecules CD80 or CD86 found on APCs. CTLA4 is abundantly expressed on T-regs, but interestingly in this pool of cells anti CTLA4 antibodies can lead to their depletion (414, 415).

Immune checkpoint inhibition lends itself to augment the antitumour immunogenic potential of OVT and indeed vice versa. This was tested recently with Newcastle Disease Virus (NDV) in a preclinical model of malignant melanoma. NDV injection into B16 tumours channelled the infiltration of CD4+ and CD8+ lymphocytes into both injected and uninjected tumours and thereby loosely focussed the systemically administered CTLA4 antibodies to the TME (416). T-Vec is currently being used in conjunction with ipilimumab in a randomised phase two clinical trial (http://www.clinicaltrials.gov; trial identifier: NCT01740297).

An immune checkpoint that has hitherto received little investigation in the context of virotherapy is PD-1(on T cells)/ PD-L1. This could be directly inhibited by PD1 antibodies or indirectly via the sequestration of PD-L1 by soluble PD1 receptor molecules. Genes coding for the inhibitory antibody (against CTLA4 or PD1) or the decoy PD1 receptor, could be transcribed into an OV and hence the disinhibition of antigen triggered T cells would be localised to the TME following administration of the virus. Our group is currently investigating this strategy with VVL recombinant viruses.

Regardless of whether we ultimately chose to translate our work with single viral or heterologous viral platforms, or indeed in combination with other immunochemotherapeutics, OVT may find most success if it is used early on in the disease process, perhaps in a neoadjuvant setting; in patients whose immune systems have not been compromised by advanced cancer or treatment. The therapeutic could be administered with little hindrance to existing patient treatment protocols. Recombinant VVL15ΔN1L mediated oncolysis could commence the priming of antitumour immunity to establish long term surveillance, as well as to combat MRD following eradication of the primary tumour by other modalities. A significant cause of cancer mortality is due to recurrence of tumour following apparent eradication, often many years later. It is this group of patients that may be the ultimate beneficiaries of our and other groups work with OVT.

4.3 Conclusion

The results from experiments conducted in this project provide optimism for the potential use of VVL15ΔN1L as a platform upon which to build a novel set of immunogenic oncolytic VVL recombinants; a set of viruses that could potentially focus both innate and adaptive arms of a developing host antitumour immune response into the TME. The IL12 armed VVL15ΔN1L recombinant holds particular promise as a treatment modality against pancreatic and other solid cancers. Excitingly VVL15-IL12 has also demonstrated dramatic efficacy as a neoadjuvant to oncologic surgery, where its properties may minimise post-operative tumour metastasis and prevent long term recurrence; from which many patients with solid cancers ultimately succumb.

Appendix

Sequences of pUC19 based VV super-shuttle vectors

1. The sequenced insert cassette between L024 and L026 genes in pUC19- LA-H5-H5-RFP-H5- RA

Key:

L024-Overlap-L025(remnant)-H5-H5-RFP-H5-L025(remnant)-L026

See section 3.1 for further details and abbreviations

AATGTTTCTTTGGTTATACTAGTATAGTCACTATCGGACAAATAAAGAAAAT
CAGATGATCGATGAATAATACATTTAAATTCATCATCTGTAAGATTTTTGAG
ATGTCTCATTAGAATATTATTAGGGTTAGTACTCATTATCATTCGGCAGCTA
TTACTTATTTTATTATTTTTCACCATATAGATCAATCATTAGATCAAAAATTG
AAAATAAATACAAAGGTTCTTGAGGGTTGTGTTAAATTGAAAGCGAGAAAT
AATCATAAATAGTCGACAATCGAATTCCCGCGGCCGGGAATTCGATTAGAT
CTAAAAATTGAAAATAAATACAAAGGTTCTTGAGGGTTGTGTTAAATTGAA
AGCGAGAAATAATCATAAATAGCTACCGGACTCAGATCCACCGGTCGCCAC
CATGGCCTCCTCCGAGGACGTCATCAAGGAGTTCATGCGCTTCAAGGTGCG
CATGGAGGGCTCCGTGAACGGCCACGAGTTCGAGATCGAGGGCGAGGGCG
AGGGCCGCCCCTACGAGGGCACCCAGACCGCCAAGCTGAAGGTGACCAAG
GGCGGCCCCCTGCCCTTCGCCTGGGACATCCTGTCCCCCCAGTTCCAGTACG
GCTCCAAGGTGTACGTGAAGCACCCCGCCGACATCCCCGACTACAAGAAGC
TGTCCTTCCCCGAGGGCTTCAAGTGGGAGCGCGTGATGAACTTCGAGGACG
GCGGCGTGGTGACCGTGACCCAGGACTCCTCCCTGCAGGACGGCTCCTTCAT
CTACAAGGTGAAGTTCATCGGCGTGAACTTCCCCTCCGACGGCCCCGTAATG
CAGAAGAAGACTATGGGCTGGGAGGCCTCCACCGAGCGCCTGTACCCCCGC
GACGGCGTGCTGAAGGGCGAGATCCACAAGGCCCTGAAGCTGAAGGACGG
CGGCCACTACCTGGTGGAGTTCAAGTCCATCTACATGGCCAAGAAGCCCGT
GCAGCTGCCCGGCTACTACTACGTGGACTCCAAGCTGGACATCACCTCCCAC
AACGAGGACTACACTATCGTGGAGCAGTACGAGCGCGCCGAGGGCCGCCAC
CACCTGTTCCTGTAGCGGCCGCGACTCTAGATCATAATCAGCCATACCACAT
TTGTAGAGGTTTTACTTGCTTTAAAAAACCTCCCACACCTCCCCCTGAACCT
GAAACATAAAATGAATGCAATTGTTGTTGTTAACTTGTTTATTGCAGCTTAT
AATGGTTACAAATAAAGCAATAGCATCACAAATTTCACAAATAAAGCATTT
TTTTCACTGCATTCTAGTTGTGGTTTGTCCAAACTCATCAATGTATCTTAAGG
CGAAAAATTGAAAATAAATACAAAGGTTCTTGAGGGTTGTGTTAAATTGAA
AGCGAGAAATAATCATAAATAAAGCTTCCCGGGACGCGTATCTAATAAGTA
GAGTCCTCATGCTTAGTTAACAACTATTTTTTATGTTAAATCAATTAGTACA

CCGCTATGTTTAATACTTATTCATATTTTAGTTTTTAGGATTGAGAATCAATA
CAAAAA TTAATGCATCATTAATTTTAGAAATACTTAGTTTCCACGTAGTCA
ATGAAACATTTGAACTCATCGTACAGGACGTTCTCGTACAGGACGTAACTAT
AAACCGGTTTATATTTGTTCAAGATAGATACAAATCCGATAACTTTTTTTAC
GAATTCTACG

2. The sequenced insert cassette between L024 and L026 genes in pUC19- LA-H5- mGMCSF -H5- RFP –H5 RA

Key:

L024-Overlap-L025(remnant)-H5-mGMCSF -H5-RFP-H5-L025(remnant)-L026

See section 3.1 for further details and abbreviations

TTTGGTTATACTAGTATAGTCACTATCGGACAAATAAAGAAAATCAGATGA
TCGATGAATAATACATTTAAATTCATCATCTGTAAGATTTTTGAGATGTCTC
ATTAGAATATTATTAGGGTTAGTACTCATTATCATTCGGCAGCTATTACTTA
TTTTATTATTTTTCACCATATAGATCAATCATTAGATCAAAAATTGAAAATA
AATACAAAGGTTCTTGAGGGTTGTGTTAAATTGAAAGCGAGAAATAATCAT
AAATAGTCGACAGGGGCTCGCATCTCTCCTTCACGCGCCCGCCGCCCTACCT
GAGGCCGCCATCCACGCCGGTTGAGTCGCGTTCTGCCGCCTCCCGCCTGTGG
TGCCTCCTGAACTGCGTCCGCCGTCTAGGTAAGTTTAAAGCTCAGGTCGAGA
CCGGGCCTTTGTCCGGCGCTCCCTTGGAGCCTACCTAGACTCAGCCGGCTCT
CCACGCTTTGCCTGACCCTGCTTGCTCAACTCTACGTCTTTGTTTCGTTTTCT
GTTCTGCGCCGTTACAGATCCAAGCTGTGACCGGCGCCTACCTGAGATCACC
GGTAGAGGGCCAACATGTGGCTGCAGAATTTACTTTTCCTGGGCATTGTGGT
CTACAGCCTCTCAGCACCCACCCGCTCACCCATCACTGTCACCCGGCCTTGG
AAGCATGTAGAGGCCATCAAAGAAGCCCTGAACCTCCTGGATGACATGCCT
GTCACGTTGAATGAAGAGGTAGAAGTCGTCTCTAACGAGTTCTCCTTCAAG
AAGCTAACATGTGTGCAGACCCGCCTGAAGATATTCGAGCAGGGTCTACGG
GGCAATTTCACCAAACTCAAGGGCGCCTTGAACATGACAGCCAGCTACTAC
CAGACATACTGCCCCCCAACTCCGGAAACGGACTGTGAAACACAAGTTACC
ACCTATGCGGATTTCATAGACAGCCTTAAAACCTTTCTGACTGATATCCCCT
TTGAATGCAAAAAACCAGGCCAAAAATGAGGAAGCCCAGCTAGCTCGACAT
GATAAGATACATTGATGAGTTTGGACAAACCACAACTAGAATGCAGTGAAA
AAAATGCTTTATTTGTGAAATTTGTGATGCTATTGCTTTATTTGTGAAATTTG
TGATGCTATTGCTTTATTTGTAACCATTATAAGCTGCAATAAACAAGTTAAC
AACAACAATTGCATTCATTTTATGTTTCAGGTTCAGGGGGAGGTGTGGGAG
GTTTTTTAAAGCAAGTAAAACCTCTACAAATGTGGTAGATCCATTTAAATGT
TAATTAGATCTAAAAATTGAAAATAAATACAAAGGTTCTTGAGGGTTGTGTT
AAATTGAAAGCGAGAAATAATCATAAATAGCTACCGGACTCAGATCCACCG
GTCGCCACCATGGCCTCCTCCGAGGACGTCATCAAGGAGTTCATGCGCTTCA
AGGTGCGCATGGAGGGCTCCGTGAACGGCCACGAGTTCGAGATCGAGGGCG

AGGGCGAGGGCCGCCCCTACGAGGGCACCCAGACCGCCAAGCTGAAGGTG
ACCAAGGGCGGCCCCCTGCCCTTCGCCTGGGACATCCTGTCCCCCCAGTTCC
AGTACGGCTCCAAGGTGTACGTGAAGCACCCCGCCGACATCCCCGACTACA
AGAAGCTGTCCTTCCCCGAGGGCTTCAAGTGGGAGCGCGTGATGAACTTCG
AGGACGGCGGCGTGGTGACCGTGACCCAGGACTCCTCCCTGCAGGACGGCT
CCTTCATCTACAAGGTGAAGTTCATCGGCGTGAACTTCCCCTCCGACGGCCC
CGTAATGCAGAAGAAGACTATGGGCTGGGAGGCCTCCACCGAGCGCCTGTA
CCCCCGCGACGGCGTGCTGAAGGGCGAGATCCACAAGGCCCTGAAGCTGAA
GGACGGCGGCCACTACCTGGTGGAGTTCAAGTCCATCTACATGGCCAAGAA
GCCCGTGCAGCTGCCCGGCTACTACTACGTGGACTCCAAGCTGGACATCAC
CTCCCACAACGAGGACTACACTATCGTGGAGCAGTACGAGCGCGCCGAGGG
CCGCCACCACCTGTTCCTGTAGCGGCCGCGACTCTAGATCATAATCAGCCAT
ACCACATTTGTAGAGGTTTTACTTGCTTTAAAAAACCTCCCACACCTCCCCC
TGAACCTGAAACATAAAATGAATGCAATTGTTGTTGTTAACTTGTTTATTGC
AGCTTATAATGGTTACAAATAAAGCAATAGCATCACAAATTTCACAAATAA
AGCATTTTTTTCACTGCATTCTAGTTGTGGTTTGTCCAAACTCATCAATGTAT
CTTAAGGCGAAAAATTGAAAATAAATACAAAGGTTCTTGAGGGTTGTGTTA
AATTGAAAGCGAGAAATAATCATAAATAAAGCTTCCCGGGACGCGTATCTA
ATAAGTAGAGTCCTCATGCTTAGTTAACAACTATTTTTTATGTTAAATCAAT
TAGTACACCGCTATGTTTAATACTTATTCATATTTTAGTTTTTAGGATTGAGA
ATCAATACAAAAA_TTAATGCATCATTAATTTTAGAAATACTTAGTTTCCAC
GTAGTCAATGAAACATTTGAACTCATCGTACAGGACGTTCTCGTACAGGAC
GTAACTATAAACCGGTTTATATTTGTTCAAGATAGATACAAATCCGATAACT
TTTTTTACGAATTCTACG

3. The sequenced insert cassette between L024 and L026 genes in pUC19-LA-H5-H5-RFP-H5-mIL12-RA

Key:

L024-Overlap-L025(remnant)-H5-H5-RFP-H5-mIL12-L025(remnant)-L026

See section 3.1 for further details and abbreviations

TTTGGTTATACTAGTATAGTCACTATCGGACAAATAAAGAAAATCAGATGA
TCGATGAATAATACATTTAAATTCATCATCTGTAAGATTTTTGAGATGTCTC
ATTAGAATATTATTAGGGTTAGTACTCATTATCATTCGGCAGCTATTACTTA
TTTTATTATTTTTCACCATATAGATCAATCATTAGATCAAAAATTGAAAATA
AATACAAAGGTTCTTGAGGGTTGTGTTAAATTGAAAGCGAGAAATAATCAT
AAATAGTCGACAATCGAATTCGATTAGATCTAAAAATTGAAAATAAATACA
AAGGTTCTTGAGGGTTGTGTTAAATTGAAAGCGAGAAATAATCATAAATAG
CTACCGGACTCAGATCCACCGGTCGCCACCATGGCCTCCTCCGAGGACGTC
ATCAAGGAGTTCATGCGCTTCAAGGTGCGCATGGAGGGCTCCGTGAACGGC

CACGAGTTCGAGATCGAGGGCGAGGGCGAGGGCCGCCCCTACGAGGGCAC
CCAGACCGCCAAGCTGAAGGTGACCAAGGGCGGCCCCCTGCCCTTCGCCTG
GGACATCCTGTCCCCCCAGTTCCAGTACGGCTCCAAGGTGTACGTGAAGCA
CCCCGCCGACATCCCCGACTACAAGAAGCTGTCCTTCCCCGAGGGCTTCAA
GTGGGAGCGCGTGATGAACTTCGAGGACGGCGGCGTGGTGACCGTGACCCA
GGACTCCTCCCTGCAGGACGGCTCCTTCATCTACAAGGTGAAGTTCATCGGC
GTGAACTTCCCCTCCGACGGCCCCGTAATGCAGAAGAAGACTATGGGCTGG
GAGGCCTCCACCGAGCGCCTGTACCCCCGCGACGGCGTGCTGAAGGGCGAG
ATCCACAAGGCCCTGAAGCTGAAGGACGGCGGCCACTACCTGGTGGAGTTC
AAGTCCATCTACATGGCCAAGAAGCCCGTGCAGCTGCCCGGCTACTACTAC
GTGGACTCCAAGCTGGACATCACCTCCCACAACGAGGACTACACTATCGTG
GAGCAGTACGAGCGCGCCGAGGGCCGCCACCACCTGTTCCTGTAGCGGCCG
CGACTCTAGATCATAATCAGCCATACCACATTTGTAGAGGTTTTACTTGCTT
TAAAAAACCTCCCACACCTCCCCCTGAACCTGAAACATAAAATGAATGCAA
TTGTTGTTGTTAACTTGTTTATTGCAGCTTATAATGGTTACAAATAAAGCAA
TAGCATCACAAATTTCACAAATAAAGCATTTTTTTCACTGCATTCTAGTTGT
GGTTTGTCCAAACTCATCAATGTATCTTAAGGCGAAAAATTGAAAATAAAT
ACAAAGGTTCTTGAGGGTTGTGTTAAATTGAAAGCGAGAAATAATCATAAA
TAAAGCTTCGAGGGGCTCGCATCTCTCCTTCACGCGCCCGCCGCCCTACCTG
AGGCCGCCATCCACGCCGGTTGAGTCGCGTTCTGCCGCCTCCCGCCTGTGGT
GCCTCCTGAACTGCGTCCGCCGTCTAGGTAAGTTTAAAGCTCAGGTCGAGAC
CGGGCCTTTGTCCGGCGCTCCCTTGGAGCCTACCTAGACTCAGCCGGCTCTC
CACGCTTTGCCTGACCCTGCTTGCTCAACTCTACGTCTTTGTTTCGTTTTCTG
TTCTGCGCCGTTACAGATCCAAGCTGTGACCGGCGCCTACGTAAGTGATATC
TACTAGATTTATCAAAAAGAGTGTTGACTTGTGAGCGCTCACAATTGATACT
TAGATTCATCGAGAGGGACACGTCGACTACTAACCTTCTTCTCTTTCCTACA
GCTGAGATCACCGGCGAAGGAGGGCCACCATGGGTCAATCACGCTACCTCC
TCTTTTTGGCCACCCTTGCCCTCCTAAACCACCTCAGTTTGGCCAGGGTCATT
CCAGTCTCTGGACCTGCCAGGTGTCTTAGCCAGTCCCGAAACCTGCTGAAGA
CCACAGATGACATGGTGAAGACGGCCAGAGAAAAGCTGAAACATTATTCCT
GCACTGCTGAAGACATCGATCATGAAGACATCACACGGGACCAAACCAGCA
CATTGAAGACCTGTTTACCACTGGAACTACACAAGAACGAGAGTTGCCTGG
CTACTAGAGAGACTTCTTCCACAACAAGAGGGAGCTGCCTGCCCCCACAGA
AGACGTCTTTGATGATGACCCTGTGCCTTGGTAGCATCTATGAGGACTTGAA
GATGTACCAGACAGAGTTCCAGGCCATCAACGCAGCACTTCAGAATCACAA
CCATCAGCAGATCATTCTAGACAAGGGCATGCTGGTGGCCATCGATGAGCT
GATGCAGTCTCTGAATCATAATGGCGAGACTCTGCGCCAGAAACCTCCTGT
GGGAGAAGCAGACCCTTACAGAGTGAAAATGAAGCTCTGCATCCTGCTTCA
CGCCTTCAGCACCCGCGTCGTGACCATCAACAGGGTGATGGGCTATCTGAG
CTCCGCCGTTCCTGGAGTAGGGGTACCTGGAGTGGGCGGATCTATGTGGGA
GCTGGAGAAAGACGTTTATGTTGTAGAGGTGGACTGGACTCCCGATGCCCC
TGGAGAAACAGTGAACCTCACCTGTGACACGCCTGAAGAAGATGACATCAC
CTGGACCTCAGACCAGAGACATGGAGTCATAGGCTCTGGAAAGACCCTGAC
CATCACTGTCAAAGAGTTTCTAGATGCTGGCCAGTACACCTGCCACAAAGG
AGGCGAGACTCTGAGCCACTCACATCTGCTGCTCCACAAGAAGGAAAATGG
AATTTGGTCCACTGAAATTTTAAAAAATTTCAAAAACAAGACTTTCCTGAAG
TGTGAAGCACCAAATTACTCCGGACGGTTCACGTGCTCATGGCTGGTGCAA
AGAAACATGGACTTGAAGTTCAACATCAAGAGCAGTAGCAGTCCCCCCGAC

TCTCGGGCAGTGACATGTGGAATGGCGTCTCTGTCTGCAGAGAAGGTCACA
CTGGACCAAAGGGACTATGAGAAGTATTCAGTGTCCTGCCAGGAGGATGTC
ACCTGCCCAACTGCCGAGGAGACCCTGCCCATTGAACTGGCGTTGGAAGCA
CGGCAGCAGAATAAATATGAGAACTACAGCACCAGCTTCTTCATCAGGGAC
ATCATCAAACCAGACCCGCCCAAGAACTTGCAGATGAAGCCTTTGAAGAAC
TCACAGGTGGAGGTCAGCTGGGAGTACCCTGACTCCTGGAGCACTCCCCAT
TCCTACTTCTCCCTCAAGTTCTTTGTTCGAATCCAGCGCAAGAAAGAAAAGA
TGAAGGAGACAGAGGAGGGGTGTAACCAGAAAGGTGCGTTCCTCGTAGAG
AAGACATCTACCGAAGTCCAATGCAAAGGCGGGAATGTCTGCGTGCAAGCT
CAGGATCGCTATTACAATTCCTCATGCAGCAAGTGGGCATGTGTTCCCTGCA
GGGTCCGATCCTAGGATGCAACGGATGCTAGCTCGACATGATAAGATACAT
TGATGAGTTTGGACAAACCACAACTAGAATGCAGTGAAAAAAATGCTTTAT
TTGTGAAATTTGTGATGCTATTGCTTTATTTGTGAAATTTGTGATGCTATTGC
TTTATTTGTAACCATTATAAGCTGCAATAAACAAGTTAACAACAACAATTGC
ATTCATTTTATGTTTCAGGTTCAGGGGGAGGTGTGGGAGGTTTTTTAAAGCA
AGTAAAACCTCTACAAATGTGGTAGATCATTTGGGACGCGTATCTAATAAG
TAGAGTCCTCATGCTTAGTTAACAACTATTTTTTATGTTAAATCAATTAGTAC
ACCGCTATGTTTAATACTTATTCATATTTTAGTTTTTAGGATTGAGAATCAAT
ACAAAAA TTAATGCATCATTAATTTTAGAAATACTTAGTTTCCACGTAGTC
AATGAAACATTTGAACTCATCGTACAGGACGTTCTCGTACAGGACGTAACT
ATAAACCGGTTTATATTTGTTCAAGATAGATACAAATCCGATAACTTTTTTT
ACGAATTCTACG

4. The sequenced insert cassette between L024 and L026 genes in pUC19- LA-H5-H5-RFP-H5-hGMCSF- RA

Key:

L024-Overlap-L025(remnant)-H5-H5-RFP-H5-hGMCSF-L025(remnant)-L026

See section 3.1 for further details and abbreviations

TTTGGTTATACTAGTATAGTCACTATCGGACAAATAAAGAAAATCAGATGA
TCGATGAATAATACATTTAAATTCATCATCTGTAAGATTTTTGAGATGTCTC
ATTAGAATATTATTAGGGTTAGTACTCATTATCATTCGGCAGCTATTACTTA
TTTTATTATTTTTCACCATATAGATCAATCATTAGATCAAAAATTGAAAATA
AATACAAAGGTTCTTGAGGGTTGTGTTAAATTGAAAGCGAGAAATAATCAT
AAATAGTCGACAATCGAATTCCCGCGGCCGGGAATTCGATTAGATCTAAAA
ATTGAAAATAAATACAAAGGTTCTTGAGGGTTGTGTTAAATTGAAAGCGAG
AAATAATCATAAATAGCTACCGGACTCAGATCCACCGGTCGCCACCATGGC
CTCCTCCGAGGACGTCATCAAGGAGTTCATGCGCTTCAAGGTGCGCATGGA
GGGCTCCGTGAACGGCCACGAGTTCGAGATCGAGGGCGAGGGCGAGGGCC
GCCCCTACGAGGGCACCCAGACCGCCAAGCTGAAGGTGACCAAGGGCGGC
CCCCTGCCCTTCGCCTGGGACATCCTGTCCCCCCAGTTCCAGTACGGCTCCA

AGGTGTACGTGAAGCACCCCGCCGACATCCCCGACTACAAGAAGCTGTCCT
TCCCCGAGGGCTTCAAGTGGGAGCGCGTGATGAACTTCGAGGACGGCGGCG
TGGTGACCGTGACCCAGGACTCCTCCCTGCAGGACGGCTCCTTCATCTACAA
GGTGAAGTTCATCGGCGTGAACTTCCCCTCCGACGGCCCCGTAATGCAGAA
GAAGACTATGGGCTGGGAGGCCTCCACCGAGCGCCTGTACCCCCGCGACGG
CGTGCTGAAGGGCGAGATCCACAAGGCCCTGAAGCTGAAGGACGGCGGCC
ACTACCTGGTGGAGTTCAAGTCCATCTACATGGCCAAGAAGCCCGTGCAGC
TGCCCGGCTACTACTACGTGGACTCCAAGCTGGACATCACCTCCCACAACG
AGGACTACACTATCGTGGAGCAGTACGAGCGCGCCGAGGGCCGCCACCACC
TGTTCCTGTAGCGGCCGCGACTCTAGATCATAATCAGCCATACCACATTTGT
AGAGGTTTTACTTGCTTTAAAAAACCTCCCACACCTCCCCCTGAACCTGAAA
CATAAAATGAATGCAATTGTTGTTGTTAACTTGTTTATTGCAGCTTATAATG
GTTACAAATAAAGCAATAGCATCACAAATTTCACAAATAAAGCATTTTTTTC
ACTGCATTCTAGTTGTGGTTTGTCCAAACTCATCAATGTATCTTAAGGCGAA
AAATTGAAAATAAATACAAAGGTTCTTGAGGGTTGTGTTAAATTGAAAGCG
AGAAATAATCATAAATAAAGCTTCGAGGGGCTCGCATCTCTCCTTCACGCG
CCCGCCGCCCTACCTGAGGCCGCCATCCACGCCGGTTGAGTCGCGTTCTGCC
GCCTCCCGCCTGTGGTGCCTCCTGAACTGCGTCCGCCGTCTAGGTAAGTTTA
AAGCTCAGGTCGAGACCGGGCCTTTGTCCGGCGCTCCCTTGGAGCCTACCTA
GACTCAGCCGGCTCTCCACGCTTTGCCTGACCCTGCTTGCTCAACTCTACGT
CTTTGTTTCGTTTTCTGTTCTGCGCCGTTACAGATCCAAGCTGTGACCGGCGC
CTACGTAAGTGATATCTACTAGATTTATCAAAAAGAGTGTTGACTTGTGAGC
GCTCACAATTGATACTTAGATTCATCGAGAGGGACACGTCGACTACTAACCT
TCTTCTCTTTCCTACAGCTGAGATCACCGGCGAAGGAGGGCCACCATGTGGC
TGCAGAGCCTGCTGCTCTTGGGCACTGTGGCCTGCAGCATCTCTGCACCCGC
CCGCTCGCCCAGCCCCAGCACGCAGCCCTGGGAGCATGTGAATGCCATCCA
GGAGGCCCGGCGTCTCCTGAACCTGAGTAGAGACACTGCTGCTG*A*GATGAA
TGAAACAGTAGAAGTCATCTCAGAAATGTTTGACCTCCAGGAGCCGACCTG
CCTACAGACCCGCCTGGAGCTGTACAAGCAGGGCCTGCGGGGCAGCCTCAC
CAAGCTCAAGGGCCCCTTGACCATGATGGCCAGCCACTACAAGCAGCACTG
CCCTCCAACCCCGGAAACTTCCTGTGCAACCCAGACTATCACCTTTGAAAGT
TTCAAAGAGAACCTGAAGGACTTTCTGCTTGTCATCCCCTTTGACTGCTGGG
AGCCAGTCCAGGAGTGAATTCGCTAGCTCGACATGATAAGATACATTGATG
AGTTTGGACAAACCACAACTAGAATGCAGTGAAAAAAATGCTTTATTTGTG
AAATTTGTGATGCTATTGCTTTATTTGTGAAATTTGTGATGCTATTGCTTTAT
TTGTAACCATTATAAGCTGCAATAAACAAGTTAACAACAACAATTGCATTC
ATTTTATGTTTCAGGTTCAGGGGGAGGTGTGGGAGGTTTTTTAAAGCAAGTA
AAACCTCTACAAATGTGGTAGATCATTTGGGACGCGTATCTAATAAGTAGA
GTCCTCATGCTTAGTTAACAACTATTTTTTATGTTAAATCAATTAGTACACCG
CTATGTTTAATACTTATTCATATTTTAGTTTTTAGGATTGAGAATCAATACAA
AAA TTAATGCATCATTAATTTTAGAAATACTTAGTTTCCACGTAGTCAATG
AAACATTTGAACTCATCGTACAGGACGTTCTCGTACAGGACGTAACTATAA
ACCGGTTTATATTTGTTCAAGATAGATACAAATCCGATAACTTTTTTTACGA
ATTCTACG

5. The sequenced insert cassette between L024 and L026 genes in pUC19- LA-H5-H5-RFP-H5-hIL12-RA

Key:

L024-Overlap-L025(remnant)-H5-H5-RFP-H5-hIL12-L025(remnant)-L026

See section 3.1 for further details and abbreviations

TTTGGTTATACTAGTATAGTCACTATCGGACAAATAAAGAAAATCAGATGA
TCGATGAATAATACATTTAAATTCATCATCTGTAAGATTTTTGAGATGTCTC
ATTAGAATATTATTAGGGTTAGTACTCATTATCATTCGGCAGCTATTACTTA
TTTTATTATTTTTCACCATATAGATCAATCATTAGATCAAAAATTGAAAATA
AATACAAAGGTTCTTGAGGGTTGTGTTAAATTGAAAGCGAGAAATAATCAT
AAATAGTCGACAATCGAATTCCCGCGGCCGGGAATTCGATTAGATCTAAAA
ATTGAAAATAAATACAAAGGTTCTTGAGGGTTGTGTTAAATTGAAAGCGAG
AAATAATCATAAATAGCTACCGGACTCAGATCCACCGGTCGCCACCATGGC
CTCCTCCGAGGACGTCATCAAGGAGTTCATGCGCTTCAAGGTGCGCATGGA
GGGCTCCGTGAACGGCCACGAGTTCGAGATCGAGGGCGAGGGCGAGGGCC
GCCCCTACGAGGGCACCCAGACCGCCAAGCTGAAGGTGACCAAGGGCGGC
CCCCTGCCCTTCGCCTGGGACATCCTGTCCCCCCAGTTCCAGTACGGCTCCA
AGGTGTACGTGAAGCACCCCGCCGACATCCCCGACTACAAGAAGCTGTCCT
TCCCCGAGGGCTTCAAGTGGGAGCGCGTGATGAACTTCGAGGACGGCGGCG
TGGTGACCGTGACCCAGGACTCCTCCCTGCAGGACGGCTCCTTCATCTACAA
GGTGAAGTTCATCGGCGTGAACTTCCCCTCCGACGGCCCCGTAATGCAGAA
GAAGACTATGGGCTGGGAGGCCTCCACCGAGCGCCTGTACCCCCGCGACGG
CGTGCTGAAGGGCGAGATCCACAAGGCCCTGAAGCTGAAGGACGGCGGCC
ACTACCTGGTGGAGTTCAAGTCCATCTACATGGCCAAGAAGCCCGTGCAGC
TGCCCGGCTACTACTACGTGGACTCCAAGCTGGACATCACCTCCCACAACG
AGGACTACACTATCGTGGAGCAGTACGAGCGCGCCGAGGGCCGCCACCACC
TGTTCCTGTAGCGGCCGCGACTCTAGATCATAATCAGCCATACCACATTTGT
AGAGGTTTTACTTGCTTTAAAAAACCTCCCACACCTCCCCCTGAACCTGAAA
CATAAAATGAATGCAATTGTTGTTGTTAACTTGTTTATTGCAGCTTATAATG
GTTACAAATAAAGCAATAGCATCACAAATTTCACAAATAAAGCATTTTTTTC
ACTGCATTCTAGTTGTGGTTTGTCCAAACTCATCAATGTATCTTAAGGCGAA
AAATTGAAAATAAATACAAAGGTTCTTGAGGGTTGTGTTAAATTGAAAGCG
AGAAATAATCATAAATAAAGCTTCGAGGGGCTCGCATCTCTCCTTCACGCG
CCCGCCGCCCTACCTGAGGCCGCCATCCACGCCGGTTGAGTCGCGTTCTGCC
GCCTCCCGCCTGTGGTGCCTCCTGAACTGCGTCCGCCGTCTAGGTAAGTTTA
AAGCTCAGGTCGAGACCGGGCCTTTGTCCGGCGCTCCCTTGGAGCCTACCTA
GACTCAGCCGGCTCTCCACGCTTTGCCTGACCCTGCTTGCTCAACTCTACGT
CTTTGTTTCGTTTTCTGTTCTGCGCCGTTACAGATCCAAGCTGTGACCGGCGC
CTACGTAAGTGATATCTACTAGATTTATCAAAAAGAGTGTTGACTTGTGAGC
GCTCACAATTGATACTTAGATTCATCGAGAGGGACACGTCGACTACTAACCT
TCTTCTCTTTCCTACAGCTGAGATCACCGGCGAAGGAGGGCCACCATGGGTC
ACCAGCAGTTGGTCATCTCTTGGTTTTCCCTGGTTTTTCTGGCATCTCCCCTC
GTGGCCATATGGGAACTGAAGAAAGATGTTTATGTCGTAGAATTGGATTGG

TATCCGGATGCCCCTGGAGAAATGGTGGTCCTCACCTGTGACACCCCTGAA
GAAGATGGTATCACCTGGACCTTGGACCAGAGCAGTGAGGTCTTAGGCTCT
GGCAAAACCCTGACCATCCAAGTCAAAGAGTTTGGAGATGCTGGCCAGTAC
ACCTGTCACAAAGGAGGCGAGGTTCTAAGCCATTCGCTCCTGCTGCTTCACA
AAAAGGAAGATGGAATTTGGTCCACTGATATTTTAAAGGACCAGAAAGAAC
CCAAAAATAAGACCTTTCTAAGATGCGAGGCCAAGAATTATTCTGGACGTT
TCACCTGCTGGTGGCTGACGACAATCAGTACTGATTTGACATTCAGTGTCAA
AAGCAGCAGAGGCTCTTCTGACCCCCAAGGGGTGACGTGCGGAGCTGCTAC
ACTCTCTGCAGAGAGAGTCAGAGGGGACAACAAGGAGTATGAGTACTCAGT
GGAGTGCCAGGAGGACAGTGCCTGCCCAGCTGCTGAGGAGAGTCTGCCCAT
TGAGGTCATGGTGGATGCCGTTCACAAGCTCAAGTATGAAAACTACACCAG
CAGCTTCTTCATCAGGGACATCATCAAACCTGACCCACCCAAGAACTTGCA
GCTGAAGCCATTAAAGAATTCTCGGCAGGTGGAGGTCAGCTGGGAGTACCC
TGACACCTGGAGTACTCCACATTCCTACTTCTCCCTGACATTCTGCGTTCAG
GTCCAGGGCAAGAGCAAGAGAGAAAAGAAAGATAGAGTCTTCACGGACAA
GACCTCAGCCACGGTCATCTGCCGCAAAAATGCCAGCATTAGCGTGCGGGC
CCAGGACCGCTACTATAGCTCATCTTGGAGCGAATGGGCATCTGTGCCCTGC
AGTGTTCCTGGAGTAGGGGTACCTGGGGTGGGCGCCAGAAACCTCCCCGTG
GCCACTCCAGACCCAGGAATGTTCCCATGCCTTCACCACTCCCAAAACCTGC
TGAGGGCCGTCAGCAACATGCTCCAGAAGGCCAGACAAACTCTAGAATTTT
ACCCTTGCACTTCTGAAGAGATTGATCATGAAGATATCACAAAAGATAAAA
CCAGCACAGTGGAGGCCTGTTTACCATTGGAATTAACCAAGAATGAGAGTT
GCCTAAATTCCAGAGAGACCTCTTTCATAACTAATGGGAGTTGCCTGGCCTC
CAGAAAGACCTCTTTTATGATGGCCCTGTGCCTTAGTAGTATTTATGAAGAC
TTGAAGATGTACCAGGTGGAGTTCAAGACCATGAATGCAAAGCTGCTGATG
GATCCTAAGAGGCAGATCTTTCTAGATCAAAACATGCTGGCAGTTATTGATG
AGCTGATGCAGGCCCTGAATTTCAACAGTGAGACTGTGCCACAAAAATCCT
CCCTTGAAGAACCGGATTTTTATAAAACTAAAATCAAGCTCTGCATACTTCT
TCATGCTTTCAGAATTCGGGCAGTGACTATTGATAGAGTGATGAGCTATCTG
AATGCTTCCTAAAAAGCGAGGTCCCTCCAAACCGTTGTCATTTTTATAAAAC
TTTGAAATGAGGAAACTTTGATAGGATGTGGATTAAGAACTAGGGAGGGGC
TAGCTCGACATGATAAGATACATTGATGAGTTTGGACAAACCACAACTAGA
ATGCAGTGAAAAAAATGCTTTATTTGTGAAATTTGTGATGCTATTGCTTTAT
TTGTGAAATTTGTGATGCTATTGCTTTATTTGTAACCATTATAAGCTGCAATA
AACAAGTTAACAACAACAATTGCATTCATTTTATGTTTCAGGTTCAGGGGGA
GGTGTGGGAGGTTTTTTAAAGCAAGTAAAACCTCTACAAATGTGGTAGATC
CATTTGGGACGCGTATCTAATAAGTAGAGTCCTCATGCTTAGTTAACAACTA
TTTTTTATGTTAAATCAATTAGTACACCGCTATGTTTAATACTTATTCATATT
TTAGTTTTTAGGATTGAGAATCAATACAAAAA TTAATGCATCATTAATTTT
AGAAATACTTAGTTTCCACGTAGTCAATGAAACATTTGAACTCATCGTACAG
GACGTTCTCGTACAGGACGTAACTATAAACCGGTTTATATTTGTTCAAGATA
GATACAAATCCGATAACTTTTTTTACGAATTCTACG

Acknowledgments

I would like to extend my deepest gratitude to Ghassan Alusi, who introduced me to the Viral Gene Therapy group at the Molecular Oncology Department, BCI and who has been a continual source of support and mentorship throughout this project. The inspiration for this work was provided by Yaohe Wang and Nick Lemoine. I am grateful for their availability, guidance and infectious enthusiasm; and without whom the completion of this work would not have been possible. I am also indebted to Ming Yuan and Louisa Chard, from the Molecular Oncology Department, BCI, who patiently taught me a wide range of technical laboratory and animal experimental skills necessary to perform the experiments outlined in this project. My thanks also to Guglielmo Rosignoli and his team at the Flow Cytometry Department, BCI, for their expert tuition and guidance; to Mark Ferguson for help with setting up and interpreting CT images of murine lungs and to Vipul Bhakta (our laboratory manager) and his team for ensuring the constant and seamless availability of experimental resources. My heartfelt thanks also to Yaohe Wang and his team at the Sino-British Research Centre for Molecular Oncology (Zhengzhou University, China), who completed vital animal experiments.

Finally I would like to acknowledge my beloved wife, Sadia for her eternal support, encouragement and understanding and my baby son, Isaq who ensures I always have a smile on my face.

This project was financially supported by The Royal College of Surgeons of England, Barts and London Charity and The Wellcome Trust.

References

1. Ahmed J, Yuan M, Alusi G, Lemoine NR, Wang Y. The Lister Strain of Vaccinia Virus as an Anticancer Therapeutic Agent. In: Lattime EC, Gerson SL, editors. Gene Therapy of Cancer. San Diego: Academic Press; 2013.
2. Fenner F. A successful eradication campaign. Global eradication of smallpox. Rev Infect Dis. 1982;4(5):916-30.
3. Henderson DA. Edward Jenner's vaccine. Public Health Rep. 1997;112(2):116-21.
4. Baxby D. Edward Jenner's Inquiry; a bicentenary analysis. Vaccine. 1999;17(4):301-7.
5. Amara RR, Villinger F, Altman JD, Lydy SL, O'Neil SP, Staprans SI, et al. Control of a mucosal challenge and prevention of AIDS by a multiprotein DNA/MVA vaccine. Science. 2001;292(5514):69-74.
6. Guse K, Cerullo V, Hemminki A. Oncolytic vaccinia virus for the treatment of cancer. Expert Opin Biol Ther. 2011;11(5):595-608.
7. Baroudy BM, Venkatesan S, Moss B. Incompletely base-paired flip-flop terminal loops link the two DNA strands of the vaccinia virus genome into one uninterrupted polynucleotide chain. Cell. 1982;28(2):315-24.
8. Smith GL, Moss B. Infectious poxvirus vectors have capacity for at least 25 000 base pairs of foreign DNA. Gene. 1983;25(1):21-8.
9. Moss B. Poxviridae: the viruses and their replication. In: Fields BN, Knipe DM, Howley PM, editors. Fields Virology. Philadelphia: Lippincott Williams & Wilkins; 2001.
10. Broyles SS. Vaccinia virus transcription. J Gen Virol. 2003;84(Pt 9):2293-303.
11. Mallardo M, Leithe E, Schleich S, Roos N, Doglio L, Krijnse Locker J. Relationship between vaccinia virus intracellular cores, early mRNAs, and DNA replication sites. J Virol. 2002;76(10):5167-83.
12. Joklik WK, Becker Y. The replication and coating of vaccinia DNA. J Mol Biol. 1964;10:452-74.
13. SALZMAN NP. The rate of formation of vaccinia deoxyribonucleic acid and vaccinia virus. Virology. 1960;10:150-2.

14. Mercer J, Helenius A. Vaccinia virus uses macropinocytosis and apoptotic mimicry to enter host cells. Science. 2008;320(5875):531-5.
15. Moss B. Poxvirus entry and membrane fusion. Virology. 2006;344(1):48-54.
16. Smith GL, Vanderplasschen A, Law M. The formation and function of extracellular enveloped vaccinia virus. J Gen Virol. 2002;83(Pt 12):2915-31.
17. Vanderplasschen A, Hollinshead M, Smith GL. Intracellular and extracellular vaccinia virions enter cells by different mechanisms. J Gen Virol. 1998;79 (Pt 4):877-87.
18. Wang Y, Gangeswaran R, Zhao X, Wang P, Tysome J, Bhakta V, et al. CEACAM6 attenuates adenovirus infection by antagonizing viral trafficking in cancer cells. J Clin Invest. 2009;119(6):1604-15.
19. Tysome JR, Briat A, Alusi G, Cao F, Gao D, Yu J, et al. Lister strain of vaccinia virus armed with endostatin-angiostatin fusion gene as a novel therapeutic agent for human pancreatic cancer. Gene Ther. 2009;16(10):1223-33.
20. Thorne SH, Hwang TH, O'Gorman WE, Bartlett DL, Sei S, Kanji F, et al. Rational strain selection and engineering creates a broad-spectrum, systemically effective oncolytic poxvirus, JX-963. J Clin Invest. 2007;117(11):3350-8.
21. Ichihashi Y. Extracellular enveloped vaccinia virus escapes neutralization. Virology. 1996;217(2):478-85.
22. Law M, Hollinshead R, Smith GL. Antibody-sensitive and antibody-resistant cell-to-cell spread by vaccinia virus: role of the A33R protein in antibody-resistant spread. J Gen Virol. 2002;83(Pt 1):209-22.
23. Smith GL, Symons JA, Khanna A, Vanderplasschen A, Alcamí A. Vaccinia virus immune evasion. Immunol Rev. 1997;159:137-54.
24. Vanderplasschen A, Mathew E, Hollinshead M, Sim RB, Smith GL. Extracellular enveloped vaccinia virus is resistant to complement because of incorporation of host complement control proteins into its envelope. Proc Natl Acad Sci U S A. 1998;95(13):7544-9.
25. Vanderplasschen A, Hollinshead M, Smith GL. Antibodies against vaccinia virus do not neutralize extracellular enveloped virus but prevent virus release from infected cells and comet formation. J Gen Virol. 1997;78 (Pt 8):2041-8.

26. Thorne SH. Strategies to achieve systemic delivery of therapeutic cells and microbes to tumors. Expert Opin Biol Ther. 2007;7(1):41-51.
27. Kirn DH, Wang Y, Liang W, Contag CH, Thorne SH. Enhancing poxvirus oncolytic effects through increased spread and immune evasion. Cancer Res. 2008;68(7):2071-5.
28. Sun HC, Qiu ZJ, Liu J, Sun J, Jiang T, Huang KJ, et al. Expression of hypoxia-inducible factor-1 alpha and associated proteins in pancreatic ductal adenocarcinoma and their impact on prognosis. Int J Oncol. 2007;30(6):1359-67.
29. Yokoi K, Fidler IJ. Hypoxia increases resistance of human pancreatic cancer cells to apoptosis induced by gemcitabine. Clin Cancer Res. 2004;10(7):2299-306.
30. Pipiya T, Sauthoff H, Huang YQ, Chang B, Cheng J, Heitner S, et al. Hypoxia reduces adenoviral replication in cancer cells by downregulation of viral protein expression. Gene Ther. 2005;12(11):911-7.
31. Shen BH, Bauzon M, Hermiston TW. The effect of hypoxia on the uptake, replication and lytic potential of group B adenovirus type 3 (Ad3) and type 11p (Ad11p). Gene Ther. 2006;13(12):986-90.
32. Shen BH, Hermiston TW. Effect of hypoxia on Ad5 infection, transgene expression and replication. Gene Ther. 2005;12(11):902-10.
33. Hiley CT, Yuan M, Lemoine NR, Wang Y. Lister strain vaccinia virus, a potential therapeutic vector targeting hypoxic tumours. Gene Ther. 2010;17(2):281-7.
34. Wang H, Chen NG, Minev BR, Szalay AA. Oncolytic vaccinia virus GLV-1h68 strain shows enhanced replication in human breast cancer stem-like cells in comparison to breast cancer cells. J Transl Med. 2012;10:167.
35. Russell SJ, Peng KW, Bell JC. Oncolytic virotherapy. Nat Biotechnol. 2012;30(7):658-70.
36. Al-Hajj M, Becker MW, Wicha M, Weissman I, Clarke MF. Therapeutic implications of cancer stem cells. Curr Opin Genet Dev. 2004;14(1):43-7.
37. Li F, Tiede B, Massagué J, Kang Y. Beyond tumorigenesis: cancer stem cells in metastasis. Cell Res. 2007;17(1):3-14.
38. Wicha MS, Liu S, Dontu G. Cancer stem cells: an old idea--a paradigm shift. Cancer Res. 2006;66(4):1883-90; discussion 95-6.

39. Wittek R. Vaccinia immune globulin: current policies, preparedness, and product safety and efficacy. Int J Infect Dis. 2006;10(3):193-201.
40. De Clercq E. Cidofovir in the treatment of poxvirus infections. Antiviral Res. 2002;55(1):1-13.
41. Yu YA, Shabahang S, Timiryasova TM, Zhang Q, Beltz R, Gentschev I, et al. Visualization of tumors and metastases in live animals with bacteria and vaccinia virus encoding light-emitting proteins. Nat Biotechnol. 2004;22(3):313-20.
42. Ziauddin MF, Bartlett DL. Oncolytic Vaccinia. In: Harrington KJ, Vile RG, Pandha HS, editors. Viral Therapy of Cancer. Chicherster, England: John Wiley & Sons Ltd; 2008.
43. Hanahan D, Weinberg RA. Hallmarks of cancer: the next generation. Cell. 2011;144(5):646-74.
44. Lichty BD, Breitbach CJ, Stojdl DF, Bell JC. Going viral with cancer immunotherapy. Nat Rev Cancer. 2014;14(8):559-67.
45. Luker KE, Hutchens M, Schultz T, Pekosz A, Luker GD. Bioluminescence imaging of vaccinia virus: effects of interferon on viral replication and spread. Virology. 2005;341(2):284-300.
46. Parato KA, Breitbach CJ, Le Boeuf F, Wang J, Storbeck C, Ilkow C, et al. The oncolytic poxvirus JX-594 selectively replicates in and destroys cancer cells driven by genetic pathways commonly activated in cancers. Mol Ther. 2012;20(4):749-58.
47. Hanahan D, Weinberg RA. The hallmarks of cancer. Cell. 2000;100(1):57-70.
48. Tzahar E, Moyer JD, Waterman H, Barbacci EG, Bao J, Levkowitz G, et al. Pathogenic poxviruses reveal viral strategies to exploit the ErbB signaling network. EMBO J. 1998;17(20):5948-63.
49. McCart JA, Ward JM, Lee J, Hu Y, Alexander HR, Libutti SK, et al. Systemic cancer therapy with a tumor-selective vaccinia virus mutant lacking thymidine kinase and vaccinia growth factor genes. Cancer Res. 2001;61(24):8751-7.
50. Goel S, Duda DG, Xu L, Munn LL, Boucher Y, Fukumura D, et al. Normalization of the vasculature for treatment of cancer and other diseases. Physiol Rev. 2011;91(3):1071-121.

51. Chang E, Chalikonda S, Friedl J, Xu H, Phan GQ, Marincola FM, et al. Targeting vaccinia to solid tumors with local hyperthermia. Hum Gene Ther. 2005;16(4):435-44.
52. Hiley CT, Chard LS, Gangeswaran R, Tysome JR, Briat A, Lemoine NR, et al. Vascular endothelial growth factor A promotes vaccinia virus entry into host cells via activation of the Akt pathway. J Virol. 2013;87(5):2781-90.
53. Chen B, Timiryasova TM, Haghighat P, Andres ML, Kajioka EH, Dutta-Roy R, et al. Low-dose vaccinia virus-mediated cytokine gene therapy of glioma. J Immunother. 2001;24(1):46-57.
54. Zhang Q, Yu YA, Wang E, Chen N, Danner RL, Munson PJ, et al. Eradication of solid human breast tumors in nude mice with an intravenously injected light-emitting oncolytic vaccinia virus. Cancer Res. 2007;67(20):10038-46.
55. Zhang Q, Liang C, Yu YA, Chen N, Dandekar T, Szalay AA. The highly attenuated oncolytic recombinant vaccinia virus GLV-1h68: comparative genomic features and the contribution of F14.5L inactivation. Mol Genet Genomics. 2009;282(4):417-35.
56. Zeh HJ, Bartlett DL. Development of a replication-selective, oncolytic poxvirus for the treatment of human cancers. Cancer Gene Ther. 2002;9(12):1001-12.
57. Aoyagi M, Zhai D, Jin C, Aleshin AE, Stec B, Reed JC, et al. Vaccinia virus N1L protein resembles a B cell lymphoma-2 (Bcl-2) family protein. Protein Sci. 2007;16(1):118-24.
58. Chen NG, Yu YA, Zhang Q, Szalay AA. Replication efficiency of oncolytic vaccinia virus in cell cultures prognosticates the virulence and antitumor efficacy in mice. J Transl Med. 2011;9:164.
59. Guo ZS, Naik A, O'Malley ME, Popovic P, Demarco R, Hu Y, et al. The enhanced tumor selectivity of an oncolytic vaccinia lacking the host range and antiapoptosis genes SPI-1 and SPI-2. Cancer Res. 2005;65(21):9991-8.
60. Lee CY, Bu LX, DeBenedetti A, Williams BJ, Rennie PS, Jia WW. Transcriptional and translational dual-regulated oncolytic herpes simplex virus type 1 for targeting prostate tumors. Mol Ther. 2010;18(5):929-35.
61. Cuevas Y, Hernández-Alcoceba R, Aragones J, Naranjo-Suárez S, Castellanos MC, Esteban MA, et al. Specific oncolytic effect of a new hypoxia-inducible

factor-dependent replicative adenovirus on von Hippel-Lindau-defective renal cell carcinomas. Cancer Res. 2003;63(20):6877-84.

62. Post DE, Van Meir EG. A novel hypoxia-inducible factor (HIF) activated oncolytic adenovirus for cancer therapy. Oncogene. 2003;22(14):2065-72.
63. Hikichi M, Kidokoro M, Haraguchi T, Iba H, Shida H, Tahara H, et al. MicroRNA regulation of glycoprotein B5R in oncolytic vaccinia virus reduces viral pathogenicity without impairing its antitumor efficacy. Mol Ther. 2011;19(6):1107-15.
64. Morita M, Aoyama Y, Arita M, Amona H, Yoshizawa H, Hashizume S, et al. Comparative studies of several vaccinia virus strains by intrathalamic inoculation into cynomolgus monkeys. Arch Virol. 1977;53(3):197-208.
65. Soekawa M, Morita C, Moriguchi R, Nakamura M. Neurovirulence of vaccinia viruses for mice. Zentralbl Bakteriol Orig A. 1974;226(4):434-42.
66. Beranek CF, Schäfer R, Bologa L, Herschkowitz N. Viral tropisms in mouse brain cell cultures. Med Microbiol Immunol. 1982;170(3):201-8.
67. Kenner J, Cameron F, Empig C, Jobes DV, Gurwith M. LC16m8: an attenuated smallpox vaccine. Vaccine. 2006;24(47-48):7009-22.
68. Garcel A, Crance JM, Drillien R, Garin D, Favier AL. Genomic sequence of a clonal isolate of the vaccinia virus Lister strain employed for smallpox vaccination in France and its comparison to other orthopoxviruses. J Gen Virol. 2007;88(Pt 7):1906-16.
69. Gubser C, Bergamaschi D, Hollinshead M, Lu X, van Kuppeveld FJ, Smith GL. A new inhibitor of apoptosis from vaccinia virus and eukaryotes. PLoS Pathog. 2007;3(2):e17.
70. Saraiva M, Alcami A. CrmE, a novel soluble tumor necrosis factor receptor encoded by poxviruses. J Virol. 2001;75(1):226-33.
71. Parker RF, Bronson LH, Green RH. Further studies of the infectious unit of vaccinia. J Exp Med. 1941;74(3):263-81.
72. Garcel A, Perino J, Crance JM, Drillien R, Garin D, Favier AL. Phenotypic and genetic diversity of the traditional Lister smallpox vaccine. Vaccine. 2009;27(5):708-17.

73. Morikawa S, Sakiyama T, Hasegawa H, Saijo M, Maeda A, Kurane I, et al. An attenuated LC16m8 smallpox vaccine: analysis of full-genome sequence and induction of immune protection. J Virol. 2005;79(18):11873-91.
74. Salek-Ardakani S, Flynn R, Arens R, Yagita H, Smith GL, Borst J, et al. The TNFR family members OX40 and CD27 link viral virulence to protective T cell vaccines in mice. J Clin Invest. 2011;121(1):296-307.
75. Ascierto ML, Worschech A, Yu Z, Adams S, Reinboth J, Chen NG, et al. Permissivity of the NCI-60 cancer cell lines to oncolytic Vaccinia Virus GLV-1h68. BMC Cancer. 2011;11:451.
76. Weinstein JN. Spotlight on molecular profiling: "Integromic" analysis of the NCI-60 cancer cell lines. Mol Cancer Ther. 2006;5(11):2601-5.
77. Gentschev I, Donat U, Hofmann E, Weibel S, Adelfinger M, Raab V, et al. Regression of human prostate tumors and metastases in nude mice following treatment with the recombinant oncolytic vaccinia virus GLV-1h68. J Biomed Biotechnol. 2010;2010:489759.
78. Worschech A, Haddad D, Stroncek DF, Wang E, Marincola FM, Szalay AA. The immunologic aspects of poxvirus oncolytic therapy. Cancer Immunol Immunother. 2009;58(9):1355-62.
79. Worschech A, Chen N, Yu YA, Zhang Q, Pos Z, Weibel S, et al. Systemic treatment of xenografts with vaccinia virus GLV-1h68 reveals the immunologic facet of oncolytic therapy. BMC Genomics. 2009;10:301.
80. Chen N, Zhang Q, Yu YA, Stritzker J, Brader P, Schirbel A, et al. A novel recombinant vaccinia virus expressing the human norepinephrine transporter retains oncolytic potential and facilitates deep-tissue imaging. Mol Med. 2009;15(5-6):144-51.
81. Gholami S, Haddad D, Chen CH, Chen NG, Zhang Q, Zanzonico PB, et al. Novel therapy for anaplastic thyroid carcinoma cells using an oncolytic vaccinia virus carrying the human sodium iodide symporter. Surgery. 2011;150(6):1040-7.
82. Haddad D, Chen NG, Zhang Q, Chen CH, Yu YA, Gonzalez L, et al. Insertion of the human sodium iodide symporter to facilitate deep tissue imaging does not alter oncolytic or replication capability of a novel vaccinia virus. J Transl Med. 2011;9:36.

83. Frentzen A, Yu YA, Chen N, Zhang Q, Weibel S, Raab V, et al. Anti-VEGF single-chain antibody GLAF-1 encoded by oncolytic vaccinia virus significantly enhances antitumor therapy. Proc Natl Acad Sci U S A. 2009;106(31):12915-20.
84. Timiryasova TM, Chen B, Haghighat P, Fodor I. Vaccinia virus-mediated expression of wild-type p53 suppresses glioma cell growth and induces apoptosis. Int J Oncol. 1999;14(5):845-54.
85. Denes B, Gridley DS, Fodor N, Takatsy Z, Timiryasova TM, Fodor I. Attenuation of a vaccine strain of vaccinia virus via inactivation of interferon viroceptor. J Gene Med. 2006;8(7):814-23.
86. Shinoura N, Yoshida Y, Asai A, Kirino T, Hamada H. Adenovirus-mediated transfer of p53 and Fas ligand drastically enhances apoptosis in gliomas. Cancer Gene Ther. 2000;7(5):732-8.
87. Jiang G, Li J, Zeng Z, Xian L. Lentivirus-mediated gene therapy by suppressing survivin in BALB/c nude mice bearing oral squamous cell carcinoma. Cancer Biol Ther. 2006;5(4):435-40.
88. Timiryasova TM, Chen B, Fodor I. Replication-deficient vaccinia virus gene therpay vector: evaluation of exogenous gene expression mediated by PUV-inactivated virus in glioma cells. J Gene Med. 2001;3(5):468-77.
89. Timiryasova TM, Gridley DS, Chen B, Andres ML, Dutta-Roy R, Miller G, et al. Radiation enhances the anti-tumor effects of vaccinia-p53 gene therapy in glioma. Technol Cancer Res Treat. 2003;2(3):223-35.
90. Fodor I, Timiryasova T, Denes B, Yoshida J, Ruckle H, Lilly M. Vaccinia virus mediated p53 gene therapy for bladder cancer in an orthotopic murine model. J Urol. 2005;173(2):604-9.
91. Smith E, Breznik J, Lichty BD. Strategies to enhance viral penetration of solid tumors. Hum Gene Ther. 2011;22(9):1053-60.
92. Breitbach CJ, Thorne SH, Bell JC, Kirn DH. Targeted and Armed Oncolytic Poxviruses for Cancer: The Lead Example of JX-594. Curr Pharm Biotechnol. 2011.
93. Kirn DH, Thorne SH. Targeted and armed oncolytic poxviruses: a novel multi-mechanistic therapeutic class for cancer. Nat Rev Cancer. 2009;9(1):64-71.

94. Yu YA, Galanis C, Woo Y, Chen N, Zhang Q, Fong Y, et al. Regression of human pancreatic tumor xenografts in mice after a single systemic injection of recombinant vaccinia virus GLV-1h68. Mol Cancer Ther. 2009;8(1):141-51.
95. McCart JA, Puhlmann M, Lee J, Hu Y, Libutti SK, Alexander HR, et al. Complex interactions between the replicating oncolytic effect and the enzyme/prodrug effect of vaccinia-mediated tumor regression. Gene Ther. 2000;7(14):1217-23.
96. Schepelmann S, Springer CJ. Viral vectors for gene-directed enzyme prodrug therapy. Curr Gene Ther. 2006;6(6):647-70.
97. Seubert CM, Stritzker J, Hess M, Donat U, Sturm JB, Chen N, et al. Enhanced tumor therapy using vaccinia virus strain GLV-1h68 in combination with a beta-galactosidase-activatable prodrug seco-analog of duocarmycin SA. Cancer Gene Ther. 2011;18(1):42-52.
98. Tietze LF, Krewer B. Novel analogues of CC-1065 and the duocarmycins for the use in targeted tumour therapies. Anticancer Agents Med Chem. 2009;9(3):304-25.
99. Ottolino-Perry K, Diallo JS, Lichty BD, Bell JC, McCart JA. Intelligent design: combination therapy with oncolytic viruses. Mol Ther. 2010;18(2):251-63.
100. Gridley DS, Andres ML, Li J, Timiryasova T, Chen B, Fodor I. Evaluation of radiation effects against C6 glioma in combination with vaccinia virus-p53 gene therapy. Int J Oncol. 1998;13(5):1093-8.
101. McCart JA, Mehta N, Scollard D, Reilly RM, Carrasquillo JA, Tang N, et al. Oncolytic vaccinia virus expressing the human somatostatin receptor SSTR2: molecular imaging after systemic delivery using 111In-pentetreotide. Mol Ther. 2004;10(3):553-61.
102. Wein RO, Weber RS. Anaplastic thyroid carcinoma: palliation or treatment? Curr Opin Otolaryngol Head Neck Surg. 2011;19(2):113-8.
103. Bergers G, Benjamin LE. Tumorigenesis and the angiogenic switch. Nat Rev Cancer. 2003;3(6):401-10.
104. Kirn DH, Wang Y, Le Boeuf F, Bell J, Thorne SH. Targeting of interferon-beta to produce a specific, multi-mechanistic oncolytic vaccinia virus. PLoS Med. 2007;4(12):e353.

105. Tysome JR, Wang P, Alusi G, Briat A, Gangeswaran R, Wang J, et al. Lister vaccine strain of vaccinia virus armed with the endostatin-angiostatin fusion gene: an oncolytic virus superior to dl1520 (ONYX-015) for human head and neck cancer. Hum Gene Ther. 2011;22(9):1101-8.
106. Jain RK, Finn AV, Kolodgie FD, Gold HK, Virmani R. Antiangiogenic therapy for normalization of atherosclerotic plaque vasculature: a potential strategy for plaque stabilization. Nat Clin Pract Cardiovasc Med. 2007;4(9):491-502.
107. Tysome JR, Lemoine NR, Wang Y. Combination of anti-angiogenic therapy and virotherapy: arming oncolytic viruses with anti-angiogenic genes. Curr Opin Mol Ther. 2009;11(6):664-9.
108. Cavallo F, De Giovanni C, Nanni P, Forni G, Lollini PL. 2011: the immune hallmarks of cancer. Cancer Immunol Immunother. 2011;60(3):319-26.
109. Schreiber RD, Old LJ, Smyth MJ. Cancer immunoediting: integrating immunity's roles in cancer suppression and promotion. Science. 2011;331(6024):1565-70.
110. Finn OJ. Immuno-oncology: understanding the function and dysfunction of the immune system in cancer. Ann Oncol. 2012;23 Suppl 8:viii6-9.
111. Hanahan D, Coussens LM. Accessories to the crime: functions of cells recruited to the tumor microenvironment. Cancer Cell. 2012;21(3):309-22.
112. Jochems C, Schlom J. Tumor-infiltrating immune cells and prognosis: the potential link between conventional cancer therapy and immunity. Exp Biol Med (Maywood). 2011;236(5):567-79.
113. Janeway CA. Approaching the asymptote? Evolution and revolution in immunology. Cold Spring Harb Symp Quant Biol. 1989;54 Pt 1:1-13.
114. Janeway CA, Medzhitov R. Innate immune recognition. Annual review of immunology. 2002;20:197-216.
115. Tapia K, Kim WK, Sun Y, Mercado-López X, Dunay E, Wise M, et al. Defective viral genomes arising in vivo provide critical danger signals for the triggering of lung antiviral immunity. PLoS Pathog. 2013;9(10):e1003703.
116. Tang D, Kang R, Coyne CB, Zeh HJ, Lotze MT. PAMPs and DAMPs: signal 0s that spur autophagy and immunity. Immunol Rev. 2012;249(1):158-75.
117. Bianchi ME. DAMPs, PAMPs and alarmins: all we need to know about danger. J Leukoc Biol. 2007;81(1):1-5.

118. Joffre O, Nolte MA, Spörri R, Reis e Sousa C. Inflammatory signals in dendritic cell activation and the induction of adaptive immunity. Immunol Rev. 2009;227(1):234-47.
119. Zanoni I, Granucci F. Regulation of antigen uptake, migration, and lifespan of dendritic cell by Toll-like receptors. J Mol Med (Berl). 2010;88(9):873-80.
120. Matzinger P. The danger model: a renewed sense of self. Science. 2002;296(5566):301-5.
121. Gallucci S, Matzinger P. Danger signals: SOS to the immune system. Curr Opin Immunol. 2001;13(1):114-9.
122. Shi Y, Evans JE, Rock KL. Molecular identification of a danger signal that alerts the immune system to dying cells. Nature. 2003;425(6957):516-21.
123. Klune JR, Dhupar R, Cardinal J, Billiar TR, Tsung A. HMGB1: endogenous danger signaling. Mol Med. 2008;14(7-8):476-84.
124. Melcher A, Todryk S, Hardwick N, Ford M, Jacobson M, Vile RG. Tumor immunogenicity is determined by the mechanism of cell death via induction of heat shock protein expression. Nat Med. 1998;4(5):581-7.
125. Prestwich RJ, Harrington KJ, Pandha HS, Vile RG, Melcher AA, Errington F. Oncolytic viruses: a novel form of immunotherapy. Expert Rev Anticancer Ther. 2008;8(10):1581-8.
126. Mantovani A, Allavena P, Sica A, Balkwill F. Cancer-related inflammation. Nature. 2008;454(7203):436-44.
127. Cheever MA, Allison JP, Ferris AS, Finn OJ, Hastings BM, Hecht TT, et al. The prioritization of cancer antigens: a national cancer institute pilot project for the acceleration of translational research. Clin Cancer Res. 2009;15(17):5323-37.
128. Mellman I, Coukos G, Dranoff G. Cancer immunotherapy comes of age. Nature. 2011;480(7378):480-9.
129. Zou W. Immunosuppressive networks in the tumour environment and their therapeutic relevance. Nat Rev Cancer. 2005;5(4):263-74.
130. Du C, Wang Y. The immunoregulatory mechanisms of carcinoma for its survival and development. J Exp Clin Cancer Res. 2011;30:12.
131. Groh V, Wu J, Yee C, Spies T. Tumour-derived soluble MIC ligands impair expression of NKG2D and T-cell activation. Nature. 2002;419(6908):734-8.

132. Stewart TJ, Smyth MJ. Improving cancer immunotherapy by targeting tumor-induced immune suppression. Cancer Metastasis Rev. 2011;30(1):125-40.
133. Whiteside TL. Tumor-induced death of immune cells: its mechanisms and consequences. Semin Cancer Biol. 2002;12(1):43-50.
134. Nakamura K, Kitani A, Fuss I, Pedersen A, Harada N, Nawata H, et al. TGF-beta 1 plays an important role in the mechanism of CD4+CD25+ regulatory T cell activity in both humans and mice. J Immunol. 2004;172(2):834-42.
135. Grütz G. New insights into the molecular mechanism of interleukin-10-mediated immunosuppression. J Leukoc Biol. 2005;77(1):3-15.
136. Devaud C, John LB, Westwood JA, Darcy PK, Kershaw MH. Immune modulation of the tumor microenvironment for enhancing cancer immunotherapy. Oncoimmunology. 2013;2(8):e25961.
137. Lutz MB, Kurts C. Induction of peripheral CD4+ T-cell tolerance and CD8+ T-cell cross-tolerance by dendritic cells. Eur J Immunol. 2009;39(9):2325-30.
138. Saied A, Pillarisetty VG, Katz SC. Immunotherapy for solid tumors--a review for surgeons. J Surg Res. 2014;187(2):525-35.
139. Kalos M, Levine BL, Porter DL, Katz S, Grupp SA, Bagg A, et al. T cells with chimeric antigen receptors have potent antitumor effects and can establish memory in patients with advanced leukemia. Sci Transl Med. 2011;3(95):95ra73.
140. Grosso JF, Jure-Kunkel MN. CTLA-4 blockade in tumor models: an overview of preclinical and translational research. Cancer Immun. 2013;13:5.
141. Weiss JM, Subleski JJ, Wigginton JM, Wiltrout RH. Immunotherapy of cancer by IL-12-based cytokine combinations. Expert Opin Biol Ther. 2007;7(11):1705-21.
142. Jinushi M, Tahara H. Cytokine gene-mediated immunotherapy: current status and future perspectives. Cancer Sci. 2009;100(8):1389-96.
143. Crompton AM, Kirn DH. From ONYX-015 to armed vaccinia viruses: the education and evolution of oncolytic virus development. Curr Cancer Drug Targets. 2007;7(2):133-9.
144. Halldén G, Portella G. Oncolytic virotherapy with modified adenoviruses and novel therapeutic targets. Expert Opin Ther Targets. 2012;16(10):945-58.
145. Garber K. China approves world's first oncolytic virus therapy for cancer treatment. J Natl Cancer Inst. 2006;98(5):298-300.

146. Vacchelli E, Eggermont A, Sautès-Fridman C, Galon J, Zitvogel L, Kroemer G, et al. Trial watch: Oncolytic viruses for cancer therapy. Oncoimmunology. 2013;2(6):e24612.
147. Romagnani C, Della Chiesa M, Kohler S, Moewes B, Radbruch A, Moretta L, et al. Activation of human NK cells by plasmacytoid dendritic cells and its modulation by CD4+ T helper cells and CD4+ CD25hi T regulatory cells. Eur J Immunol. 2005;35(8):2452-8.
148. Dörner T, Radbruch A. Antibodies and B cell memory in viral immunity. Immunity. 2007;27(3):384-92.
149. Stoermer KA, Morrison TE. Complement and viral pathogenesis. Virology. 2011;411(2):362-73.
150. Hu W, Davis JJ, Zhu H, Dong F, Guo W, Ang J, et al. Redirecting adaptive immunity against foreign antigens to tumors for cancer therapy. Cancer Biol Ther. 2007;6(11):1773-9.
151. Ferguson MS, Lemoine NR, Wang Y. Systemic delivery of oncolytic viruses: hopes and hurdles. Adv Virol. 2012;2012:805629.
152. Thorne SH. Immunotherapeutic potential of oncolytic vaccinia virus. Immunol Res. 2011;50(2-3):286-93.
153. Prestwich RJ, Errington F, Diaz RM, Pandha HS, Harrington KJ, Melcher AA, et al. The case of oncolytic viruses versus the immune system: waiting on the judgment of Solomon. Hum Gene Ther. 2009;20(10):1119-32.
154. Cairns R, Papandreou I, Denko N. Overcoming physiologic barriers to cancer treatment by molecularly targeting the tumor microenvironment. Mol Cancer Res. 2006;4(2):61-70.
155. Guedan S, Rojas JJ, Gros A, Mercade E, Cascallo M, Alemany R. Hyaluronidase expression by an oncolytic adenovirus enhances its intratumoral spread and suppresses tumor growth. Mol Ther. 2010;18(7):1275-83.
156. De Silva N, Atkins H, Kirn DH, Bell JC, Breitbach CJ. Double trouble for tumours: exploiting the tumour microenvironment to enhance anticancer effect of oncolytic viruses. Cytokine Growth Factor Rev. 2010;21(2-3):135-41.

157. Breitbach CJ, Paterson JM, Lemay CG, Falls TJ, McGuire A, Parato KA, et al. Targeted inflammation during oncolytic virus therapy severely compromises tumor blood flow. Mol Ther. 2007;15(9):1686-93.
158. Bridle BW, Hanson S, Lichty BD. Combining oncolytic virotherapy and tumour vaccination. Cytokine Growth Factor Rev. 2010;21(2-3):143-8.
159. Gujar SA, Lee PW. Oncolytic virus-mediated reversal of impaired tumor antigen presentation. Front Oncol. 2014;4:77.
160. Kaczmarek A, Vandenabeele P, Krysko DV. Necroptosis: the release of damage-associated molecular patterns and its physiological relevance. Immunity. 2013;38(2):209-23.
161. Galluzzi L, Kroemer G. Autophagy mediates the metabolic benefits of endurance training. Circ Res. 2012;110(10):1276-8.
162. Martins I, Kepp O, Schlemmer F, Adjemian S, Tailler M, Shen S, et al. Restoration of the immunogenicity of cisplatin-induced cancer cell death by endoplasmic reticulum stress. Oncogene. 2011;30(10):1147-58.
163. Inoue H, Tani K. Multimodal immunogenic cancer cell death as a consequence of anticancer cytotoxic treatments. Cell Death Differ. 2014;21(1):39-49.
164. Green DR, Ferguson T, Zitvogel L, Kroemer G. Immunogenic and tolerogenic cell death. Nat Rev Immunol. 2009;9(5):353-63.
165. Guo ZS, Liu Z, Bartlett DL. Oncolytic Immunotherapy: Dying the Right Way is a Key to Eliciting Potent Antitumor Immunity. Front Oncol. 2014;4:74.
166. Bartlett DL, Liu Z, Sathaiah M, Ravindranathan R, Guo Z, He Y, et al. Oncolytic viruses as therapeutic cancer vaccines. Mol Cancer. 2013;12(1):103.
167. Obeid M, Tesniere A, Ghiringhelli F, Fimia GM, Apetoh L, Perfettini JL, et al. Calreticulin exposure dictates the immunogenicity of cancer cell death. Nat Med. 2007;13(1):54-61.
168. Tesniere A, Apetoh L, Ghiringhelli F, Joza N, Panaretakis T, Kepp O, et al. Immunogenic cancer cell death: a key-lock paradigm. Curr Opin Immunol. 2008;20(5):504-11.
169. Sukkurwala AQ, Martins I, Wang Y, Schlemmer F, Ruckenstuhl C, Durchschlag M, et al. Immunogenic calreticulin exposure occurs through a phylogenetically

conserved stress pathway involving the chemokine CXCL8. Cell Death Differ. 2014;21(1):59-68.

170. Ghiringhelli F, Apetoh L, Tesniere A, Aymeric L, Ma Y, Ortiz C, et al. Activation of the NLRP3 inflammasome in dendritic cells induces IL-1beta-dependent adaptive immunity against tumors. Nat Med. 2009;15(10):1170-8.
171. Huang B, Sikorski R, Kirn DH, Thorne SH. Synergistic anti-tumor effects between oncolytic vaccinia virus and paclitaxel are mediated by the IFN response and HMGB1. Gene Ther. 2011;18(2):164-72.
172. John LB, Howland LJ, Flynn JK, West AC, Devaud C, Duong CP, et al. Oncolytic virus and anti-4-1BB combination therapy elicits strong antitumor immunity against established cancer. Cancer Res. 2012;72(7):1651-60.
173. Whilding LM, Archibald KM, Kulbe H, Balkwill FR, Öberg D, McNeish IA. Vaccinia virus induces programmed necrosis in ovarian cancer cells. Mol Ther. 2013;21(11):2074-86.
174. Rodriguez-Rocha H, Gomez-Gutierrez JG, Garcia-Garcia A, Rao XM, Chen L, McMasters KM, et al. Adenoviruses induce autophagy to promote virus replication and oncolysis. Virology. 2011;416(1-2):9-15.
175. Meng C, Zhou Z, Jiang K, Yu S, Jia L, Wu Y, et al. Newcastle disease virus triggers autophagy in U251 glioma cells to enhance virus replication. Arch Virol. 2012;157(6):1011-8.
176. Thirukkumaran CM, Shi ZQ, Luider J, Kopciuk K, Gao H, Bahlis N, et al. Reovirus modulates autophagy during oncolysis of multiple myeloma. Autophagy. 2013;9(3):413-4.
177. English L, Chemali M, Duron J, Rondeau C, Laplante A, Gingras D, et al. Autophagy enhances the presentation of endogenous viral antigens on MHC class I molecules during HSV-1 infection. Nature immunology. 2009;10(5):480-7.
178. Thorburn J, Horita H, Redzic J, Hansen K, Frankel AE, Thorburn A. Autophagy regulates selective HMGB1 release in tumor cells that are destined to die. Cell Death Differ. 2009;16(1):175-83.
179. Endo Y, Sakai R, Ouchi M, Onimatsu H, Hioki M, Kagawa S, et al. Virus-mediated oncolysis induces danger signal and stimulates cytotoxic T-lymphocyte activity via proteasome activator upregulation. Oncogene. 2008;27(17):2375-81.

180. Michaud M, Martins I, Sukkurwala AQ, Adjemian S, Ma Y, Pellegatti P, et al. Autophagy-dependent anticancer immune responses induced by chemotherapeutic agents in mice. Science. 2011;334(6062):1573-7.
181. Ayna G, Krysko DV, Kaczmarek A, Petrovski G, Vandenabeele P, Fésüs L. ATP release from dying autophagic cells and their phagocytosis are crucial for inflammasome activation in macrophages. PLoS One. 2012;7(6):e40069.
182. Li Y, Wang LX, Yang G, Hao F, Urba WJ, Hu HM. Efficient cross-presentation depends on autophagy in tumor cells. Cancer Res. 2008;68(17):6889-95.
183. Li Y, Wang LX, Pang P, Cui Z, Aung S, Haley D, et al. Tumor-derived autophagosome vaccine: mechanism of cross-presentation and therapeutic efficacy. Clin Cancer Res. 2011;17(22):7047-57.
184. Gauvrit A, Brandler S, Sapede-Peroz C, Boisgerault N, Tangy F, Gregoire M. Measles virus induces oncolysis of mesothelioma cells and allows dendritic cells to cross-prime tumor-specific CD8 response. Cancer Res. 2008;68(12):4882-92.
185. Meng S, Xu J, Wu Y, Ding C. Targeting autophagy to enhance oncolytic virus-based cancer therapy. Expert Opin Biol Ther. 2013;13(6):863-73.
186. Han W, Li L, Qiu S, Lu Q, Pan Q, Gu Y, et al. Shikonin circumvents cancer drug resistance by induction of a necroptotic death. Mol Cancer Ther. 2007;6(5):1641-9.
187. Leone P, Shin EC, Perosa F, Vacca A, Dammacco F, Racanelli V. MHC class I antigen processing and presenting machinery: organization, function, and defects in tumor cells. J Natl Cancer Inst. 2013;105(16):1172-87.
188. Motz GT, Coukos G. Deciphering and reversing tumor immune suppression. Immunity. 2013;39(1):61-73.
189. Hargadon KM. Tumor-altered dendritic cell function: implications for anti-tumor immunity. Front Immunol. 2013;4:192.
190. Murphy K, Janeway C, Travers P, Walport M, Mowat A, Weaver C. Janeway's Immunobiology. New York: Garland Science, Taylor and Francis group; 2011.
191. Joffre OP, Segura E, Savina A, Amigorena S. Cross-presentation by dendritic cells. Nat Rev Immunol. 2012;12(8):557-69.
192. Martin-Orozco N, Dong C. Inhibitory costimulation and anti-tumor immunity. Semin Cancer Biol. 2007;17(4):288-98.

193. Sharpe AH, Freeman GJ. The B7-CD28 superfamily. Nat Rev Immunol. 2002;2(2):116-26.
194. Gujar SA, Marcato P, Pan D, Lee PW. Reovirus virotherapy overrides tumor antigen presentation evasion and promotes protective antitumor immunity. Mol Cancer Ther. 2010;9(11):2924-33.
195. Errington F, Steele L, Prestwich R, Harrington KJ, Pandha HS, Vidal L, et al. Reovirus activates human dendritic cells to promote innate antitumor immunity. J Immunol. 2008;180(9):6018-26.
196. Kawai T, Akira S. The role of pattern-recognition receptors in innate immunity: update on Toll-like receptors. Nature immunology. 2010;11(5):373-84.
197. Kawai T, Akira S. Toll-like receptors and their crosstalk with other innate receptors in infection and immunity. Immunity. 2011;34(5):637-50.
198. Greiner S, Humrich JY, Thuman P, Sauter B, Schuler G, Jenne L. The highly attenuated vaccinia virus strain modified virus Ankara induces apoptosis in melanoma cells and allows bystander dendritic cells to generate a potent anti-tumoral immunity. Clin Exp Immunol. 2006;146(2):344-53.
199. Schulz O, Diebold SS, Chen M, Näslund TI, Nolte MA, Alexopoulou L, et al. Toll-like receptor 3 promotes cross-priming to virus-infected cells. Nature. 2005;433(7028):887-92.
200. Guillerme JB, Boisgerault N, Roulois D, Ménager J, Combredet C, Tangy F, et al. Measles virus vaccine-infected tumor cells induce tumor antigen cross-presentation by human plasmacytoid dendritic cells. Clin Cancer Res. 2013;19(5):1147-58.
201. Waldhauer I, Steinle A. NK cells and cancer immunosurveillance. Oncogene. 2008;27(45):5932-43.
202. Coca S, Perez-Piqueras J, Martinez D, Colmenarejo A, Saez MA, Vallejo C, et al. The prognostic significance of intratumoral natural killer cells in patients with colorectal carcinoma. Cancer. 1997;79(12):2320-8.
203. Villegas FR, Coca S, Villarrubia VG, Jiménez R, Chillón MJ, Jareño J, et al. Prognostic significance of tumor infiltrating natural killer cells subset CD57 in patients with squamous cell lung cancer. Lung Cancer. 2002;35(1):23-8.

204. Ishigami S, Natsugoe S, Tokuda K, Nakajo A, Che X, Iwashige H, et al. Prognostic value of intratumoral natural killer cells in gastric carcinoma. Cancer. 2000;88(3):577-83.
205. Burshtyn DN. NK cells and poxvirus infection. Front Immunol. 2013;4:7.
206. Weibel S, Raab V, Yu YA, Worschech A, Wang E, Marincola FM, et al. Viral-mediated oncolysis is the most critical factor in the late-phase of the tumor regression process upon vaccinia virus infection. BMC Cancer. 2011;11:68.
207. Langers I, Renoux VM, Thiry M, Delvenne P, Jacobs N. Natural killer cells: role in local tumor growth and metastasis. Biologics. 2012;6:73-82.
208. Kärre K, Ljunggren HG, Piontek G, Kiessling R. Selective rejection of H-2-deficient lymphoma variants suggests alternative immune defence strategy. Nature. 1986;319(6055):675-8.
209. Orr MT, Lanier LL. Inhibitory Ly49 receptors on mouse natural killer cells. Curr Top Microbiol Immunol. 2011;350:67-87.
210. Jamil KM, Khakoo SI. KIR/HLA interactions and pathogen immunity. J Biomed Biotechnol. 2011;2011:298348.
211. Stewart CA, Laugier-Anfossi F, Vély F, Saulquin X, Riedmuller J, Tisserant A, et al. Recognition of peptide-MHC class I complexes by activating killer immunoglobulin-like receptors. Proc Natl Acad Sci U S A. 2005;102(37):13224-9.
212. Brown MG, Dokun AO, Heusel JW, Smith HR, Beckman DL, Blattenberger EA, et al. Vital involvement of a natural killer cell activation receptor in resistance to viral infection. Science. 2001;292(5518):934-7.
213. Sivori S, Pende D, Bottino C, Marcenaro E, Pessino A, Biassoni R, et al. NKp46 is the major triggering receptor involved in the natural cytotoxicity of fresh or cultured human NK cells. Correlation between surface density of NKp46 and natural cytotoxicity against autologous, allogeneic or xenogeneic target cells. Eur J Immunol. 1999;29(5):1656-66.
214. Mandelboim O, Lieberman N, Lev M, Paul L, Arnon TI, Bushkin Y, et al. Recognition of haemagglutinins on virus-infected cells by NKp46 activates lysis by human NK cells. Nature. 2001;409(6823):1055-60.

215. Jarahian M, Fiedler M, Cohnen A, Djandji D, Hämmerling GJ, Gati C, et al. Modulation of NKp30- and NKp46-mediated natural killer cell responses by poxviral hemagglutinin. PLoS Pathog. 2011;7(8):e1002195.
216. Martinez J, Huang X, Yang Y. Direct TLR2 signaling is critical for NK cell activation and function in response to vaccinia viral infection. PLoS Pathog. 2010;6(3):e1000811.
217. Nimmerjahn F, Ravetch JV. Antibodies, Fc receptors and cancer. Curr Opin Immunol. 2007;19(2):239-45.
218. Lee SH, Miyagi T, Biron CA. Keeping NK cells in highly regulated antiviral warfare. Trends Immunol. 2007;28(6):252-9.
219. Clément MV, Haddad P, Soulié A, Legros-Maida S, Guillet J, Cesar E, et al. Involvement of granzyme B and perforin gene expression in the lytic potential of human natural killer cells. Res Immunol. 1990;141(6):477-89.
220. Natuk RJ, Welsh RM. Accumulation and chemotaxis of natural killer/large granular lymphocytes at sites of virus replication. J Immunol. 1987;138(3):877-83.
221. Smyth MJ, Thia KY, Street SE, MacGregor D, Godfrey DI, Trapani JA. Perforin-mediated cytotoxicity is critical for surveillance of spontaneous lymphoma. J Exp Med. 2000;192(5):755-60.
222. Colucci F, Caligiuri MA, Di Santo JP. What does it take to make a natural killer? Nat Rev Immunol. 2003;3(5):413-25.
223. Street SE, Cretney E, Smyth MJ. Perforin and interferon-gamma activities independently control tumor initiation, growth, and metastasis. Blood. 2001;97(1):192-7.
224. Angiolillo AL, Sgadari C, Taub DD, Liao F, Farber JM, Maheshwari S, et al. Human interferon-inducible protein 10 is a potent inhibitor of angiogenesis in vivo. J Exp Med. 1995;182(1):155-62.
225. Biron CA, Nguyen KB, Pien GC, Cousens LP, Salazar-Mather TP. Natural killer cells in antiviral defense: function and regulation by innate cytokines. Annual review of immunology. 1999;17:189-220.

226. Tugues S, Burkhard SH, Ohs I, Vrohlings M, Nussbaum K, Vom Berg J, et al. New insights into IL-12-mediated tumor suppression. Cell Death Differ. 2015;22(2):237-46.
227. Vivier E, Ugolini S, Blaise D, Chabannon C, Brossay L. Targeting natural killer cells and natural killer T cells in cancer. Nat Rev Immunol. 2012;12(4):239-52.
228. Kim S, Iizuka K, Aguila HL, Weissman IL, Yokoyama WM. In vivo natural killer cell activities revealed by natural killer cell-deficient mice. Proc Natl Acad Sci U S A. 2000;97(6):2731-6.
229. Smyth MJ, Crowe NY, Godfrey DI. NK cells and NKT cells collaborate in host protection from methylcholanthrene-induced fibrosarcoma. Int Immunol. 2001;13(4):459-63.
230. Halfteck GG, Elboim M, Gur C, Achdout H, Ghadially H, Mandelboim O. Enhanced in vivo growth of lymphoma tumors in the absence of the NK-activating receptor NKp46/NCR1. J Immunol. 2009;182(4):2221-30.
231. Imai K, Matsuyama S, Miyake S, Suga K, Nakachi K. Natural cytotoxic activity of peripheral-blood lymphocytes and cancer incidence: an 11-year follow-up study of a general population. Lancet. 2000;356(9244):1795-9.
232. Zhou S, Kawakami S, Higuchi Y, Yamashita F, Hashida M. The involvement of NK cell activation following intranasal administration of CpG DNA lipoplex in the prevention of pulmonary metastasis and peritoneal dissemination in mice. Clin Exp Metastasis. 2012;29(1):63-70.
233. Ksienzyk A, Neumann B, Nandakumar R, Finsterbusch K, Grashoff M, Zawatzky R, et al. IRF-1 expression is essential for natural killer cells to suppress metastasis. Cancer Res. 2011;71(20):6410-8.
234. Sobolev O, Stern P, Lacy-Hulbert A, Hynes RO. Natural killer cells require selectins for suppression of subcutaneous tumors. Cancer Res. 2009;69(6):2531-9.
235. Grégoire C, Chasson L, Luci C, Tomasello E, Geissmann F, Vivier E, et al. The trafficking of natural killer cells. Immunol Rev. 2007;220:169-82.
236. Dokun AO, Kim S, Smith HR, Kang HS, Chu DT, Yokoyama WM. Specific and nonspecific NK cell activation during virus infection. Nature immunology. 2001;2(10):951-6.

237. Orange JS, Biron CA. An absolute and restricted requirement for IL-12 in natural killer cell IFN-gamma production and antiviral defense. Studies of natural killer and T cell responses in contrasting viral infections. J Immunol. 1996;156(3):1138-42.
238. Sivori S, Falco M, Della Chiesa M, Carlomagno S, Vitale M, Moretta L, et al. CpG and double-stranded RNA trigger human NK cells by Toll-like receptors: induction of cytokine release and cytotoxicity against tumors and dendritic cells. Proc Natl Acad Sci U S A. 2004;101(27):10116-21.
239. Schmidt KN, Leung B, Kwong M, Zarember KA, Satyal S, Navas TA, et al. APC-independent activation of NK cells by the Toll-like receptor 3 agonist double-stranded RNA. J Immunol. 2004;172(1):138-43.
240. Hart OM, Athie-Morales V, O'Connor GM, Gardiner CM. TLR7/8-mediated activation of human NK cells results in accessory cell-dependent IFN-gamma production. J Immunol. 2005;175(3):1636-42.
241. Cooper MA, Elliott JM, Keyel PA, Yang L, Carrero JA, Yokoyama WM. Cytokine-induced memory-like natural killer cells. Proc Natl Acad Sci U S A. 2009;106(6):1915-9.
242. Paust S, Gill HS, Wang BZ, Flynn MP, Moseman EA, Senman B, et al. Critical role for the chemokine receptor CXCR6 in NK cell-mediated antigen-specific memory of haptens and viruses. Nature immunology. 2010;11(12):1127-35.
243. O'Leary JG, Goodarzi M, Drayton DL, von Andrian UH. T cell- and B cell-independent adaptive immunity mediated by natural killer cells. Nature immunology. 2006;7(5):507-16.
244. Bukowski JF, Biron CA, Welsh RM. Elevated natural killer cell-mediated cytotoxicity, plasma interferon, and tumor cell rejection in mice persistently infected with lymphocytic choriomeningitis virus. J Immunol. 1983;131(2):991-6.
245. Sun JC, Beilke JN, Lanier LL. Adaptive immune features of natural killer cells. Nature. 2009;457(7229):557-61.
246. Wang LC, Lynn RC, Cheng G, Alexander E, Kapoor V, Moon EK, et al. Treating Tumors With a Vaccinia Virus Expressing IFNβ Illustrates the Complex Relationships Between Oncolytic Ability and Immunogenicity. Mol Ther. 2011.

247. Smith GL, Benfield CT, Maluquer de Motes C, Mazzon M, Ember SW, Ferguson BJ, et al. Vaccinia virus immune evasion: mechanisms, virulence and immunogenicity. J Gen Virol. 2013;94(Pt 11):2367-92.
248. Bartlett N, Symons JA, Tscharke DC, Smith GL. The vaccinia virus N1L protein is an intracellular homodimer that promotes virulence. J Gen Virol. 2002;83(Pt 8):1965-76.
249. Gratz MS, Suezer Y, Kremer M, Volz A, Majzoub M, Hanschmann KM, et al. N1L is an ectromelia virus virulence factor and essential for in vivo spread upon respiratory infection. J Virol. 2011;85(7):3557-69.
250. Billings B, Smith SA, Zhang Z, Lahiri DK, Kotwal GJ. Lack of N1L gene expression results in a significant decrease of vaccinia virus replication in mouse brain. Ann N Y Acad Sci. 2004;1030:297-302.
251. Hayasaka D, Ennis FA, Terajima M. Pathogeneses of respiratory infections with virulent and attenuated vaccinia viruses. Virol J. 2007;4:22.
252. Mohan KV, Zhang CX, Atreya CD. The proteoglycan bamacan is a host cellular ligand of vaccinia virus neurovirulence factor N1L. J Neurovirol. 2009;15(3):229-37.
253. Mathew A, O'Bryan J, Marshall W, Kotwal GJ, Terajima M, Green S, et al. Robust intrapulmonary CD8 T cell responses and protection with an attenuated N1L deleted vaccinia virus. PLoS One. 2008;3(10):e3323.
254. Jacobs N, Bartlett NW, Clark RH, Smith GL. Vaccinia virus lacking the Bcl-2-like protein N1 induces a stronger natural killer cell response to infection. J Gen Virol. 2008;89(Pt 11):2877-81.
255. Maluquer de Motes C, Cooray S, Ren H, Almeida GM, McGourty K, Bahar MW, et al. Inhibition of apoptosis and NF-κB activation by vaccinia protein N1 occur via distinct binding surfaces and make different contributions to virulence. PLoS Pathog. 2011;7(12):e1002430.
256. Graham SC, Bahar MW, Cooray S, Chen RA, Whalen DM, Abrescia NG, et al. Vaccinia virus proteins A52 and B14 Share a Bcl-2-like fold but have evolved to inhibit NF-kappaB rather than apoptosis. PLoS Pathog. 2008;4(8):e1000128.

257. Cooray S, Bahar MW, Abrescia NG, McVey CE, Bartlett NW, Chen RA, et al. Functional and structural studies of the vaccinia virus virulence factor N1 reveal a Bcl-2-like anti-apoptotic protein. J Gen Virol. 2007;88(Pt 6):1656-66.
258. DiPerna G, Stack J, Bowie AG, Boyd A, Kotwal G, Zhang Z, et al. Poxvirus protein N1L targets the I-kappaB kinase complex, inhibits signaling to NF-kappaB by the tumor necrosis factor superfamily of receptors, and inhibits NF-kappaB and IRF3 signaling by toll-like receptors. J Biol Chem. 2004;279(35):36570-8.
259. Stark GR, Darnell JE. The JAK-STAT pathway at twenty. Immunity. 2012;36(4):503-14.
260. Chen RA, Ryzhakov G, Cooray S, Randow F, Smith GL. Inhibition of IkappaB kinase by vaccinia virus virulence factor B14. PLoS Pathog. 2008;4(2):e22.
261. Hayden MS, Ghosh S. Shared principles in NF-kappaB signaling. Cell. 2008;132(3):344-62.
262. Zhang Z, Abrahams MR, Hunt LA, Suttles J, Marshall W, Lahiri DK, et al. The vaccinia virus N1L protein influences cytokine secretion in vitro after infection. Ann N Y Acad Sci. 2005;1056:69-86.
263. Tait SW, Green DR. Mitochondria and cell death: outer membrane permeabilization and beyond. Nat Rev Mol Cell Biol. 2010;11(9):621-32.
264. Youle RJ, Strasser A. The BCL-2 protein family: opposing activities that mediate cell death. Nat Rev Mol Cell Biol. 2008;9(1):47-59.
265. Restifo NP, Dudley ME, Rosenberg SA. Adoptive immunotherapy for cancer: harnessing the T cell response. Nat Rev Immunol. 2012;12(4):269-81.
266. Bridle BW, Stephenson KB, Boudreau JE, Koshy S, Kazdhan N, Pullenayegum E, et al. Potentiating cancer immunotherapy using an oncolytic virus. Mol Ther. 2010;18(8):1430-9.
267. Wongthida P, Diaz RM, Pulido C, Rommelfanger D, Galivo F, Kaluza K, et al. Activating systemic T-cell immunity against self tumor antigens to support oncolytic virotherapy with vesicular stomatitis virus. Hum Gene Ther. 2011;22(11):1343-53.

268. Kottke T, Errington F, Pulido J, Galivo F, Thompson J, Wongthida P, et al. Broad antigenic coverage induced by vaccination with virus-based cDNA libraries cures established tumors. Nat Med. 2011;17(7):854-9.
269. Pulido J, Kottke T, Thompson J, Galivo F, Wongthida P, Diaz RM, et al. Using virally expressed melanoma cDNA libraries to identify tumor-associated antigens that cure melanoma. Nat Biotechnol. 2012;30(4):337-43.
270. Burke JM. GM-CSF-armed, replication-competent viruses for cancer. Cytokine Growth Factor Rev. 2010;21(2-3):149-51.
271. Ju DW, Cao X, Acres B. Intratumoral injection of GM-CSF gene encoded recombinant vaccinia virus elicits potent antitumor response in a mixture melanoma model. Cancer Gene Ther. 1997;4(2):139-44.
272. Dranoff G, Jaffee E, Lazenby A, Golumbek P, Levitsky H, Brose K, et al. Vaccination with irradiated tumor cells engineered to secrete murine granulocyte-macrophage colony-stimulating factor stimulates potent, specific, and long-lasting anti-tumor immunity. Proc Natl Acad Sci U S A. 1993;90(8):3539-43.
273. Lapteva N, Aldrich M, Weksberg D, Rollins L, Goltsova T, Chen SY, et al. Targeting the intratumoral dendritic cells by the oncolytic adenoviral vaccine expressing RANTES elicits potent antitumor immunity. J Immunother. 2009;32(2):145-56.
274. Edukulla R, Ramakrishna E, Woller N, Mundt B, Knocke S, Gürlevik E, et al. Antitumoral immune response by recruitment and expansion of dendritic cells in tumors infected with telomerase-dependent oncolytic viruses. Cancer Res. 2009;69(4):1448-58.
275. Kaufman HL, Cohen S, Cheung K, DeRaffele G, Mitcham J, Moroziewicz D, et al. Local delivery of vaccinia virus expressing multiple costimulatory molecules for the treatment of established tumors. Hum Gene Ther. 2006;17(2):239-44.
276. Feder-Mengus C, Schultz-Thater E, Oertli D, Marti WR, Heberer M, Spagnoli GC, et al. Nonreplicating recombinant vaccinia virus expressing CD40 ligand enhances APC capacity to stimulate specific CD4+ and CD8+ T cell responses. Hum Gene Ther. 2005;16(3):348-60.
277. Mukherjee S, Haenel T, Himbeck R, Scott B, Ramshaw I, Lake RA, et al. Replication-restricted vaccinia as a cytokine gene therapy vector in cancer:

persistent transgene expression despite antibody generation. Cancer Gene Ther. 2000;7(5):663-70.

278. Kaufman HL, Flanagan K, Lee CS, Perretta DJ, Horig H. Insertion of interleukin-2 (IL-2) and interleukin-12 (IL-12) genes into vaccinia virus results in effective anti-tumor responses without toxicity. Vaccine. 2002;20(13-14):1862-9.
279. Carroll MW, Overwijk WW, Surman DR, Tsung K, Moss B, Restifo NP. Construction and characterization of a triple-recombinant vaccinia virus encoding B7-1, interleukin 12, and a model tumor antigen. J Natl Cancer Inst. 1998;90(24):1881-7.
280. Ruby J, Bluethmann H, Aguet M, Ramshaw IA. CD40 ligand has potent antiviral activity. Nat Med. 1995;1(5):437-41.
281. Sambhi SK, Kohonen-Corish MR, Ramshaw IA. Local production of tumor necrosis factor encoded by recombinant vaccinia virus is effective in controlling viral replication in vivo. Proc Natl Acad Sci U S A. 1991;88(9):4025-9.
282. Breitbach CJ, Burke J, Jonker D, Stephenson J, Haas AR, Chow LQ, et al. Intravenous delivery of a multi-mechanistic cancer-targeted oncolytic poxvirus in humans. Nature. 2011;477(7362):99-102.
283. Hodge JW, Poole DJ, Aarts WM, Gomez Yafal A, Gritz L, Schlom J. Modified vaccinia virus ankara recombinants are as potent as vaccinia recombinants in diversified prime and boost vaccine regimens to elicit therapeutic antitumor responses. Cancer Res. 2003;63(22):7942-9.
284. Hodge JW, Higgins J, Schlom J. Harnessing the unique local immunostimulatory properties of modified vaccinia Ankara (MVA) virus to generate superior tumor-specific immune responses and antitumor activity in a diversified prime and boost vaccine regimen. Vaccine. 2009;27(33):4475-82.
285. Zhang YQ, Tsai YC, Monie A, Wu TC, Hung CF. Enhancing the therapeutic effect against ovarian cancer through a combination of viral oncolysis and antigen-specific immunotherapy. Mol Ther. 2010;18(4):692-9.
286. Mastrangelo MJ, Maguire HC, Eisenlohr LC, Laughlin CE, Monken CE, McCue PA, et al. Intratumoral recombinant GM-CSF-encoding virus as gene therapy in patients with cutaneous melanoma. Cancer Gene Ther. 1999;6(5):409-22.

287. Senzer NN, Kaufman HL, Amatruda T, Nemunaitis M, Reid T, Daniels G, et al. Phase II clinical trial of a granulocyte-macrophage colony-stimulating factor-encoding, second-generation oncolytic herpesvirus in patients with unresectable metastatic melanoma. J Clin Oncol. 2009;27(34):5763-71.
288. Coffey JC, Wang JH, Smith MJ, Bouchier-Hayes D, Cotter TG, Redmond HP. Excisional surgery for cancer cure: therapy at a cost. Lancet Oncol. 2003;4(12):760-8.
289. Demicheli R, Valagussa P, Bonadonna G. Does surgery modify growth kinetics of breast cancer micrometastases? Br J Cancer. 2001;85(4):490-2.
290. Iversen P, Madsen PO, Corle DK. Radical prostatectomy versus expectant treatment for early carcinoma of the prostate. Twenty-three year follow-up of a prospective randomized study. Scand J Urol Nephrol Suppl. 1995;172:65-72.
291. Lange PH, Hekmat K, Bosl G, Kennedy BJ, Fraley EE. Acclerated growth of testicular cancer after cytoreductive surgery. Cancer. 1980;45(6):1498-506.
292. Baum M. Does surgery disseminate or accelerate cancer? Lancet. 1996;347(8996):260.
293. O'Reilly MS, Boehm T, Shing Y, Fukai N, Vasios G, Lane WS, et al. Endostatin: an endogenous inhibitor of angiogenesis and tumor growth. Cell. 1997;88(2):277-85.
294. Pidgeon GP, Harmey JH, Kay E, Da Costa M, Redmond HP, Bouchier-Hayes DJ. The role of endotoxin/lipopolysaccharide in surgically induced tumour growth in a murine model of metastatic disease. Br J Cancer. 1999;81(8):1311-7.
295. Mitsudomi T, Nishioka K, Maruyama R, Saitoh G, Hamatake M, Fukuyama Y, et al. Kinetic analysis of recurrence and survival after potentially curative resection of nonsmall cell lung cancer. J Surg Oncol. 1996;63(3):159-65.
296. Maniwa Y, Kanki M, Okita Y. Importance of the control of lung recurrence soon after surgery of pulmonary metastases. Am J Surg. 2000;179(2):122-5.
297. Lacy AM, Delgado S, Castells A, Prins HA, Arroyo V, Ibarzabal A, et al. The long-term results of a randomized clinical trial of laparoscopy-assisted versus open surgery for colon cancer. Ann Surg. 2008;248(1):1-7.

298. Da Costa ML, Redmond HP, Finnegan N, Flynn M, Bouchier-Hayes D. Laparotomy and laparoscopy differentially accelerate experimental flank tumour growth. Br J Surg. 1998;85(10):1439-42.
299. Da Costa ML, Redmond P, Bouchier-Hayes DJ. The effect of laparotomy and laparoscopy on the establishment of spontaneous tumor metastases. Surgery. 1998;124(3):516-25.
300. Patel H, Le Marer N, Wharton RQ, Khan ZA, Araia R, Glover C, et al. Clearance of circulating tumor cells after excision of primary colorectal cancer. Ann Surg. 2002;235(2):226-31.
301. Holmgren L, O'Reilly MS, Folkman J. Dormancy of micrometastases: balanced proliferation and apoptosis in the presence of angiogenesis suppression. Nat Med. 1995;1(2):149-53.
302. Pidgeon GP, Barr MP, Harmey JH, Foley DA, Bouchier-Hayes DJ. Vascular endothelial growth factor (VEGF) upregulates BCL-2 and inhibits apoptosis in human and murine mammary adenocarcinoma cells. Br J Cancer. 2001;85(2):273-8.
303. Lee SW, Gleason NR, Southall JC, Allendorf JD, Blanco I, Huang EH, et al. A serum-soluble factor(s) stimulates tumor growth following laparotomy in a murine model. Surg Endosc. 2000;14(5):490-4.
304. O'Reilly MS, Holmgren L, Shing Y, Chen C, Rosenthal RA, Moses M, et al. Angiostatin: a novel angiogenesis inhibitor that mediates the suppression of metastases by a Lewis lung carcinoma. Cell. 1994;79(2):315-28.
305. Li TS, Kaneda Y, Ueda K, Hamano K, Zempo N, Esato K. The influence of tumour resection on angiostatin levels and tumour growth--an experimental study in tumour-bearing mice. Eur J Cancer. 2001;37(17):2283-8.
306. Snyder GL, Greenberg S. Effect of anaesthetic technique and other perioperative factors on cancer recurrence. Br J Anaesth. 2010;105(2):106-15.
307. Lejeune FJ. Is surgical trauma prometastatic? Anticancer Res. 2012;32(3):947-51.
308. Miki C, Hiro J, Ojima E, Inoue Y, Mohri Y, Kusunoki M. Perioperative allogeneic blood transfusion, the related cytokine response and long-term survival after potentially curative resection of colorectal cancer. Clin Oncol (R Coll Radiol). 2006;18(1):60-6.

309. Vallejo R, Hord ED, Barna SA, Santiago-Palma J, Ahmed S. Perioperative immunosuppression in cancer patients. J Environ Pathol Toxicol Oncol. 2003;22(2):139-46.
310. Tai LH, de Souza CT, Bélanger S, Ly L, Alkayyal AA, Zhang J, et al. Preventing postoperative metastatic disease by inhibiting surgery-induced dysfunction in natural killer cells. Cancer Res. 2013;73(1):97-107.
311. Benish M, Bartal I, Goldfarb Y, Levi B, Avraham R, Raz A, et al. Perioperative use of beta-blockers and COX-2 inhibitors may improve immune competence and reduce the risk of tumor metastasis. Ann Surg Oncol. 2008;15(7):2042-52.
312. Goldfarb Y, Sorski L, Benish M, Levi B, Melamed R, Ben-Eliyahu S. Improving postoperative immune status and resistance to cancer metastasis: a combined perioperative approach of immunostimulation and prevention of excessive surgical stress responses. Ann Surg. 2011;253(4):798-810.
313. Glasner A, Avraham R, Rosenne E, Benish M, Zmora O, Shemer S, et al. Improving survival rates in two models of spontaneous postoperative metastasis in mice by combined administration of a beta-adrenergic antagonist and a cyclooxygenase-2 inhibitor. J Immunol. 2010;184(5):2449-57.
314. Ho CS, López JA, Vuckovic S, Pyke CM, Hockey RL, Hart DN. Surgical and physical stress increases circulating blood dendritic cell counts independently of monocyte counts. Blood. 2001;98(1):140-5.
315. Decker D, Schondorf M, Bidlingmaier F, Hirner A, von Ruecker AA. Surgical stress induces a shift in the type-1/type-2 T-helper cell balance, suggesting down-regulation of cell-mediated and up-regulation of antibody-mediated immunity commensurate to the trauma. Surgery. 1996;119(3):316-25.
316. Tai LH, Tanese de Souza C, Sahi S, Zhang J, Alkayyal AA, Ananth AA, et al. A mouse tumor model of surgical stress to explore the mechanisms of postoperative immunosuppression and evaluate novel perioperative immunotherapies. J Vis Exp. 2014(85).
317. Nichols PH, Ramsden CW, Ward U, Sedman PC, Primrose JN. Perioperative immunotherapy with recombinant interleukin 2 in patients undergoing surgery for colorectal cancer. Cancer Res. 1992;52(20):5765-9.

318. Deehan DJ, Heys SD, Ashby J, Eremin O. Interleukin-2 (IL-2) augments host cellular immune reactivity in the perioperative period in patients with malignant disease. Eur J Surg Oncol. 1995;21(1):16-22.
319. Sedman PC, Ramsden CW, Brennan TG, Giles GR, Guillou PJ. Effects of low dose perioperative interferon on the surgically induced suppression of antitumour immune responses. Br J Surg. 1988;75(10):976-81.
320. Houvenaeghel G, Bladou F, Blache JL, Olive D, Monges G, Jacquemier J, et al. Tolerance and feasibility of perioperative treatment with interferon-alpha 2a in advanced cancers. Int Surg. 1997;82(2):165-9.
321. Dranoff G. Cytokines in cancer pathogenesis and cancer therapy. Nat Rev Cancer. 2004;4(1):11-22.
322. Brandstadter JD, Yang Y. Natural killer cell responses to viral infection. J Innate Immun. 2011;3(3):274-9.
323. Tai LH, Zhang J, Scott KJ, de Souza CT, Alkayyal AA, Ananth AA, et al. Perioperative influenza vaccination reduces postoperative metastatic disease by reversing surgery-induced dysfunction in natural killer cells. Clin Cancer Res. 2013;19(18):5104-15.
324. Poland GA, Grabenstein JD, Neff JM. The US smallpox vaccination program: a review of a large modern era smallpox vaccination implementation program. Vaccine. 2005;23(17-18):2078-81.
325. Lane JM, Ruben FL, Neff JM, Millar JD. Complications of smallpox vaccination, 1968. N Engl J Med. 1969;281(22):1201-8.
326. Kretzschmar M, Wallinga J, Teunis P, Xing S, Mikolajczyk R. Frequency of adverse events after vaccination with different vaccinia strains. PLoS Med. 2006;3(8):e272.
327. Nalca A, Zumbrun EE. ACAM2000: the new smallpox vaccine for United States Strategic National Stockpile. Drug Des Devel Ther. 2010;4:71-9.
328. Kemper AR, Davis MM, Freed GL. Expected adverse events in a mass smallpox vaccination campaign. Eff Clin Pract. 2002;5(2):84-90.
329. Lane JM, Goldstein J. Evaluation of 21st-century risks of smallpox vaccination and policy options. Ann Intern Med. 2003;138(6):488-93.

330. Artenstein AW. New generation smallpox vaccines: a review of preclinical and clinical data. Rev Med Virol. 2008;18(4):217-31.
331. Hingorani SR, Petricoin EF, Maitra A, Rajapakse V, King C, Jacobetz MA, et al. Preinvasive and invasive ductal pancreatic cancer and its early detection in the mouse. Cancer Cell. 2003;4(6):437-50.
332. Hingorani SR, Wang L, Multani AS, Combs C, Deramaudt TB, Hruban RH, et al. Trp53R172H and KrasG12D cooperate to promote chromosomal instability and widely metastatic pancreatic ductal adenocarcinoma in mice. Cancer Cell. 2005;7(5):469-83.
333. Reed LJ, Muench H. A simple method of estimating fifty percent endpoints. A J Epidemiol. 1938;27(3):493-7.
334. Workman P, Aboagye EO, Balkwill F, Balmain A, Bruder G, Chaplin DJ, et al. Guidelines for the welfare and use of animals in cancer research. Br J Cancer. 2010;102(11):1555-77.
335. Wyatt LS, Shors ST, Murphy BR, Moss B. Development of a replication-deficient recombinant vaccinia virus vaccine effective against parainfluenza virus 3 infection in an animal model. Vaccine. 1996;14(15):1451-8.
336. Hassan R, Ho M. Mesothelin targeted cancer immunotherapy. Eur J Cancer. 2008;44(1):46-53.
337. Wang HL, Ning T, Li M, Lu ZJ, Yan X, Peng Q, et al. Effect of endostatin on preventing postoperative progression of distant metastasis in a murine lung cancer model. Tumori. 2011;97(6):787-93.
338. Sato M, Iwakabe K, Kimura S, Nishimura T. Functional skewing of bone marrow-derived dendritic cells by Th1- or Th2-inducing cytokines. Immunol Lett. 1999;67(1):63-8.
339. Palma JP, Yauch RL, Kang HK, Lee HG, Kim BS. Preferential induction of IL-10 in APC correlates with a switch from Th1 to Th2 response following infection with a low pathogenic variant of Theiler's virus. J Immunol. 2002;168(8):4221-30.
340. Iwasaki A, Kelsall BL. Freshly isolated Peyer's patch, but not spleen, dendritic cells produce interleukin 10 and induce the differentiation of T helper type 2 cells. J Exp Med. 1999;190(2):229-39.

341. Menten P, Wuyts A, Van Damme J. Macrophage inflammatory protein-1. Cytokine Growth Factor Rev. 2002;13(6):455-81.
342. Griffith JW, Sokol CL, Luster AD. Chemokines and chemokine receptors: positioning cells for host defense and immunity. Annual review of immunology. 2014;32:659-702.
343. Dorner BG, Scheffold A, Rolph MS, Huser MB, Kaufmann SH, Radbruch A, et al. MIP-1alpha, MIP-1beta, RANTES, and ATAC/lymphotactin function together with IFN-gamma as type 1 cytokines. Proc Natl Acad Sci U S A. 2002;99(9):6181-6.
344. Zitvogel L, Kepp O, Galluzzi L, Kroemer G. Inflammasomes in carcinogenesis and anticancer immune responses. Nature immunology. 2012;13(4):343-51.
345. Gerlic M, Faustin B, Postigo A, Yu EC, Proell M, Gombosuren N, et al. Vaccinia virus F1L protein promotes virulence by inhibiting inflammasome activation. Proc Natl Acad Sci U S A. 2013;110(19):7808-13.
346. Latz E, Xiao TS, Stutz A. Activation and regulation of the inflammasomes. Nat Rev Immunol. 2013;13(6):397-411.
347. Hoebe K, Janssen E, Beutler B. The interface between innate and adaptive immunity. Nature immunology. 2004;5(10):971-4.
348. Iwasaki A, Medzhitov R. Regulation of adaptive immunity by the innate immune system. Science. 2010;327(5963):291-5.
349. Schenten D, Medzhitov R. The control of adaptive immune responses by the innate immune system. Adv Immunol. 2011;109:87-124.
350. Postigo A, Way M. The vaccinia virus-encoded Bcl-2 homologues do not act as direct Bax inhibitors. J Virol. 2012;86(1):203-13.
351. Airoldi I, Cocco C, Giuliani N, Ferrarini M, Colla S, Ognio E, et al. Constitutive expression of IL-12R beta 2 on human multiple myeloma cells delineates a novel therapeutic target. Blood. 2008;112(3):750-9.
352. Airoldi I, Di Carlo E, Cocco C, Caci E, Cilli M, Sorrentino C, et al. IL-12 can target human lung adenocarcinoma cells and normal bronchial epithelial cells surrounding tumor lesions. PLoS One. 2009;4(7):e6119.
353. Cocco C, Pistoia V, Airoldi I. New perspectives for melanoma immunotherapy: role of IL-12. Curr Mol Med. 2009;9(4):459-69.

354. Ferretti E, Di Carlo E, Cocco C, Ribatti D, Sorrentino C, Ognio E, et al. Direct inhibition of human acute myeloid leukemia cell growth by IL-12. Immunol Lett. 2010;133(2):99-105.
355. Baldwin GC, Gasson JC, Kaufman SE, Quan SG, Williams RE, Avalos BR, et al. Nonhematopoietic tumor cells express functional GM-CSF receptors. Blood. 1989;73(4):1033-7.
356. Mueller MM, Fusenig NE. Constitutive expression of G-CSF and GM-CSF in human skin carcinoma cells with functional consequence for tumor progression. Int J Cancer. 1999;83(6):780-9.
357. Ninck S, Reisser C, Dyckhoff G, Helmke B, Bauer H, Herold-Mende C. Expression profiles of angiogenic growth factors in squamous cell carcinomas of the head and neck. Int J Cancer. 2003;106(1):34-44.
358. Gutschalk CM, Herold-Mende CC, Fusenig NE, Mueller MM. Granulocyte colony-stimulating factor and granulocyte-macrophage colony-stimulating factor promote malignant growth of cells from head and neck squamous cell carcinomas in vivo. Cancer Res. 2006;66(16):8026-36.
359. Pei XH, Nakanishi Y, Takayama K, Bai F, Hara N. Granulocyte, granulocyte-macrophage, and macrophage colony-stimulating factors can stimulate the invasive capacity of human lung cancer cells. Br J Cancer. 1999;79(1):40-6.
360. Gutschalk CM, Yanamandra AK, Linde N, Meides A, Depner S, Mueller MM. GM-CSF enhances tumor invasion by elevated MMP-2, -9, and -26 expression. Cancer Med. 2013;2(2):117-29.
361. Mueller MM, Fusenig NE. Friends or foes - bipolar effects of the tumour stroma in cancer. Nat Rev Cancer. 2004;4(11):839-49.
362. Aliper AM, Frieden-Korovkina VP, Buzdin A, Roumiantsev SA, Zhavoronkov A. A role for G-CSF and GM-CSF in nonmyeloid cancers. Cancer Med. 2014;3(4):737-46.
363. Joosten SA, Ottenhoff TH. Human CD4 and CD8 regulatory T cells in infectious diseases and vaccination. Human immunology. 2008;69(11):760-70.
364. Josefowicz SZ, Lu LF, Rudensky AY. Regulatory T cells: mechanisms of differentiation and function. Annual review of immunology. 2012;30:531-64.

365. Mueller SN, Gebhardt T, Carbone FR, Heath WR. Memory T cell subsets, migration patterns, and tissue residence. Annual review of immunology. 2013;31:137-61.
366. Gregory AD, Houghton AM. Tumor-associated neutrophils: new targets for cancer therapy. Cancer Res. 2011;71(7):2411-6.
367. Colombo MP, Lombardi L, Stoppacciaro A, Melani C, Parenza M, Bottazzi B, et al. Granulocyte colony-stimulating factor (G-CSF) gene transduction in murine adenocarcinoma drives neutrophil-mediated tumor inhibition in vivo. Neutrophils discriminate between G-CSF-producing and G-CSF-nonproducing tumor cells. J Immunol. 1992;149(1):113-9.
368. Di Carlo E, Forni G, Lollini P, Colombo MP, Modesti A, Musiani P. The intriguing role of polymorphonuclear neutrophils in antitumor reactions. Blood. 2001;97(2):339-45.
369. Matsushima H, Geng S, Lu R, Okamoto T, Yao Y, Mayuzumi N, et al. Neutrophil differentiation into a unique hybrid population exhibiting dual phenotype and functionality of neutrophils and dendritic cells. Blood. 2013;121(10):1677-89.
370. Albanesi M, Mancardi DA, Jönsson F, Iannascoli B, Fiette L, Di Santo JP, et al. Neutrophils mediate antibody-induced antitumor effects in mice. Blood. 2013;122(18):3160-4.
371. Broder CC, Kennedy PE, Michaels F, Berger EA. Expression of foreign genes in cultured human primary macrophages using recombinant vaccinia virus vectors. Gene. 1994;142(2):167-74.
372. Drillien R, Spehner D, Bohbot A, Hanau D. Vaccinia virus-related events and phenotypic changes after infection of dendritic cells derived from human monocytes. Virology. 2000;268(2):471-81.
373. Jenne L, Hauser C, Arrighi JF, Saurat JH, Hügin AW. Poxvirus as a vector to transduce human dendritic cells for immunotherapy: abortive infection but reduced APC function. Gene Ther. 2000;7(18):1575-83.
374. Sánchez-Puig JM, Sánchez L, Roy G, Blasco R. Susceptibility of different leukocyte cell types to Vaccinia virus infection. Virol J. 2004;1:10.

375. Byrd D, Shepherd N, Lan J, Hu N, Amet T, Yang K, et al. Primary human macrophages serve as vehicles for vaccinia virus replication and dissemination. J Virol. 2014;88(12):6819-31.
376. Chanmee T, Ontong P, Konno K, Itano N. Tumor-associated macrophages as major players in the tumor microenvironment. Cancers (Basel). 2014;6(3):1670-90.
377. Asano K, Nabeyama A, Miyake Y, Qiu CH, Kurita A, Tomura M, et al. CD169-positive macrophages dominate antitumor immunity by crosspresenting dead cell-associated antigens. Immunity. 2011;34(1):85-95.
378. Martinez-Pomares L, Gordon S. CD169+ macrophages at the crossroads of antigen presentation. Trends Immunol. 2012;33(2):66-70.
379. Chard LS, Maniati E, Wang P, Zhang Z, Gao D, Wang J, et al. A vaccinia virus armed with interleukin-10 is a promising therapeutic agent for treatment of murine pancreatic cancer. Clin Cancer Res. 2015;21(2):405-16.
380. Parmiani G, Castelli C, Pilla L, Santinami M, Colombo MP, Rivoltini L. Opposite immune functions of GM-CSF administered as vaccine adjuvant in cancer patients. Ann Oncol. 2007;18(2):226-32.
381. Clive KS, Tyler JA, Clifton GT, Holmes JP, Mittendorf EA, Ponniah S, et al. Use of GM-CSF as an adjuvant with cancer vaccines: beneficial or detrimental? Expert Rev Vaccines. 2010;9(5):519-25.
382. Odukoya O, Schwartz J, Weichselbaum R, Shklar G. An epidermoid carcinoma cell line derived from hamster 7,12-dimethylbenz[a]anthracene-induced buccal pouch tumors. J Natl Cancer Inst. 1983;71(6):1253-64.
383. Gimenez-Conti IB, Slaga TJ. The hamster cheek pouch carcinogenesis model. J Cell Biochem Suppl. 1993;17F:83-90.
384. Parviainen S, Ahonen M, Diaconu I, Kipar A, Siurala M, Vähä-Koskela M, et al. GMCSF-armed vaccinia virus induces an antitumor immune response. Int J Cancer. 2015;136(5):1065-72.
385. Nelles MJ, Duncan WR, Streilein JW. Immune response to acute virus infection in the Syrian hamster. II. Studies on the identity of virus-induced cytotoxic effector cells. J Immunol. 1981;126(1):214-8.

386. Liu BL, Robinson M, Han ZQ, Branston RH, English C, Reay P, et al. ICP34.5 deleted herpes simplex virus with enhanced oncolytic, immune stimulating, and anti-tumour properties. Gene Ther. 2003;10(4):292-303.
387. Pol J, Bloy N, Obrist F, Eggermont A, Galon J, Cremer I, et al. Trial Watch:: Oncolytic viruses for cancer therapy. Oncoimmunology. 2014;3:e28694.
388. Harrington KJ, Hingorani M, Tanay MA, Hickey J, Bhide SA, Clarke PM, et al. Phase I/II study of oncolytic HSV GM-CSF in combination with radiotherapy and cisplatin in untreated stage III/IV squamous cell cancer of the head and neck. Clin Cancer Res. 2010;16(15):4005-15.
389. Heo J, Reid T, Ruo L, Breitbach CJ, Rose S, Bloomston M, et al. Randomized dose-finding clinical trial of oncolytic immunotherapeutic vaccinia JX-594 in liver cancer. Nat Med. 2013;19(3):329-36.
390. Jaime JC, Young AM, Mateo J, Yap TA, Denholm KA, Shah KJ, et al., editors. Phase I clinical trial of a genetically modified and oncolytic vaccinia virus GL-ONC1 with green fluorescent protein imaging. American society of clinical oncology; 2012; Chicago, Illinois.
391. Mell LK, Yu YA, Brumund KT, Advani SJ, Onyeama S, Daniels GA, et al., editors. Phase I Trial Of Attenuated Vaccinia Virus (GL-ONC1) Delivered Intravenously With Concurrent Cisplatin And Radiotherapy In Patients With Locoregionally Advanced Head And Neck Carcinoma. Multidisciplinary Head and Neck Cancer Symposium; 2014; Scottsdale, Arizona.
392. Nguyen A, Ho L, Wan Y. Chemotherapy and Oncolytic Virotherapy: Advanced Tactics in the War against Cancer. Front Oncol. 2014;4:145.
393. Nguyên TL, Abdelbary H, Arguello M, Breitbach C, Leveille S, Diallo JS, et al. Chemical targeting of the innate antiviral response by histone deacetylase inhibitors renders refractory cancers sensitive to viral oncolysis. Proc Natl Acad Sci U S A. 2008;105(39):14981-6.
394. Alvarez-Breckenridge CA, Yu J, Price R, Wei M, Wang Y, Nowicki MO, et al. The histone deacetylase inhibitor valproic acid lessens NK cell action against oncolytic virus-infected glioblastoma cells by inhibition of STAT5/T-BET signaling and generation of gamma interferon. J Virol. 2012;86(8):4566-77.

395. Kim HS, Kim-Schulze S, Kim DW, Kaufman HL. Host lymphodepletion enhances the therapeutic activity of an oncolytic vaccinia virus expressing 4-1BB ligand. Cancer Res. 2009;69(21):8516-25.
396. Banissi C, Ghiringhelli F, Chen L, Carpentier AF. Treg depletion with a low-dose metronomic temozolomide regimen in a rat glioma model. Cancer Immunol Immunother. 2009;58(10):1627-34.
397. Chen CA, Ho CM, Chang MC, Sun WZ, Chen YL, Chiang YC, et al. Metronomic chemotherapy enhances antitumor effects of cancer vaccine by depleting regulatory T lymphocytes and inhibiting tumor angiogenesis. Mol Ther. 2010;18(6):1233-43.
398. Hermans IF, Chong TW, Palmowski MJ, Harris AL, Cerundolo V. Synergistic effect of metronomic dosing of cyclophosphamide combined with specific antitumor immunotherapy in a murine melanoma model. Cancer Res. 2003;63(23):8408-13.
399. Ghiringhelli F, Menard C, Puig PE, Ladoire S, Roux S, Martin F, et al. Metronomic cyclophosphamide regimen selectively depletes CD4+CD25+ regulatory T cells and restores T and NK effector functions in end stage cancer patients. Cancer Immunol Immunother. 2007;56(5):641-8.
400. Kottke T, Thompson J, Diaz RM, Pulido J, Willmon C, Coffey M, et al. Improved systemic delivery of oncolytic reovirus to established tumors using preconditioning with cyclophosphamide-mediated Treg modulation and interleukin-2. Clin Cancer Res. 2009;15(2):561-9.
401. Kottke T, Galivo F, Wongthida P, Diaz RM, Thompson J, Jevremovic D, et al. Treg depletion-enhanced IL-2 treatment facilitates therapy of established tumors using systemically delivered oncolytic virus. Mol Ther. 2008;16(7):1217-26.
402. Cerullo V, Diaconu I, Kangasniemi L, Rajecki M, Escutenaire S, Koski A, et al. Immunological effects of low-dose cyclophosphamide in cancer patients treated with oncolytic adenovirus. Mol Ther. 2011;19(9):1737-46.
403. Gabrilovich DI, Nagaraj S. Myeloid-derived suppressor cells as regulators of the immune system. Nat Rev Immunol. 2009;9(3):162-74.

404. Sinha P, Clements VK, Bunt SK, Albelda SM, Ostrand-Rosenberg S. Cross-talk between myeloid-derived suppressor cells and macrophages subverts tumor immunity toward a type 2 response. J Immunol. 2007;179(2):977-83.
405. Huang B, Pan PY, Li Q, Sato AI, Levy DE, Bromberg J, et al. Gr-1+CD115+ immature myeloid suppressor cells mediate the development of tumor-induced T regulatory cells and T-cell anergy in tumor-bearing host. Cancer Res. 2006;66(2):1123-31.
406. Esaki S, Goshima F, Kimura H, Murakami S, Nishiyama Y. Enhanced antitumoral activity of oncolytic herpes simplex virus with gemcitabine using colorectal tumor models. Int J Cancer. 2013;132(7):1592-601.
407. Kaneno R, Shurin GV, Kaneno FM, Naiditch H, Luo J, Shurin MR. Chemotherapeutic agents in low noncytotoxic concentrations increase immunogenicity of human colon cancer cells. Cell Oncol (Dordr). 2011;34(2):97-106.
408. Ghebeh H, Lehe C, Barhoush E, Al-Romaih K, Tulbah A, Al-Alwan M, et al. Doxorubicin downregulates cell surface B7-H1 expression and upregulates its nuclear expression in breast cancer cells: role of B7-H1 as an anti-apoptotic molecule. Breast Cancer Res. 2010;12(4):R48.
409. Workenhe ST, Mossman KL. Rewiring cancer cell death to enhance oncolytic viro-immunotherapy. Oncoimmunology. 2013;2(12):e27138.
410. Krysko DV, Garg AD, Kaczmarek A, Krysko O, Agostinis P, Vandenabeele P. Immunogenic cell death and DAMPs in cancer therapy. Nat Rev Cancer. 2012;12(12):860-75.
411. Workenhe ST, Pol JG, Lichty BD, Cummings DT, Mossman KL. Combining oncolytic HSV-1 with immunogenic cell death-inducing drug mitoxantrone breaks cancer immune tolerance and improves therapeutic efficacy. Cancer Immunol Res. 2013;1(5):309-19.
412. Tysome JR, Li X, Wang S, Wang P, Gao D, Du P, et al. A novel therapeutic regimen to eradicate established solid tumors with an effective induction of tumor-specific immunity. Clin Cancer Res. 2012;18(24):6679-89.

413. Wolchok JD, Hodi FS, Weber JS, Allison JP, Urba WJ, Robert C, et al. Development of ipilimumab: a novel immunotherapeutic approach for the treatment of advanced melanoma. Ann N Y Acad Sci. 2013;1291:1-13.
414. Gao Q, Qiu SJ, Fan J, Zhou J, Wang XY, Xiao YS, et al. Intratumoral balance of regulatory and cytotoxic T cells is associated with prognosis of hepatocellular carcinoma after resection. J Clin Oncol. 2007;25(18):2586-93.
415. Walker LS. Treg and CTLA-4: two intertwining pathways to immune tolerance. J Autoimmun. 2013;45:49-57.
416. Zamarin D, Holmgaard RB, Subudhi SK, Park JS, Mansour M, Palese P, et al. Localized oncolytic virotherapy overcomes systemic tumor resistance to immune checkpoint blockade immunotherapy. Sci Transl Med. 2014;6(226):226ra32.